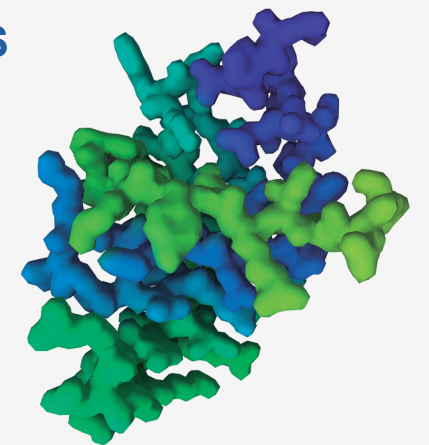




VNIVERSITAT
E VALÈNCIA

Doctoral Program in Biomedicine and Biotechnology

CHARACTERIZATION OF THE METABOLIC PROFILE AND IDENTIFICATION OF POTENTIAL THERAPEUTIC TARGETS IN ADVANCED PROSTATE CANCER PATIENTS



DOCTORAL THESIS

Author:

Nuria Gómez Cebrían

Supervised by:

Dra. Leonor Puchades Carrasco

Dr. Antonio Pineda Lucena

Dr. José Antonio López Guerrero

Valencia, January, 2023

2023

DOCTORAL THESIS

Nuria Gómez Cebrían



ivo

IIS La Fe
Instituto de
Investigación Sanitaria



VNIVERSITAT
ID VALÈNCIA

Doctoral Program in Biomedicine and Biotechnology

CHARACTERIZATION OF THE METABOLIC
PROFILE AND IDENTIFICATION OF POTENTIAL
THERAPEUTIC TARGETS IN ADVANCED
PROSTATE CANCER PATIENTS

Doctoral Thesis

Author:

Nuria Gómez Cebrián

Supervised by:

Dra. Leonor Puchades Carrasco

Dr. Antonio Pineda Lucena

Dr. José Antonio López Guerrero

January, 2023

Leonor Puchades Carrasco, Doctora en Bioquímica, Investigadora Principal en la Unidad de Descubrimiento de Fármacos del Instituto de Investigación Sanitaria La Fe en Valencia.

Antonio Pineda Lucena, Doctor en Ciencias Químicas, Director Científico del Centro de Investigación Médica Aplicada en Pamplona.

José Antonio López Guerrero, Doctor en Ciencias Biológicas, Investigador Principal en el Laboratorio de Biología Molecular de la Fundación Instituto Valenciano de Oncología en Valencia.

INFORMAN:

Que **Nuria Gómez Cebrián**, Licenciada en Biotecnología por la Universidad Católica de Valencia, ha realizado en la Unidad de Descubrimiento de Fármacos del Instituto de Investigación Sanitaria La Fe, bajo su dirección, el trabajo de investigación titulado **“CHARACTERIZATION OF THE METABOLIC PROFILE AND IDENTIFICATION OF POTENTIAL THERAPEUTIC TARGETS IN ADVANCED PROSTATE CANCER PATIENTS”** y que hallándose concluida, reúne todos los requisitos para su juicio y calificación, por tanto, autorizan su presentación, a fin de que pueda ser juzgado por el tribunal correspondiente para la obtención del grado de Doctor por la Universidad de Valencia.

Y para que conste, en cumplimiento con la legislación, firman el presente informe en Valencia, a 13 de Enero de 2023.



Dra. Leonor Puchades Carrasco
DNI: 24373634M



Dr. Antonio Pineda Lucena
DNI: 30517484A



Dr. José Antonio López Guerrero
DNI: 21655332G

La realización de esta tesis doctoral ha sido financiada con los siguientes proyectos:

- Programa Prometeo para grupos de investigación de excelencia PROMETEO/2016/103. Conselleria de Educación, Investigación, Cultura y Deporte (IP: José Antonio López Guerrero).

- “Contribuciones de la metabolómica por RMN a la clasificación clínica de pacientes: un paso adelante”. Plan Nacional I+D+I MINECO SAF2017-89229-R. Ministerio de Economía y Competitividad (IP: Antonio Pineda Lucena).

- “New integrative analysis of genetic vulnerabilities in advanced prostate cancer for the identification of novel pharmaceutically relevant protein targets”. Subvenciones a grupos de investigación emergentes GV/2021/154. Conselleria de Innovación, Universidades, Ciencia y Sociedad Digital (IP: Leonor Puchades Carrasco).

A mis padres

A Jorge

A David

Agradecimientos

En primer lugar, a mis directores de tesis, la Dra. Leonor Puchades, el Dr. Antonio Pineda y el Dr. José Antonio López, por haberme dado la oportunidad de realizar esta tesis, y por todos los consejos que me han dado durante esta etapa. Especialmente, me gustaría darle las gracias a Leo por toda la confianza que ha depositado en mí, por darme la oportunidad de aprender en el campo de la biología molecular y los cultivos celulares, y por su implicación a lo largo de toda esta tesis. He aprendido mucho de ella tanto a nivel profesional como personal.

Gracias a todo el departamento de Biología Molecular del IVO por acogerme tan bien en su laboratorio. A María por su ayuda y consejos cuando los he necesitado, y por adentrarme en el mundo de la PCR. A Belén, con quien he compartido todos los horrores de los cultivos celulares. Siempre recordaré esos mensajes de buenos días en los que nos contábamos todos los problemas y la frustración que teníamos con las células.

Gracias a todos los vecinos de Infección Grave, con los que he compartido buenos momentos durante este tiempo. Especialmente a Geles y a Rosa Ana, que han hecho que los almuerzos y las comidas fuera más amenas.

Agradecer también a todos los compañeros que han pasado por el laboratorio. A Leti, Rubén, Marta y Arturo, que me enseñaron a manejarme en el laboratorio y a entender mejor la metabolómica. Muchas gracias también a Inés. Hemos compartido gran parte del proceso de nuestras tesis, y me has escuchado y apoyado siempre que lo he necesitado. ¡Ánimo que ya te queda nada!

Gracias a todos los estudiantes de prácticas con los que he tenido la oportunidad de trabajar. Especialmente, quiero dar las gracias al trío calavera: Lien, Inés y Dani. Siempre llegáis al laboratorio con una sonrisa y con ganas de aprender y trabajar. Gracias por vuestra ayuda y por vuestro apoyo durante estos meses.

Me gustaría agradecer a las cuatro grandes amistades que me llevo de esta etapa, con las que he tenido la suerte de coincidir en distintas etapas de la tesis y con las que he

compartido muchos momentos. Primero fue María. Al principio no congeniamos muy bien, pero con el tiempo nos convertimos en inseparables y pudimos compartir risas, lloros, viajes a por café, miles de comidas, y ahora, hasta carreras. ¡Nos queda nuestro viaje! Luego me crucé con Ayelén y con Mercedes, mis compañeras de despachito. Nunca un espacio tan pequeño ha dado para tanto. Hemos compartido momentos de crisis, incertidumbres y lágrimas, pero también tardes de chocolate, bombones y cafés. Miles de gracias por escucharme y por cada uno de los consejos que me distéis. ¡Sé que nos quedan muchos momentos por vivir fuera! Y finalmente agradecer a Patri, mi gran compañera durante esta última etapa. Empezamos a conocernos mejor por las restricciones del COVID, y nos hemos convertido en muy buenas amigas. Gracias por venir siempre con una sonrisa, y por escucharme y ayudarme siempre que lo he necesitado. Hemos compartido miles de confesiones en nuestras comidas interminables y hemos creado nuevas tradiciones que espero que continúen por mucho tiempo. ¡Espero seguir compartiendo muchos más momentos en los próximos años!

Quiero agradecer a mi familia, que han estado apoyándome durante todos estos años. En especial, quiero agradecer a mis padres y a mi hermano Jorge, que han compartido mis alegrías, mis frustraciones y algún momento de sufrimiento. Mamá y papá, millones de gracias por la comprensión y por todo el cariño que me habéis dado, esto no hubiese sido posible sin vuestro apoyo y sacrificio. Mamá, gracias por creer en mí ni cuando yo misma lo hago, por estar a mi lado cada día, y por interesarte cada día por mi trabajo.

Miles de gracias a ti, David. Gracias por compartir esta etapa conmigo, por todo el interés que demuestras hacia mi trabajo, y por acompañarme los fines o festivos al laboratorio. Pero especialmente, gracias por tu apoyo constante, por tu paciencia infinita, por tu ayuda, por tu comprensión, por aguantarme durante estos años, por creer en mí, y por estar siempre a mi lado.

Finalmente me gustaría agradecer a mis yayos. Os echo mucho de menos, especialmente a ti yaya. Ojalá pudierais estar aquí compartiendo este momento conmigo, pero espero que lo podáis ver dondequiera que estéis.

INDEX

LIST OF FIGURES	17
LIST OF TABLES	19
ABBREVIATIONS	21
RESUMEN	25
I. INTRODUCTION	41
I.1. PROSTATE CANCER	43
I.1.1. PROSTATE CANCER	43
I.1.2. DIAGNOSIS	43
I.1.3. TUMOR STAGING	46
I.1.4. TREATMENT	47
I.1.4.1. Localized PCa	48
I.1.4.2. Advanced PCa	50
I.1.5. MOLECULAR SUBTYPES	51
I.1.6. CURRENT CHALLENGES IN THE LANDSCAPE OF PCA	54
I.2. OMICS TECHNOLOGIES IN CANCER	55
I.2.1. OMICS TECHNOLOGIES FOR THE IDENTIFICATION OF NEW THERAPEUTIC TARGETS	59
I.2.1.1. DEFINITION AND CHARACTERISTICS OF A DRUG TARGET	59
I.2.1.2. GENETIC SCREENING	60
I.2.1.3. IDENTIFICATION OF GENETIC VULNERABILITIES	62
I.2.2. OMICS TECHNOLOGIES FOR THE IDENTIFICATION OF NON-INVASIVE BIOMARKERS	62
I.2.2.1. MULTI-OMICS CHARACTERIZATION OF CANCER-RELATED METABOLIC PHENOTYPES	63
I.2.2.2. ANALYTICAL PLATFORMS FOR METABOLIC STUDIES	66
I.2.2.3. STEPS OF A METABOLIC STUDY	68
II. HYPOTHESIS AND OBJECTIVES	73
III. MATERIALS AND METHODS	77
III.1. IDENTIFICATION OF METABOLIC BIOMARKERS FOR ADVANCED PCA	79
III.1.1. SAMPLE COLLECTION FOR METABOLOMICS ANALYSES	79
III.1.2. SELECTION OF TRANSCRIPTOMIC STUDIES	80
III.1.3. ACQUISITION OF NMR METABOLIC PROFILE	81
III.1.3.1. Spectra acquisition	81

III.1.3.2.	NMR data processing	82
III.1.4.	METABOLITE ASSIGNMENT	83
III.1.5.	MULTIVARIATE STATISTICAL ANALYSIS	83
III.1.6.	DIFFERENTIAL EXPRESSION ANALYSES	84
III.1.7.	GENE SET ENRICHMENT ANALYSIS	84
III.2.	IDENTIFICATION OF POTENTIAL THERAPEUTIC TARGETS FOR ADVANCED PCA.....	85
III.2.1.	CALCULATION OF THE ESSENTIALITY SCORE	85
III.2.2.	SELECTION OF TRANSCRIPTOMIC STUDIES.....	85
III.2.3.	DIFFERENTIAL EXPRESSION ANALYSES	86
III.2.4.	SURVIVAL ANALYSES.....	86
III.2.5.	EVALUATION OF THE THERAPEUTIC POTENTIAL.....	87
III.2.5.1.	Databases.....	87
III.2.5.2.	Characterization of gene expression levels in cellular models.....	87
III.2.5.3.	Generation of shRNA knockdown models	90
III.2.5.4.	Cell proliferation assay.....	93
III.2.5.5.	Colony formation assay.....	93
III.2.5.6.	Wound healing assay.....	94
III.2.5.7.	Co-immunoprecipitation assay	94
IV.	RESULTS AND DISCUSSION.....	95
IV.1.	CHARACTERIZATION OF METABOLIC CHANGES RELATED TO PCA PROGRESSION.....	97
IV.1.1.	PCA METABOLIC PROFILE	97
IV.1.2.	SAMPLE HETEROGENEITY AND OUTLIER DETECTION	100
IV.1.3.	UNTARGETED METABOLOMICS ANALYSIS OF LOW- AND HIGH-GS PCA PATIENTS.....	106
IV.1.4.	IDENTIFICATION OF DYSREGULATED METABOLIC PATHWAYS BETWEEN LOW- AND HIGH-GS PCA PATIENTS.....	108
IV.1.5.	TARGETED ANALYSIS OF LOW- AND HIGH-GS PCA PATIENTS' METABOLIC PROFILE	110
IV.1.6.	BIOLOGICAL INTERPRETATION.....	113
IV.2.	CHARACTERIZATION OF NOVEL SPECIFIC GENETIC VULNERABILITIES IN ADVANCED PCA.....	117
IV.2.1.	IDENTIFICATION OF ESSENTIAL GENES IN PCA CELL LINES	117
IV.2.2.	ANALYSIS OF THE POTENTIAL ASSOCIATION BETWEEN ESSENTIAL GENES AND PCA PROGRESSION.....	119
IV.2.3.	ESSENTIAL GENES OVER-EXPRESSED IN PCA.....	120
IV.2.4.	ESSENTIAL GENES OVER-EXPRESSED IN AGGRESSIVE/METASTATIC PCA TUMORS	120
IV.2.5.	CORRELATION BETWEEN ESSENTIAL GENE EXPRESSION AND PCA PROGRESSION	122

IV.2.6.	EVALUATION OF ESSENTIAL GENES AS POTENTIAL PCA THERAPEUTIC TARGETS	122
IV.2.7.	EVALUATION OF EIF3H AS A VALUABLE THERAPEUTIC TARGET IN PCA.....	128
IV.2.7.1.	Role of EIF3H in cancer progression	128
IV.2.7.2.	EIF3H is a druggable target.....	129
IV.2.7.3.	EIF3H is over-expressed in PCa and is correlated with patient's prognosis	131
IV.2.8.	VALIDATION OF EIF3H AS A VALUABLE THERAPEUTIC TARGET IN PCA	132
IV.2.8.1.	EIF3H is over-expressed in PCa cell lines	132
IV.2.8.2.	EIF3H silencing reduces proliferation and migration in PCa cell lines	133
IV.2.8.3.	EIF3H over-expression increases proliferation and migration in PCa cell lines.....	136
IV.2.8.4.	Changes in EIF3H levels promote epithelial-mesenchymal transition	138
IV.2.9.	IDENTIFICATION OF POTENTIAL EIF3H-EFFECTOR PROTEINS.....	140
IV.2.9.1.	EIF3H directly interacts with STAU1 in PCa cell lines	140
IV.2.9.2.	STAU1 is a druggable target	141
<u>V.</u>	<u>FUTURE PERSPECTIVES.....</u>	<u>145</u>
<u>VI.</u>	<u>CONCLUSIONS.....</u>	<u>149</u>
<u>VII.</u>	<u>REFERENCES.....</u>	<u>153</u>
<u>VIII.</u>	<u>APPENDICES.....</u>	<u>189</u>
<u>IX.</u>	<u>PUBLICATIONS.....</u>	<u>205</u>

List of figures

Figure 1. Definition of histological patterns used to determine the ISUP Grade Group based on the Gleason Scores	47
Figure 2. Therapeutic strategies for localized tumors based on the risk of the PCa progression...	49
Figure 3. Representation of the most common genetic alterations identified in localized PCa	52
Figure 4. Capabilities and characteristics that facilitate the transformation of normal cells into a neoplastic condition.....	56
Figure 5. Overview of the relationship between omics technologies	57
Figure 6. Overview of the basic workflow followed in a LOF genetic screen.	61
Figure 7. Schematic representative of the most consistently metabolic pathways reported to be dysregulated across different PCa multi-omics studies	64
Figure 8. General workflow followed in an NMR-based metabolomic study.....	68
Figure 9. Schematic representation of the lentivirus production strategy	92
Figure 10. Metabolite assignation of a representative ¹ H-CPMG serum spectrum of a PCa sample	98
Figure 11. Metabolite assignation of a representative ¹ H-NOESY urine spectrum of a PCa sample	99
Figure 12. PCA score plots of serum and urine global metabolic profile of low- and high-GS PCa patients	100
Figure 13. Outlier identification based on the non-supervised PCA.....	101
Figure 14. Identification of an outlier sample exhibiting peaks corresponding to EDTA.....	102
Figure 15. Outlier identification after sample exclusion, based on the non-supervised PCA.....	103
Figure 16. Score plot of all urine samples of low- and high-GS PCa patients	103
Figure 17. PCA score plots of serum and urine samples included in the study	105
Figure 18. Unsupervised statistical analysis	106
Figure 19. Supervised statistical analysis	106
Figure 20. Internal validation of the OPLS-DA models using the permutation test.....	107
Figure 21. Venn diagram representing the overlap between the results obtained for the GSEA of the different PCa transcriptomic datasets included in the analysis	109
Figure 22. Boxplot representing the normalized serum and urine intensities of the metabolites showing higher variations in intensity between the groups of study.....	113
Figure 23. Schematic representation of the genetic and metabolic alterations found for the comparison between low- and high-GS PCa patients	113
Figure 24. Overview of the strategy followed during the analysis for the identification of potential therapeutic targets in PCa.....	117

List of figures

Figure 25. Comparison of essential genes identified after calculating genetic dependencies using the Hart approach or following the DEMETER2 model.....	118
Figure 26. Overview of the filtering steps and the final subset of essential genes	122
Figure 27. Protein-protein interaction regulatory network constructed using STRING.....	123
Figure 28. 3D structures of the PDB ID 6YBD	130
Figure 29. Network for the known and predicted substrates that may be deubiquitinated by EIF3H	131
Figure 30. <i>EIF3H</i> is over-expressed in PCa and associated with PCa progression	132
Figure 31. EIF3H is over-expressed at the transcriptomic and proteomic level in more aggressive PCa stages.....	132
Figure 32. Lentivirus infection of PC3 PCa cell lines with the control and the <i>EIF3H</i> shRNA vectors	133
Figure 33. Silencing <i>EIF3H</i> expression in PC3 cell line using lentivirus-mediated shRNA	134
Figure 34. <i>EIF3H</i> knockdown inhibits the proliferation and colony formation of PC3 cells	135
Figure 35. Silencing <i>EIF3H</i> expression has an effect on PC3 migration	136
Figure 36. Over-expression of EIF3H in PC3 cell line using lentivirus-mediated shRNA.....	137
Figure 37. <i>EIF3H</i> over-expression enhances the proliferation and colony formation of PC3 cells	137
Figure 38. Over-expression of <i>EIF3H</i> expression has an effect on PC3 migration	138
Figure 39. EIF3H induces epithelial-mesenchymal transition in PC3 cells.....	139
Figure 40. <i>STAU1</i> is over-expressed in PCa and associated with PCa progression	141
Figure 41. 3D structure of the PDB ID 6HTU.....	142

List of tables

Table 1. Overview of commercially available PCa biomarker tests	54
Table 2. Metabolic alterations observed in different multi-omics studies focused on the characterization of the metabolic profile of specific PCa subtypes	65
Table 3. Summary of the advantages and limitations of MS and NMR in metabolomics studies	66
Table 4. Number of samples included in each experimental group for each collected biofluid....	79
Table 5. Acquisition parameters for each ¹ H-RMN biofluid spectra	82
Table 6. Summary of the processing steps followed in each biofluid	82
Table 7. Description of the master mix used for reverse transcription of purified RNA.....	88
Table 8. Description of the reaction master mix used for RT-PCR.....	89
Table 9. Primer sequences used for the qPCR.....	89
Table 10. Information about the antibodies used in the western blot analyses	90
Table 11. shRNA constructions and over-expression plasmids used for EIF3H gene	90
Table 12. Subset of samples excluded from the study	104
Table 13. Clinical characteristics of PCa patients included in the metabolic study.....	104
Table 14. Characteristics of selected PCa transcriptomic studies	109
Table 15. Top ten most significantly enriched metabolic pathways.....	110
Table 16. Mean intensities and variations for the metabolites identified in the serum samples of low- and high-GS PCa patients.....	111
Table 17. Mean intensities and variations for the metabolites identified in the urine samples of low- and high-GS PCa patients.....	112
Table 18. Characteristics of the selected PCa transcriptomic studies.....	119
Table 19. Number of samples included in each experimental group for the differential expression analyses	120
Table 20. Number of samples included in each experimental group for the differential expression analyses	120
Table 21. Number of samples included in each experimental group for the differential expression analyses	121
Table 22. Extracted characteristics and literature information of the potential therapeutic targets involved in the mRNA translation pathway	125
Table 23. Extracted characteristics and literature information of the potential therapeutic targets involved in the spliceosome pathway	127

ABBREVIATIONS

1D	One dimension
¹ H-NMR	Proton nuclear magnetic resonance
Å	Angstrom
ADT	Androgen deprivation therapy
AR	Androgen receptor
BCR	Biochemical recurrence
BF	Bayes factor
BPH	Benign prostatic hyperplasia
cDNA	Complementary deoxyribonucleic acid
CPMG	Carr-Purcell-Meiboom-Gill
CRISPR	Clustered regularly interspace short palindromic repeat
CRPC	Castration resistant prostate cancer
GEO	Gene expression omnibus
GS	Gleason score
Da	Dalton
EIF3H	Eukaryotic translation initiation factor 3 subunit H
EMT	Epithelial-mesenchymal transition
FC	Fold-change
GFP	Green fluorescent protein
GSEA	Gene set enrichment analysis
LOF	Loss-of-function
MNA	1-methylnicotinamide
MS	Mass spectroscopy
mRNA	Messenger ribonucleic acid
NMR	Nuclear magnetic resonance
NOESY	Nuclear overhauser effect spectroscopy
OPLS-DA	Orthogonal partial least square discriminant analysis
OXPHOS	Oxidative phosphorylation
PCa	Prostate cancer
PCA	Principal component analysis
PPI	Protein-protein interaction
Ppm	Parts per million

Abbreviations

PQN	Probabilistic quotient normalization
PSA	Prostate specific antigen
qPCR	Quantitative polymerase chain reaction
shRNA	Small hairpin RNA
snRNPs	Small nuclear ribonucleoproteins
TCA	Tricarboxylic acid
TSP	Trimethylsilylpropanoic acid

RESUMEN

INTRODUCCIÓN

El cáncer de próstata (CaP) representa el segundo tumor en incidencia en hombres y es la quinta causa de muerte por cáncer a nivel global. El CaP es un tumor hormono-dependiente, que requiere de la activación del receptor de andrógenos (AR) para su proliferación. Clínicamente, se caracteriza por una gran variabilidad en su evolución, progresando desde una condición indolente hasta un fenotipo agresivo que puede diseminarse y metastatizar a los nodos linfáticos y huesos.

Actualmente, el diagnóstico temprano del CaP se realiza mediante la determinación sérica del antígeno prostático específico (PSA) y el examen rectal digital (DRE). Si estas pruebas dan resultados anómalos y hay sospecha de CaP, se realiza una biopsia guiada por ultrasonido transrectal (TRUS) para la confirmación histológica. Sin embargo, estas pruebas presentan una baja sensibilidad y especificidad, y conllevan un alto riesgo de sobre-diagnóstico y sobre-tratamiento de los pacientes, especialmente en los casos de CaP indolente. Una vez se ha confirmado el diagnóstico, se utiliza el sistema de gradación de la escala de Gleason (GS) para evaluar la agresividad del tumor, en base a sus características histológicas, y estratificar a los pacientes según su pronóstico. Aunque el sistema de Gleason ha sido modificado varias veces, todavía presenta ciertas limitaciones que dificultan distinguir con precisión entre tumores indolentes y agresivos de CaP.

El tratamiento del CaP depende del estadio tumoral y del pronóstico de cada paciente. Así, los tumores en etapas tempranas se tratan, inicialmente, mediante radioterapia o prostatectomía radical. Debido a la dependencia del CaP a los andrógenos para proliferar, estos tratamientos suelen combinarse con la terapia de deprivación androgénica (TDA) con el objetivo de reducir los niveles de testosterona circulante. Sin embargo, la respuesta a este tratamiento es transitoria debido a que, tras 18-36 meses, la mayoría de los pacientes desarrollarán resistencia a la TDA y progresarán a un CaP resistente a la castración (CPRC). Para estos pacientes, los tratamientos disponibles se basan en quimioterapia, hormonoterapia, inmunoterapia o inhibidores de PARP. A pesar de los avances realizados para comprender mejor los procesos moleculares y biológicos involucrados en la progresión del CaP, actualmente no existen biomarcadores específicos

ni estrategias terapéuticas eficientes para la detección y tratamiento de este tumor en estadios avanzados.

La metabolómica representa una herramienta muy prometedora y particularmente apropiada para la identificación de biomarcadores no invasivos con utilidad clínica en el diagnóstico y el seguimiento de pacientes. Esto se debe a que el metaboloma está muy ligado al fenotipo de la enfermedad, proporcionando información sobre alteraciones debidas a cambios en la expresión génica, estilo de vida, patologías y/o respuesta a tratamientos. Esta aproximación se puede integrar con otros datos, obtenidos mediante técnicas ómicas complementarias y otros estudios clínicos, consiguiendo así obtener un visión global y más precisa de la enfermedad, así como una descripción más detallada del estado del paciente y de la evolución de la enfermedad.

Por otro lado, la medicina de precisión constituye una de las vías con mayor potencial en la mejora de la atención médica y el tratamiento de los pacientes con cáncer. Mediante la regulación específica de la actividad de algunas dianas terapéuticas claves, se podría llegar a controlar el crecimiento tumoral y la formación de metástasis. Aunque el concepto de medicina de precisión no es nuevo, la aparición de las ciencias ómicas junto con los notables avances tecnológicos en las plataformas de análisis, han sentado las bases de esta aproximación. Las terapias dirigidas se basan en el estudio del estatus genético específico de las células tumorales. Una aplicación muy útil de este tipo de estudios es la identificación de vulnerabilidades genéticas específicas que puedan ayudar a descubrir nuevas dianas terapéuticas. En este contexto, mediante cribados de silenciamiento de genes, se pueden analizar los efectos inducidos a partir del bloqueo parcial de la actividad de un gen por ARN de interferencia (*knock-down*), o del bloqueo total del gen (*knock-out*) utilizando técnicas de edición génica (CRISPR). Estos cribados pueden ayudar a identificar perfiles moleculares específicos, requeridos por las células tumorales para su proliferación. Además, la comparación en estos cribados entre tejidos sanos y tumorales puede contribuir a identificar genes esenciales únicamente en el tumor, siendo éstos considerados potenciales dianas terapéuticas para el desarrollo de terapias anticancerosas específicas.

OBJETIVOS

Como se ha descrito en la introducción, el CaP se define como un cáncer biológicamente heterogéneo y con un curso clínico muy variable. El manejo óptimo del CaP presenta muchos retos debido a la dificultad en predecir qué pacientes con tumores en estadios tempranos desarrollarán una progresión metastática del tumor. Además, no existe un sistema de clasificación que permita discriminar con precisión entre tumores de CaP indolentes y agresivos. Por tanto, la identificación de nuevos biomarcadores asociados a la progresión de la enfermedad podría contribuir a mejorar el panorama actual de estos pacientes. Por otro lado, el CaP continúa siendo incurable cuando progresa a etapas más avanzadas, por lo que nuevas opciones terapéuticas, basadas en la medicina personalizada, podrían contribuir a aumentar la supervivencia y mejorar la calidad de vida de los pacientes con CaP. En este contexto, la aplicación de distintas tecnologías ómicas representa una estrategia prometedora para el desarrollo de nuevos biomarcadores no invasivos, y para la identificación de vulnerabilidades genéticas, esenciales para la proliferación tumoral, que podrían ser evaluadas en profundidad como posibles dianas terapéuticas para el desarrollo de nuevos fármacos.

Por tanto, teniendo en cuenta estos antecedentes, el presente trabajo de investigación tiene como finalidad abordar los siguientes objetivos y sub-objetivos:

1. Caracterizar cambios metabólicos asociados a la progresión del CaP.
 - i. Caracterizar el perfil metabólico de orina y suero de pacientes con CaP avanzado.
 - ii. Identificar alteraciones metabólicas específicas en los pacientes con CaP avanzado.
2. Caracterizar vulnerabilidades genéticas específicas del CaP avanzado.
 - i. Identificar nuevas y potenciales dianas terapéuticas para el tratamiento del CaP avanzado.
 - ii. Validar funcionalmente las potenciales dianas terapéuticas.

METODOLOGÍA Y RESULTADOS

1. Caracterización de cambios metabólicos asociados a la progresión del CaP

Para el estudio de la caracterización del perfil metabólico del CaP agresivo se analizaron 78 muestras de suero y 84 muestras de orina de pacientes con CaP, recogidas por el departamento de urología y el biobanco del Instituto Valenciano de Oncología y congeladas a -80°C . Se utilizó el valor del GS para clasificar a los pacientes en dos grupos (GS bajo y GS alto), definiendo un valor de GS de 7 como punto de corte.

Las muestras se procesaron siguiendo protocolos descritos para estudios de metabolómica por resonancia magnética nuclear (RMN) y se analizaron en un espectrómetro de 500 MHz. La adquisición de los espectros de las muestras de suero se realizó a 310 K, utilizando la secuencia de pulso 1D-CPMG, mientras que para la adquisición de los espectros de las muestras de orina se utilizó una temperatura de 300 K y la secuencia de pulso 1D-NOESY. Los espectros obtenidos fueron transformados, faseados y se corrigió la línea base de manera automática.

Tras la adquisición, y teniendo en cuenta las características de cada biofluido, los espectros fueron procesados siguiendo distintos protocolos. Primero, se definió la región del espectro a integrar, y se excluyeron las señales del agua y la urea en ambos biofluidos. A continuación, los espectros de suero se referenciaron con la señal del TSP (0.00 ppm), se dividieron en regiones de tamaño constante (0.01 ppm), y se normalizaron respecto al área total de cada espectro. Por otro lado, los espectros de orina se dividieron en regiones constantes de 0.001 ppm, se alinearon utilizando el paquete de R *'speaq'*, y se normalizaron respecto al área total de cada espectro y mediante la normalización con cociente probabilístico. Una vez procesados, se utilizaron diferentes bases de datos para asignar los metabolitos presentes en los espectros de cada biofluido. Finalmente, para cada metabolito identificado, las regiones de integración para las señales correspondientes fueron definidas. Se utilizó el programa Mnova para integrar y cuantificar las regiones seleccionadas.

Con el objetivo de evaluar la homogeneidad de las muestras incluidas en cada grupo de estudio e identificar muestras presentando un comportamiento anómalo (potenciales

outliers), se realizó un análisis exploratorio mediante la combinación de métodos no supervisados de reconocimiento por patrones (análisis de componentes principales - PCA), utilizando el programa SIMCA-P, y la inspección visual de los espectros. En los espectros de suero, este análisis reveló un conjunto de muestras que presentaban señales intensas correspondientes a etanol, una muestra con picos correspondientes a una contaminación por EDTA y un subgrupo de pacientes que presentaban niveles inusualmente elevados de glucosa. Los picos correspondientes a EDTA pueden deberse al tipo de tubos que se utilizó para recoger la muestra. Para evitar que estas señales pudieran interferir con otras señales del espectro y debido a que este compuesto se utiliza para la recogida de muestras de plasma, esta muestra fue eliminada del análisis. En cuanto a los pacientes que presentaban señales de etanol y niveles anormalmente altos de glucosa, se examinaron los espectros de estos mismos pacientes en las muestras de orina y se observó que se reproducía el mismo perfil metabólico que en las muestras de suero. La presencia de las señales de etanol no se pudo asociar con ninguna de las variables recogidas en la historia clínica, por lo que podría deberse a la ingesta. Debido a que uno de los criterios de recogida de las muestras era que debía hacerse en ayunas, estos pacientes fueron excluidos del análisis en ambos biofluidos. En cuanto a los pacientes que presentaban niveles anormalmente altos de glucosa, se examinó su historia clínica y se observó que todos ellos eran diabéticos. Para evitar que estas señales tan intensas pudieran interferir con otras señales del espectro, y debido a que uno de los criterios de inclusión era que los pacientes de CaP no debían presentar ninguna otra enfermedad, todos los pacientes diabéticos fueron excluidos del análisis tanto de suero como de orina.

Tras la exclusión justificada de los *outliers*, los análisis estadísticos multivariantes finalmente incluyeron 66 muestras de suero y 73 muestras de orina. En primer lugar, se utilizó el PCA, un método no supervisado, para evaluar el potencial impacto de las diferentes variables clínicas (edad, PSA, IMC, enfermedad metastática y GS) sobre la distribución de las muestras de suero y orina. En ninguno de los modelos construidos, se observó un impacto significativo de las variables clínicas estudiadas sobre la distribución de las muestras en el espacio. A continuación, se definió la clase (GS bajo vs GS alto) a la que pertenecía cada individuo, y se empleó el método supervisado de análisis discriminante de mínimos cuadrados con corrección ortogonal (OPLS-DA) como método de discriminación.

El modelo construido para cada biofluido reveló una capacidad reducida para la discriminación entre los grupos de estudio. A continuación, se evaluó la validez de ambos modelos mediante el test de permutación ($n = 100$). Para las muestras de suero, se observó que no había diferencias al comparar los valores estadísticos permutados con respecto a los valores obtenidos en el modelo real. Por otro lado, en la validación interna del modelo de orina, el valor estadístico R^2Y superaba los valores aconsejables, indicando que el modelo obtenido estaba sobreajustado, además de presentar una capacidad de predicción baja.

Con el fin de poder identificar diferencias metabólicas específicas entre los pacientes con GS bajo y alto, se realizó un análisis dirigido de los datos de RMN utilizando la información transcriptómica disponible en muestras de tejidos tumorales de CaP. Para ello, se llevó a cabo una búsqueda en el repositorio de GEO y se seleccionaron los estudios transcriptómicos que cumplieran con los siguientes criterios de selección: analizar muestras de CaP en tejido humano, analizar el perfil de expresión génica utilizando *microarrays*, incluir información disponible de la variable clínica de GS, y tamaño muestral mayor de 30 muestras. En los tres estudios en esta revisión (*gse16560*, *gse46602* y *gse70768*) se normalizaron los datos a escala logarítmica en base 2 (\log_2) cuando fue necesario y, en el caso de existir varias sondas para el mismo gen, se calculó la media de todas las sondas para obtener el valor más representativo. Adicionalmente, se evaluó la homogeneidad de las muestras mediante análisis no supervisado. A continuación, para cada gene, se calculó el *fold-change* (FC) entre los grupos de GS bajo y alto, y se utilizó el test no paramétrico de Mann-Whitney U para realizar un análisis de expresión diferencial entre ambos grupos. El FC y el p-valor obtenido del análisis de expresión diferencial se utilizaron para identificar rutas metabólicas alteradas entre los grupos de estudios mediante un análisis de enriquecimiento de genes centrado en genes relacionados con metabolismo. Para ello, se utilizaron las funciones incluidas en el paquete de R “*mdgsa*”, y se seleccionaron las rutas metabólicas que presentaban diferencias estadísticamente significativas ($p\text{-valor} < 0.05$).

En total, se identificaron 36 rutas significativamente alteradas entre los grupos de GS bajo y alto. A continuación, se identificaron los metabolitos involucrados en cada ruta y se asignaron las señales correspondientes en los espectros de RMN. En total, se identificaron 23 y 22 metabolitos en los espectros de suero y orina, respectivamente. Tras la

cuantificación de las señales, se llevó a cabo un análisis univariante utilizando el test de Mann-Whitney U para comparar las intensidades de cada metabolito entre los pacientes con GS bajo y alto. Este análisis reveló que, en comparación con los pacientes con GS bajo, el suero de los pacientes con GS alto presentaba concentraciones significativamente elevadas de glucosa y glicina, mientras que la orina de estos mismos pacientes exhibía niveles significativamente más altos de 1-metilnicotinamida. Además, en ambos biofluidos se observaron niveles más elevados de fenilalanina en los pacientes con GS alto, aunque en ningún caso las diferencias fueron estadísticamente significativas.

2. Caracterización de vulnerabilidades genéticas específicas en CaP avanzado

Para la caracterización de vulnerabilidades genéticas en CaP avanzado, se utilizaron los datos de cribados genéticos en 501 líneas celulares disponibles en la base de datos DepMap. En primer lugar, se seleccionaron los datos de las siete líneas celulares de CaP disponibles en la base de datos. A continuación, para cada gen analizado en cada una de las líneas celulares, se calculó el valor de esencialidad siguiendo una aproximación muy similar a la descrita por Hart *et al.* Brevemente, esta estrategia se basa en la utilización de una lista de referencia de genes clasificados como esenciales y no esenciales para la proliferación celular, a partir de la cuál, para cada gen, se calcula un clasificador bayesiano (factor bayesiano (FB)) que define la probabilidad de que un determinado gen pertenezca a la lista de genes esenciales ($FB > 0$) o no esenciales ($FB < 0$). Una vez clasificados, se normalizaron los valores de FB a Z-scores para ordenar los genes dentro de cada línea celular. Finalmente, se combinaron en una única lista todos los genes con un Z-score > 1.96 en alguna de las líneas celulares de CaP, y se seleccionaron aquellos genes clasificados como esenciales en al menos el 50% de las líneas de CaP analizadas. Siguiendo esta estrategia, se detectaron un total de 199 vulnerabilidades genéticas asociadas al CaP.

Para evaluar la relevancia terapéutica de estas vulnerabilidades genéticas, se analizó la expresión de los 199 genes en muestras de tejido de individuos sanos y de pacientes diagnosticados con diferentes estadios de CaP. Para ello, se realizó una revisión de los datos disponibles en el repositorio GEO y se seleccionaron los estudios transcriptómicos de CaP que cumplieran con los criterios de selección definidos: analizar muestras de tejido humano, analizar el perfil de expresión génica utilizando *microarrays*, incluir un tamaño muestral

mayor de 50 muestras, y analizar muestras de al menos dos de los grupos de estudio (tejido sano, CaP primario, CaP metastático). Otros criterios que también se tuvieron en cuenta para la selección de los estudios fueron la disponibilidad de datos relativos a la recurrencia de la enfermedad y la supervivencia del paciente. En base a estos criterios, se seleccionaron cinco estudios centrados en CaP (gse6919, gse35988, gse21035, gse10645 y gse46602). A continuación, los datos se normalizaron a escala logarítmica en base 2 (\log_2) cuando fue necesario y se evaluó la homogeneidad de las muestras en los distintos estudios. En el caso de existir varias sondas para el mismo gen, se calculó la media de todas las sondas para obtener el valor más representativo.

En base a los datos disponibles en cada estudio, se llevó a cabo el análisis de expresión diferencial para los 199 genes seleccionados entre: i) tejido sano *vs* CaP, ii) tumores indolentes *vs* agresivos, o iii) CaP primario *vs* metastático. En la segunda comparación se utilizó la variable clínica de recurrencia bioquímica (RB) para clasificar a los pacientes en el grupo de tumores indolentes (no RB) o tumores agresivos (RB). Para cada comparación, la significancia estadística de la expresión diferencial de cada gen entre los grupos de estudio se evaluó utilizando el test de Mann-Whitney U. Se utilizó el método de Benjamin-Hochberg para ajustar el p-valor, y se seleccionaron los genes con un p-valor ajustado < 0.05 como estadísticamente significativos.

Para la identificación de genes sobre-expresados en CaP con respecto a individuos sanos, se utilizaron dos de los estudios (gse6919 y gse35988). Tras el análisis de expresión diferencial entre los dos grupos, se determinó que 61 de los 199 genes definidos como esenciales en CaP estaban sobre-expresados de manera significativa en CaP en al menos uno de los estudios. La expresión de estos genes se evaluó entre tumores indolentes *vs* agresivos y entre CaP primario *vs* metastático. En la primera comparación, se utilizaron dos estudios (gse10645 y gse46602), y se identificaron 29 genes cuyos niveles de expresión eran significativamente más elevados en tumores agresivos en al menos uno de los estudios incluidos. Para la comparación de CaP primario *vs* metastático, se utilizaron tres estudios (gse6919, gse35988 y gse21035), y 17 genes fueron identificados como significativamente sobre-expresados en dos de los tres estudios analizados. En total, se seleccionaron 27 genes cuyos niveles de expresión eran significativamente más elevados en tumores agresivos o

metastáticos en al menos el 50% de los estudios evaluados, 5 de ellos estaban sobre-expresados en ambas condiciones.

A continuación, se evaluó la potencial correlación entre los niveles de expresión de cada uno de estos genes y la progresión del CaP en los pacientes. Para ello, se llevaron a cabo análisis de supervivencia utilizando el paquete de R “*survminer*”, que permite representar la estimación de la función de supervivencia (método de Kaplan-Meier). Se seleccionaron los cuartiles inferior y superior como puntos de corte, y los pacientes se clasificaron, según los niveles de expresión del gen a analizar, en el grupo de baja o alta expresión. La significancia estadística del análisis se determinó mediante la prueba de Matel-Cox (*log-rank test*). y se seleccionaron los genes con un p-valor < 0.05 como estadísticamente significativos. Este análisis reveló que, para 16 de los genes evaluados, una mayor expresión estaba significativamente asociada a un peor pronóstico en los pacientes de CaP.

Con el objetivo de evaluar potenciales interacciones entre los 16 genes seleccionados, así como su posible implicación funcional en el CaP, se utilizó la base de datos *Search Tool for the Retrieval of Interacting Genes* (STRING) para construir una red de interacción proteína-proteína. En este análisis se observó que existían interacciones entre 11 de las proteínas seleccionadas, y que algunos de los grupos estaban significativamente asociados a funciones biológicas concretas. El análisis funcional de la red reveló que tres procesos biológicos estaban sobre-representados: la formación del complejo de iniciación de la transducción citoplasmática, la iniciación de la traducción citoplasmática, y el ensamblaje de las ribonucleoproteínas nucleares pequeñas (snRNPs) del espliceosoma. De estas 11 proteínas, tres de ellas estaban directamente asociadas con los procesos de traducción (EIF2S3, EIF3B y EIF3H), y otras tres con el ensamblaje del espliceosoma (LSM4, PRPF3 y SNRPE). En base a estos resultados, estas seis proteínas fueron seleccionadas para continuar con su evaluación como posibles dianas terapéuticas para el desarrollo de nuevos fármacos en CaP.

En primer lugar, se evaluó la posibilidad de poder modular la actividad de estas proteínas utilizando pequeñas moléculas (*druggability*) utilizando la información disponible en las bases de datos Uniprot, Protein Data Bank, CanSAR y Pharos. Para cada

potencial diana terapéutica, se extrajo información relacionada con sus características biológicas, farmacológicas y estructurales. En particular, se determinó la disponibilidad de datos de estructura tridimensional, la presencia de potenciales sitios de unión en la estructura de la proteína, la existencia de inhibidores o ligandos conocidos, la localización subcelular, y la información disponible sobre su implicación en la progresión del CaP u otros cánceres. De acuerdo a la información recogida para cada una de las dianas implicadas en los procesos de traducción, se decidió evaluar el potencial de EIF3H como diana terapéutica para estadios avanzados del CaP. Por otro lado, LSM4 y SNRPE, relacionadas con el ensamblaje del espliceosoma, fueron seleccionados como candidatos preferentes para evaluar su posible papel como dianas terapéuticas en CaP en futuros análisis.

La subunidad H del factor 3 de iniciación de la traducción (EIF3H) es una de las 13 subunidades que forman el complejo EIF3, el cual está implicado en varios pasos del proceso de iniciación de la traducción. Esta subunidad se localiza en el citoplasma, tiene un peso molecular de 39.930 dalton y está constituida por una secuencia de 352 aminoácidos. Existe información disponible sobre 11 estructuras 3D de la proteína, determinadas por microscopía electrónica. Aunque no hay ningún inhibidor o ligando descrito contra EIF3H, la base de datos canSAR predice un potencial sitio de unión en su estructura en base al análisis de diferentes características. Esta subunidad contiene un dominio MPN que se encuentra en las proteínas metaloproteasas y que ha sido relacionado con funciones de ubiquitinación y deubiquitinación. De hecho, varios artículos han descrito que EIF3H tiene actividad deubiquitinasa favoreciendo a la estabilidad de proteínas implicadas en la promoción de la agresividad tumoral (ej. SNAIL, YAP). Además, la base de datos UbiBrowser 2.0 incluye una predicción de 7 proteínas como posibles sustratos de EIF3H.

En relación a los resultados obtenidos de los análisis de expresión diferencial en los datos de pacientes diagnosticados con CaP, se observó que *EIF3H* estaba sobre-expresado de manera significativa en CaP con respecto a tejidos sanos, así como en tumores agresivos y metastáticos en comparación con pacientes con tumores indolentes o primarios, respectivamente. Además, los análisis de supervivencia revelaron que una mayor expresión

de *EIF3H* se correlacionaba significativamente con un tiempo de RB más corto y con peor supervivencia global.

Con el objetivo de investigar en profundidad la implicación de *EIF3H* en la progresión del CaP, se utilizaron cuatro modelos celulares de próstata: uno representando la condición sana (RWPE-1), y tres líneas de CaP (22rv1, LnCaP y PC3) que difieren en su dependencia a andrógenos y su potencial metastático. En primer lugar, se extrajo RNA y proteínas de las cuatro líneas celulares, y se analizaron los niveles de expresión a nivel de RNA mensajero (mRNA), utilizando la técnica de RT-qPCR (*Quantitative Reverse Transcription Polymerase Chain Reaction*), y a nivel de proteína mediante el análisis por *western blot*. Los resultados obtenidos mostraron que las líneas de CaP presentaban niveles significativamente más elevados de mRNA y de proteína en comparación con la línea sana. A continuación, se generó un modelo estable de inhibición (*knock-down*) y de sobre-expresión de *EIF3H* en el modelo celular de PC3. Para la generación del modelo *knock-down*, se utilizó el plásmido pLV, con resistencia a puromicina, conteniendo dos RNA de interferencia dirigidos al silenciamiento de *EIF3H* (sh-2 y sh-4) y un RNA control (sh-C), mientras que para el modelo de sobre-expresión se utilizó el plásmido pLV, incluyendo la secuencia para la sobre-expresión para *EIF3H* (Myc-*EIF3H*). Ambos plásmidos contenían además la secuencia para expresar la proteína de fluorescencia verde (GFP) y poder así detectar la eficiencia de la transfección. Tras clonar y purificar los vectores correspondientes, se transfectaron las células HEK 293T junto con los vectores necesarios para generar lentivirus (Gag/Pol, Rev y VSV-G). La eficiencia de la transfección se evaluó por la detección de la expresión de GFP. Tras 48 horas, las partículas virales generadas se utilizaron para infectar las células PC3. A las 24 horas de la infección, se comprobó la expresión de GFP y se utilizó una dosis de 1 µg/mL de puromicina para seleccionar las células infectadas.

Para evaluar la eficiencia del silenciamiento y de la sobre-expresión del gen, se llevaron a cabo experimentos de RT-qPCR y *western blot*. Los resultados revelaron que el vector sh-4, en comparación con el vector sh-C, reducía en un 90% los niveles de mRNA y de proteína, respectivamente. En cuanto al vector de sobre-expresión, se observó que, con respecto al vector pLV, los niveles de mRNA eran 2.2 veces más elevados mientras que los niveles de proteína de *EIF3H* aumentaban en un 50%. A continuación, se evaluó el efecto

del silenciamiento y de la sobre-expresión de EIF3H en la proliferación, la eficiencia clonogénica, y la capacidad de migración de las células de CaP. Los resultados de estos experimentos demostraron que el silenciamiento de EIF3H reducía, de manera significativa, la proliferación, la capacidad clonogénica y la migración de las células PC3, mientras que la sobre-expresión de EIF3H favorece a la capacidad proliferativa, la capacidad clonogénica y de migración de las mismas células.

Debido a que las células necesitan realizar la transición epitelio-mesenquimal (EMT) para poder aumentar su capacidad de migración e invasión, se examinaron los cambios en niveles de proteína de algunos de los marcadores de la EMT tras el silenciamiento y sobre-expresión de EIF3H. Este análisis reveló que, mientras los niveles de E-cadherina aumentaban y que los de vimentina disminuían tras la inhibición de EIF3H, en el modelo de sobre-expresión se obtuvieron resultados opuestos, sugiriendo una posible implicación de EIF3H en la regulación de la EMT en las células de PC3.

Finalmente, en base a la actividad deubiquitinasa de EIF3H, se llevó a cabo un ensayo de co-inmunoprecipitación con el objetivo de identificar distintas proteínas cuya estabilidad pudiera estar siendo regulada por los cambios en la expresión de EIF3H y estar además implicadas en la progresión del CaP. Con este fin, se realizó una inmunoprecipitación de EIF3H en los extractos proteicos obtenidos a partir de células PC3 infectadas con los vectores pLV y Myc-EIF3H, respectivamente. Posteriormente, se analizaron mediante espectrometría de masas todas las proteínas contenidas en la fracción eluida junto con EIF3H. Entre las proteínas que aparecían en las tres réplicas que sobre-expresaban EIF3H y no lo hacían en las réplicas infectadas con el vector pLV, destacó Staufen 1 (STAU1) debido a su potencial implicación en el proceso de tumorigénesis.

STAU1 es una proteína de unión al ARN, implicada en varios procesos relevantes del metabolismo del ARN, cuya desregulación puede contribuir a la fisiopatología de varias enfermedades, entre ellas el cáncer. De hecho, distintos estudios han destacado su implicación en la promoción tumoral, y recientemente, se ha observado una posible implicación de STAU1 en la regulación del crecimiento, migración e invasión de modelos

celulares de CaP. Además, distintos estudios han mostrado como STAU1 puede ser ubiquitinada y degradada por el sistema ubiquitina-proteasoma (UPS). Dado que EIF3H ha sido descrita como una enzima deubiquitinasa, un posible efecto de la interacción directa observada podría ser la deubiquitinación de STAU1 por EIF3H, lo que podría contribuir a su estabilización, promoviendo así la progresión tumoral

Futuros experimentos irán dirigidos a confirmar esta hipótesis y comprobar si el efecto de EIF3H sobre la progresión del CaP está mediada por la estabilización de STAU1. En ese caso, STAU1 podría representar una buena diana terapéutica para el futuro desarrollo de fármacos. STAU1 es una proteína que se encuentra en el citoplasma, tiene un peso molecular de 63.182 dalton y una secuencia formada por 577 aminoácidos. Existen datos sobre 4 estructuras 3D disponibles con resoluciones por debajo de los 3.0 Å. En relación a los datos de expresión en pacientes con CaP, se observó que *STAU1* se encuentra sobre-expresada de manera significativa en CaP con respecto a individuos sanos, así como en tumores agresivos y metastáticos en comparación a pacientes con tumores indolentes o primarios, respectivamente. Además, los análisis de supervivencia revelaron que existe una correlación significativa entre una mayor expresión de *STAU1* y un valor de GS más elevado, así como con un tiempo de RB más corto.

CONCLUSIONES

1. El análisis combinado de datos transcriptómicos y metabolómicos representa una estrategia relevante para la caracterización de alteraciones metabólicas relacionadas con la progresión del CaP y la identificación de biomarcadores no invasivos, con potencial clínico para el manejo de pacientes de CaP.
2. Los cambios metabólicos observados en muestras de pacientes con CaP, revelan la existencia de alteraciones en la ruta de la síntesis de nucleótidos y en el metabolismo energético en los pacientes de CaP con GS alto.

3. A nivel transcriptómico, los pacientes con CaP con GS alto muestran un aumento de la biosíntesis de purinas unido a mayor actividad del ciclo del folato, y una reducción en el flujo de la glicólisis. Estas alteraciones se reflejan a nivel sistémico por niveles elevados de glicina y glucosa en suero, y concentraciones más altas de 1-metilnicotinamida en orina.
4. El análisis combinado de datos de esencialidad génica, basado en resultados de cribados funcionales, junto con resultados de análisis de expresión diferencial y correlación con la progresión de la enfermedad, representa un enfoque prometedor para caracterizar vulnerabilidades genéticas de gran valor para la identificación de nuevas dianas terapéuticas en pacientes con CaP avanzado.
5. Las vulnerabilidades genéticas asociadas a pacientes con CaP avanzado están principalmente relacionadas con procesos de iniciación de la traducción del ARN mensajero y el ensamblaje del espliceosoma.
6. EIF3H, LSM4 y SNRPE representan nuevas dianas terapéuticas con potencial para el desarrollo de nuevos fármacos para el tratamiento de pacientes con CaP avanzado.
7. Los cambios en la expresión de EIF3H están correlacionados significativamente con la proliferación celular, la capacidad de formación de colonias y la capacidad de migración en los modelos celulares de CaP evaluados.
8. Existe una correlación entre la expresión de EIF3H y los niveles de expresión de distintos marcadores de la transición EMT en los modelos celulares de CaP evaluados, sugiriendo una posible implicación de EIF3H en la progresión de la EMT.

I. INTRODUCTION

I.1. PROSTATE CANCER

I.1.1. Prostate cancer

Prostate cancer (PCa) is a malignant urologic disease triggered by the rapidly and uncontrollably growth rate of epithelial prostate cells, that finally leads to the development of a tumor. PCa is defined as a hormone-dependent cancer that requires the activation of the androgen receptor (AR) to survive and proliferate (Q. Yang et al., 2005). It is considered a multi-focal disease, with 60-90% of the patients presenting multiple distinct cancer foci within the prostate at the time of diagnosis (Andreoiu & Cheng, 2010). In addition, PCa is characterized by an extremely variable clinical course, ranging from patients showing an indolent condition with a slow progression rate, to others exhibiting an aggressive phenotype that rapidly disseminates and metastasizes to the lymph nodes and bones (Sathianathen et al., 2018).

Regarding PCa incidence, it is the second most frequent cancer and the fifth leading cause of cancer-related death in men worldwide, with an estimated of almost 1.5 million cases (7.3% of all cancers) and 374.000 cancer-related deaths (3.8% of all cancer deaths) in 2020 (Sung et al., 2021). Due to the growth and aging of global population, these numbers are expected to increase to approximately 2.4 million new cases and 740.000 deaths by 2040 (Ferlay et al., 2020). In Spain, according to the Spanish Society of Medical Oncology, PCa is expected to be the first diagnosed male cancer and the fourth cause of death, with more than 34.000 new cases and over 6.000 PCa-related deaths. In particular, Spain is the seventeenth European country in PCa incidence rate (70.6 per 100.000 population) and ninth European country with the lowest mortality rate (7.3) (Ferlay et al., 2020).

I.1.2. Diagnosis

An adequate PCa diagnosis is fundamental to provide a better clinical management of PCa patients and offer more precise and accurate treatment options. At early stages, PCa does not usually exhibit any symptoms, and the determination of the prostate specific antigen (PSA) serum levels and the digital rectal examination (DRE) are the two main screenings methods used for its early detection.

PSA is a glycoprotein, encoded by the *KLK3* gene, that is synthesized by epithelial prostate cells, and is then secreted into the ducts to be part of the seminal fluid. In normal prostate cells, PSA is mainly confined in the prostate gland and only small quantities are leaked into blood. However, during PCa development, there is a loss of basal cells and a disruption of the lumen architecture (Salman et al., 2015), that can cause the release of PSA into circulation, resulting in an increase of its serum levels. In general, a PSA level of 4 ng/ml is considered to be normal, but concentrations between 4 and 10 ng/ml are suspicious of PCa. When abnormal PSA levels are detected, a biopsy is required to confirm the presence of PCa (Hübner et al., 2018). Notably, the quantification of PSA levels as a screening method remains controversial as this test suffers from a number of limitations. In particular, as high PSA levels have also been detected in men diagnosed with benign prostatic hyperplasia (BPH), it exhibits poor specificity for the accurate diagnosis of PCa (Chistiakov et al., 2018). In this context, the low specificity of the PSA test has led not only to perform many unnecessary biopsies, but also to overtreat tumors with low malignant potential. Furthermore, it also presents low specificity for differentiating indolent from more aggressive tumors (Chistiakov et al., 2018). Consequently, depending on the study, PCa overdiagnosis and overtreatment account for over 30% to 80% of the cases (Etzioni et al., 2002; Postma & Schröder, 2005).

DRE consists in examining the surface of the peripheral zone of the prostate to detect changes in the texture of the prostate gland (Salman et al., 2015). Although palpable abnormalities during DRE are considered suspicious of PCa, regardless the PSA levels (Loeb & Catalona, 2009), this screening method also presents several limitations regarding its sensitivity and specificity for PCa detection (Cui et al., 2016; Jones et al., 2018; Philip et al., 2005).

When there is suspicion of PCa based on abnormal results provided by these two tests, a transrectal ultrasound (TRUS)-guided biopsy is performed to confirm the presence of a tumor. TRUS is the most used technique for sampling prostate tissue, and consists of inserting an ultrasound probe to take prostate images and to perform a needled biopsy for collecting between 10 to 12 prostate biopsies cores (Bjurlin & Taneja, 2014). Similar to the other tests, this procedure also has some disadvantages, including low sensitivity and

specificity that results in missing clinically significant cases on the initial biopsy (Fütterer et al., 2015; X. Wang, Bao, et al., 2018), or over-detecting clinically insignificant tumors leading to over-treatment (Boesen, 2019; F. K. Chen et al., 2016). Thus, repeated prostate biopsies, that may cause health discomforts such as haematospermia and bleeding, are normally performed (Kawachi et al., 2010). Furthermore, TRUS cannot differentiate between indolent and aggressive tumor tissues, finally resulting in misclassification of PCa patients (Harvey et al., 2012; Pokorny et al., 2014).

Besides these diagnostic strategies, imaging tools such as positron emission tomography (PET) and multiparametric magnetic resonance imaging (mpMRI), have emerged as promising approaches for PCa diagnosis. PET consists in introducing radiolabeled tracers into the patient to detect their location in the body. As this technique is based on the metabolic and molecular adaptations of cancer cells (e.g., increase glucose consumption or cellular membrane synthesis), the tracer selection depends on the metabolic characteristics of each tumor. Among the most widely used tracers are ^{18}F -fluorodeoxyglucose, ^{11}C -acetate, ^{11}C -choline and ^{18}F -fluorocholine. Despite the established role of PET in the clinical practice, this approach still presents some limitations, including limited availability and short half-life of some radiotracers, poor imaging resolution, and inability to distinguish tumors from non-malignant hypermetabolic processes (D. R. Schmidt et al., 2021). On the other hand, mpMRI combines three different MRI sequences (T2-weighted image, diffusion-weighted imaging and dynamic contrast-enhanced) to characterize the tumor in the prostate. Notably, radiomic features have emerged as promising tools for defining different cancer subtypes (Z. Liu et al., 2019). However, although this strategy may improve the detection and localization of primary PCa, some improvements have to be made, with a particular focus on clinical interpretation (M. Li et al., 2021) and optimization of the Prostate Imaging Reporting and Data System (PI-RADS) (Sosnowski et al., 2016). Moreover, other omics technologies, such as genomics, epigenomics or transcriptomics, have demonstrated their potential in the definition of specific molecular tumor subgroups, that may improve patient classification according to disease aggressiveness and guide in treatment decision-making (Meng et al., 2021; Q.-H. Nguyen et al., 2020; Qi et al., 2021; H. Zhang et al., 2018), therefore, achieving a more personalized medicine.

Early detection of PCa is essential as the 5-year survival rate for PCa patients drops from 100% when the diagnosis is performed at early stages, to 30% when patients are diagnosed with a tumor that has disseminated to other organs (Cancer.Net, 2012). Nevertheless, although some advances have been made to improve survival and life quality of these patients, there remain some limitations that need to be overcome in the management of PCa patients, mainly those related to accuracy of early diagnosis, risk stratification, and treatment of advanced disease.

I.1.3. Tumor staging

Histological evaluation of tumor tissues is important to evaluate the grade of tumor development and its prognosis (Gordetsky & Epstein, 2016; Hoogland et al., 2014). In PCa, the histological evaluation is assessed based on the Gleason Score (GS) system, that determines the tumor aggressiveness and its metastatic potential using predefined histological patterns. The GS system was developed by Donald Gleason in 1960 (Gleason & Mellinger, 1974), and is currently considered one of the most powerful prognostic predictors in PCa and a relevant criterion for tumor staging, prognosis and treatment selection.

However, despite the efforts made to improve grading accuracy, the system still suffers from several limitations, including variability when assigning the GS due to the higher complexity of the system (Gordetsky & Epstein, 2016). Thus, in an attempt to improve PCa grading, a new grading system, known as the International Society of Urological Pathology (ISUP) grade group was proposed in 2013 (Pierorazio et al., 2013). This system defines five grade groups that accurately reflect tumor prognosis and provide an outcome that can be more easily interpreted by clinicians and patients (Epstein, et al., 2016). Thus, in 2016, the ISUP groups were incorporated into the World Health Organization, and were recommended as a classification system, in combination with other clinical variables, due to its higher potential in predicting the risk of potentially lethal PCa (Epstein, Zelefsky, et al., 2016; Epstein, 2016; Ross et al., 2012). Based on the grade group system, tumors are classified as low risk (ISUP grade 1), intermediate risk (ISUP grade 2 or 3), and high risk (ISUP grade > 3), and these categories are used to guide the clinical management of PCa patients (Mottet et al., 2017).

Notably, the individual introduction of the \leq G D may oversimplify the complexity of the system and lead to lose relevant prognostic information required for decision making (Pierorazio et al., 2013). Thus, to avoid this problem and accurately reflect the PCa biology, it is recommended to combine the \leq G D with the GS system (Epstein, Egevad, et al., 2016; Epstein, Zelefsky, et al., 2016; Pierorazio et al., 2013) (Figure 1).

		Gleason score	ISUP grade group	Characteristics
Well differentiated ↓ Moderately differentiated ↓ Poorly differentiated ↓	Gleason pattern 1 2 3 4 5	$GS \leq 6$	1	Only individual discrete well-formed glands.
		$GS = 7 (3+4)$	2	Predominantly well-formed glands with lesser component of poorly-formed/fused/cirriiform glands.
		$GS = 7 (4+3)$	3	Predominantly poorly-formed/fused/cirriiform glands with lesser component of well-formed glands.
		$GS = 8 (4+4, 5+3, 3+5)$	4	i) Only poorly-formed/fused/cirriiform glands, ii) Predominantly well-formed glands and lesser component lacking glands, or iii) Predominantly lacking glands and lesser component of well-formed glands.
		$GS \geq 9$	5	Lacks gland formations (or with necrosis) with or without poorly-formed/fused/cirriiform glands.

Figure 1. Definition of histological patterns used to determine the ISUP Grade Group based on the Gleason Scores. Lower values represent more favorable tumors. Adapted from Epstein et al., 2016.

Together with histopathological tumor grading, the tumor, node, metastasis (TNM) staging system, that determines tumor location and spreading, is also employed to aid in PCa clinical decision-making (Buyyounouski et al., 2017). If the tumor is located within the prostate gland it is defined as an organ-confined PCa, but when the tumor has spread or metastasized to any other part of the body, it is defined as metastatic PCa.

I.1.4. Treatment

Accurate clinical management of PCa accounts for different factors, including clinical features at different tumor stages (localized, advanced or metastatic stage, and castration-sensitive or castration-resistant disease), histopathological and molecular traits, and patient-related characteristics (age, comorbidities, life expectancy, overall health, family history and preferences) (Rebello et al., 2021). However, as diagnostic tests are not accurate enough to differentiate low- from high-risk phenotypes, treatment is frequently similar in both cases. Consequently, indolent tumors tend to be overtreated and patients have worse quality of life due to the side effects caused by such aggressive treatments.

1.1.4.1. Localized PCa

Particularly, for localized PCa tumors, therapeutic options involve expectant management (mainly through active surveillance (AS)), and radical local treatments (radiation or radical prostatectomy (RP)) with or without androgen deprivation therapy (ADT). Given that PCa is highly dependent on androgens, that bind to the androgen receptor (AR) and subsequently regulate the expression of genes involved in tumorigenesis processes (Lamb et al., 2014), ADT aims at reducing circulating these hormone levels to prevent cancer growth. In general, ADT can be achieved with surgical (orchiectomy) or chemical castration (e.g., agonists or antagonists of the luteinizing hormone-releasing hormone).

Importantly, the optimal management for men with localized disease remains controversial (Parker et al., 2020). In order to evaluate tumor staging and guide treatment decision (D'Amico et al., 1998; Mottet et al., 2017), patients are stratified into different risk groups based on the risk of biochemical recurrence (BCR), that is defined by two consecutive rising PSA levels > 0.2 ng/mL following RP (Cookson et al., 2007; Cornford et al., 2017), or PSA value ≥ 2 ng/ml above the PSA nadir after radiotherapy (Roach et al., 2006). One of the most commonly used classifications for risk-stratification of PCa patients is the one proposed by the National Comprehensive Cancer Network, combines serum PSA levels, ISUP grade groups and clinical T category from the TNM system. Thus, patients are classified into low risk (PSA < 10 ng/ml, T1-T2a and ISUP grade 1), intermediate risk (PSA > 10 -20 ng/ml, T2b, and ISUP grade 2 or 3), and high risk (PSA > 20 ng/ml, \geq T2c, and ISUP grade > 3) groups (Mohler et al., 2019). As showed in Figure 2 treatment options vary between these groups, ranging from minimal intervention to more aggressive therapeutic strategies for high-risk tumors.

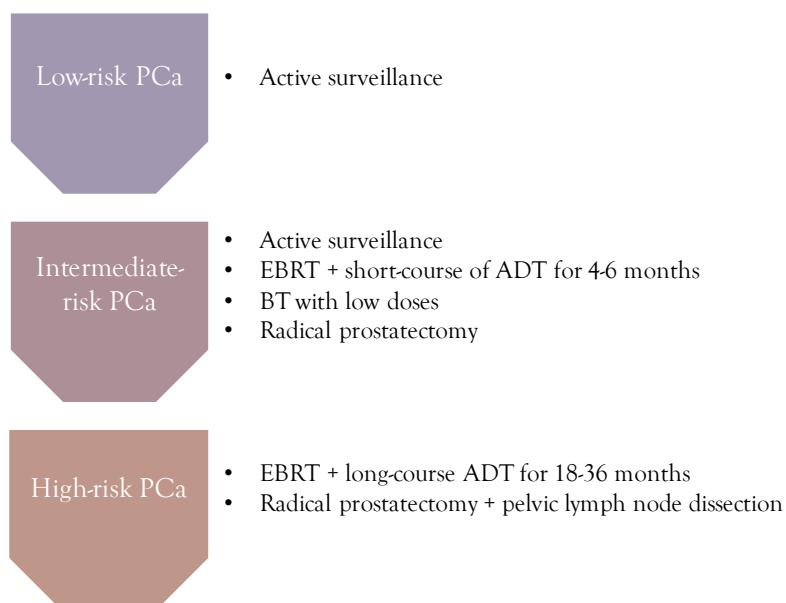


Figure 2. Therapeutic strategies for localized tumors based on the risk of the PCa progression. ADT: androgen deprivation therapy, BT: brachytherapy, EBRT: external beam radiation therapy.

Patients with low-risk tumors are generally followed by AS as first option (Parker et al., 2020). AS aims at monitoring patient progression, allowing for early intervention if the tumor progresses, and involves DRE examinations, PSA levels monitoring and repeated biopsies. This strategy has shown promising results in terms of minimizing overdiagnoses (Dall’Era et al., 2012), and avoiding overtreatment and unwanted side effects (Mahal et al., 2019). In addition, several studies have reported that patients monitored with AS have similar clinical outcomes than those with immediate definitive treatment (Dall’Era et al., 2012; Iremashvili et al., 2012).

For patients diagnosed with intermediate-risk, disease therapeutic options rely on local treatments to remove cancer from a specific part of the body (Parker et al., 2020). Radiation is a therapeutic strategy that can be administrated using either brachytherapy (BT) or external beam radiation therapy (EBRT). BT relies on placing radioactive sources within the prostate gland to deliver a maximum dose of radiation to the prostate, and minimizing radiation to the surroundings tissues. On the other hand, EBRT is based on delivering targeted radiation beams to a specific part of the body and can be administrated in any tumor stage. BT should be administrated with low doses, while EBRT should be combined with a short-course of ADT for 4-6 months (Parker et al., 2020). Another local

therapy is RP, a surgical approach that consists in removing the entire prostate gland and tissue around it. RP is the most common therapeutic option for patients younger than 70 years, with low- or intermediate-risk PCa, with a life expectancy greater than 10 years and no or minimal comorbidities (Keyes et al., 2013).

Men diagnosed with high-risk PCa have higher risk of rapid progression and of metastatic disease, therefore, more aggressive therapies are recommended, including EBRT combined with a long-course of ADT (for 18-36 months) or RP combined with pelvic lymph node dissection (Parker et al., 2020).

1.1.4.2. Advanced PCa

This stage represents the most lethal form of PCa, and patients are generally treated according to the tumor sensitivity to androgen-based therapies. Currently, ADT combined with different therapies, including EBRT, AR-targeting drugs and chemotherapy, have showed improved clinical outcomes for patients with metastatic hormone-dependent tumors and suitable for taking these treatments (reviewed in Rebello et al., 2021).

Notably, despite most patients initially respond well to ADT, testosterone suppression can only be controlled for an average of 18-36 months until BCR occurs. This can be explained by the intratumour heterogeneity of PCa. As tumor cells may exhibit varying degrees of androgen sensitivity (Klotz & Toren, 2012), some cell populations may become resistant to ADT and, therefore, androgen suppression may no longer be effective to stop cancer cell proliferation (Ceder et al., 2016) in these patients. In this context, over 10-20% of PCa patients will finally develop a new cancer phenotype known as castration resistant prostate cancer (CRPC) (Gravis et al., 2016; Heidenreich et al., 2014; Lam et al., 2006; Petrylak et al., 2004), that has a median survival rate of approximately 14 months (Ritch & Cookson, 2016).

Although the underlying mechanisms of castration resistance development are not well understood, ADT usually leads to molecular alterations of the AR that may contribute to resistance to androgen therapy. Genetic changes involve AR over-expression by gene amplification (Chan & Dehm, 2014), activating AR mutations (Robins, 2012), and post-

translational mutations that increase AR sensitivity to androgens (van der Steen et al., 2013). In addition, other AR-independent signaling pathways, including activation of kinases (J. M. Drake et al., 2013) or of steroid receptor pathways (Arora et al., 2013), may also be involved in PCa progression.

Given that AR signaling remains activated, the AR remains an important target in CRPC phenotype (Azzouni & Mohler, 2012; Y. Chen et al., 2009). In this context, androgen pathway inhibitors such as abiraterone, a CYP17A1 inhibitor that blocks androgen biosynthesis in the adrenal glands, tumor cells and testis, or enzalutamide, an AR antagonist that inhibits androgens binding to the AR, have improved survival outcome in these patients (Sridhar et al., 2014). For patients that have developed metastatic disease (mCRPC), docetaxel, a chemotherapy agent, have showed beneficial effect in life quality and overall survival of mCRPC patients (Petrylak et al., 2004; Tannock et al., 2004). Notably, androgen pathway inhibitors are recommended in patients with mCRPC after docetaxel administration (Parker et al., 2020). For those tumors that have metastasized to the bone, immunotherapy and bone-targeted (e.g., Sipeleucel-T, denosumab and ^{223}Ra) are recommended (Parker et al., 2020). Finally, tumors harboring mutations in genes related to DNA repair mechanisms (e.g., *BRCA1* or *BRCA2*) may benefit from genome-targeted strategies such as PARP inhibitors (Hussain et al., 2020).

As each therapeutic option has its own strengths and limitations (e.g., more localized administration, higher costs or worse side effects profiles), it is crucial to identify which patients are more likely to benefit from a specific treatment. Although, all these therapeutic strategies aim to increase overall survival and improve quality of life of PCa patients at advanced stages, CRPC remains incurable, exhibits poor prognosis and, for those patients that have developed mCRPC, the expected average survival time is of 18-20 months (Fizazi et al., 2012; Karantanos et al., 2013; Scher et al., 2012).

I.1.5. Molecular subtypes

Although pathological grading continues to be used as the gold prognostic system for risk stratification, the classification of PCa patients into low- and high-risk groups is not accurate enough due to the high degree of clinical heterogeneity. As similarly graded

tumors can have very variable clinical outcomes, it is important to better understand the high heterogeneity in genomic and molecular features that define each tumor in order to improve patient stratification and help in treatment selection. In this context, the emergence of high-throughput sequencing technologies can provide a detailed genomic profiling and better define specific tumor subtypes based on genomic and molecular alterations. The characterization of such molecular subgroups may allow to precisely identify high-risk tumors harboring specific genetic alterations and potentially identify novel candidates for the development of new therapeutic strategies.

In the PCa field, genome-wide sequencing of primary tumors has revealed seven major molecular subgroups, represented in Figure 3, that allow to classify over 75% of all cases (Cancer Genome Atlas Research Network, 2015). These subtypes are grouped into two main categories, that are defined by the presence or absence of translocations between androgen-regulated genes and the ETS family of transcription factors. Depending on the ETS gene involved in the rearrangement, tumors positive for a genetic translocation can be divided into four subclasses: i) TMPRSS2:ERG, ii) TMPRSS2:ETV1, iii) TMPRSS2:ETV4, and iv) TMPRSS2:FLI1. On the other hand, negative ETS genetic subtypes can be classified into three categories based on the presence of point mutations in *SPOP*, *FOXA1* or *IDH1* genes.

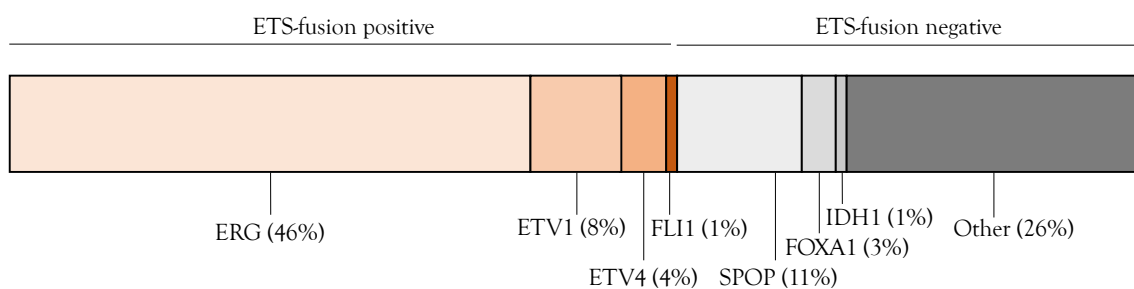


Figure 3. Representation of the most common genetic alterations identified in localized PCa. Adapted from Christenson et al., 2022.

Molecular characterization of the genomic landscape has also identified genomic alterations specifically associated with the prognosis of the disease, that may contribute to improve stratification of PCa patients. For instance, ETS-fusion positive tumors frequently

harbor alterations in *PTEN* (Cancer Genome Atlas Research Network, 2015; Robinson et al., 2015), and deletions of this gene are correlated with greater GS, worse prognosis and higher metastatic rate (Pourmand et al., 2007; Taylor et al., 2010). In addition, overexpression of *SPINK1* is restricted to ETS-negative phenotypes, and is associated with aggressiveness and recurrence after RP (Brooks et al., 2015; Tomlins et al., 2008). Furthermore, SPOP and FOXA1 mutant tumors exhibit higher AR activity (Geng et al., 2013), and SPOP-mutated subtypes are more sensitive to therapeutic strategies based on PARP inhibitors (Boysen et al., 2015).

Genomic studies have also been extended to the metastatic PCa phenotype, showing a similar subgroup distribution as primary tumors, but with some specific molecular features. In particular, SPOP mutations are mainly restricted to localized PCa, and the IDH1 group is absent in mCRPC phenotypes (Fraser & Rouette, 2019). Furthermore, mCRPC tumors exhibit higher AR activity, mainly due to gene amplifications or mutations, that has been associated with the development of castration-resistant and resistance to hormone therapy (Antonarakis et al., 2014; Henzler et al., 2016). In addition, mCRPC tumors also present alterations in DNA repair genes (e.g., *BRCA2*, *BRCA1* and *ATM*), making them more sensitive to DNA damaging agents like PARP inhibitors (Cheng et al., 2016; Mateo et al., 2015).

Notably, genomic technologies have not only contributed to define specific PCa genomic subtypes, but also to identify molecular alterations that may be used as molecular markers for early detection, disease stratification and prediction of treatment response, resulting in more personalized medicine approaches. As shown in Table 1, the use of different analytical approaches has given rise to a wide range of diagnostic, prognostic and predictive biomarker tests with potential applicability in the clinical practice (reviewed in Frantzi et al., 2020). However, despite many molecular markers have been developed for PCa management, only a few (e.g., PSA, PC3) have been approved by the Food and Drug Administration to be used in the clinic.

Table 1. Overview of commercially available PCa biomarker tests. Adapted from Frantzi et al., 2020

Biomarker test	Omics Markers	Molecular Feature	Assay Method	Specimen Type	Clinical Application
4k score	4 kallikreins	Proteins	Immunoassay	Serum	Diagnostic
STHLM3 nomogram	PSA, free PSA, intact PSA, KLK2, MSMB, MIC1, 232 SNPs, age, family history, DRE	SNPs	PSA immunoassays and SNP genotyping	Serum	Diagnostic
AR-V7	AR-V7	CTCs	RT-PCR, ddPCR	Serum	Predictive
Confirm MDx	GSTP1, APC, RASSF	Methylation	Multiplex PCR	Tissue	Diagnostic
OncotypeDx	12 cancer-related and 5 reference genes	mRNAs	RT-PCR	Tissue	Diagnostic Prognostic
DNA repair genes	BRCA1, BRCA2 or ATM	DNA	NGS	Tissue	Predictive
Decipher	22 coding and non-protein coding regions	mRNAs	Affymetrix microarrays	Tissue	Prognostic
Prolaris	31 cell cycle progression and 15 reference genes	mRNAs	RT-PCR	Tissue	Prognostic
SChLAP1	SChLAP1	lnc RNA	Microarray hybridization	Tissue	Prognostic
Select MDx	HOXC6 and DLX1	mRNAs	RT-PCR	Urine	Diagnostic
ExoDX	PCA3, ERG and SPDEF	Exosomal mRNAs and lnc RNA	RT-PCR	Urine	Diagnostic
ProgenSA PCA3	PCA3	lnc RNA	RT-PCR	Urine	Diagnostic
MiProstate (mips)	TMPRSS2-ERG and PCA3	Gene fusion and lnc RNA	RT-PCR	Urine	Diagnostic

I.1.6. Current challenges in the landscape of PCa

As stated in previous sections, PCa is defined as a biologically heterogeneous disease characterized by a highly variable clinical course. Notably, depending on the time of diagnosis, patients' survival significantly increases when the tumor is diagnosed at early stages. Optimal management of PCa patients remains challenging due to the difficulties in

accurately predicting and discriminating indolent patients from those that may develop aggressive and metastatic progression. Currently clinical available prognostic methods mainly rely on the histopathological evaluation of biopsies, graded on the basis of the GS system. Although it suffers from a number of limitations, the GS system remains to be the best clinical variable to determine tumor aggressiveness and metastatic potential. Notably, omics technologies have contributed to molecularly characterize the landscape of certain tumors and to develop novel biomarkers for discriminating between indolent and aggressive tumor subtypes. Nevertheless, despite the great advances made in biomarker discovery, very few are actually being used in the clinical practice, and there is still a need for more precise and robust biomarkers to improve the diagnosis and risk stratification of PCa patients.

On the other hand, despite the efforts made in developing new therapeutic strategies for PCa treatment, the disease remains incurable when it progresses to more aggressive stages. ADT is the common treatment option for men diagnosed with hormone-sensitive tumors. This is an effective strategy that improves prognosis and symptoms, but it can only control the tumor for 18-36 months before it progresses to a CRPC phenotype (Sanhueza & Kohli, 2018). Although there exists a wide range of different approved therapeutic strategies (i.e., chemo- and hormone-therapy, radium-223, sipuleucel-T) to treat CRPC and mCRPC and extend patients' life time, these agents provide small survival benefits and the disease still presents an unfavorable prognosis. Thus, the development of new treatments to avoid the unwanted side-effects caused by currently available therapies, increase the overall survival rate and improve life quality of patients diagnosed with aggressive PCa tumors is highly needed. In this context, the identification of molecular tumor alterations using omics-based approaches could improve treatment selection and contribute to the development of more specific therapeutic strategies.

I.2. OMICS TECHNOLOGIES IN CANCER

The tumorigenesis process involves the acquisition of genomic changes that promote the transformation of a healthy human cell into a tumor cell. Although there are more than 100 different types of tumors, they all share commonalities that need to be acquired by any cancerous cell during tumor development. These molecular changes were

first grouped by Hanahan & Weinberg into six distinct hallmark capabilities (Hanahan & Weinberg, 2000), and were later expanded to ten (Hanahan & Weinberg, 2011). Among the described essential characteristics are sustaining proliferative signaling, avoiding immune destruction, genome stability and mutation, and deregulating cellular metabolism. In a third revision, four more capabilities, known as emerging hallmarks related to tumor plasticity and reprogramming, senescent cells and polymorphic microbiomes (Hanahan, 2022), have been proposed and incorporated into the set of cancer hallmarks (Figure 4).

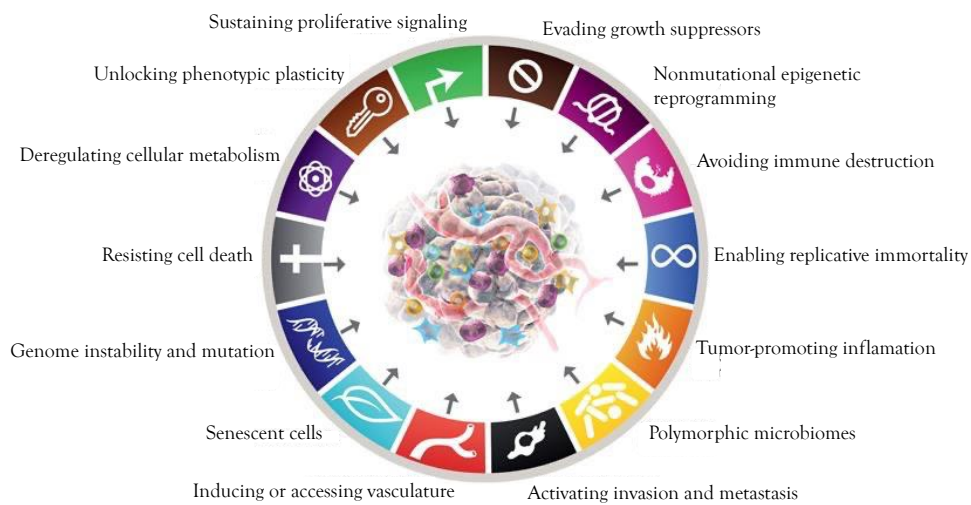


Figure 4. Capabilities and characteristics that facilitate the transformation of normal cells into a neoplastic condition. From Hanahan, 2022

Omics technologies are defined as high-throughput strategies that allow to simultaneously study and analyze large numbers of small molecules such as genes, RNA, proteins or metabolites, among others. The advances made during the last decades in omics profiling techniques and big data analysis have enabled the development and progression of several research areas, including the well-known genomics, transcriptomics, proteomics and metabolomics fields (Figure 5). Recently, other omics technologies, such as lipidomics, metagenomics, glycomics and radiomics, have emerged as complementary strategies to contribute to the detailed characterization of biological systems (Banerjee et al., 2015; R. R. Drake, 2015; Shur et al., 2021; K. Yang & Han, 2016).

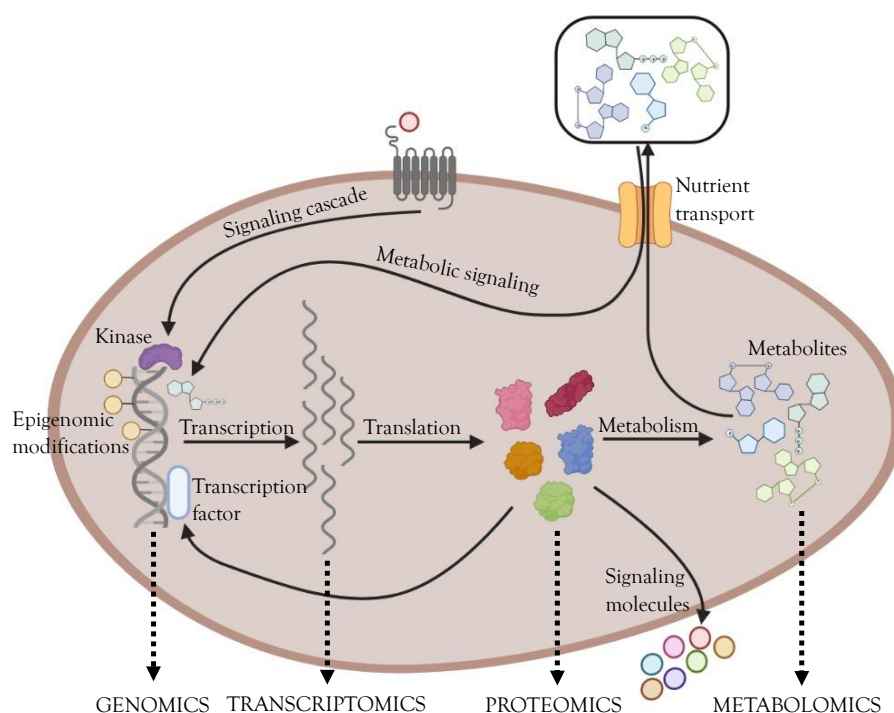


Figure 5. Overview of the relationship between omics technologies. Changes at the genomic level result in altered mRNA transcription and protein expression and activity, that are finally reflected in the metabolome composition. Metabolic dysregulations also affect DNA replication, RNA transcription and protein function. Adapted from Schmidt et al., 2021.

Genomics aims at studying the entire genome of a certain organism using DNA sequencing technologies. In the human body, the genome contains over 3 billion DNA base pairs, and it is estimated that each of the approximately 25,000 genes codes for an average of three proteins. In the oncology area, DNA sequence is mainly applied for the identification of cancer-specific mutations and for the analysis of chromosomal rearrangements that may allow to define different cancer subtypes (Olivier et al., 2019). This technology has enabled the development of different gene panels, summarized in Table 1, and the identification of other genes that may be used as biomarkers for tumor aggressiveness and/or predicting treatment response (Graf et al., 2022; Jamaspishvili et al., 2018; Joseph et al., 2013).

The transcriptomics field is focused on analyzing the expression of all genes present in an organism to reveal differences in their expression by measuring the levels of mRNA transcripts. There are several strategies available to study gene expression, such as

microarrays and RNA sequencing, that have generated large amounts of data deposited in public domain repositories. The Gene Expression Omnibus (GEO) is a well-known public repository that stores more than 4.300 high-throughput datasets from microarray and RNA sequencing analyses. The detection of changes in gene expression may be used to gain deeper knowledge of the molecular processes underlying the development and progression of a specific disease. In addition, the identification of alterations in gene expression levels can contribute to develop gene signatures for predicting patient outcome, prognosis, recurrence risk or treatment response (Olivier et al., 2019). By measuring gene expression levels, a number of studies have identified promising biomarkers associated with PCa progression (Sandsmark et al., 2017; N. Xu et al., 2020; Yi et al., 2018), and others have characterized potential drug targets (Vainio et al., 2012; P. Zhang et al., 2022).

Proteomics involves the analysis of cellular proteins present in an organism, including their structure, physiological roles and functions. For the identification and quantification of proteins, mass spectroscopy (MS) and affinity-based protein arrays methodologies are frequently used. Furthermore, complementary approaches such as nuclear magnetic resonance (NMR) and X-ray crystallography can provide information on protein structure. In the cancer field, proteomics has focused on characterizing changes in protein levels between healthy individuals and patients to identify potential biomarkers or drug targets, predicting drug sensitivity and performing drug resistance analysis to detect putative proteins (Olivier et al., 2019; K.-H. Yu & Snyder, 2016). Several studies have applied proteomics for the identification of potential protein biomarkers for PCa diagnosis and/or prognosis (Alaiya et al., 2011; Davaliev et al., 2015; Geisler et al., 2015; Iglesias-Gato et al., 2016), and for the development of therapeutic strategies (Endoh et al., 2012; Khamis et al., 2010; Sugie et al., 2015; Ummanni et al., 2011).

Finally, metabolomics is based on the systemic measurement of all metabolites, defined as low molecular weight compounds (≤ 1500 Da), that are present in a biological sample such as a cell, a tissue or an organism. Metabolites include amino acids, carbohydrates, organic acids, vitamins, lipids or drugs, among others. An important concept of this field is that the synthesis of metabolites is the downstream of the biological processes, which ranges from genome to transcriptome, to proteasome and finally to

metabolome. Thus, metabolomics provides a final overview of the functional genetic status of an organism, and allows to understand the relationships between metabolic changes, related biochemical pathways, and gene functions (Lajis et al., 2017). In the cancer research, oncology-based metabolomics studies are mainly focused on detecting metabolic differences between normal and cancer phenotypes and between stages of a specific health condition, or monitoring patient's response to a treatment. Metabolomics has greatly contributed to the identification of biomarkers that can potentially be used for the diagnosis and prognosis of PCa (Fujita et al., 2017; Kumar et al., 2016; Pérez-Rambla et al., 2017; J. A. Schmidt et al., 2017).

Particularly, in the oncology field, different omics-based approaches have shown great potential for the development of novel targeted therapies (Hoang et al., 2019; Luo et al., 2019; Sun et al., 2019; von Rundstedt et al., 2016), as well as for the identification of non-invasive diagnostic and prognostic biomarkers valuable for the early diagnosis of cancer and for predicting the course of the disease, respectively.

1.2.1. Omics technologies for the identification of new therapeutic targets

1.2.1.1. Definition and characteristics of a drug target

A druggable target is defined as a protein that plays an important role in the pathophysiology of a disease, and whose activity can be modulated by a drug, including a small molecular weight chemical compound (e.g., inhibitors, agonists, etc.) or a biologic (e.g., antibodies, recombinant proteins, etc.) (Gashaw et al., 2012). This type of proteins can be identified by analyzing gene and/or protein expression profiling, in target tumor tissues (comparing different cancer stages) or comparing healthy against disease tissues (Narayan et al., 2016; Wei et al., 2016; N. Xu et al., 2020), or by assessing gene essentiality in different cellular models (Behan et al., 2019; Cowley et al., 2014; Hart et al., 2014; Meyers et al., 2017; Tsherniak et al., 2017). A relevant aspect to consider is to know whether the selected candidates are context-specific or core fitness genes. Core fitness or pan-cancer genes are required for cell fitness in multiple normal tissues or cell types, while context-specific genes play important roles in cell proliferation but only in a specific molecular context or cancer type (Behan et al., 2019; Chang et al., 2021). As core fitness vulnerabilities are commonly identified in the majority of tested cell lines, these genes are

more likely to be involved in essential processes and may have greater non-selective toxic effects and low therapeutic index (Behan et al., 2019; Chang et al., 2021). Thus, context-specific candidates are more likely to be selected as promising drug targets as they show lower potential of inducing toxic effects in healthy tissues (Behan et al., 2019).

In addition, assessment of the target tractability or druggability can also contribute to identify the most promising targets that may be amenable to interactions. In this context, there are several characteristics that can provide further evidence about the likelihood that a target may interact with small molecules. For instance, drug targets with known crystalized 3D structure are advantageous over others, as it may help to predict potential binding sites by analyzing their structural properties (e.g., size, shape, protein atoms exposed to interactions) (Brown et al., 2018; Gashaw et al., 2012). Moreover, previously available bioactivity data on the candidate protein is also a key feature and it can allow to early determine whether the target can be effectively modulated by chemical compounds (Brown et al., 2018). Finally, protein cellular location is also an important aspect to consider, as many biopharmaceutical approaches require the target to be cell surface exposed or secreted (Brown et al., 2018).

1.2.1.2. Genetic screening

Gene modulation or perturbation aims at studying and understanding biological functions of genes and identifying essential molecular processes that occur during cell growth (Hart et al., 2014). Notably, this type of studies enables the identification of genes that are essential for cell fitness. Thus, a genetic dependency can be defined as a gene that is required for cell proliferation or survival, and its ablation or inhibition will result in a complete loss of cell viability (Lin & Sheltzer, 2020; Tsherniak et al., 2017).

In particular, one approach to uncover genetic cancer dependencies is to perform loss-of-functions (LOF) screens (Figure 6) across a wide variety of well-characterized cancer cells lines reflecting molecular tumor heterogeneity (Tsherniak et al., 2017). In these studies, a mixture of reagents is randomly integrated in individual cells and only one gene is targeted in each generated cell clone (Boettcher & Hoheisel, 2010). Two different types of reagents are employed in LOF experiments: RNA interference (RNAi), mediated by

short interfering RNAs (siRNAs) that are frequently obtained from small hairpin RNA (shRNA) precursors, and Clustered Regularly Interspaced Short Palindromic Repeat (CRISPR). Notably, LOF screening requires a library of reagents that are designed *in-silico* and are then cloned to generate a plasmid library for virus production and screening (Shalem et al., 2015). A low multiplicity of infection is used to ensure that each cell is targeted by only one reagent (J. Liu & Li, 2019). Once reagents are introduced into cells, either positive or negative selections are applied to select the population exhibiting the phenotype of interest. Among these two strategies, negative selection screens aim at discovering genetic alterations that cause cell loss of fitness and may be further selected for drug-targeting purposes. Monitoring cell growth over time is the simplest method for negative phenotype selection.

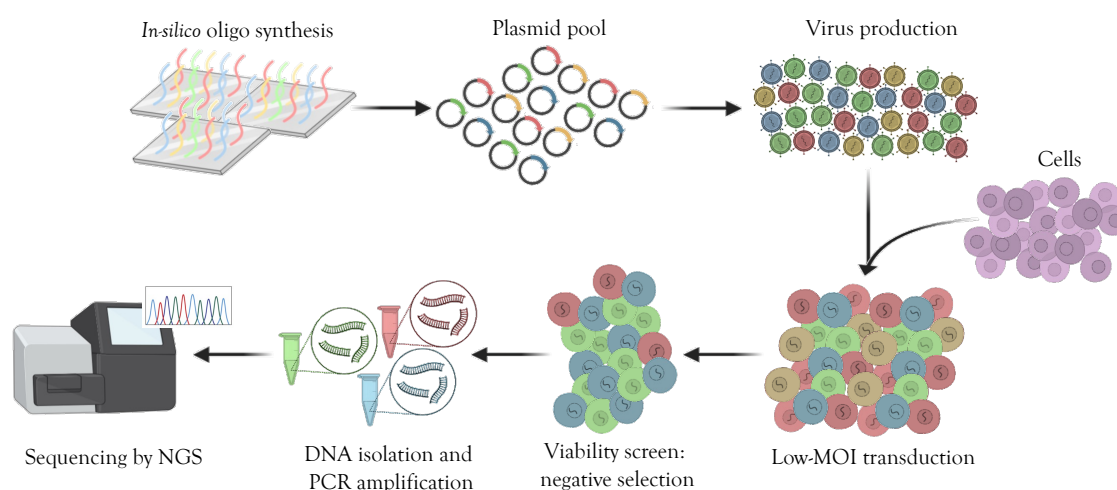


Figure 6. Overview of the basic workflow followed in a LOF genetic screen.

After phenotypic selection, DNA is extracted from the cell population of interest and reagents targeting each gene are amplified through polymerase chain reaction by deep sequencing. Since each reagent has a gene-specific fingerprint, known as the molecular barcode (Brummelkamp & Bernards, 2003), they can be easily identified by mapping the raw sequencing reads against the original reagent library containing the annotation to its corresponding target gene (Agrotis & Ketteler, 2015; Shalem et al., 2015). In general, as each reagent is sequenced at different times during the experiment (e.g., at the beginning and end of the screening), the detection of enriched/depleted reagents is performed by comparing their frequencies along time.

1.2.1.3. Identification of genetic vulnerabilities

Different computational approaches have been developed to characterize genetic dependencies in LOF screening assays. One of the available strategies for analyzing shRNA screenings is described by Hart *et al.* (Hart et al., 2014). Briefly, this approach employs gold-standard positive (essential genes) and negative (non-essential genes) reference gene sets to train a Bayesian classifier of gene essentiality. In particular, the classifier is used to determine the likelihood that a certain gene belongs to the essential or non-essential group by evaluating whether the distribution of the fold-changes of its shRNA is more similar to the distributions of the shRNA targeting essential or non-essential genes from the gold-standard lists. Finally, the obtained value, defined as the Bayes Factor (BF), gives information about the essentiality of the gene, and is used to classify genes into essential (BF scores > 0) or non-essential (BF scores < 0) groups.

The reference lists used to train the classifier are derived from a set of human cell lines. Hart *et al.* defines essential genes as those required for cell proliferation across all tested screening assays, while genes not expressed in the majority of cell lines are included in the non-essential set (Hart et al., 2014). The developed python scripts and the references sets required to calculate the Bayes Factor are available as supplementary data in the authors' paper. Data from whole-genome essentiality screens, conducted using either shRNA or CRISPR technology, are available from different public databases, including the DepMap portal (<https://depmap.org/portal/>) or the Project Score (<https://score.depmap.sanger.ac.uk>). While the Project database only contains genetic screens performed using CRISPR libraries, data from both shRNA and CRISPR screening assays can be downloaded from the DepMap repository.

1.2.2. Omics technologies for the identification of non-invasive biomarkers

The application of omics technologies, and in particular metabolomics, into the biomarker discovery field offers the possibility of identifying novel biomarkers through the analysis of biofluid samples, that can be collected using minimally or non-invasive approaches. Notably, as metabolites represent the end products of biochemical pathways, they can be strongly influenced by any pathological process and reflect alterations closely associated with the disease progression and/or remission. These changes may provide new

insights to develop promising biomarkers with clinical utility for early diagnosis, disease progression and treatment response monitoring. Systemic metabolic alterations measured in biofluids provide a picture of the metabolic changes occurring in the whole organism, that can be affected by the tumor itself and also by external factors (e.g., diet, lifestyle, treatment administration). Systemic changes, like diet composition, are known to affect metabolism within tumor cells (Bose et al., 2020; Sullivan et al., 2019) and impact on tumor progression (Goncalves et al., 2019; M. Lv et al., 2014). In addition to metabolomics, other omics-based approaches, such as transcriptomics, have contributed to the characterization of local transcriptomic changes. In particular, the analysis of tumor tissues enables the study of local molecular changes driving different cancer metabolic phenotypes.

However, each omics on its own fails to capture the entire biological complexity a human disease like cancer (Karczewski & Snyder, 2018). Thus, the combination of metabolomics with other omics data may provide a more sensitive strategy to detect metabolic alterations related to the disease for the development of clinically relevant biomarkers (Hasin et al., 2017; Karczewski & Snyder, 2018; D. R. Schmidt et al., 2021). In this context, the combined analysis of tissue and biofluid metabolomic profiles, using different omics approaches, could provide broader information about the systemic and local metabolic changes related to a disease condition (Lewis & Kemp, 2021; Y. Li et al., 2018). These analyses may provide insights to which molecular pathways contribute to the onset and progression of the disease and ultimately lead to the identification of metabolic biomarkers associated with a specific health condition (Hasin et al., 2017).

1.2.2.1. Multi-omics characterization of cancer-related metabolic phenotypes

In the context of PCa, the integration of data generated from different omics studies has contributed to better characterize the specific metabolic phenotype of PCa when compared to benign prostate (reviewed in Gómez-Cebrián et al., 2022). Particularly, as shown in Figure 7, based on the combined analysis of different omics data, the metabolic profile of PCa patients is characterized by alterations in the TCA cycle, polyamine synthesis, hexosamine biosynthetic pathway, and nucleotide and lipid metabolism. Notably, these metabolic alterations are in agreement with the findings observed in other studies where only metabolomics was applied to characterize the metabolic profile of PCa tumors

(Braadland et al., 2017; Dereziński et al., 2017; Goto et al., 2015; Huang et al., 2017; Lima et al., 2019; Madhu et al., 2016; Mondul et al., 2015; Struck-Lewicka et al., 2015).

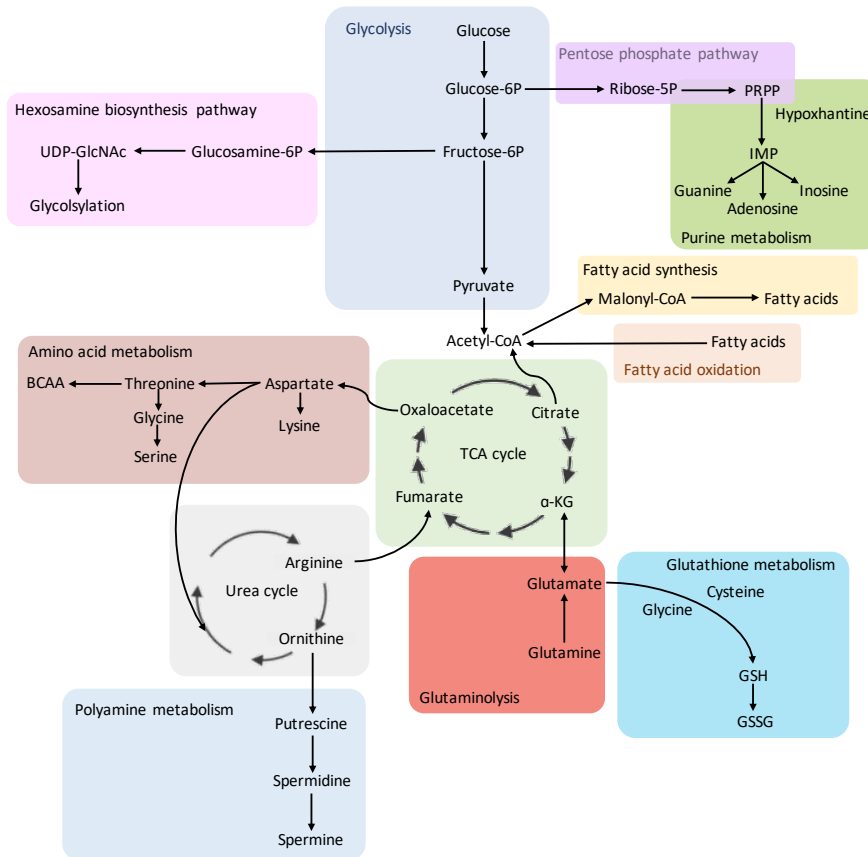


Figure 7. Schematic representative of the most consistently metabolic pathways reported to be dysregulated across different PCa multi-omics studies. From Gómez-Cebrián et al., 2022. Thick lines highlight the metabolic pathways found to be up-regulated in PCa tumors when compared with benign prostate tissue. KG: alpha-ketoglutarate, Fructose-6P: fructose-6-phosphate, Glucosamine-6P: glucosamine-6-phosphate, Glucose-6P: glucose-6-phosphate, IMP: inosine monophosphate, PRPP: phosphoribosyl diphosphate, Ribose-5P: ribose-5-phosphate.

Similarly, other multi-omics studies have also characterized metabolic alterations associated with specific subgroups of PCa patients (reviewed in Gómez-Cebrián et al., 2022). Table 2 summarizes the most relevant metabolic changes associated to the different PCa subgroups, including dysregulations in the TCA cycle, and amino acid, nucleotide and lipid metabolism. Interestingly, while many of the multi-omics studies characterized the local tumor metabolic profile by directly analyzing the tumor origin source (tissue samples), only one study used minimally invasive approaches (serum) to detect systemic metabolic alterations (Kiebish et al., 2020).

Table 2. Metabolic alterations observed in different multi-omics studies focused on the characterization of the metabolic profile of specific PCa subtypes. From Gómez-Cebrián et al., 2022.

Study	Sample	Omics Data	Group Comparison	Major Findings
Kiebish et al., 2020	Serum	L + M + P	non-BCR vs. BCR	BCR: ↑ TNC, APOA-IV, and 1-methyladenosine and ↓ phosphatidic acid
W. Liu et al., 2015	Tissue	G + M	PCa vs. metastatic	Metastatic PCa: ↑ <i>CYP11A1</i> , <i>PNP</i> , <i>SMS</i> , proline, cholesterol, sarcosine, spermidine, and spermine
C. Li et al., 2013	Tissue	M + T	PCa vs. metastatic	Metastatic PCa: ↓ histamine
Latonen et al., 2018	Tissue	E + G + P + T	PCa vs. CRPC	CRPC: ↓ <i>ACO2</i> , <i>OGDH</i> , <i>SUCLG1</i> , and <i>IDH3A</i> ; ↑ <i>MDH2</i>
; U' YhU'z&S%7ell lines	Cell lines	L + M + T	LNCaP vs. SCNC	LNCaP: ↑ <i>PHGDH</i> , <i>PSAT1</i> , <i>PSPH</i> , <i>TDH</i> , <i>GCAT</i> , citrate, isocitrate, and succinate; ↓ fumarate, glutamate, glutamine, <i>IDH1</i> , <i>GLUD1</i> , <i>GLUD2</i> , carnitine, and short-chain acylcarnitines SCNC: ↑ lactate and <i>LDH</i> ; ↓ <i>G6P</i>
Joshi et al., 2020	Cell lines	M + T	<i>CPT1A</i> KD vs. <i>CPT1A</i> OE	<i>CPT1A</i> OE: ↑ <i>PHGDH</i> , <i>PSAT1</i> , <i>SHMT2</i> , <i>CTH</i> , <i>GSTO2</i> , dimethylglycine, cystathionine, cystathionine, and cysteine; ↓ glycolysis
Y. Chen et al., 2020	Cell lines	M + T	ARCaP _E vs. ARCaP _M	ARCaP _M : ↑ malate, <i>ACO2</i> , <i>SDHA</i> , aspartate, <i>ASS1</i> , and <i>SRR</i> ; ↓ glycolysis, succinate, and citrate
Hansen et al., 2016	Tissue	L + M	<i>ERG</i> _{low} vs. <i>ERG</i> _{high}	<i>ERG</i> _{high} : ↑ ethanolamine, glycine, phosphocholine, phosphoethanolamine, <i>ACACA</i> , <i>FASN</i> , and <i>SAT1</i> ; ↓ <i>ACO2</i> , citrate, spermine, putrescine, and glucose

Yan et al., 2017	Tissue	L + M + T	<i>SPOP</i> _{wt} vs. <i>SPOP</i> _{mutant}	<i>SPOP</i> _{mutant} : ↑ <i>ACADL</i> , <i>ELOVL2</i> , <i>FH</i> , fatty acids, fumarate, and malate
Andersen et al., 2018	Tissue	M + T	Low vs. high reactive stroma	High reactive stroma: ↑ taurine and leucine; ↓ citrate, spermine, and scyllo-inositol
Oberhuber et al., 2020	Tissue	M + P + T	<i>STAT3</i> _{low} vs. <i>STAT3</i> _{high}	<i>STAT3</i> _{low} : ↑ <i>OXPHOS</i> , TCA cycle, ribosomal activity, pyruvate, fumarate, and malate; ↓ <i>PDK4</i>

Thus, the metabolic characterization of different PCa phenotypes has enabled to identify metabolic alterations associated with a specific phenotype (Joshi et al., 2020; Oberhuber et al., 2020), with poor prognosis (Andersen et al., 2018; Hansen et al., 2016; Kiebish et al., 2020) or with advanced stages of the disease (Latonen et al., 2018; C. Li et al., 2013; W. Liu et al., 2015).

1.2.2.2. Analytical platforms for metabolic studies

The most commonly used analytical strategies for metabolomics analyses are MS and NMR. Each of these analytical platform presents different advantages and limitations (Table 3). Importantly, none of these platforms can completely identify and quantify the metabolomic composition of a biological sample, therefore, they may be considered as complementary methods. Their selection mainly depends on the objective of the study and the sample to be analyzed (A.-H. M. Emwas, 2015).

Table 3. Summary of the advantages and limitations of MS and NMR in metabolomics studies. Adapted from A.-H. Emwas et al., 2019.

	MS	NMR
Reproducibility	Low reproducibility	High reproducibility
Sensitivity	High sensitivity	Low sensitivity
Selectivity	Selective	Generally used for nonselective analysis
Sample measurement	Requires different ionization methods to increase the number of detected metabolites	Relatively fast measurements and all detectable metabolites can be observed in one measurement

Sample preparation	More demanding procedures	Minimal sample preparation
Sample recovery	Destructive technique, though only small amount of sample is needed	Non-destructive, several analyses can be performed on the same sample, and the sample can be recovered and stored for a long time
Quantitative analysis	The intensity is often not correlated with metabolite concentrations	Inherently quantitative since the signal intensity is directly proportional to the metabolite concentration
Fluxomics analysis	Enables <i>in vitro</i> and <i>in vivo</i> metabolic flux analysis	Although it is less sensitive, it provides unique labeling information complementary to MS, and allows to distinguish between isotopes of different elements (e.g., ^{13}C and ^{15}N)
Tissue samples	Some approaches can be used though these are far from being routine	Possible to detect metabolites in tissue samples using HRMAS NMR
Number of detectable metabolites	Possible to detect hundreds or thousands of metabolites	Unambiguously identified and detected less than 200 in one measurement
Targeted analysis	GC-MS and LC-MS are superior for targeted analysis	Can be used for targeted and untargeted analysis
In vivo studies	Is not used for <i>in vivo</i> metabolomics studies	<i>In vivo</i> analysis can be carried out using MRS

GC-MS: Gas Chromatography, HRMAS: High-Resolution Magic-Angle Sample Spinning, LC-MS: Liquid Chromatography, MRS: Magnetic Resonance Spectroscopy, MS: Mass Spectroscopy, NMR: Nuclear Magnetic Resonance.

Depending on the objective of the study, two different data analysis approaches can be applied to conduct a metabolomic study:

- The targeted analysis aims at accurately identifying and quantifying a predefined group of metabolites present in a biological sample. Thus, for this type of analysis, previously known information about the disease of interest (e.g., metabolites involved in a particular metabolic pathway) is required. A major drawback of the targeted approach is the limited metabolite coverage, therefore, it may not be useful for discovery-based biomarker studies.

- The untargeted strategy is focused on the identification and quantification of a large number of metabolites (between 100 to 1000), including unknown compounds, present in a biological sample. This approach is widely used in biomarker discovery, and it is usually combined with multivariate analyses to reduce data complexity due to the extensive data generated (Roberts et al., 2012).

1.2.2.3. Steps of a metabolic study

The common workflow that is followed in many metabolic studies focused on biomarker identification is represented in Figure 8.

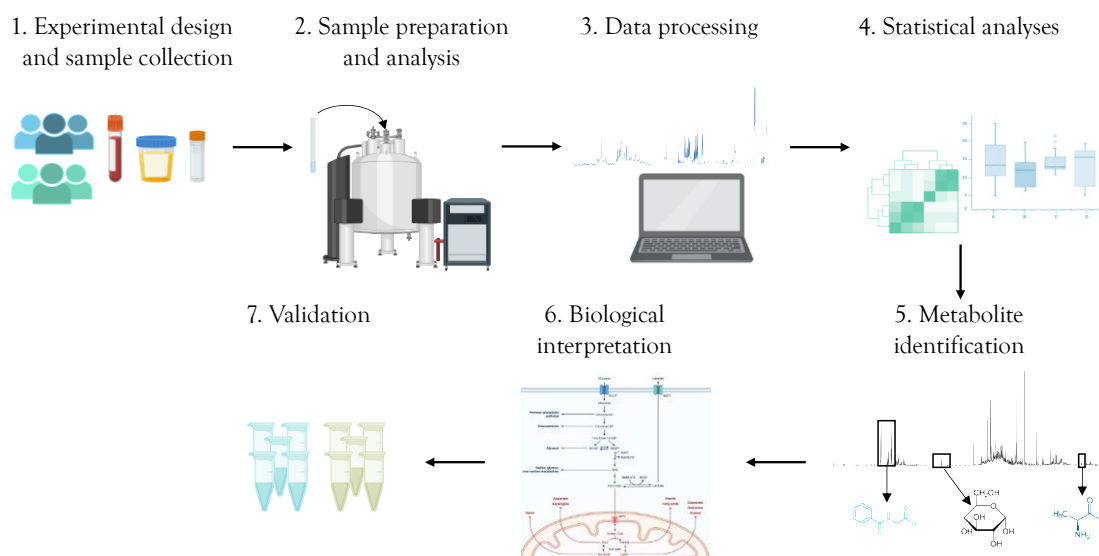


Figure 8. General workflow followed in an NMR-based metabolomic study

a) Experimental design and sample collection

In any clinical metabolic study, it is essential to perform an appropriate experimental design that allows to answer the initial biological question. There exist different designs of studies, but retrospective case-control studies, where patients with a specific medical condition (cases) are compared to individuals that do not present that condition (controls), are frequently used for biomarker identification purposes.

Regarding sample type, metabolomics studies are mainly conducted on biofluids, feces or tissue samples. Contrary to tumor samples, biofluids allow to detect large number of metabolites using non- or minimally-invasive sample collection procedures. Sample

preparation procedures mainly depend on the sample type. While urine requires minimal sample preparation, serum and plasma samples are collected either by allowing blood to clot or by adding anti-coagulants, respectively. In addition, during this step, samples are normally mixed with a phosphate buffer to reduce variations associated with differences in the pH or viscosity (Beckonert et al., 2007).

Finally, a relevant aspect to consider is sample size, as it has a significant impact on the statistical power of the analysis. Thus, it is important to include large sample cohorts and external datasets to increase the statistical power of the analyses, obtain more accurate and robust findings, and evaluate the clinical significance of the metabolic findings using independent cohorts.

b) NMR spectra acquisition

For metabolomics studies, one-dimensional (1D) proton NMR experiments are the most frequently used. They allow to detect any molecule, present in the sample at a certain concentration, that contains hydrogen atoms in its chemical structure. Two different pulse sequences are generally used for 1D-NMR spectra acquisition:

- NOESY (Nuclear Overhauser Effect Spectroscopy). This experiment provides a good water suppression spectrum while maintaining a flat baseline, and enables the detection of small and large molecular weight metabolites (Gowda et al., 2008). Urine spectra are often acquired using the NOESY pulse sequence.
- CPMG (Carr-Purcell-Meiboom-Gill). This NMR method is generally used when aiming at suppressing broad signals from large weight molecules (Gowda et al., 2008). Thus, due to the elevated protein and lipid content, this sequence is mainly applied to analyze serum and plasma samples.

c) Data processing

After spectra acquisition, several processing steps are applied to improve signal quality and reduce biases. Phasing and baseline correction are firstly performed to correct phase distortions, ensure spectral quality, and remove spectral artefacts. These steps result in a spectrum with flat signal-free regions and horizontal lines with zero intensity. Spectra alignment is also important to avoid the construction of an inappropriate metabolic model

and ensure that the same peaks corresponding to the same compound are comparable and quantifiable across all spectra. Several alignment algorithms have been developed to achieve this goal, including internal correlation shifting (Savorani et al., 2010), correlation optimized warping (Nielsen et al., 1998), and hierarchical cluster-based peak alignment (Vu et al., 2011).

Following steps include sub-spectral selection to remove uninformative spectral regions, and bucketing to divide the NMR spectra into small buckets. In the resulting data matrix, the intensity of each variable is calculated using the area under the curve. To account for the overall concentration of each sample and enable sample comparison, the data matrix can be normalized. This is a critical step specially in urine studies, as large differences in excreted volume, and therefore in urinary concentration and subsequently in metabolite dilution, are found between patients. The most frequently used normalization method in NMR experiments is the numerical or integral normalization, though probabilistic quotient normalization (PQN) is often applied for urine normalization. Finally, prior to the statistical analyses, the data matrix can be transformed to make it more normally distributed and to scale the metabolite intensities. There exists a number of scaling methods, but Pareto is frequently chosen to scale NMR data.

d) Multivariate statistical analysis

Once NMR data has been processed, the next step is multivariate statistical analysis, where all data features are simultaneously taken into account, contributing to reduce data dimensionality and identify potential relationships between them. These analyses can be divided into two categories: unsupervised and supervised methods.

In the unsupervised analysis, the data matrix is explored to detect underlying patterns and sample outliers in the sample dataset. Principal component analysis (PCA) is commonly used in NMR analysis, and is based on reducing data to a combination of linearly uncorrelated variables, known as principal components, that explain the variance in the data. The major variance is associated with the first component, while the following components explain increasingly reduced percentages of variance. On the other hand, supervised methods are used to identify correlations between metabolic features and the

phenotypic variable of interest, therefore, reducing the contribution of data variance. Contrary to the PCA, previous knowledge about group classification is needed to detect the buckets that differ between the groups of interest. Examples of supervised analyses conducted on NMR experiments include partial least squares discriminant analysis (PLS-DA) and orthogonal PLS-DA (OPLS-DA).

Importantly, as the processed data matrix presents a greater number of columns (predictor variables or buckets) than rows (samples), these supervised models may tend to be overfitted and overestimate their predictability (Triba et al., 2015). Thus, cross-validation procedures are highly recommended to assess the quality of the built model. Two values are normally extracted for quality evaluation, R^2 and Q^2 parameters. While R^2 represents a measure of the goodness of fit (models that perfectly describes the data are defined by $R^2 = 1$), Q^2 gives a measure of the predictability of the model ($Q^2 = 1$ describes a perfect predictive ability of the model). In addition, another important test to evaluate the supervised models is the permutation analysis, that evaluates whether the classification of samples into their predefined groups is better than any other random classification randomly performed (Westerhuis et al., 2008). In this test, the labels of each group (case/control) are randomly assigned to different individuals, and a new supervised model is generated. This process is repeated n times. As this model has been calculated by classifying the individual randomly, it is expected that the calculated model has lower fitness and predictability values than the original model. A good validation result is considered when the R^2Y and the Q^2Y values of the permuted model are not higher than 0.3-0.4 and 0.05, respectively (Eriksson et al., 2013).

e) Metabolite identification

For metabolite identification, NMR peaks of the spectra are matched against a set of reference metabolites. There exists a number of high-quality, publicly available databases (e.g., HMDB BMRB) that contain reference NMR spectra for hundreds of metabolites collected under different experimental conditions, including different nuclei and a diverse range of spectrometer frequencies. Notably, this step represents one of the major challenges faced in any metabolomic study.

f) Univariate statistical analyses

In contrast to multivariate analyses, univariate methods analyze each metabolic characteristic independently to detect, based on a pre-defined statistical threshold, whether a certain variable exhibits significant differences in its values between the groups of study. In addition, these methods are normally used to confirm that the metabolic regions that are found to be informative in the multivariate model, remain significant in a univariate context. This is particularly notable to validate potential biomarkers (Percival et al., 2020). A number of univariate tests are available for the analysis of metabolomic data, and the selection of the proper method is based on data properties such as number of groups to compare, sample size and data distribution.

g) Biological interpretation

The final step of a metabolic analysis attempts to integrate all identified metabolites with functional analyses to provide a consistent biological explanation of the observed metabolic alterations on the context of the disease of study. To achieve this purpose, information from several compound databases as well as relevant literature, is combined to identify related metabolites, as those involved in the same metabolic pathway, and gain insights into the biological function or the metabolic pathway that each metabolite is involved in.

II. HYPOTHESIS AND OBJECTIVES

PCa is defined as a biologically heterogeneous tumor with a variable clinical course. Optimal management of PCa is challenging due to the difficulties in predicting which patients with indolent tumors will develop metastatic progression. There still remains no classification scheme that allows to accurately discriminate indolent from aggressive PCa tumors. Thus, there is an urgent need of more robust biomarkers to improve the current landscape of the disease. In addition, PCa remains incurable when it progresses to advanced stages, and new therapies based on personalized medicine, are highly crucial to increase overall survival rate and improve life quality of PCa patients. In this context, the application of different omics technologies may represent a powerful approach for the development of non-invasive prognostic biomarkers, and for the identification of genetic vulnerabilities required for tumor proliferation that may be further investigated as potential therapeutic targets.

Considering these two aspects, the present work aims to address the following main objectives and subobjectives:

1. Characterization of metabolic changes related to PCa progression.
 - i. Characterization of the urine and serum metabolic phenotype of advanced PCa patients.
 - ii. Identification of specific metabolic alterations in advanced PCa patients.
2. Characterization of specific genetic vulnerabilities in advanced PCa.
 - i. Identification of novel potential therapeutic targets for the treatment of advanced PCa.
 - ii. Functional validation of potential therapeutic targets for the treatment of advanced PCa.

III. MATERIALS AND METHODS

III.1. IDENTIFICATION OF METABOLIC BIOMARKERS FOR ADVANCED PCa

III.1.1. Sample collection for metabolomics analyses

Patient recruitment and sampling procedures were carried out following all applicable local regulatory requirements and laws, in accordance with the Declaration of Helsinki, and after approval from the Ethics Committee of the Instituto Valenciano de Oncología (CAPROSIVO, GVA, PROMETEO/2016/103) on May 2015. Before being included in the study, a written informed consent from each participant was obtained. The study included 78 serum and 84 urine samples from PCa patients between the ages of 46 and 92, that were recruited at the Urology Department and the Biobank of the Instituto Valenciano de Oncología (Valencia, Spain) between November 2016 and October 2018. PCa patients included in the study did not have any other diseases and were not receiving any therapy for PCa at the time of sample collection.

Clinical variables, including PSA value, prostate volume, GS and body mass index (BMI), were collected for all patients. Patients were classified into two groups according to the GS score, using a $GS < 7$ as cut-off as it has been shown to be the optimal parameter for PCa patient clinical management (De Nunzio et al., 2018). Following this criterium, classification of urine and serum samples into the low- ($GS < 7$) or the high-GS ($GS \geq 7$) group is summarized in Table 4.

Table 4. Number of samples included in each experimental group for each collected biofluid

	Serum	Urine
Low-GS ($GS < 7$)	41	46
High-GS ($GS \geq 7$)	37	38

Sample processing, storage and preparation for NMR analyses was performed following the procedures described for NMR metabolic studies (Beckonert et al., 2007):

- SERUM

Blood samples were collected in 7.5 ml S-Monovette® Serum-gel tubes (SARSTEDT AG&Co Nümbrecht) and centrifugated at 1600 g for 15 min at 4°C after coagulation. Then, supernatant was collected, aliquoted in 1.5 ml cryotubes, freeze in liquid nitrogen and finally stored at -80°C for NMR analyses.

For NMR measurements, serum samples were thawed on ice, and 300 µL of serum were added to 300 µL of phosphate buffer (75 mM of Na₂HPO₄, 4.6 mM of trimethylsilylpropanoic acid (TSP) and 0.04% NaN₃, pH = 7.4, in D₂O). Finally, 550 µL of each sample were transferred to a 5 mm NMR tube.

- URINE

On the other hand, urine samples were collected in a 100 ml sterile container (Ref. 409726, Deltalab). Then, 6 ml of NaN₃ (0.05%) were immediately added to 3 ml of urine, and 2 aliquots of 1.5 ml each were freeze in liquid nitrogen. Urine samples were finally stored at -80°C until NMR analyses.

Before NMR analyses, urine samples were first thawed on ice and then centrifugated at 6000 rpm for 10 min at room temperature (RT). After centrifugation, 60 µL of phosphate buffer (1.5 M KH₂PO₄, 0.1% TSP and 0.05% NaN₃, pH = 7.4, in D₂O) were added to 540 µL of urine sample supernatant. Then, 550 µL of each sample were transferred to a 5 mm NMR tube.

III.1.2. Selection of transcriptomic studies

The Gene Expression Omnibus (GEO; <https://www.ncbi.nlm.nih.gov/geo/>) database was examined to identify publicly available PCa transcriptomic studies. The search was limited to *Homo sapiens* as organism and microarrays as analytical platform. Only those studies that met the following features were included in the analysis: 1) analyzed human PCa tumor samples, 2) analyzed the gene expression profiling by array, 3) available information of the GS variable, and 4) included more than 30 samples.

All processing steps were conducted using the R language (3.6.0 version) and environment for statistical computing (R Core Team, 2020). To verify data integrity, all datasets underwent quality control using the *affy* R package (Gautier et al., 2004), and PCA plots were individually generated for each dataset and visualized using the *FactoMineR* and the *factoextra* R packages (Kassambara & Mundt, 2020; Lê et al., 2008) for outlier detection and bias in sample distribution. If not previously performed, gene expression data was subjected to \log_2 transformation for normalization. The \log_2 transformation is the most widely used approach for processing transcriptomic data, and different bioinformatics tools, such as *limma* R package (Ritchie et al., 2015), are developed to use \log_2 data as input. Notably, as microarrays had different probes for the same gene, the median of all probes was calculated for each gene. Finally, similar to the metabolic analysis, samples were classified according to the GS value into low- (GS < 7) and high-GS (GS \geq 7) groups.

III.1.3. Acquisition of NMR metabolic profile

III.1.3.1. Spectra acquisition

As shown in Table 5, the acquisition parameters were modified according to each biofluid. All NMR measurements were acquired using a 500 MHz spectrometer, collecting a 1D-CPMG spin-echo pulse sequence at 310 K for serum samples, and a 1D-NOESY pulse sequence at 300 K for urine samples. For spectra acquisition, the following commands were used: probe adjust, stabilization and homogeneity of the magnetic field, automatic calculation of the 90° pulse (P1), and automatic transformation and pre-process of the spectra.

Table 5. Acquisition parameters for each ¹H-RMN biofluid spectra

	Serum	Urine
Pulse program	cpmgpr1d.comp	noesygppr1d
Temperature (K)	310	300
NS	256	256
DS	8	4
TD	61440	65536
SW (ppm)	20.05	29.99
D1 (s)	4	4
RG	80.6	90.5

1D: one-dimensional, D1: relaxation delay between free induction decays (FIDs), DS: number of dummy scans, K: kelvin, NS: number of scans, RG: receiver gain, SW: spectral width, TD: size of fid

III.1.3.2. NMR data processing

Serum and urine spectra were multiplied by a line-broadening factor of 1 Hz and Fourier transformed. Finally, all spectra were automatically phased, baseline corrected, and internally referenced to the methyl group signal of TSP (0.00 ppm). Then, spectra were binned and integrated using Amix 3.9.7 program (Bruker Biospin), and the parameters (bucket width, spectral region and excluded regions) were modified according to the characteristics of each biofluid. The followed protocol for processing serum and urine spectra is summarized in Table 6. The integration mode used in both biofluids was sum of absolute intensities.

Table 6. Summary of the processing steps followed in each biofluid

	Serum	Urine
Bucketing	Spectral region: 8.5–0.5 ppm	Spectral region: 9.38–0.07 ppm
	Excluded regions:	Excluded regions:
	- Water: 4.87–4.51 ppm	- Water: 4.86–4.72 ppm
	- Urea: 6.65–5.53 ppm	- Urea: 6.10–5.45 ppm
	Bucket width: 0.01 ppm	Bucket width: 0.001 ppm
	Integration mode: sum of absolute intensities	Integration mode: sum of absolute intensities
Alignment	TSP	speaq
Normalization	Integral normalization	Integral normalization and PQN

PQN: probabilistic quotient normalization, ppm: part per million, speaq: spectrum alignment and quantitation, TSP: trimethylsilylpropanoic acid

After integration, a peak alignment algorithm was applied to urine samples to improve their alignment. Samples were aligned using the *speaq* R package (Beirnaert et al., 2018; Vu et al., 2011), that is based on the hierarchical Cluster-based Peak Alignment method (Vu et al., 2011) for spectra alignment. Integral normalization was employed to normalized serum samples, that individually divides each bucket by the spectrum total area. This process was automatically performed using Amix 3.9.7 program (Bruker Biospin). Urine spectra were normalized by integral normalization and PQN (Dieterle et al., 2006). PQN is frequently applied to normalize urine samples due to the great variation in urine chemical concentrations as a consequence of high salt contents. For each spectrum, this method calculates a dilution factor as the quotient between the signal intensities of the corresponding spectrum and a reference spectrum. The PQN method was applied in R 3.6.0 version (RStudio) following the instructions described in Dieterle et al., 2006.

III.1.4. Metabolite assignment

Metabolites were identified based on publicly available information from two different databases (HMDB and BMRB) and the commercial database BBIOREFCODE (Bruker Biospin). Optimal integration regions were defined for each metabolite (Appendix 1), integrated and quantified using the Mnova program (MestreNova 8.0). The relative intensity of metabolite signals was quantified using variable size bucketing tool. The metabolic regions of interest were defined by visual inspection, integrating one signal for each identified metabolite.

III.1.5. Multivariate statistical analysis

Multivariate statistical analyses were performed using SIMCA-P 14.0 program (Umetrics AB). The scaling method was adjusted to the NMR data, using Pareto and unit variance (UV) for scaling serum and urine samples, respectively. UV uses the standard deviation to scale the data, while Pareto relies on the square root of the standard deviation as scaling factor. After scaling, non-supervised analyses based on PCA were performed to evaluate homogeneity between groups and identify potential outliers, that were individually examined and excluded from further analyses when considered.

Then, supervised analyses using OPLS-DA models were carried out to relate the metabolic dataset with the clinical variable of interest. In this work, the supervised analysis was used to assess the discriminatory potential between low- and high-GS groups. The default method of 7-fold internal cross validation was applied, from which Q^2Y and R^2Y values were extracted. Those parameters were used to evaluate the quality of all OPLS-DA models. In addition, the permutation test was calculated from the original OPLS-DA models, using 100 iterations for each of the models.

III.1.6. Differential expression analyses

Univariate analyses on metabolic and transcriptomic data were carried out using the R language (3.6.0 version). In the metabolic and transcriptomic datasets, differences between low- and high-GS groups were assessed using the two-tailed Mann-Whitney U test from the *stats* R package. Statistically significant differences were considered as a p-value < 0.05. Finally, fold-change (FC) values were calculated for each metabolite and gene.

III.1.7. Gene Set Enrichment Analysis

To identify altered metabolic pathways between the groups of interest, a gene set enrichment analysis (GSEA) was individually performed on each PCa transcriptomic dataset using the functions implemented in the *mdgsa* R package (Montaner & Dopazo, 2010). The metabolic pathways defined by the Kyoto Encyclopedia of Genes and Genomes (KEGG) database (Kanehisa, 2019; Kanehisa et al., 2019; Kanehisa & Goto, 2000) were used for the functional enrichment. Metabolic pathways with a log odds ratio > 0 indicated enriched metabolic pathways in the high-GS group. Finally, pathways showing a p-value < 0.05 were defined as significantly dysregulated.

III.2. IDENTIFICATION OF POTENTIAL THERAPEUTIC TARGETS FOR ADVANCED PCa

III.2.1. Calculation of the essentiality score

Publicly available data from genome-wide shRNA LOF screens, comprising viability data on over 18000 genes in a total of 501 cell lines (v.2.4.3 and v.2.19.2 (Cowley et al., 2014; Tsherniak et al., 2017)), were downloaded from the DepMap portal (<https://depmap.org/portal/download/all/>). These data files had quantile normalized log fold-change gene level dependencies, calculated as ATARiS scores (Shao et al., 2013), and filtered according to a quality threshold. The cell line annotation file containing information on cell line name, cancer type and primary/metastatic site, was downloaded from the same portal.

Based on these data, the essentiality score for each gene was calculated in each screened PCa cell line using the approach firstly described by Hart *et al* (Hart et al., 2014) and extensively applied in later studies (Apaolaza et al., 2017; Davoli et al., 2016; Ilic et al., 2017). Briefly, a Bayesian classifier was employed to calculate the essentiality value based on the log likelihood (BF values) that a specific gene belonged to the gold-standard reference set of essential ($BF > 0$) or non-essential ($BF < 0$) genes. Then, genes were rank-ordered by the BF score, and the BF values were Z-score normalized across each tested cell line. Genes with a Z-score > 1.96 (Witwicki et al., 2018) were extracted from each cell line, and the lists of all significant genes were combined to select those detected in more than 50% of the screened PCa cell lines.

III.2.2. Selection of transcriptomic studies

An advanced search was conducted on the GEO database to identify studies analyzing the transcriptomic profile of prostate samples, excluding all studies not performed on human samples. Studies that met the following conditions were selected: 1) analyzed human tumor samples, 2) analyzed the gene expression profiling by array, 3) included 50 or more samples, and 4) analyzed samples from at least two of the groups of interest (healthy, primary, metastatic stage). In addition, other considered but not selective

criteria included available information on disease recurrence, patient status, or survival / recurrence time.

All processing steps were conducted using the R language (3.6.0 version). Data quality control using the *affy* R package (Gautier et al., 2004) was conducted on all transcriptomic datasets, and data was \log_2 normalized when needed. For each microarray, when different probes were available for the same gene, the median of all probes was calculated for each gene to get the most informative value. A PCA was individually conducted in each transcriptomic dataset to detect outliers and evaluate potential bias in sample distribution. PCA plots were generated and visualized using the *FactoMineR* and the *factoextra* R packages, respectively (Kassambara & Mundt, 2020; Lê et al., 2008).

III.2.3. Differential expression analyses

Based on the experimental groups, transcriptomic studies were used for comparing: i) healthy vs PCa, ii) indolent *vs* aggressive or iii) primary *vs* metastatic tissue samples. For the second comparison, the BCR variable was used to classify patients into indolent (non-BCR) or aggressive (BCR) groups. In each comparison, differences in the gene expression levels between both groups were assessed using the two-tailed Mann-Whitney U test from the “*stats*” R package. Statistical p-values were adjusted using the Benjamin-Hochberg (BH) method, and significant genes were defined as those showing an adjusted p-value < 0.05 .

III.2.4. Survival analyses

Kaplan-Meier survival analyses were conducted using the “*survminer*” R package to evaluate the individual role of each gene in disease progression. Lower and upper quartiles were selected as cut-off points to divide samples into low- and high-expression groups. The log-rank test was applied to detect significant survival differences between groups, considering a p-value < 0.05 as significant.

III.2.5. Evaluation of the therapeutic potential

III.2.5.1. Databases

Protein-protein interaction (PPI) network and functional enrichment analyses were constructed using the Search Tool for the Retrieval of Interacting Genes (STRING, <http://string.embl.de>) (Szkłarczyk et al., 2021). A confidence score of 0.4 was set as the cut-off criterion. Potential druggability of the selected candidates was assessed using the information available at Uniprot (UniProt Consortium, 2021), Protein Data Bank (PDB) (Berman et al., 2000), CanSAR (Coker et al., 2019) and Pharos (Sheils et al., 2021) databases. In particular, information regarding biological, pharmacological and structural features was extracted from these web portals. The UbiBrowser 2.0 database (X. Wang et al., 2022) was used to identify potential interactions between ubiquitin E3 ligases or deubiquitinases and substrates.

III.2.5.2. Characterization of gene expression levels in cellular models

- PCa cell lines

A total of four human prostate cell lines were used for molecular biology experiments: one representing a healthy condition (RWPE-1) and three PCa (22rv1, LnCaP and PC3) cellular models exhibiting different biological and molecular characteristics. RWPE-1 is defined as epithelial cell line, derived from the peripheral zone, that expresses PSA and AR. The 22rv1 line represents a primary stage of PCa, is an androgen-dependent cell line derived from a human xenograft, and expresses PSA and AR. The other two PCa cell lines are metastatic models that differ in their androgen sensitivity, metastasis origin and metastatic potential. LnCaP is established from a lymph node metastasis, is sensitive to androgens and has the lowest metastatic potential. On the other hand, PC3 cells are used as an androgen-resistant model. This cell line is initiated from a bone metastasis of a grade IV adenocarcinoma and is characterized by a high metastatic potential.

- Cell culture and reagents

The 22rv1, LNCaP and PC3 cells were cultured in RPMI 1640 medium (GIBCO), supplemented with 10% fetal bovine serum (FBS) and 100 U/mL penicillin/streptomycin. The RWPE-1 cell line was cultured in keratinocyte serum free medium (K-SFM), supplemented with 0.05 mg/mL bovine pituitary extract, 5 ng/mL epidermal growth

factor, 10% FBS and 100 U/mL penicillin/streptomycin. Human embryonic kidney (HEK) 293T cells were cultured in Dulbecco's modified Eagle's medium (DMEM), supplemented with 10% FBS and 100 U/mL penicillin/streptomycin. All cells were grown in an incubator at 37°C containing 5% CO₂, and the culture medium was replaced every 2 days.

- Real-time qPCR

200.000 cells were seeded on 6-wells plates and incubated in 5% CO₂ at 37°C for 48 h. After removing medium from cells and rinsing them with 1X cold PBS, total RNA was isolated using the RNeasy Mini Kit (Quiagen GmbH, Hilden, Germany) and quantified using a nanodrop. Complementary DNA (cDNA) was synthesized from 500 ng of total RNA using the QuantiTect Reverse Transcription kit (Quiagen), following instructions provided by the manufacturer. Briefly, total RNA was firstly incubated at 42°C for 2 min to remove contaminant genomic DNA. Then, samples were incubated at 42°C for 15 min after adding the Master mix prepared with the kit (Table 7). Individual test was carried out on triplicates.

Table 7. Description of the master mix used for reverse transcription of purified RNA

Reactive	µl
Quantiscript Reverse Transcriptase	1
Quantiscript RT Buffer	4
RT Primer Mix	1

After reverse transcription, Master mix from the TB Green® Premix EX Taq™ kit (Takara, Shiga, Japan) and primers were added to 10 ng of cDNA to prepare the reaction mix (Table 8). The RT-PCR was conducted on a ViiA 7 Real-Time PCR System (Applied Biosystems), with 60°C annealing temperature and 40 amplification cycles. Individual test was carried out on duplicates.

Table 8. Description of the reaction master mix used for RT-PCR

Reactive	μl
DNA	2
ROX Dye II (50X)	0.2
Primer Sense (10X)	0.3
Primer Antisense (10X)	0.3
DNA master SYBR Premix Ex Taq Takara (2X)	5
H ₂ O	2.2

The expression values were quantified using the $2^{-\Delta\Delta C}$ method and normalized to beta-2-microglobulin (B2M) expression levels. DNA sequence of oligonucleotides used for qPCR reactions are included in Table 9.

Table 9. Primer sequences used for the qPCR

Gene	Sense	Antisense
<i>B2M</i>	AAGCAGCATCATGGAGGTTTG	GAGCTACCTGTGGAGCAACC
<i>EIF3H</i>	CCAGCAGCAATCATTTGGGG	ATATTCTCCTGCTGGCGACG

- Western blot analysis

1.5 x 10⁶ cells were seeded on 100 mm dishes and incubated in 5% CO₂ at 37°C for 48 h. The medium was removed, and cells were rinsed with 1X cold PBS. Proteins were extracted by adding 150 μL of lysis buffer (1 mL of RiPA buffer containing 0.25 mM β -glycerophosphate, 1 mM DTT, 4 μM leupeptin, 40 μM PMSF, 100 μM calyculin, 1 μM sodium orthovanadate, and 0.4 μM pepstatin) to each dish. Cells were scraped, and lysates were transferred to 1.5 mL Eppendorf tubes, incubated on ice for 30 min, and spined at maximum speed for 30 min at 4°C. Supernatants were transferred to a new tube and protein concentration was measured using the PierceTM BSA Protein Assay kit (Thermo Scientific), following manufacturer's instructions.

Protein aliquots were prepared to a final concentration of 1 $\mu\text{g}/\mu\text{L}$, and 20 μg of protein was loaded and separated by size on a 4-15% polyacrylamide gel (Bio-Rad Laboratories Inc.), and then transferred to a nitrocellulose membrane (Bio-Rad Laboratories Inc.). Non-specific binding sites were blocked using 1X Tris-buffered saline-

Tween (TBS-T) buffer (100 mL 10X TBS (200 mM Tris pH = 7.5, 1.5 M NaCl), 900 mL H₂O, 1 mL Tween 20%) with 5% nonfat milk at RT for 1 h, followed by incubation with primary antibodies (diluted 1:1000 in 1X TBS-T with 5% BSA) at 4°C overnight. Then, membranes were washed three times with 1X TBS-T for 10 min each at RT, and incubated with peroxidase-conjugated secondary antibodies (diluted 1:10000 in 1X TBS-T containing 5% nonfat milk) at RT for 1 h. After washing membranes three more times with 1X TBS-T, immunoreactive bands were detected using an enhanced chemiluminescence (ECL) detection system (Bio-Rad Laboratories Inc.) following manufacturer's instructions. Dilution conditions and antibodies used for the determination of protein levels are included in Table 10. Antibodies against E-cadherin, EIF3H, GAPDH and Vimentin were obtained from Cell Signaling or Abcam. HorseRadish Peroxidase (HRP)-conjugated goat anti-rabbit IgG was purchased from Bio-Rad (Bio-Rad Laboratories Inc.).

Table 10. Information about the antibodies used in the western blot analyses

Antibody	Manufacture reference number	Dilution
E-cadherin	40772 (Abcam)	1:1000
EIF3H	3413 (Cell Signaling Technology)	1:1000
GAPDH	2118 (Cell Signaling Technology)	1:1000
Vimentin	92547 (Abcam)	1:1000

III.2.5.3. Generation of shRNA knockdown and over-expression models

- shRNA and over-expression plasmids

shRNA and over-expression constructions were purchased from Vector Builder Biotechnology (Guangzhou, China), and knockdown and over-expression models were generated following lentiviral infection. Information on each vector is detailed in Table 11.

Table 11. shRNA constructions and over-expression plasmids used for *EIF3H* gene

Name	Vector	Manufacture reference
sh-Scramble	pLV[shRNA]-EGFP:T2A:Puro-U6>Scramble_shRNA	VB010000-0009mxc
shEIF3H-2	pLV[shRNA]-EGFP:T2A:Puro-U6>hEIF3H[shRNA#2]	VB900071-1747qhr
shEIF3H-4	pLV[shRNA]-EGFP:T2A:Puro-U6>hEIF3H[shRNA#4]	VB211116-1322fzg
pLV	pLV[Exp]-EGFP:T2A:Puro-EF1A>ORF_Stuffer	VB010000-9389rbj
Myc-EIF3H	pLV[Exp]-EGFP:T2A:Puro-EF1A>Myc/hEIF3H	VB220412-1402gkc

- Plasmid preparation

Competent DH5 α *Escherichia coli* (*E. coli*) was used to clone the lentiviral vectors. Bacteria cells were thawed and kept on ice unless otherwise stated. Aseptic conditions were followed during the whole procedure. For plasmid replication, 50 μ l of *E. coli* containing the lentiviral vector were plated on an autoclaved LB agar plate (0.5 % yeast extract, 1% tryptone, 1% NaCl, 1% agar, 1:1000 ampicillin), using sterile cell spreaders. Then, plates were incubated in a static incubator at 37°C overnight.

Plasmid purification was performed following an internal protocol described in Appendix 2. Briefly, using a sterile inoculation loop, a single colony from each transformation plate was picked and inoculated in 3 mL of autoclaved LB medium with 1:1000 ampicillin. Bacteria cultures were left in a shaking incubator at 37°C until the end of the day. Then, 500 μ l of each culture were transferred to 250 mL of LB medium, and left shaking at 37°C overnight. Next day, plasmid was extracted using different freshly made solutions, and various cycles of incubation and centrifugation. DNA was precipitated and transferred to an Eppendorf tube containing 70% EtOH. Then, microtubes were spined at maximum speed at 4°C for 5 min, supernatants were removed and pellets were airdried overnight. Finally, pellets were resuspended on 1X Tris-EDTA buffer and quantified using a nanodrop.

- Lentiviral generation

An internal protocol was followed for viral production, represented in Figure 9. All required plasmids to transfect HEK 293T cells were provided, including the packaging system, that was split into two plasmids one encoding Rev and another encoding Gag and Pol proteins, and the envelope plasmid (VSV-G).

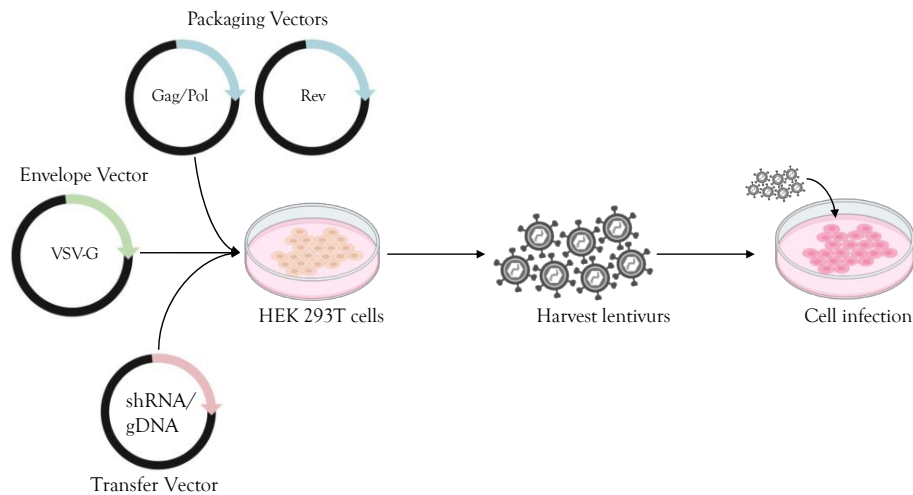


Figure 9. Schematic representation of the lentivirus production strategy. HEK 293T cells are transfected with envelope and packaging plasmids to form the virus particles and the transfer plasmid containing the vector of interest. After removing and replacing with fresh media, virus particles can be harvested after 48-72 hours and used for cell infection.

For each lentiviral vector to be infected, 1.5×10^6 HEK 293T cells were seeded in a 100 mm dish, and left incubating overnight. 24 h after seeding, shRNA constructions together with Gag/Pol, Rev and v-SVG plasmids were first thawed on ice. For each lentiviral vector, a transfection Mix with 544 μ L DMEM serum free and 24 μ L FuGENE was prepared, mixed by inversion and incubated for 5 min at RT. In addition, a DNA solution of 20 μ L, consisting of 0.4 μ g v-SVG, 3.7 μ g Gag/Pol, 3.7 μ g Rev and 4.2 μ g lentiviral vectors in sterile H₂O, was prepared and added after incubation time to each mix. The transfection mix was mixed by inversion and let stand at RT for 25-30 min. Medium from HEK 293T cells was removed and replaced with 6 mL of DMEM medium. After incubation, the transfection reaction was added to cells dropwise and dishes were swirled to mix and incubated in 5% CO₂ at 37 °C. Medium was replaced after 7 h and cells were incubated for 2 days. The green fluorescent protein (GFP) expression was observed under an automated inverted Leica DMI 4000B fluorescence microscope (Leica Microsystems GmbH, Germany) 24 h after transfection.

- Cell infection

2 days before infection, 300.000 cells were seeded in a 6-well plate and incubated in 5% CO₂ at 37°C for 2 days. At 48 h post transfection, the packaged recombinant lentiviruses were harvested from the media of HEK 293T cells, filtered with a 0.45 μ m

syringe filter, and spined at 300 g for 3 min. Then, after media removal, PC3 cells in each well were infected with each packaged lentivirus by adding 2 mL of the filtered supernatant with 4 µg/ml transfection reagent (Polybrene). Infection media was replaced with regular culture media (2 ml/well) after 7-8 h, and cells were incubated. At 24 h post infection, cells were selected in growth medium containing the appropriate puromycin concentration (1 µg/ml) and maintained under the same conditions for further analyses. The GFP expression was observed 72 h after selection.

III.2.5.4. Cell proliferation assay

Cell proliferation was measured via the colorimetric CellTiter 96 Cell Proliferation MTS assay (Promega, USA), and/or the fluorescence-based CyQUANT Cell Proliferation Assay (Thermo Scientific). In brief, between 200 and 1.000 cells were seeded in 96-well plates and cultured for 5 days at 37°C in 5% CO₂. For the MTS assay, 20 µL of the reagent were directly added to culture wells, and left incubating for 3 hours at 37°C. Then, absorbance was read at 490 nm using a microplate reader (Synergy H1, BioTek Instruments). For the CyQUANT assay, after incubation time, 200 µL of CyQUANT buffer solution was added to each well, and cells were incubated for 5 min at RT. Fluorescence measurements were made using a microplate reader (Synergy H1, BioTek Instruments) with excitation at 480 nm and emission detection at 520 nm. Twelve replicate wells were prepared for each condition. GraphPad Prism (version 9.3.0, GraphPad Software Inc., USA) was used to perform the statistical analyses. The experiment was repeated at least one time to validate the initial results.

III.2.5.5. Colony formation assay

PCa cells were seeded into 6-well plates (500 cells/well, each condition was prepared in triplicates) and cultured at 37°C in 5% CO₂. Two weeks after seeding, cells were fixed with 4% paraformaldehyde for 10 min at RT. After washing three times with water, the fixed cells were stained with Sulforhodamine B for 20 min, washed five times with 2% acetic acid, and left airdried overnight. Then, Sulforhodamine B was solubilized with 10 mM Tris-base and absorbance was measure using a microplate reader (Synergy H1, BioTek Instruments) at 570 nm. GraphPad Prism (version 9.3.0, GraphPad Software Inc.,

USA) was used to perform the statistical analyses. The experiment was repeated at least one time to validate the initial results.

III.2.5.6. Wound healing assay

A total of 200.000 cells were seeded in 12-well plates, each condition in triplicates. 24h after incubation, wounds were created by scrapping monolayer cells with a 200 μ L pipette tip, and non-adherent cells were removed from the medium. Cells were allowed to migrate across the wound, and a phase-contrast Leica Dmi8 microscope (Leica Microsystems GmbH, Germany) was used to take pictures at different times until the wound was closed. Cell migration was calculated as the rate of cells moving towards the scratch area. ImageJ software with the Wound healing size tool plug-in, was used to measure the wound area. GraphPad Prism (version 9.3.0, GraphPad Software Inc., USA) was used to perform the statistical analyses. The experiment was repeated at least one time to validate the initial results.

III.2.5.7. Co-immunoprecipitation assay

For co-immunoprecipitation assay, 1×10^6 cells were seeded on 100 mm dishes and incubated at 37°C for 48 h. Three replicates were prepared for each condition. After incubation time, 10 μ M MG132 was used and cells were incubated for 5 h before harvesting for protein extraction. Following protein extraction and quantification, 1 mg of protein lysates were incubated with PierceTM anti-Myc magnetic beads (Thermo Scientific) at RT for 1 h. Then, after washing the beds with cold 1X cell lysis buffer (Cell Signaling Technology) for three times, the immunoprecipitated protein complexes were collected and analyzed by mass spectrometry and western blot. The mass spectrometry analyses were conducted by the Proteomics Facility at the Universitat de València.

IV. RESULTS AND DISCUSSION

IV.1. CHARACTERIZATION OF METABOLIC CHANGES RELATED TO PCa PROGRESSION

IV.1.1. PCa metabolic profile

NMR experiments were acquired using a 500 MHz spectrometer, obtaining good quality spectra in urine and serum samples. A representative ^1H -CPMG and ^1H -NOESY spectrum from a serum and urine sample of a PCa patient is shown in Figure 10 and Figure 11, respectively. The metabolic profile of serum samples was dominated by a combination of signals from high- and low-molecular weight metabolites, including peaks from glycoproteins, unsaturated fatty acids, amino acids, sugars and organic acids. On the other hand, the metabolic profile of urine was characterized by signals from a wide range of low-molecular weight analytes of different chemical classes, including organic acids, amino acids, polysaccharides and simple sugars.

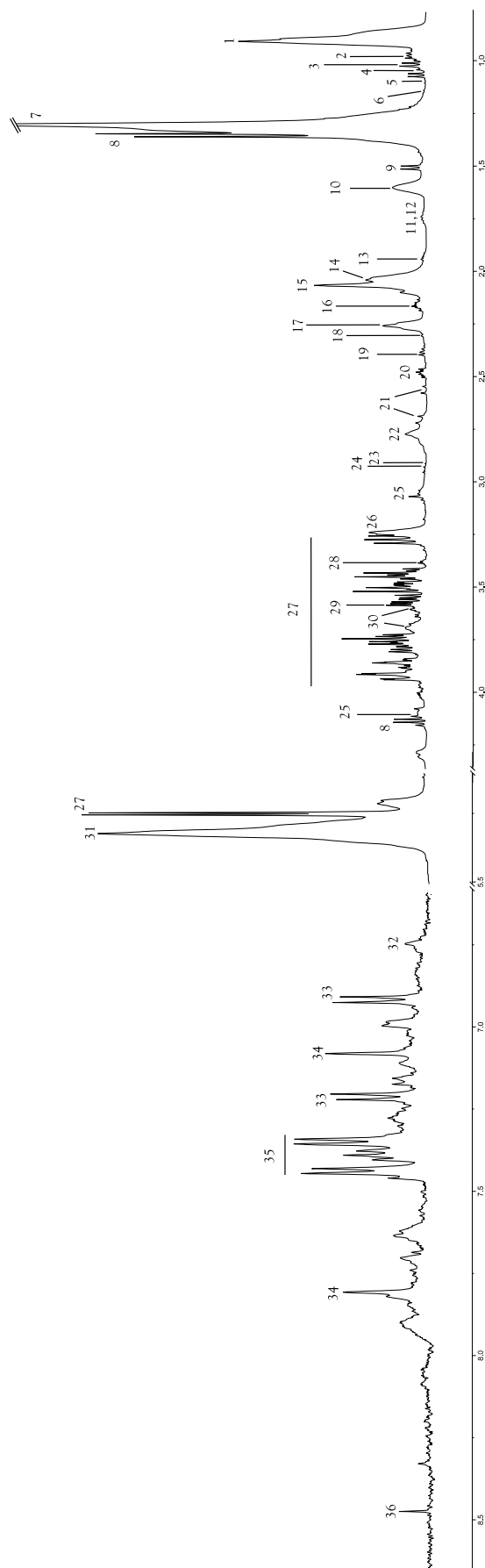


Figure 10. Metabolite assignation of a representative ^1H -CPMG serum spectrum of a PCa sample. The water and the urea region have been excluded from the spectrum. The aromatic region of the spectrum is magnified. Metabolic assignation: 1, HDL; LDL; VLDL (-CH3) lipoproteins; 2, leucine; 3, valine; 4, isoleucine; 5, methylsuccinate; 6, propylene glycol; 7, HDL; LDL; VLDL (-CH₂)_n lipoproteins; 8, lactate; 9, alanine; 10, lipids (-CH₂-CH₂CO); 11, lysine; 12, arginine; 13, acetate; 14, unsaturated fatty acids (-CH₂-CH₂-CH=CH-); 15, N-acetyl glycoproteins (NAG); 16, methionine; 17, lipids (-CH₂-CH₂CO); 18, acetoacetate; 19, succinate; 20, glutamine; 21, citrate; 22, polyunsaturated fatty acids (-CH=CH-CH₂-CH=CH₂); 23, trimethylamine; 24, N,N-dimethylglycine; 25, creatinine; 26, choline metabolites (choline; phosphocholine; glycerophosphocholine); 27, glucose; 28, scyllo-inositol; 29, glycine; 30, glycerol; 31, lipids (-CH=CH-); 32, fumarate; 33, tyrosine; 34, histidine; 35, phenylalanine; 36, formate.

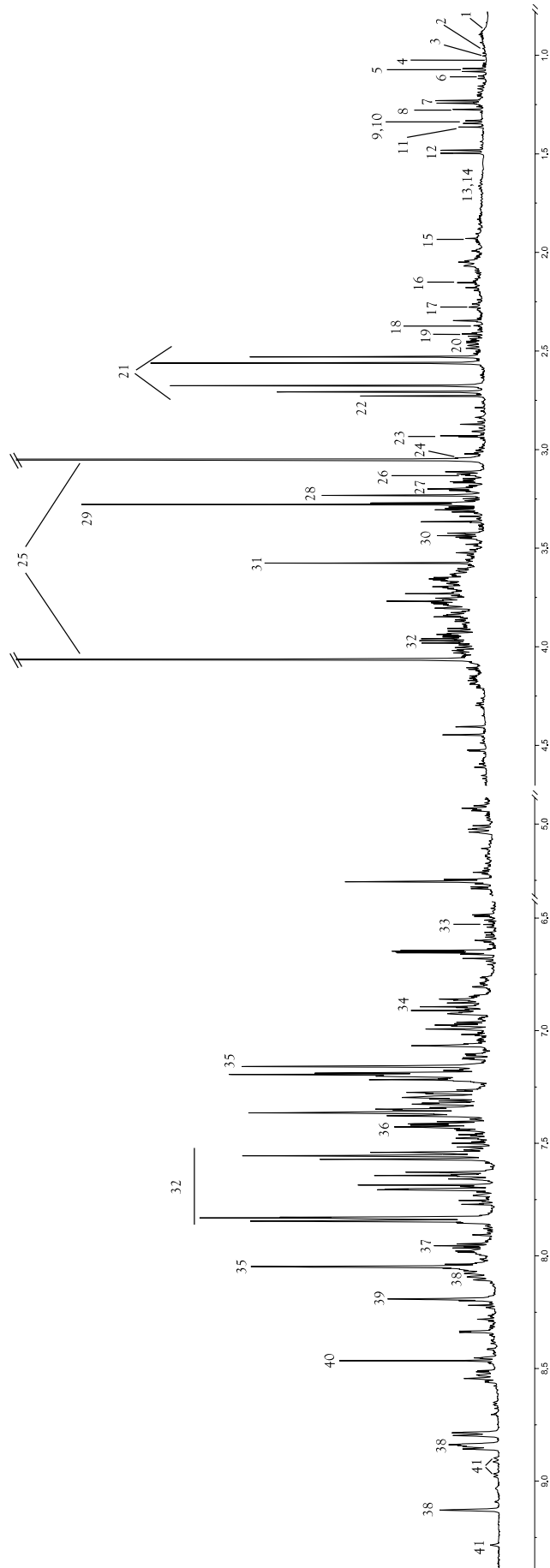


Figure 11. Metabolite assignment of a representative $^1\text{H-NOESY}$ urine spectrum of a PCa sample. The water and the urea region have been excluded from the spectrum. The aromatic region of the spectrum is magnified. Metabolic assignment: 1, 2-hydroxyisovalerate; 2, leucine; 3, valine; 4, isoleucine; 5, methylsuccinate; 6, 3-methyl-2-oxovalerate; 7, methylmalonate; 8, 3-hydroxyisovalerate; 9, lactate; 10, threonine; 11, 2-hydroxyisovalerate; 12, alanine; 13, lysine; 14, arginine; 15, acetate; 16, methionine; 17, acetoacetate; 18, pyruvate; 19, succinate; 20, glutamine; 21, citrate; 22, dimethylamine; 23, N-N-dimethylamine; 24, creatine; 25, creatinine; 26, cis-aconitate; 27, choline; 28, carnitine; 29, TMAO; 30, taurine; 31, glycine; 32, hippurate; 33, fumarate; 34, tyrosine; 35, histidine; 36, phenylalanine; 37, xanthine; 38, trigonelline; 39, oxypurinol; 40, formate; 41, 1-methylnicotinamide.

IV.1.2. Sample heterogeneity and outlier detection

Non-supervised PCA and visual inspection of the spectra were combined to conduct a preliminary analysis of the NMR data. This exploratory analysis enabled:

- i) The identification of samples exhibiting differences in their metabolic profile. Exhaustive examination of their spectra allowed to define them as outliers and remove them from the analysis.
- ii) The evaluation of sample homogeneity to identify potential trends and/or grouping due to clinical or processing variables that could interfere with the analysis.

Individual analysis of serum and urine spectra resulted in the identification of a subset of samples exhibiting unusual peaks. These samples were thoroughly analyzed to better understand the reason of their different behavior and evaluate their possible exclusion of the study. The score plot corresponding to the set of serum and urine samples is represented in Figure 12.

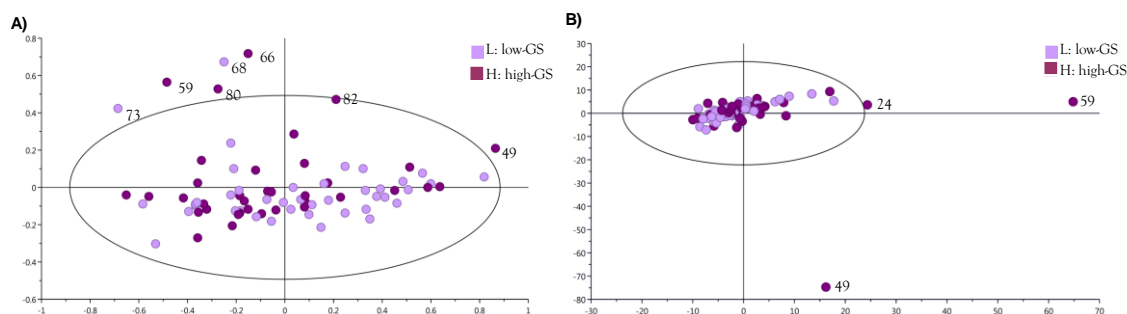


Figure 12. PCA score plots of (A) serum and (B) urine global metabolic profile of low- and high-GS PCa patients

- Outlier identification in serum samples

The analysis of the score plots generated from serum samples enabled the identification of two outliers (S66 y S68), that showed a different behavior compared to the rest of samples (Figure 13A-B). The visual inspection of their metabolic profile showed peaks at 1.20 ppm and 3.70 ppm, corresponding to ethanol (Figure 13C). In addition, although S02 sample was inside the limits of the score plot, the visual inspection of its spectrum also revealed peaks corresponding to ethanol. To determine whether these profiles were exclusively found in serum samples, the urine profile of those same patients

was also examined. Notably, unusually intense ethanol signals were also observed in the NMR spectra of urine samples from those patients (Figure 13D). Additionally, the clinical history of these patients was thoroughly revised, however, none of the available information could be associated with the presence of these signals, suggesting diet as their potential source. Taking into consideration that these spectra could not be compared to the others, and that one of the inclusion criteria in this study was the sample collection under fasting conditions, these samples were not included in the analysis.

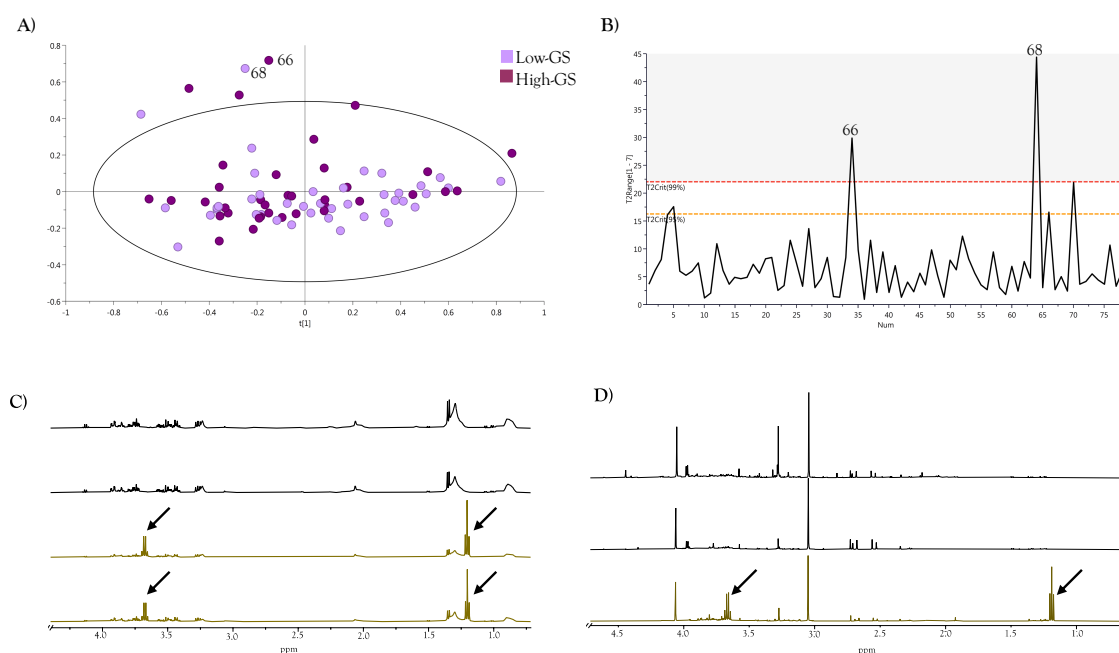


Figure 13. Outlier identification based on the non-supervised PCA. A) Score plot and B) T^2 Hotelling of all serum samples ($n = 78$) where S66 and S68 were identified as potential outliers. Comparison of C) serum ^1H -CPMG profile of S66 and S68 samples (yellow) and D) urine ^1H -NOESY spectrum of U02 sample (yellow) against a representative sample subset (black), highlighting the peaks corresponding to ethanol.

Another potential outlier (S13) was also identified during the visual inspection. This sample exhibited abnormal peaks at 2.60 ppm and 3.15 ppm corresponding to EDTA (Figure 14). The presence of EDTA signals is associated with the type of tubes used for sample collection. Considering that these peaks could interfere with the metabolic analysis and that EDTA is added to plasma samples to stop clotting, this sample was excluded from the analysis.

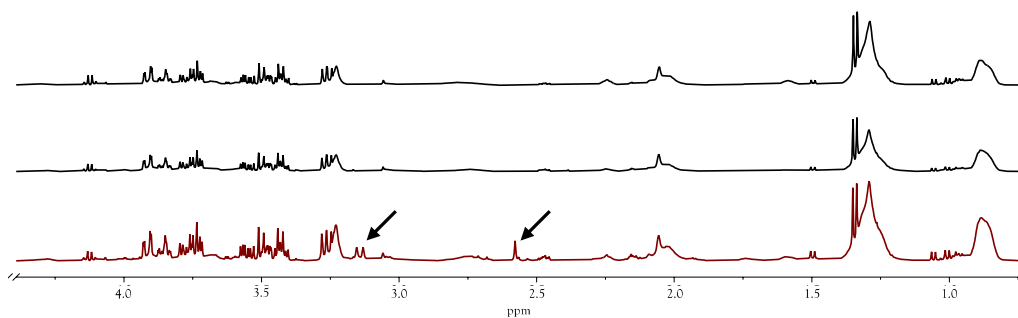


Figure 14. Identification of an outlier sample exhibiting peaks corresponding to EDTA. Comparison of the serum ^1H CPMG spectrum of the S13 sample (red) against a representative sample subset (black).

The serum score plot generated after excluding these four samples showed a small sample subset (S49, S59, S73, S80 and S82) exhibiting a different behavior compared to the rest of samples (Figure 15A). The visual inspection of their metabolic profile showed unusually elevated glucose levels (Figure 15B). To better understand this abnormal behavior, a detailed inspection of the clinical history was conducted, revealing that these patients were diabetic. To determine whether this profile was also observed in the urine of these patients, the urinary spectra was examined, also showing abnormally high glucose levels (Figure 15C). Notably, the presence of these intense signals in the NMR spectra precluded the accurate quantification of other metabolites present in the spectra due to the overlap of glucose signals with other metabolite signals. In addition, the presence of such intense signals could also affect to the intensity of the other signals in the spectra. Thus, considering that one of the inclusion criteria in this study was that PCa patients should not have any diseases, other than PCa, and that this clinical condition showed a significant reflection in the metabolomic profile, all diabetic patients were excluded for further analyses.

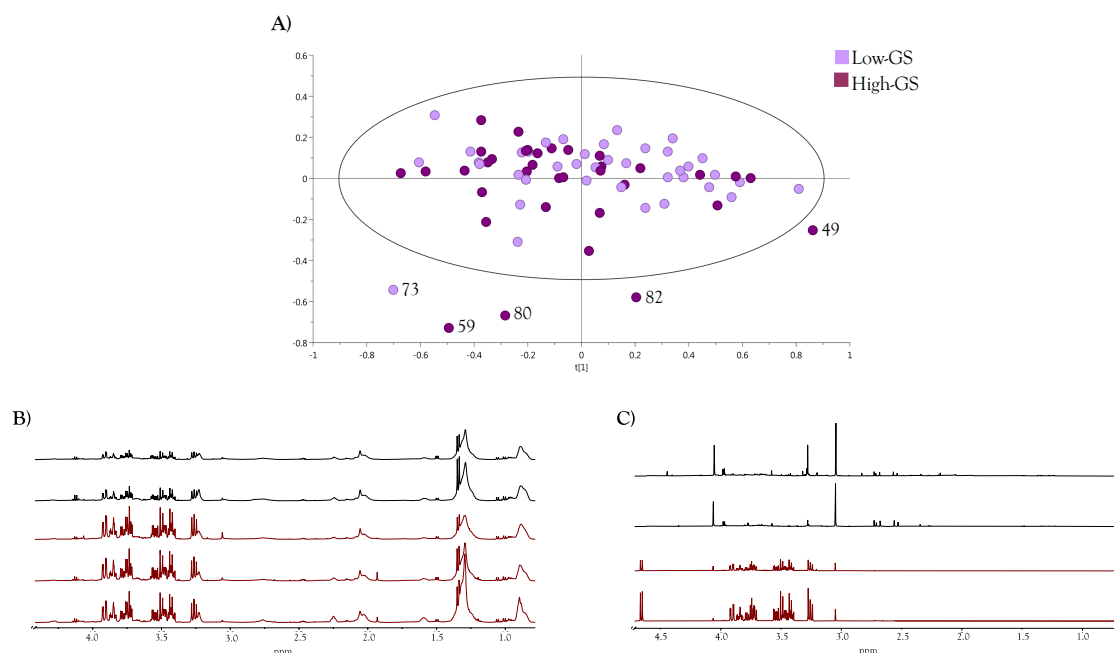


Figure 15. Outlier identification after sample exclusion, based on the non-supervised PCA. A) Score plot of serum samples ($n = 74$) where S49, S59, S73, S80 and S82 were identified as potential outliers. Comparison of B) serum ^1H -CPMG profile of S59, S80 and S82 samples (red) and C) urine ^1H -NOESY spectrum of U49 and U59 samples (red), exhibiting abnormally elevated glucose levels, against a representative sample subset (black).

○ URINE

As it is showed in the score plot of Figure 12, two of the urine samples exhibited a very different metabolic profile compared to the rest of samples. The examination of their clinical history revealed that these patients were the same diabetic samples that were identified in the analysis of the serum profile. After excluding all diabetic patients and the samples containing ethanol peaks, the PCA score plot of the urine samples is represented in Figure 16.

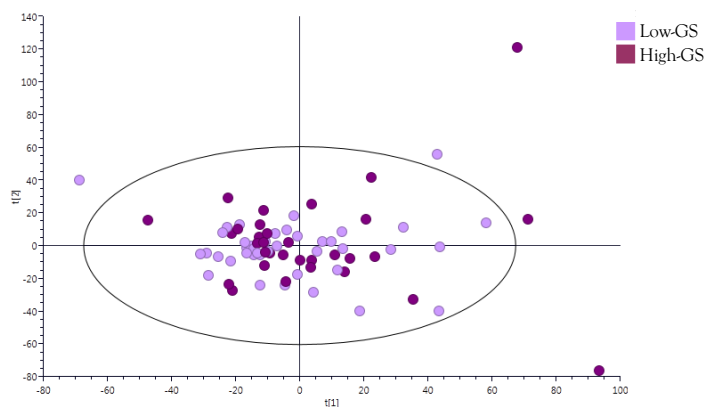


Figure 16. Score plot of all urine samples ($n = 73$) of low- and high-GS PCa patients

The metabolic profile and the clinical history of the samples found to be outside of the confidence interval in the score plot and the T^2 Hotelling graph were examined, but there was any significant clinical or technical reason to exclude them from the analysis. Thus, all samples were included in further analyses.

A summary of the reason for exclusion of serum and urine samples removed from the analysis is presented in Table 12.

Table 12. Subset of samples excluded from the study

Biofluid	Subgroup	Patient ID
Serum	(i) Presence of contaminants	EDTA: S13 Ethanol: S02, S66, S68
	(ii) Abnormal intense signals	Glucose: S16, S19, S36, S49, S59, S73, S80, S82
Urine	(i) Presence of contaminants	Ethanol: U02, U66, U68
	(ii) Abnormal intense signals	Glucose: U16, U19, U36, U49, U59, U73, U80, U82

Clinical characteristics of the individuals finally included in the study are summarized in Table 13.

Table 13. Clinical characteristics of PCa patients included in the metabolic study

	Serum (n = 66)		Urine (n = 73)	
	Low-GS	High-GS	Low-GS	High-GS
Number of patients (%)	36 (54.5%)	30 (45.5%)	41 (56.16%)	32 (43.84%)
Age (years)	65.69 ± 6.61	64.33 ± 11.60	65.66 ± 6.95	64.47 ± 11.23
BMI (kg/m ²)	25.02 ± 2.87	26.68 ± 7.66	26.43 ± 3.08	26.73 ± 7.34
Prostate volume (ml)	44.26 ± 22.71	44.18 ± 23.71	43.71 ± 22.46	42.42 ± 23.83
PSA (ng/ml)	5.93 ± 3.65	70.70 ± 179.19	5.78 ± 3.48	66.68 ± 174.04

BMI: Body Mass Index, GS: Gleason Score, PSA: Prostate Specific Antigen, SD: standard deviation. Values expressed as mean ± SD.

- Sample homogeneity

After outlier detection and exclusion, non-supervised PCA models were built to assess the potential influence of different clinical variables (age, BMI, metastatic disease and serum levels of PSA) on the metabolic profile of serum and urine samples. As shown

in Figure 17, the non-supervised analysis of the global metabolic profiles did not reveal any significant sample clustering according to any of the tested variables.

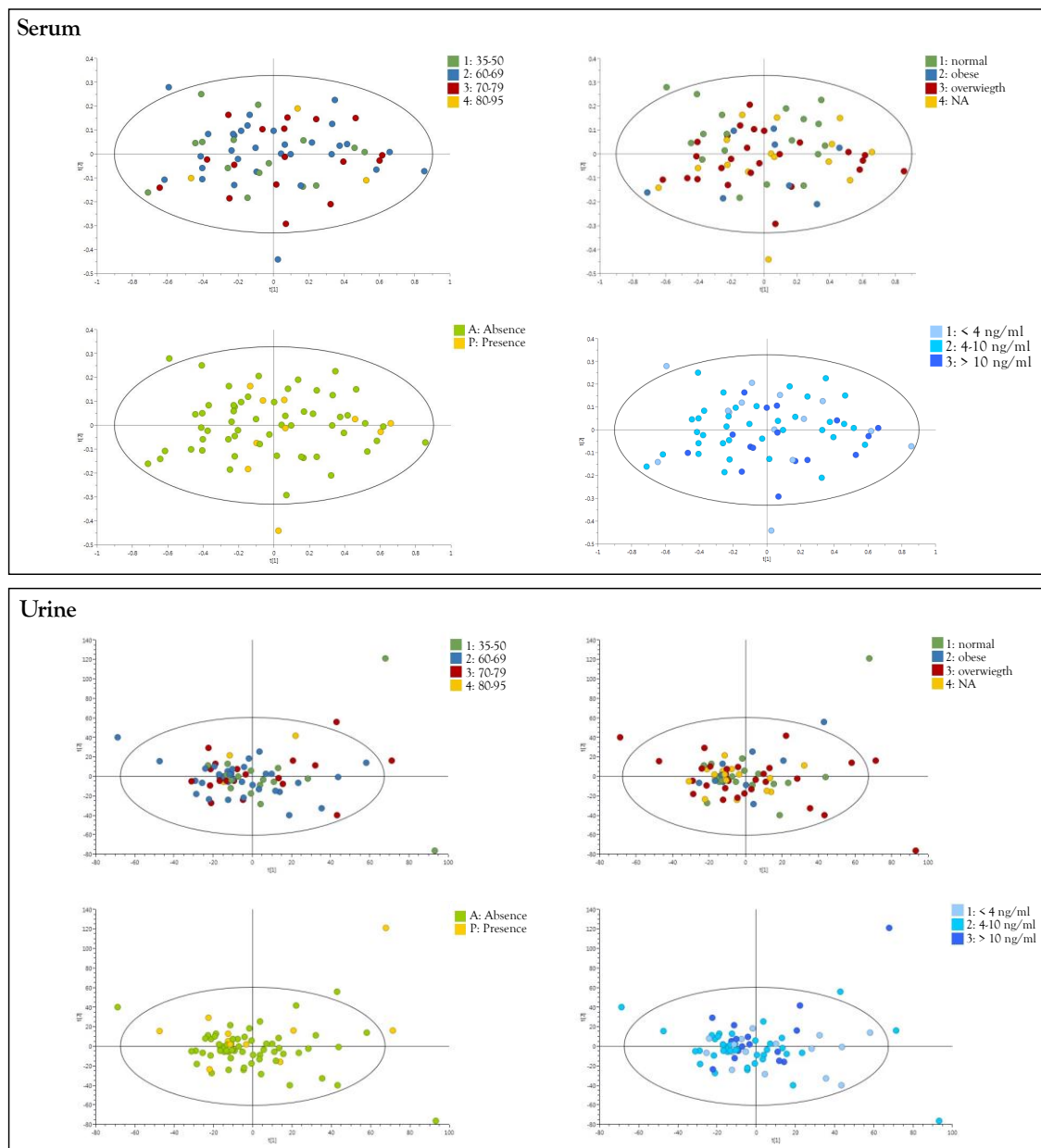


Figure 17. PCA score plots of serum and urine samples included in the study. Samples are colored based on the evaluated clinical variables. A) Age: 1, 35-50; 2, 60-69; 3, 70-79; 4, 80-95 years old, B) Body mass index: 1, normal; 2, obese; 3, overweight; 4, NA, C) Metastatic disease: A, absence; P, presence, D) PSA serum levels: 1, < 4; 2, 4-10; 3, >10 ng/ml.

In addition, a PCA model was also generated to determine whether samples were grouped according to the two defined GS groups. As shown in Figure 18, samples were not

clustered based on the GS, and exhibited a homogenous distribution in both serum and urine profiles.

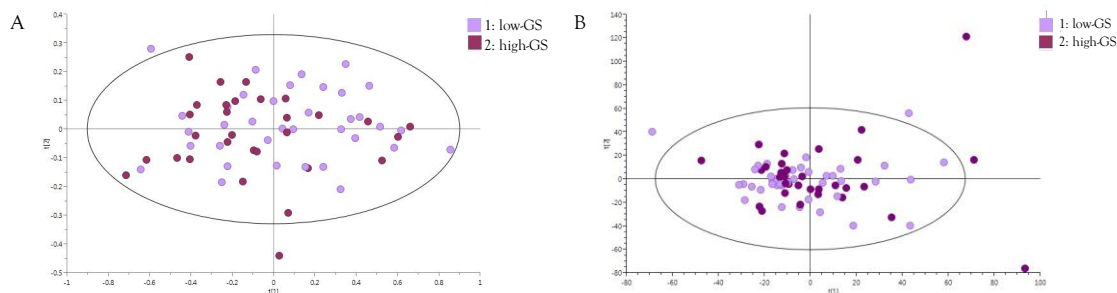


Figure 18. Unsupervised statistical analysis. PCA score plots of A) serum and B) urine global metabolic profile colored by GS variable: 1, low-GS; 2, high-GS group.

IV.1.3. Untargeted metabolomics analysis of low- and high-GS PCa patients

First, to examine potential differences between the two groups of study, supervised analysis (OPLS-DA) aiming at discriminating the serum and urinary profiles from low- and high-GS PCa patients were generated. Although both models showed a reasonable fitting of the data ($R^2Y = 0.227$ and 0.556 for serum and urine, respectively), these multivariate models revealed low discrimination between low- and high-GS groups ($Q^2 = 0.0231$ and -0.256 for serum and urine, respectively) (Figure 19). Thus, based on the Q^2 value, none of the OPLS-DA models exhibited significant predictive power.

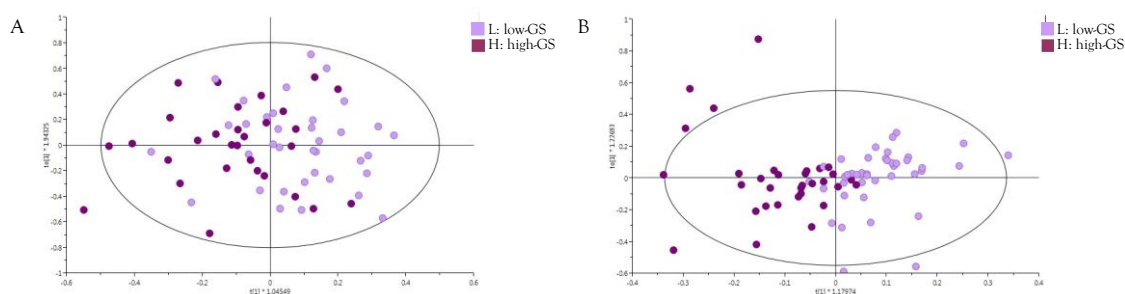


Figure 19. Supervised statistical analysis. OPLS-DA score plot of A) serum and B) urine metabolic profiles comparing PCa patients from low- (L) vs high- (H) GS groups.

This result may be reflecting that the differences between the groups of study were rather small or that there was a high intragroup variability within the groups of study. Interestingly, in a large study performed on urine samples from BPH and PCa patients,

significant metabolic differences could only be observed when conducting univariate statistical analyses (Bruzzone et al., 2020). In addition, in another metabolic study evaluating the potential use of urine samples to discriminate among control individuals (including BPH condition) and PCa patients, both groups could only be separated when considering a specific spectral interval (Zaragoza et al., 2014). Thus, the difficulty in discriminating between our groups of study may highlight the multifactorial nature of PCa, and the low impact of prostate alterations in the biofluid composition (Bruzzone et al., 2020; Dell'Atti, 2016).

Furthermore, the OPLS-DA models were internally validated by a permutation test. For the serum analysis, when comparing the random experimental $R^2(Y)$ and $Q^2(Y)$ values with the values from the original dataset, these intercept values were not significantly higher ($R^2(Y) = 0.168$ and $Q^2(Y) = -0.177$) than the ones obtained with the permutation analysis (Figure 20A). These values suggested that there were not any differences when the model was generated by correctly or randomly distributing the samples into the two groups of study, also resulting in a very low predictive ability of the model.

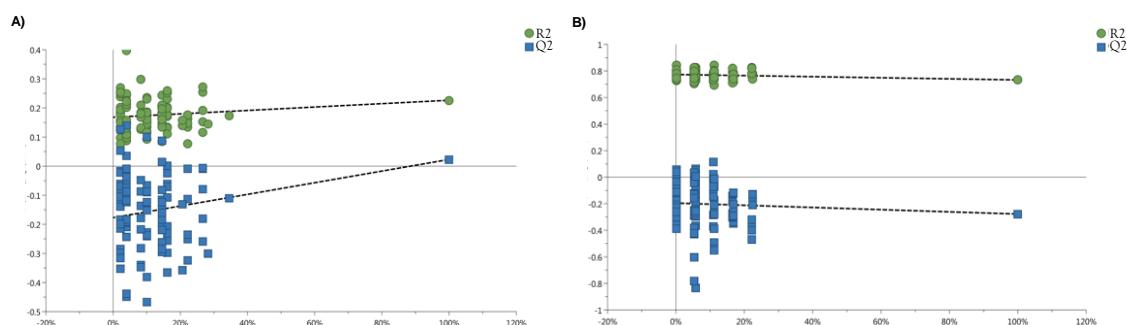


Figure 20. Internal validation of the OPLS-DA models using the permutation test. Result of the permutation tests obtained from the A) serum and B) urine OPLS-DA model obtained from 100 random permutations. The Y axis shows the values of R^2Y and Q^2Y for each of the 100 generated models, and the X axis represents the correlation coefficients between the permuted and the original model.

On the other hand, in the permutation analysis of the urine dataset (Figure 20B), the intercept values $R^2(Y)$ and $Q^2(Y)$ values were higher ($R^2(Y) = 0.773$ and $Q^2(Y) = -0.195$) than the ones from the original dataset. Although the $Q^2(Y)$ value was below 0.05, the $R^2(Y)$ was higher than 0.4, suggesting that the model was over-fitted. The overfitting observed in the urine model may be explained by the low number of samples compared to the high

number of buckets. This is particularly important in urine analysis, as spectra are divided into smaller buckets due to the high number of signals present in urine samples. In addition, another important factor that could contribute to overfitting is the high variability of urine samples, as it may complicate to uncover differences between the groups of study.

An alternative to overcome the overfitting problem could be to decrease the number of variables following a targeted approach, where variables that greatly contribute to discriminate among the groups of study would be selected, while redundant or non-informative variables would be excluded.

Notably, the overall systemic metabolism exhibits higher variations that could mask tumor-associated metabolites (e.g., biochemical processes occurring at other body parts, diet, age, drug administration, etc.). In this context, data availability of tumor samples, that are localized at the site of the disease, may contribute to investigate how much of the tumor metabolism is reflected in biofluid samples and identify more robust and sensitive biomarkers. Thus, to characterize significant metabolic differences between low- and high-GS patients, we targeted the NMR analysis on metabolites involved in specifically altered metabolic pathways between both PCa groups. To that end, data from publicly available PCa transcriptomics datasets was used to perform a GSEA for the identification of dysregulated metabolic pathways between both groups of interest.

IV.1.4. Identification of dysregulated metabolic pathways between low- and high-GS PCa patients

After searching on the GEO repository, three published PCa transcriptomics studies met the established criteria (GSE16560 (Sboner et al., 2010), GSE46602 (Mortensen et al., 2015) and GSE70768 (Ross-Adams et al., 2015)), and were used to perform a GSEA for the identification of dysregulated metabolic pathways. Characteristics of the three selected PCa studies are shown in Table 14. Data integrity was evaluated in all datasets, and any sample was removed from the analysis after generating PCA plots (Appendix 3).

Table 14. Characteristics of selected PCa transcriptomic studies

Study ID	Analytical platform ID	Number of genes	Number of samples	Experimental groups
GSE16560	GPL5474	6100	281	Low-GS (n=83); High-GS (n=198)
GSE46602	GPL570	23495	36	Low-GS (n=17); High-GS (n=19)
GSE70768	GPL10558	30947	122	Low-GS (n=17); High-GS (n=105)

GS: Gleason Score, ID: Identification

From the GSEA, a total of 36 metabolic routes were found to be significantly altered (p-value < 0.05) between the low- and high-GS groups (Appendix 4). Although different metabolic routes were dysregulated in each transcriptomic study, probably due to differences in array size and the genes included in each analytical platform, significantly dysregulated metabolic pathways were shared between all three datasets (Figure 21).

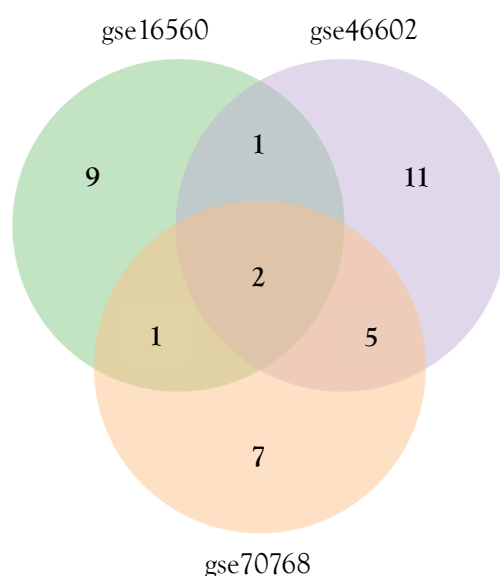


Figure 21. Venn diagram representing the overlap between the results obtained for the GSEA of the different PCa transcriptomic datasets included in the analysis

Interestingly, among the top ten most significantly altered metabolic pathways, listed in Table 15, different multi-omics studies also identified changes in purine and histidine metabolism (C. Li et al., 2013; Lima et al., 2021; W. Liu et al., 2015), and in the steroid hormone biosynthesis pathway (W. Liu et al., 2015) when comparing primary tumors *vs* benign tissue or metastatic PCa samples.

Table 15. Top ten most significantly enriched metabolic pathways

ID KEGG	Pathway name	LOR ^a	p-value ^b	FDR ^c
hsa00190	Oxidative phosphorylation	0.8950	1.33E-18	5.14E-16
hsa00240	Pyrimidine metabolism	0.6645	2.57E-09	4.94E-07
hsa00230	Purine metabolism	0.4492	4.04E-08	5.19E-06
hsa00830	Retinol metabolism	-0.8751	3.90E-06	0.0016
hsa01230	Biosynthesis of amino acids	0.5104	0.0002	0.0155
hsa00140	Steroid hormone biosynthesis	-0.6065	0.0002	0.0432
hsa00900	Terpenoid backbone biosynthesis	0.7854	0.0003	0.0228
hsa01200	Carbon metabolism	0.3306	0.0005	0.0722
hsa00350	Tyrosine metabolism	-0.6329	0.0007	0.0942
hsa00340	Histidine metabolism	-0.7859	0.0010	0.0970

FDR: False Discovery Rate, ID: Identification, KEGG: Kyoto Encyclopedia of Genes and Genomes, LOR: Log Odds Ratio. ^a Positive and negative LOR values indicate that the pathway is enriched with genes up- and down-regulated in the high-GS PCa group. ^b p-value calculated using the Mann-Whitney U test. ^c p-value corrected by the Benjamini-Yekutieli (BY) procedure.

In addition, some of these dysregulated routes, including purine and pyrimidine metabolism and oxidative phosphorylation (OXPHOS), have previously been associated with PCa progression. In particular, enhanced purine and pyrimidine metabolism has been observed in PCa and other tumor types to maintain nucleotide biosynthesis and support tumor cell proliferation (Barfeld et al., 2015; Kelly et al., 2016; Kodama et al., 2020; Y. Lv et al., 2020). The OXPHOS pathway plays a relevant role in energy production and is involved in tumor progression. In addition, given the heavy reliance of certain tumors on this pathway for ATP production, it has recently emerged as a promising target for cancer therapy (Ashton et al., 2018; Nayak et al., 2018; Sica et al., 2020). Regarding PCa, pyrimidine metabolism was associated with high Gleason grade and more aggressive tumors (Penney et al., 2011), while the OXPHOS pathway was reported to be activated in high-grade PCa (Kelly et al., 2016). These two metabolic pathways were found to be significantly dysregulated in all three transcriptomic studies.

IV.1.5. Targeted analysis of low- and high-GS PCa patients' metabolic profile

For the targeted analysis, only metabolites included in the 36 dysregulated pathways were considered. Among all selected metabolites, peaks corresponding to 23 and 22

metabolites were integrated and quantified in serum and urine $^1\text{H-NMR}$ spectra, respectively. Univariate statistical analyses were conducted to compare the intensity levels of these metabolites between low- and high-GS PCa patients, and the results are summarized in Table 16 for serum and Table 17 for urine analyses.

Table 16. Mean intensities and variations for the metabolites identified in the serum samples of low- and high-GS PCa patients

Metabolite	Mean low-GS	SD low-GS	Mean high-GS	SD high-GS	p-value ^a	FC	% variation ^b	Direction ^c
Glucose	48,5827	7,8779	53,6112	7,8767	0,0150	1,1035	10,3504	↑
Glycine	2,8665	0,6326	3,0893	0,5310	0,0369	1,0777	7,7730	↑
Phenylalanine	2,6653	0,5504	2,8567	0,4964	0,0765	1,0718	7,1806	↑
Scyllo-inositol	0,7631	0,1897	0,8178	0,1818	0,2457	1,0717	7,1655	↑
Formate	0,0630	0,0157	0,0659	0,0154	0,3872	1,0468	4,6777	↑
Acetate	1,0986	0,2009	1,1464	0,2149	0,4461	1,0435	4,3507	↑
Citrate	2,1463	0,4163	2,2267	0,3693	0,3463	1,0375	3,7484	↑
Acetoacetate	1,2676	0,1825	1,3125	0,2519	0,7443	1,0354	3,5441	↑
Arginine/Lysine	9,0840	1,1895	9,3924	1,1613	0,3732	1,0339	3,3944	↑
Valine	3,8874	0,7271	4,0092	0,6068	0,3943	1,0313	3,1337	↑
Glutamine	5,5521	1,1009	5,6804	1,0345	0,6133	1,0231	2,3116	↑
Leucine	3,9624	0,5109	4,0243	0,4131	0,4616	1,0156	1,5617	↑
Lactate	60,0575	10,4254	59,2342	8,6205	0,9643	0,9863	1,3708	↓
Fumarate	0,5427	0,0913	0,5498	0,0992	0,6589	1,0132	1,3194	↑
Trimethylamine	0,3561	0,0528	0,3608	0,0575	0,8429	1,0131	1,3053	↑
Alanine	6,6098	1,1125	6,6874	0,9480	0,5517	1,0117	1,1733	↑
N,N-dimethylglycine	0,6652	0,1027	0,6723	0,1141	0,8629	1,0107	1,0683	↑
Propylene glycol	1,2123	0,0679	1,2005	0,0482	0,2108	0,9902	0,9803	↓
Isoleucine	1,0214	0,1096	1,0147	0,0919	0,9847	0,9935	0,6549	↓
Succinate	0,9430	0,2268	0,9485	0,1862	0,7154	1,0059	0,5862	↑
Tyrosine	0,8111	0,1758	0,8153	0,1461	0,6964	1,0052	0,5168	↑
Histidine	0,7557	0,1223	0,7596	0,1227	0,9643	1,0052	0,5156	↑
Methylsuccinate	0,9494	0,0884	0,9511	0,0734	0,9847	1,0018	0,1816	↑

SD: standard deviation, FC: fold change. ^a p-value calculated using the Mann-Whitney U test. ^b Mean signal intensity variation between groups (%). ^c Direction of the variation, considering the low-GS group as a reference.

Table 17. Mean intensities and variations for the metabolites identified in the urine samples of low- and high-GS PCa patients

Metabolite	Mean low-GS	SD low-GS	Mean high-GS	SD high-GS	p-value ^a	FC	% variation ^b	Direction ^c
Phenylalanine	12,4293	6,5254	15,9270	11,5533	0,4098	1,2814	28,1407	↑
4-Py	13,8703	9,7431	11,4132	9,6532	0,1540	0,8229	17,7146	↓
Lactate	12,7163	10,8158	10,8707	3,5066	0,8727	0,8549	14,5139	↓
1-methylnicotinamide	0,2219	0,1915	0,2528	0,0911	0,0056	1,1395	13,9466	↑
Methylmalonate	9,8610	4,3057	8,5232	2,3148	0,1355	0,8643	13,5660	↓
Acetoacetate	8,4185	3,1900	9,3849	3,9161	0,3384	1,1148	11,4792	↑
Alanine	10,4308	3,1810	9,4522	1,8824	0,4226	0,9062	9,3819	↓
3-hydroxyisovalerate	4,6490	0,9309	4,2404	1,0895	0,0707	0,9121	8,7900	↓
2-furoylglycine	1,4283	0,7950	1,3033	0,6604	0,6013	0,9125	8,7542	↓
Isobutyrate	3,7875	0,8659	3,4973	0,7745	0,1348	0,9234	7,6631	↓
Citrate	44,4248	16,6546	47,8244	23,8925	0,9604	1,0765	7,6525	↑
Formate	1,1654	0,3651	1,2270	0,4054	0,4757	1,0528	5,2847	↑
Leucine	1,4110	0,3517	1,3486	0,2213	0,7445	0,9558	4,4222	↓
Carnitine	11,3446	4,8417	11,8231	7,1531	0,8727	1,0422	4,2179	↑
Methanol	6,2374	1,9472	5,9919	1,1823	0,9252	0,9606	3,9356	↓
Glycine	16,3502	5,5583	15,7644	4,8645	0,6624	0,9642	3,5828	↓
Valine	2,3994	0,4984	2,3369	0,3390	0,9164	0,9740	2,6047	↓
Trigonelline	1,2269	1,1233	1,1966	0,9148	0,4688	0,9753	2,4710	↓
Creatinine	123,5729	20,1437	122,1583	18,4016	0,9956	0,9886	1,1448	↓
Isoleucine	0,6135	0,1442	0,6095	0,1145	0,9512	0,9934	0,6559	↓
3-methyl-2-oxovalerate	4,1272	0,8293	4,1458	1,2483	0,5767	1,0045	0,4500	↑
Taurine	26,3869	5,4990	26,3335	8,7617	0,5322	0,9980	0,2023	↓

SD: standard deviation, FC: fold change, 4-Py: N1-Methyl-4-pyridone-5-carboxamide. ^ap-value calculated using the Mann-Whitney U test. ^b Mean signal intensity variation between groups (%). ^c Direction of the variation, considering the low-GS group as a reference.

From these statistical analyses, metabolites exhibiting higher variations in intensity between low- and high-GS PCa patients are represented in Figure 22. In particular, compared to the low-GS group, the serum metabolic profile of high-GS PCa patients was characterized by significantly high concentrations of glucose and glycine, while the urine of those same patients was dominated by markedly increased levels of 1-methylnicotinamide. Interestingly, although non-statistically significant, relevant alterations in the levels of phenylalanine (over 7%) were found in both biofluids for high-GS patients.

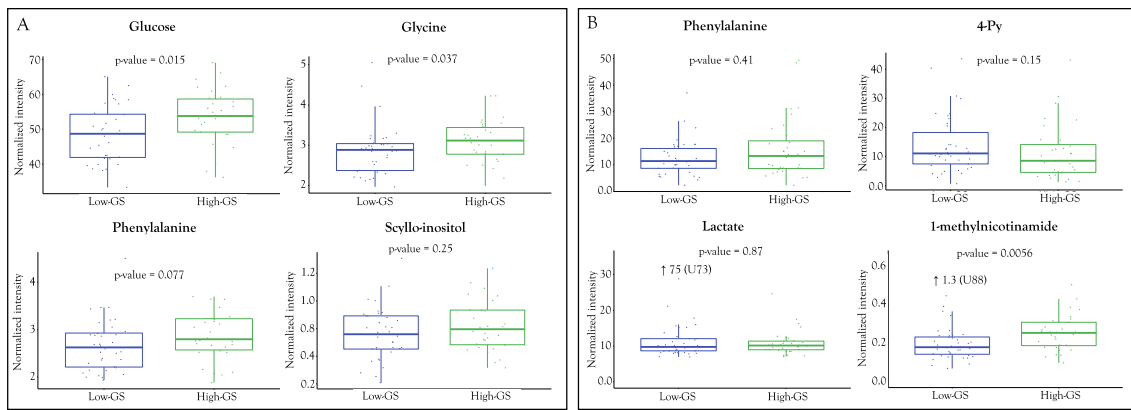


Figure 22. Boxplot representing the normalized (A) serum and (B) urine intensities of the metabolites showing higher variations in intensity between the groups of study. For each box, the central line is the median, the edges of the box are the upper and lower quartiles, the whiskers extend the box by a further ± 1.5 interquartile range (IQR), and samples are plotted as individual points. p-value represented above the boxplots and calculated using the Mann-Whitney U test. 4-Py: N1-Methyl-4-pyridone-5-carboxamide, GS: Gleason Score.

IV.1.6. Biological interpretation

The most relevant genetic and metabolic alterations found when comparing both groups of interest are summarized in Figure 23. Together, the transcriptomic and metabolic analysis revealed that high-GS PCa patients exhibited alterations in energy metabolism and nucleotide synthesis.

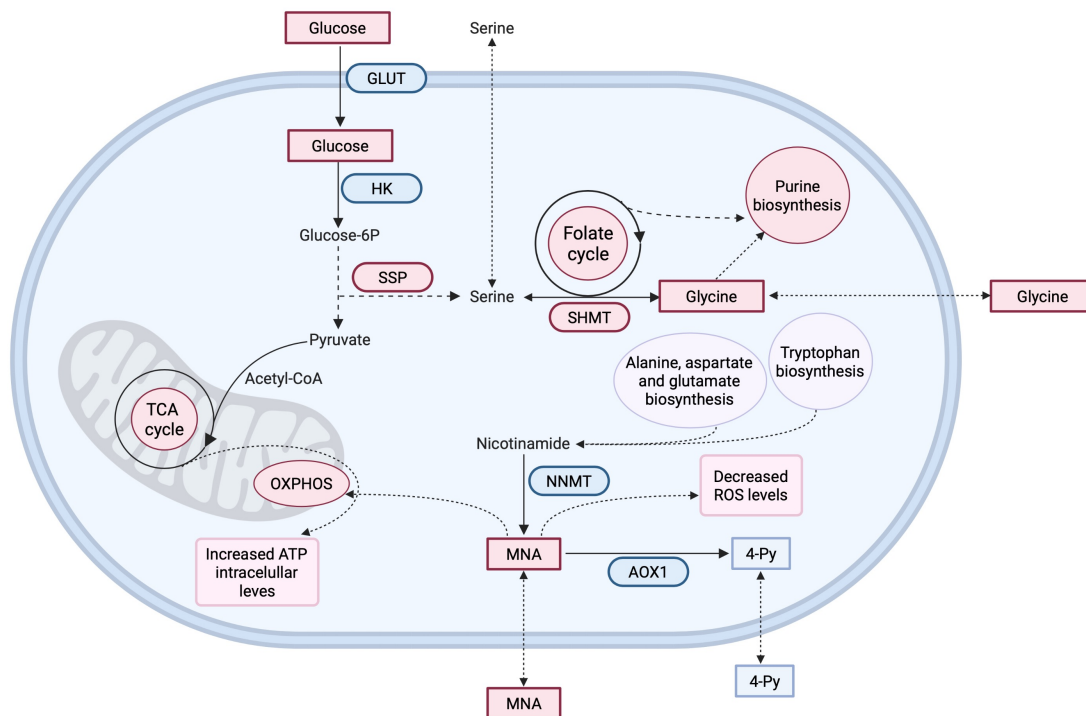


Figure 23. Schematic representation of the genetic and metabolic alterations found for the comparison between low- and high-GS PCa patients. Red and blue fonts indicate increases and decreases, respectively, in high-GS PCa patients. Solid and dashed arrows are for direct and multistep reactions, respectively. 4-Py:

N1-methyl-4-pyridone-5-carboxamide, AOX1: aldehyde oxidase 1, ATP: adenosine triphosphate, glucose-6P: glucose 6-phosphate, GLUT: glucose transporter, HK: hexokinase, NNMT: nicotinamide N-methyltransferase, OXPHOS: oxidative phosphorylation, ROS: reactive oxygen species, SHMT: serine hydroxymethyl transferase, SSP: serine synthesis pathway, TCA: tricarboxylic acid cycle.

Glucose is involved in the glycolysis pathway, being transported inside the cell by glucose transporters (GLUT), and then converted to glucose-6-phosphate by hexokinase (HK) enzyme. Interestingly, most tumor types show increased glucose consumption to meet the high energetic demands and biosynthesis needs. This high rate of glucose uptake can be detected by 18F-fluorodeoxyglucose (FDG)-PET scanning. Nevertheless, other neoplastic conditions, including PCa, do not exhibit this metabolic profile showing low glucose rate, therefore, relying on alternative energy sources such as fatty acid oxidation for energy production (Y. Liu, 2006; Y. Liu et al., 2010; Wu et al., 2014). In line with our findings, increased glucose serum levels at the time of diagnosis were found to be positively associated with increased risk of recurrence in PCa patients (Wright et al., 2013). Furthermore, a different study also reported positive correlations between glucose serum levels and PCa risk (Wulaningsih et al., 2013). In addition, in agreement with the low rate of glucose consumption observed in some tumors types, the GSEA revealed a decreased glycolysis activity in the high-GS PCa group. This particular metabolic characteristic observed in that group of patients could explain the limitation of FDG-PET scanning and the higher sensitivity observed in choline-PET scans for PCa (Richter et al., 2010). In fact, many PCa tumors have showed elevated uptake of 18F-fluciclovine (a synthetic analog of leucine) and 11C-choline, that are being used in PET imaging for patient restaging or for detecting metastasis that may be missed by other imaging approaches (Savir-Baruch et al., 2017; Umbehr et al., 2013). Analyzing the transcriptomic data from the PCa datasets, the expression levels of enzymes and transporters involved in the glycolysis pathway, including GLUT and HK, were found to be down-regulated in high-GS patients. Taken together, those findings may support the idea that glucose was not being used as a primary energy source in those patients, but it was being accumulated due to decreased GLUT and HK expression and the subsequent slow glycolysis rate.

The metabolic univariate statistical analysis also revealed significant alterations in glycine levels between both groups of study. Notably, the role of glycine in cancer is

controversial. Different studies have identified decreased serum in high-grade PCa patients (Kumar et al., 2015) and reported associations between glycine uptake and tumor proliferation (Jain et al., 2012). Nevertheless, others have observed increased serum glycine in PCa patients (Kumar et al., 2016), and described an inhibitory effect on tumorigenesis due to an excess of glycine (Labuschagne et al., 2014; Rose et al., 1999). Moreover, in PCa tissue samples, glycine was found to be statistically significantly correlated with PCa progression (McDunn et al., 2013), and in a multi-omics study conducted on tissue samples, increased glycine levels were found in PCa tumors enriched in the TMPRSS2-ERG gene fusion (Hansen et al., 2016). Glycine and serine can be interconverted through the serine hydroxymethyl transferase (SHMT) enzyme, that is also involved in the folate cycle, an important pathway that provides metabolic intermediates for purine biosynthesis. Glycine can be converted to serine using 5,10-methylenetetrahydrofolate (5,10-methyleneTHF), a metabolite required to sustain enhanced nucleotide synthesis and cell growth. As this reaction would deplete the intracellular 5,10-methyleneTHF pools and slow proliferation, tumor cells may release glycine to limit its intracellular concentration favoring serine-to-glycine conversion and 5,10-methyleneTHF production (Dolfi et al., 2013). In this context, increased glycine serum levels observed in high-GS PCa patients could be explained by the use of serine, but not glycine, to support the one-carbon pool resulting in glycine accumulation, and the subsequent need to release glycine excess outside the cell to maintain an activated purine biosynthesis and tumor proliferation. This hypothesis was supported by the enhanced activity of the one-carbon pool by folate and purine biosynthesis, observed in the GSEA, together with the over-expression of SHMT and of the enzymes involved in serine synthesis pathway, including PHGDH, PSAT and PSPH, in the high-GS group.

In the urine metabolic profile, the univariate analysis showed significantly elevated levels of 1-methylnicotinamide (MNA) in high-GS PCa patients. This metabolite is involved in the nicotinate and nicotinamide metabolism pathway, and is converted from nicotinamide through nicotinamide N-methyltransferase (NNMT), and then further catabolized to pyridones (2-Py and 4-Py) by aldehyde oxidase (AOX1). Notably, a recently published study combining different omics data from benign and PCa tissues, found enhanced nicotinate and nicotinamide metabolism in tumor samples (Lima et al., 2021).

In addition, previous studies observed associations between MNA concentration and tumor progression. Particularly, in a colorectal cancer study, this metabolite was reported to enhance cell growth, inhibit apoptosis, promote cell cycle progression, limit ROS production and increase ATP production (X. Xie et al., 2014). Furthermore, a different study showed that increased MNA levels could support OXPHOS activation in rapidly dividing cells, avoiding their shift towards glycolysis (Ramsden et al., 2017). Interestingly, these findings were in agreement with the results from the GSEA, as the high-GS group exhibited slow glycolysis and enhanced OXPHOS compared to low-GS patients. In addition, another study found that *AOX1* was down-regulated in high-GS and metastatic PCa samples (Varisli, 2013). In our analysis, although *NNMT* and *AOX1* showed decreased expression in high-GS patients, the ratio *NNMT/AOX1* was higher, indicating lower *AOX1* expression. Taken all together, those results could suggest that MNA conversion to pyridones may be slower than its synthesis from nicotinamide, resulting in its accumulation. This hypothesis would be supported by the non-significantly decreased levels of 4-Py observed in high-GS PCa patients.

Finally, phenylalanine was the only metabolite that exhibited increased levels both in the serum and urine samples of the high-GS PCa patients. Phenylalanine is metabolized to tyrosine through the phenylalanine hydroxylase (PAH) enzyme. Dysfunctional PAH were previously observed in inflammatory and malignant diseases, and elevated phenylalanine levels were also reported in other cancer types (Neurauter et al., 2008; Sirniö et al., 2019; X. Zhang et al., 2013). In this work, the decreased *PAH* expression observed in the high-GS groups may explain the accumulation of phenylalanine in both biofluids in this group of patients.

IV.2. CHARACTERIZATION OF SPECIFIC GENETIC VULNERABILITIES IN ADVANCED PCa

The proposed workflow to characterize PCa gene dependencies is represented in Figure 24. Briefly, our strategy was firstly focused on the identification of essential genes based on screening assays performed on PCa cell lines. Then, using gene expression data, essential genes were filtered to select those found to be over-expressed in PCa compared to normal tissues, as well as in aggressive and/or metastatic PCa tumors. Based on survival data, the prognostic value of each gene was evaluated to select those showing a significant association with worse disease prognosis. Finally, their biological relevance was examined using publicly available literature and different databases to select the most promising candidates, and their role in cancer was assessed and validated through functional *in vitro* experiments.

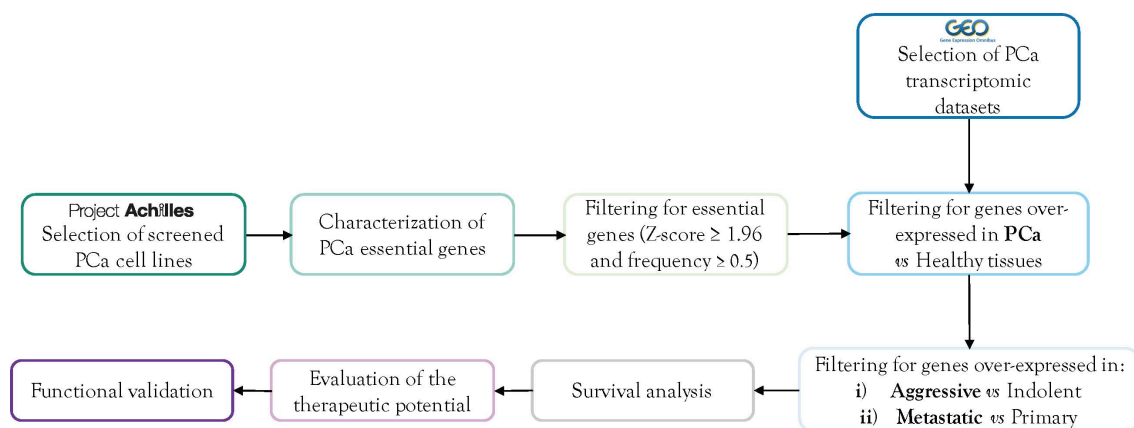


Figure 24. Overview of the strategy followed during the analysis for the identification of potential therapeutic targets in PCa

IV.2.1. Identification of essential genes in PCa cell lines

The characterization of PCa genetic vulnerabilities was performed following a similar approach as described in previously published studies (Apaolaza et al., 2017; Davoli et al., 2016; Ilic et al., 2017).

Besides the strategy described by Hart *et al.*, applied in this study, several algorithms have later been developed for calculating gene essentiality scores and identifying tumor

genetic vulnerabilities (Hart & Moffat, 2016; Meyers et al., 2017; Tsherniak et al., 2017). One of these analytical methods is DEMETER2 (McFarland et al., 2018), that models both on- and off-target effects, avoids the identification of common essential genes and accounts for differences in screen quality across cell lines. Notably, this algorithm also uses the curated reference gene lists developed by Hart *et al.* to characterize genetic vulnerabilities. Although there are noticeable differences in data modelling between both analytical strategies (e.g., mathematical function), there is a high degree of overlap when comparing essential genes identified after estimating gene dependencies based on the HART strategy used in this study with those characterized later, following the DEMETER2 approach (Figure

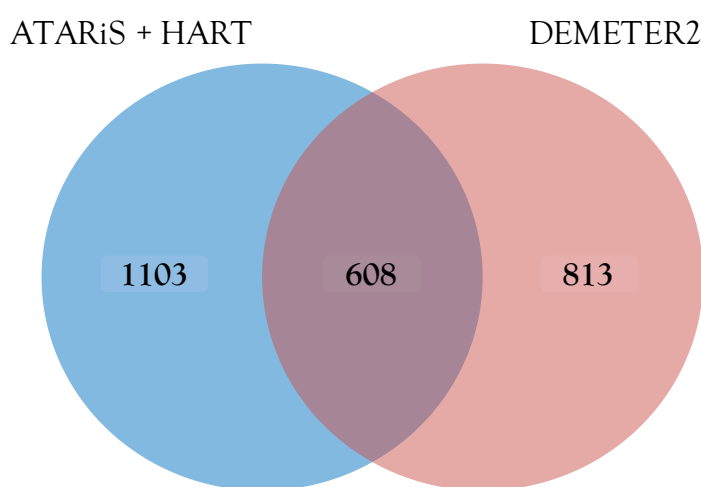


Figure 25. Comparison of essential genes identified after calculating genetic dependencies using the Hart approach or following the DEMETER2 model

Although there exists a big overlap between both analytical strategies, the differences in the number of genes identified as essential by each of them could be explained by several factors. First, the genes analyzed by both approaches are not exactly the same. Only 80% of them were screened in both approaches. Thus, more than 2000 and 1000 genes were specifically analyzed with HART and DEMETER2 methods, respectively. Another important factor to consider is how each strategy defines a gene as essential. In DEMETER2, essential genes are defined as those with a value lower than -1. On the other hand, in the HART strategy, genes are identified as essential when their BF values are higher than 0, thus being less restrictive than DEMETER2, and leading to the selection of a higher number of essential genes.

For this study, among all tested cell lines, only gene screening data from PCa cell lines ($n = 7$) were considered for further analyses. For every gene screened in each cell line, the essentiality score was calculated following the approach developed by Hart *et al.* (Hart *et al.*, 2014). Then, after Z-score normalization of the essentiality values, the subset of the 5% most essential genes ($Z\text{-score} > 1.96$) was derived for each cell line. Finally, all lists from the 7 cell lines were combined, resulting in 1711 PCa genetic vulnerabilities. Finally, from the subset of 1711 PCa genetic vulnerabilities, those genes identified as essential in more than 50% of all screened PCa cell lines (4/7 cell lines) were selected, yielding a total of 199 PCa genetic dependencies.

IV.2.2. Analysis of the potential association between essential genes and PCa progression

After the GEO database search, five PCa studies met the inclusion criteria: GSE6919 (Chandran *et al.*, 2007; Y. P. Yu *et al.*, 2004), GSE35988 (Grasso *et al.*, 2012), GSE21035 (Taylor *et al.*, 2010), GSE10645 (Nakagawa *et al.*, 2008) and GSE46602 (Mortensen *et al.*, 2015). Characteristics of the selected PCa transcriptomic studies are shown in Table 18.

Table 18. Characteristics of the selected PCa transcriptomic studies

Study ID	Analytical platform ID	Number of genes	Number of samples
GSE6919	GPL8300	5405	171
GSE35988	GPL6480	19571	112
GSE21035	GPL4091	16784	218
GSE10645	GPL5858 and GPL5873	960	596
GSE46602	GPL570	23493	50

Data integrity was assessed in all datasets included in the analysis, and expression data was \log_2 transformed, if not previously performed. After generating PCA plots for each individual study to detect outliers and non-homogenous sample distribution, any bias was detected in the studies (Appendix 5).

IV.2.3. Essential genes over-expressed in PCa

From the initial set of studies selected from GEO, two (gse6919 and gse35988) were used to conduct a differential gene expression analysis between PCa tumor samples and healthy tissues on the group of genes previously identified as essential. For each study, the number of samples included in each group is summarized in Table 19. Compared to normal tissues, a total of 61 genes out of the 199 genes identified as essential in at least 50% of PCa cell lines, were identified to be significantly over-expressed in PCa in at least one of the studies.

Table 19. Number of samples included in each experimental group for the differential expression analyses

Study ID	Essential genes included in the analytical platform	Experimental groups
gse6919	78/199	Healthy (n=81); PCa (n=90)
gse35988	173/199	Healthy (n=28); PCa (n=94)

IV.2.4. Essential genes over-expressed in aggressive/metastatic PCa tumors

Based on the experimental groups and the clinical variables included in the transcriptomic datasets, RNA expression data were used to conduct differential expression analysis between: i) aggressive *vs* indolent and ii) metastatic *vs* primary tumor samples.

- Essential genes over-expressed in aggressive PCa tumors

Before differential expression analysis, samples were classified into indolent and aggressive groups based on disease recurrence. Patients showing positive biochemical recurrence were classified in the aggressive group. For each study, the number of samples included in each group is summarized in Table 20.

Table 20. Number of samples included in each experimental group for the differential expression analyses

Study ID	Essential genes included in the analytical platform	Experimental groups
gse10645	9/199	Indolent (n=195); Aggressive (n=200)
gse46602	183/199	Indolent (n=8); Aggressive (n=17)

Only those genes previously identified as significantly over-expressed in PCa, in comparison to healthy prostate tissues, were included in this analysis. For these genes, differential expression analyses between indolent and aggressive groups were performed on each transcriptomic dataset, leading to the identification of a total of 26 up-regulated genes in the aggressive condition in any of the transcriptomics studies. All significantly up-regulated genes detected in at least one of the two studies were selected.

- Essential genes over-expressed in metastatic PCa tumors

Three datasets (gse6919, gse35988 and gse21035) were used to conduct differential gene expression analysis between primary and metastatic PCa samples. The number of samples analyzed in each study is summarized in Table 21.

Table 21. Number of samples included in each experimental group for the differential expression analyses

Study ID	Essential genes included in the analytical platform	Experimental groups
gse6919	78/199	Primary (n=65); Metastatic (n=25)
gse35988	173/199	Primary (n=59); Metastatic (n=35)
gse21035	164/199	Primary (n=181); Metastatic (n=37)

Only those genes significantly over-expressed in PCa, in comparison to healthy prostate tissues, were included in this analysis. A total of 42 genes were identified to be up-regulated in metastatic compared to primary tumor samples in at least one of the studies. Among these significantly up-regulated genes, only genes found to be up-regulated in at least two of the three datasets (n = 17) were considered for further analyses.

- Essential genes over-expressed in aggressive or metastatic PCa tumors

A total of 27 genes were significantly over-expressed either in aggressive or in metastatic tumors. Among them, 5 genes were up-regulated both in aggressive and in metastatic tumors. Notably, compared to the indolent *vs* aggressive comparison, a larger subset of genes was characterized as differently expressed when comparing metastatic *vs* primary PCa samples. As previously reported, similarities in the molecular landscape together with the high degree of intra- and inter-individual heterogeneity, may be

influencing the detection of differences in the transcriptomic profile of indolent and aggressive tumors (Sboner et al., 2010).

IV.2.5. Correlation between essential gene expression and PCa progression

The impact of the relative expression of selected genes in PCa patients' prognosis was evaluated based on available data from three transcriptomic studies (gse10645, gse21035 and gse46602). Following Kaplan-Meier curves analysis for the 27 genes found to be essential and over-expressed either in the aggressive or metastatic PCa subgroups, relative expression of 16 of these genes showed a significant positive association with a worse PCa patient's prognosis (Figure 26). For each of these genes, boxplots showing relative expression levels in the different subgroups of samples and Kaplan-Meier curves, evaluating the correlation between gene expression and disease progression and/or overall survival, are included in Appendix 6.

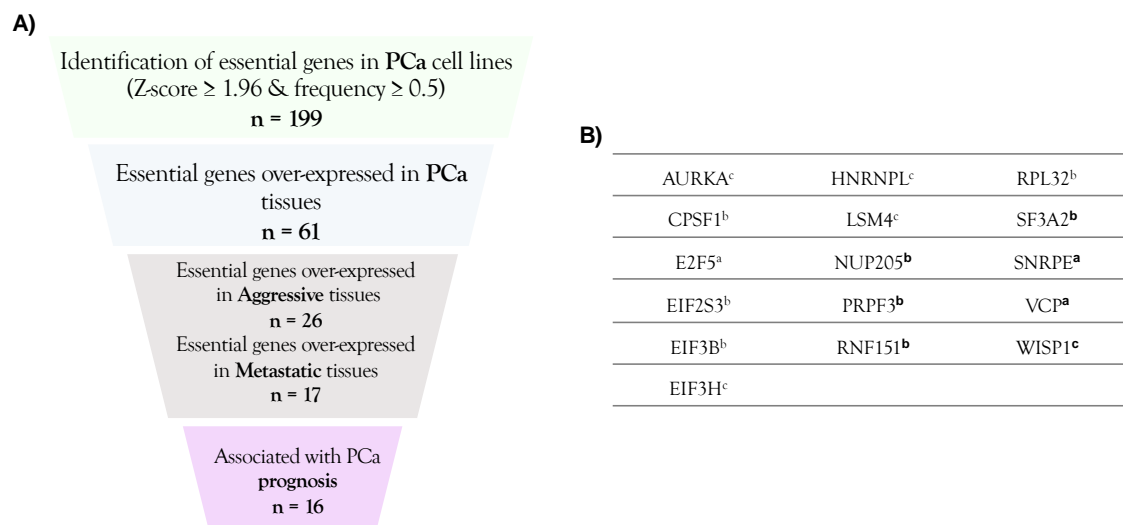


Figure 26. Overview of the filtering steps and the final subset of essential genes. A) Summary of all steps conducted to select the most relevant subset of genes associated with aggressiveness and progression of PCa. In each step, the number of genes after applying each filter is represented in bold. B) List of potential therapeutic targets associated with PCa aggressiveness and progression. Genes identified as essential and over-expressed in ^a aggressive, ^b metastatic or ^c aggressive and metastatic tumors.

IV.2.6. Evaluation of essential genes as potential PCa therapeutic targets

A PPI network (Szklarczyk et al., 2021) was constructed in order to evaluate potential interactions between the 16 selected therapeutic targets and their functional role in the disease. The STRING analysis showed direct relationships among 11 of the proteins

included in the analysis, with some groups exhibiting strong interactions, suggesting that those proteins were at least partially biologically connected as a group (Figure 27A). Functional enrichment analysis of this network revealed over-representation of three biological processes: formation of cytoplasmic translation initiation complex, cytoplasmic translational initiation, and spliceosomal snrnp assembly. Proteins involved in each of these processes are represented in Figure 27B. The statistical parameters for the constructed network and for the biological process are shown in Figure 27C.

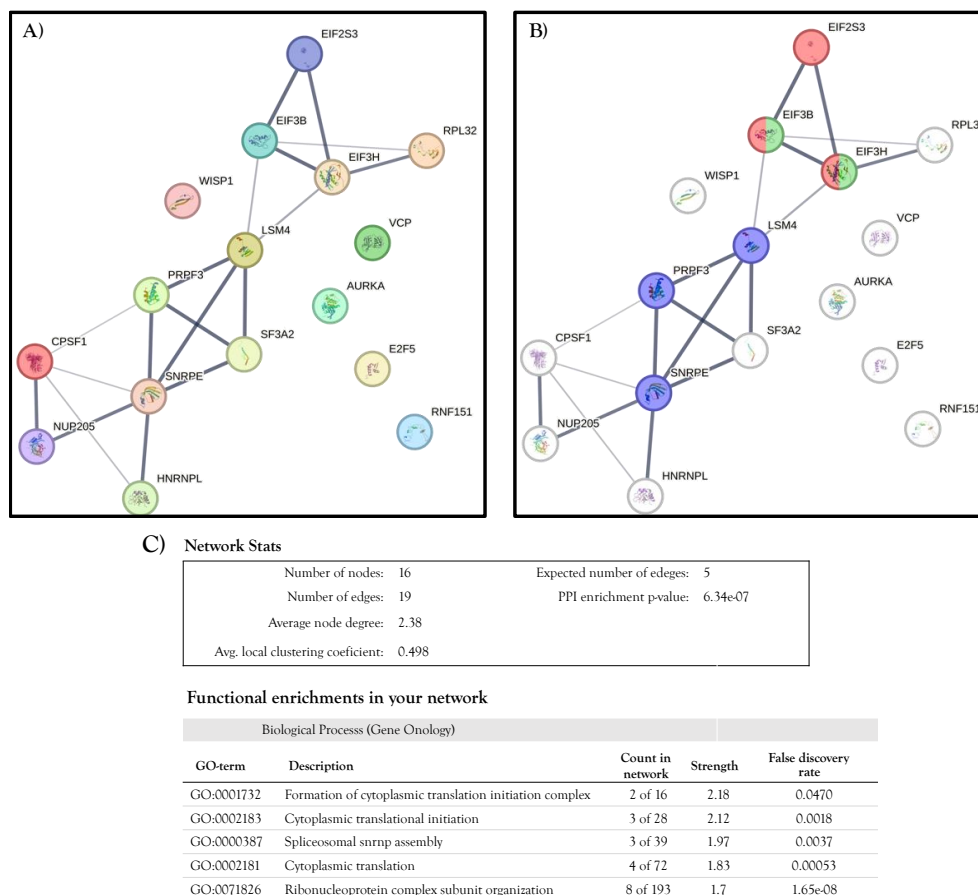


Figure 27. Protein-protein interaction regulatory network constructed using STRING. Lines represent associations between proteins, and their thickness indicate the strength of the data support. A) STRING network for all selected therapeutic targets showing the interactions among 11 of them. B) Same network colored by the top three most significantly enriched biological processes (Gene Ontology), green: formation of cytoplasmic translation initiation complex, red: cytoplasmic translational initiation, and blue: spliceosomal snrnp assembly. C) Statistical parameters of the PPI network (above) and of the biological processes obtained after the functional enrichment.

- Biological relevance of mRNA translation initiation in PCa

Dysregulations in protein synthesis or mRNA translation processes are frequently observed in tumor cells, as they require continuous protein synthesis to promote their malignant phenotype (Bhat et al., 2015; Pelletier et al., 2015; Robichaud et al., 2019; Truitt & Ruggero, 2016). Interestingly, given that tumor cells may become more dependent on mRNA translation, this process has been considered as a promising pathway to identify novel targets for cancer therapy (Ruggero, 2013; Silvera et al., 2010). In particular, translation initiation involves many different initiation factors (eIFs) and is considered the rate-limiting step for most mRNAs (Spilka et al., 2013). Thus, a potential strategy for modifying protein synthesis is through the regulation of eIFs (Ingolia et al., 2009). Indeed, several eIFs have been observed to be amplified or dysregulated in different cancer types (Ruggero, 2013), and have also been associated with tumor development (Ali et al., 2017; Robichaud et al., 2019; Sharma et al., 2016). In the context of PCa, alterations in some eIFs have been reported (Furic et al., 2010; Graff et al., 2009; Jaiswal et al., 2018; H. G. Nguyen et al., 2018), as well as dysregulation of signaling cascades that control the protein synthesis machinery (Hsieh et al., 2015; L. Liu & Dong, 2014; Proud, 2019; Roux & Topisirovic, 2018). Furthermore, therapeutic strategies targeting eIFs or other components involved in related processes have shown inhibitory effects on PCa progression. In particular, a reduction of tumor progression has been reported when inhibiting the eIF4G/eIF4E complex formation (Jaiswal et al., 2018). Another study has shown that dual inhibition of PI3K/mTOR induces cell death in a *PTEN*-deficient PCa mouse model (Carver et al., 2011). In addition, several studies have described that the use of inhibitors against mTOR affects PCa tumorigenesis (Bitting & Armstrong, 2013; D'Abronzio & Ghosh, 2018; Guertin et al., 2009; Lian et al., 2018).

Based on the analysis performed in this study, out of the 16 candidate genes being evaluated as potential targets for PCa, three proteins were directly involved in protein translation processes (Figure 27B). Given that this biological process has shown to play a relevant role in PCa development (D'Abronzio & Ghosh, 2018; Hernández et al., 2019; J. Xie et al., 2021), the potential of each of these proteins as molecular targets for advanced PCa treatment was individually evaluated. To that end, information related to availability of 3D structure, defined druggable cavities, known inhibitors or ligands, subcellular

location and association with the disease was assessed for each of them. The most relevant information found in this search, derived from different specialized databases, is summarized in Table 22.

Table 22. Extracted characteristics and literature information of the potential therapeutic targets involved in the mRNA translation pathway

	EIF2S3	EIF3B	EIF3H
Molecular weight ^a	51.109 Da	92.482 Da	39.930 Da
Subcellular location ^{a,b}	Cytoplasm	Cytoplasm / Nucleus	Cytoplasm
Available 3D structure ^{a,c,d}	Yes (Kenner et al., 2019)	Yes (Brito Querido et al., 2020; Simonetti et al., 2016)	Yes (Brito Querido et al., 2020; Erzberger et al., 2014)
Ligandable cavities ^c	Yes	No	Yes
Inhibitors/Ligands ^{c,e}	Not known	Not known	Not known
Role in cancer	Not known	- Over-expressed in LC (Wang et al., 2013), PC (Ren et al., 2021), glioma (Liang et al., 2012) and CC (Wang et al., 2012) tumors and required for tumor proliferation (Liang et al., 2012; Ren et al., 2021; H. Wang et al., 2013; Z. Wang et al., 2012).	- Over-expressed in HCC (Zhu et al., 2016), GC (Wang et al., 2018), ESCC (Guo et al., 2020), and associated with tumorigenesis (Guo et al., 2020; X. Wang, Wang, et al., 2018; Zhu et al., 2016). - Deubiquitinates YAP and SNAIL, thus promoting tumorigenesis (Guo et al., 2020). - Interacts with METTL3 enhancing translation and oncogenic transformation (Choe et al., 2018) - Its inhibition induced apoptosis through Bcl-2 and caspase-dependent way (G. Yu et al., 2018).
Role in PCa	Not known	- Over-expressed in PCa tumors and cells lines, and involved in tumor proliferation (Xiang et al., 2020)	- Frequently observed over-expressed in PCa tumors and positively correlated with GS (Nupponen et al., 1999; Saramäki et al., 2001; Savinainen et al., 2006)

			- Up-regulated in PCa cell lines and involved in tumor growth (L. Zhang et al., 2008).
Expression in PCa ^f	Up-regulated	Up-regulated	Up-regulated
Association with GS ^c	Positively associated	Positively associated	Positively associated
Other information ^g	-	-	- Deubiquitination activity (Guo et al., 2020; Zhou et al., 2020)

BC: bladder cancer, CC: colon cancer, Da: Dalton, ESCC: esophageal squamous cell carcinoma, GC: gastric cancer, GS: Gleason score, HCC: hepatocellular carcinoma, PC: pancreatic cancer, PCa: prostate cancer. Information extracted from ^a Uniprot, ^b Human protein atlas, ^c CanSAR, ^d Protein Data Bank, and ^e Pharos, ^f TCGA and Genotype-Tissue Expression (548 PCa patients vs 100 healthy individuals) and ^g UbiBrowser databases

Based on the information summarized in the table above, further analyses were focused on evaluating the potential of *EIF3H* gene, together with other proteins that might be relevant for its activity, as therapeutic target for advanced PCa stages.

- Biological relevance of spliceosome assembly in PCa

The spliceosome machinery is composed of five small nuclear ribonucleoproteins, that remove introns from the precursor mRNA. Each ribonucleoprotein consists of a small nuclear RNA and a group of associated proteins (Fabrizio et al., 2009), known as splicing factors. Alternative splicing involves the removal of introns from precursor mRNA, being an essential step in the post-transcriptional regulation of gene expression (Y. Lee & Rio, 2015). Notably, several studies have associated alternative splicing and dysregulations in this pathway with cancer development (Biamonti et al., 2014; Chabot & Shkreta, 2016; Dvinge et al., 2016; Singh & Eyra, 2017; J. Zhang & Manley, 2013). In particular, genomic mutations in the splicing machinery, including splicing factors, have been observed in solid tumors and hematological diseases (F. Liu et al., 2018, p. 1; Sheng et al., 2018; Sokół et al., 2018; H. Wang et al., 2019; R. Xie et al., 2019). In the context of PCa, changes in the expression of different components of the spliceosome have been reported to play a direct role in tumor proliferation (Fei et al., 2017; Paronetto et al., 2010; Takayama et al., 2017). In addition, alternative splicing was found to be closely associated with PCa progression and resistance to ADT by restoring AR activity through the formation of the well-known

AR splicing variant 7 (AR-V7) (Antonarakis et al., 2014; Fan et al., 2018; H. Li et al., 2018; Nadiminty et al., 2015; J. Xu & Qiu, 2016). Thus, given the relevance of alternative splicing in tumor development and proliferation, targeting splicing components has emerged as a potential therapeutic strategy for cancer treatment (Bonnal et al., 2012; S. C.-W. Lee & Abdel-Wahab, 2016; Paschalis et al., 2018).

The STRING network analysis conducted in this study revealed that three of proteins being evaluated as potential PCa therapeutic targets, were associated with the spliceosome pathway (Figure 27B). Alterations in the spliceosome machinery has shown to play a relevant role in the development and response to therapy in advanced PCa patients. Thus, these proteins were selected for their individual evaluation as potential therapeutic target for advanced PCa. Table 23 summarizes the information evaluated for each of them in order to assess their potential as therapeutic targets for advanced PCa.

Table 23. Extracted characteristics and literature information of the potential therapeutic targets involved in the spliceosome pathway

	LSM4	PRPF3	SNRPE
Molecular weight ^a	15.350 Da	77.529 Da	10.804 Da
Subcellular location ^{a,b}	Cytoplasm / Nucleus	Nucleus	Cytoplasm / Nucleus
Available 3D structure ^{a,c,d}	Yes (Zhan et al., 2018)	Yes (Bertram et al., 2017; Zhan et al., 2018)	Yes (Bai et al., 2021; Zhang et al., 2018)
Ligandable cavities ^c	No	Yes	Yes
Inhibitors/Ligands ^{c,e}	Not known	Not known	Not known
Role in cancer	- Over-expressed in HCC (Chen et al., 2021), BC (Ta et al., 2021; Yin et al., 2021), PC (Xue et al., 2018) and OC (Hou & Zhang, 2021)	- Over-expressed in HCC and associated with worse prognosis (Liu et al., 2020) - Promotes PC progression via the RAP2B/ERK pathway (Li et al., 2022)	- Over-expressed in BC and associated with poor prognosis and tumor proliferation (Xie & Xu, 2020). - Over-expressed in BC, LC and OC, and its inhibition leads to cell death through autophagy (Quidville et al., 2013)
Role in PCa	-	-	- Over-expressed in PCa, and associated with cancer proliferation and progression

	through regulation of AR expression (Anchi et al., 2012; Tamura et al., 2007)		
Expression in PCa ^f	Up-regulated	Down-regulated	Up-regulated
Association with GS ^c	- Positively associated	- Negatively associated	- Positively associated
Other information ^g	-	-	-

AR: androgen receptor, BC: breast cancer, Da: Dalton, GS: Gleason score, HCC: hepatocellular carcinoma, LC: lung cancer, OC: ovarian cancer, PC: pancreatic cancer, PCa: prostate cancer. Information extracted from ^a Uniprot, ^b Human protein atlas, ^c CanSAR, ^d Protein Data Bank, and ^e Pharos ^f TCGA and Genotype-Tissue Expression (548 PCa patients vs 100 healthy individuals) and ^g UbiBrowser databases

Based on the of the information detailed in Table 23, *LSM4* and *SNRPE* genes were classified as preferential candidates for the evaluation of their therapeutic potential as therapeutic targets for advanced PCa in future stages of this project.

IV.2.7. Evaluation of EIF3H as a valuable therapeutic target in PCa

IV.2.7.1. Role of EIF3H in cancer progression

The Eukaryotic translation Initiation Factor 3 (EIF3) is the largest multi-complex initiation factor, and has been involved in initiation and termination of protein translation and ribosomal recycling (Beznosková et al., 2013; Pisarev et al., 2007; Valásek, 2012). It is comprised by 13 different subunits (named from a to m), including the EIF3 subunit H (EIF3H), a 40 kDa protein located on chromosome 8q23.3-q24.11.

Studies conducted on different cancers types significantly associated over-expression of *EIF3H* with cell proliferation. Particularly, it was reported to be over-expressed in breast cancer tumor samples and to be a driver gene contributing to cell growth, survival and transformation, while its inhibition suppressed proliferation and colony formation (Mahmood et al., 2014). High *EIF3H* levels were also observed in other cancers (Cappuzzo et al., 2009; Hong et al., 2018; Hutter et al., 2012; Mahmood et al., 2014; Okamoto et al., 2003). In addition, increased expression was associated with proliferation, invasion and tumorigenicity in hepatocellular carcinoma (Zhu et al., 2016) and colorectal cancer (Pittman et al., 2010), and it was defined as an oncogene that promoted cell metastasis via epithelial-mesenchymal transition (EMT) activation in lung cancer (Hu et al., 2020). Moreover, the oncogenic role of *EIF3H* was confirmed by its ability

to promote malignant transform of immortal NIH3T3 cells (L. Zhang et al., 2007). From a mechanistic perspective, it was reported that EIF3H activated EMT signaling by increasing the expression of fibronectin, N-cadherin, β -catenin, vimentin and *SNAIL*, and suppressing E-cadherin (Hu et al., 2020). In addition, this gene was recently described as a potential deubiquitinating enzyme, being essential to stabilize *SNAIL* protein and promote EMT (Guo et al., 2020).

In relation to PCa, it has been reported that 30% of PCa patients exhibit overexpression of *EIF3H* (Nupponen et al., 1999; Saramäki et al., 2001; Savinainen et al., 2006). Moreover, *EIF3H* amplification was associated with advanced stage and poor cancer overall survival (Saramäki et al., 2001), suggesting that it may play a role in tumor progression. Indeed, increased EIF3H protein levels were observed in three different PCa cell models (22rv1, LnCaP and PC3), and its inhibition using siRNA reduced cell proliferation in the PC3 line (L. Zhang et al., 2008). Although EIF3H has been related to PCa progression, to date, the specific mechanism driving to PCa progression promoted by EIF3H changes is not understood.

IV.2.7.2. EIF3H is a druggable target

EIF3H is one of the subunits that constitutes the EIF3 complex, that interacts with other EIFs and is involved in many steps of the translation initiation process (des Georges et al., 2015). This subunit is localized in the cytoplasm, has a mass of 39.930 Da and a length of 352 amino acids (UniProt Consortium, 2021). According to the information available on the PDB, there exist 10 different 3D structures for mammalian EIF3H, all of them determined by electron microscopy and the majority resolved above resolutions of 3.5 Å. In these structures, EIF3H can be found in complex with other EIF3 subunits (PDB ID: 3J8B), but also with components of the 40S ribosomal subunit (PDB ID: 6YBD). Figure 28A shows the structure of the EIF3 in complex with several of its subunits and the 40S ribosomal subunit, resolved at 3.30 Å. Although there are none described inhibitors or ligands associated with EIF3H, the canSAR database has predicted, based on a number of features (e.g., volume, enclosure, hydrogen-bond donors, hydrophobic fraction, etc.) and their comparison against bona-fide drug targets like kinases (Coker et al., 2019), one potential ligandable cavity in its structure (Figure 28B).

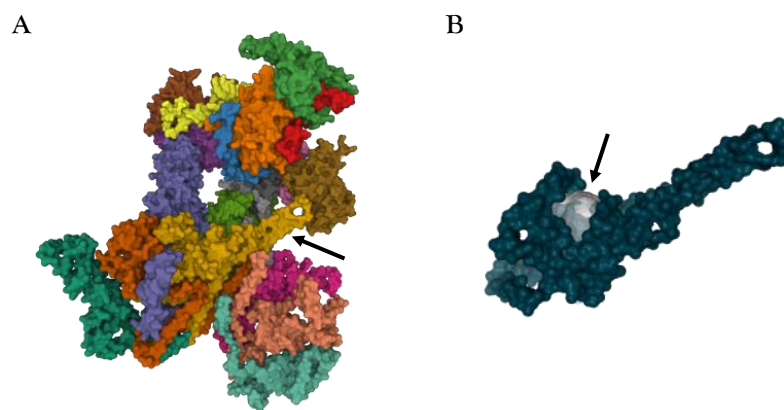


Figure 28. 3D structures of the PDB ID 6YBD. A) Structure of the human 48S translational initiation complex - EIF3, where the EIF3H subunit is represented in light brown (indicated with an arrow). The image was obtained from the PDB. B) Structure of the EIF3H subunit indicating with an arrow the potential ligandable cavity based on the canSAR predictions. The image was obtained from the canSAR database.

EIF3H recombinant protein expressed and purified in different hosts, including *E. coli*, yeast and Baculovirus, with a purity above 85% can commercially be obtained (<https://www.mybiosource.com>). The EIF3H subunit contains a MPN domain that promotes the assembly of multiprotein complexes (Enchev et al., 2010; Pena et al., 2007), and is found in metalloenzymes that function as ubiquitinases/deubiquitinases (Verma et al., 2002). The deubiquitinase activity of EIF3H has recently been described, and it has been reported to stabilize relevant proteins associated with promotion of tumor aggressiveness (Guo et al., 2020; Zhou et al., 2020). As showed in Figure 29, EIF3H is known to deubiquitinase SNAIL1, and other 7 additional proteins are predicted as high confident substrates. Thus, one of the future objectives of the project is to explore proteins interacting with EIF3H, and evaluate whether they are better valuable therapeutic targets than EIF3H by assessing different chemical and molecular features.

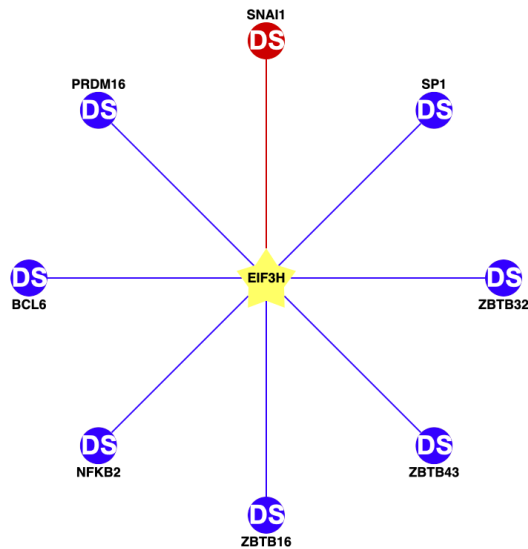


Figure 29. Network for the known (red) and predicted (blue) substrates that may be deubiquitinated by EIF3H. Information extracted from the UbiBrowser 2.0 database.

IV.2.7.3. EIF3H is over-expressed in PCa and is correlated with patient's prognosis

Based on the differential expression analysis performed in this study, *EIF3H* showed higher expression in PCa samples compared with normal tissues (Figure 30A). Moreover, *EIF3H* was significantly over-expressed in aggressive (Figure 30B) and metastatic (Figure 30C) samples when compared to indolent and primary tissues, respectively. In addition, its expression was significantly correlated with poor overall survival (Figure 30D) and shorter BCR-free time (Figure 30E).

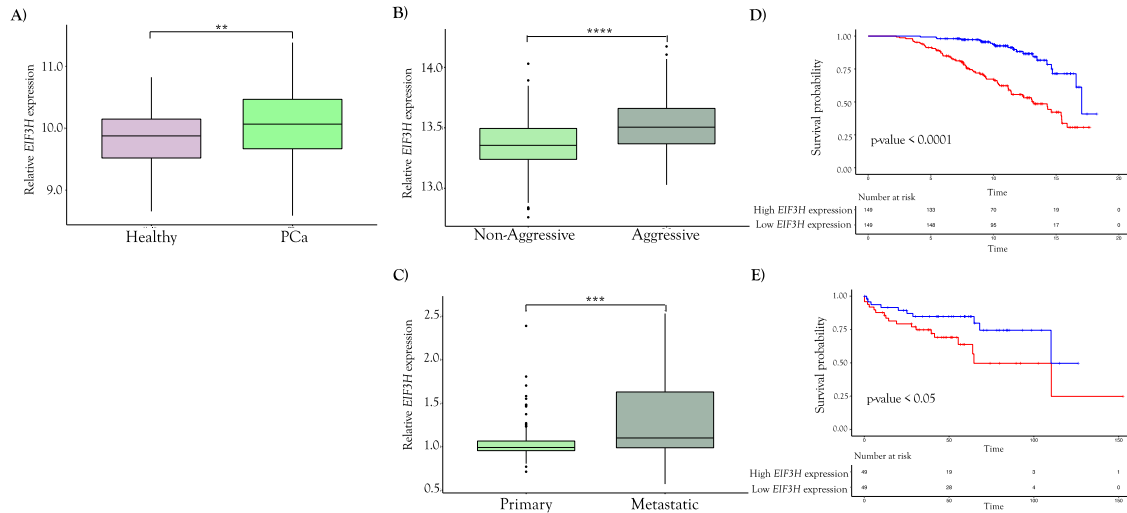


Figure 30. EIF3H is over-expressed in PCa and associated with PCa progression. A) Relative expression in PCa and normal tissues based on publicly available data from gse6919 GEO dataset. Relative expression in different PCa stages and Kaplan-Meier curves based on publicly available data from B and D) gse10645 and, C and E) gse21035 GEO studies. **** p-value < 0.0001, *** p-value < 0.001 and ** p-value < 0.01 vs reference group.

IV.2.8. Validation of EIF3H as a valuable therapeutic target in PCa

IV.2.8.1. EIF3H is over-expressed in PCa cell lines

mRNA expression and protein levels of EIF3H in four different prostate cellular models were evaluated by qPCR and western blot, respectively. As shown in Figure 31, both EIF3H mRNA and protein levels were found to be significantly higher in PCa cell lines compared to the normal prostate cellular model.

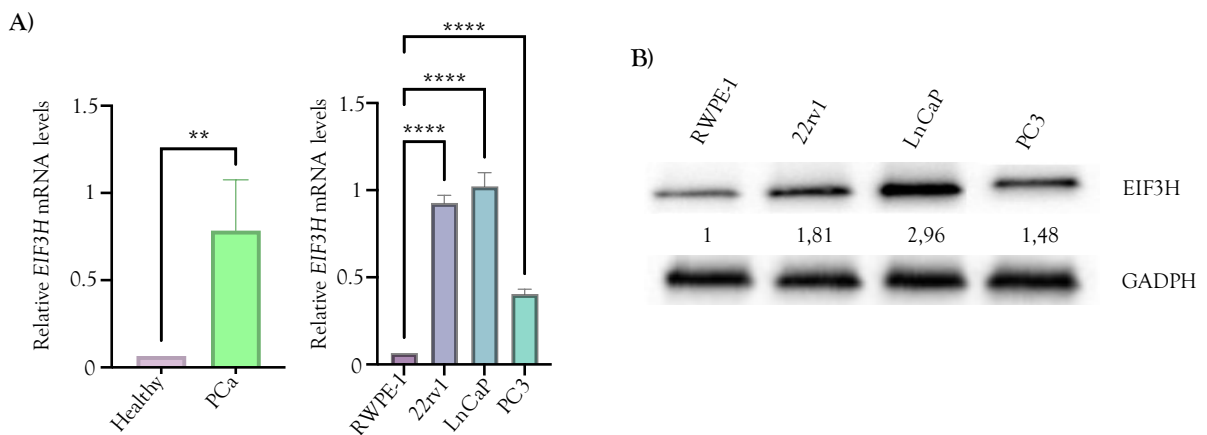


Figure 31. EIF3H is over-expressed at the transcriptomic and proteomic level in more aggressive PCa stages. A) q-PCR and B) Western blot showing higher relative EIF3H mRNA and protein levels in different PCa cell lines compared to the healthy condition. Results are expressed as mean \pm SEM in qPCR experiments. **** p-value < 0.0001 and ** p-value < 0.01 vs reference group.

Interestingly, cell lines defined as androgen-dependent (22rv1 and LnCaP) showed higher expression levels than the androgen-independent phenotype (PC3). These results may indicate that EIF3H could play a relevant role in the early development of PCa. Nevertheless, as shown in Figure 30, this gene was observed to be over-expressed in aggressive and advanced stages of the disease, and significantly correlated with poor overall survival. In addition, previous studies reported that EIF3H protein levels were increased in different PCa cell lines, and that it had an effect on proliferation when using the PC3 cell line as a model (Zhang et al., 2008). Thus, this may be an isolated result with any direct association regarding the androgen dependency status.

IV.2.8.2. EIF3H silencing reduces proliferation and migration in PCa cell lines

To study the role of EIF3H in PCa, lentivirus-mediated shRNA silencing of *EIF3H* was performed on the PC3 cell line. Control shRNA (sh-C) and two shRNAs targeting *EIF3H* (sh-2 and sh-4) were used in lentiviral infection experiments. The efficiency of the infection was assessed based on GFP expression detection after infection with selected plasmids (Figure 32).

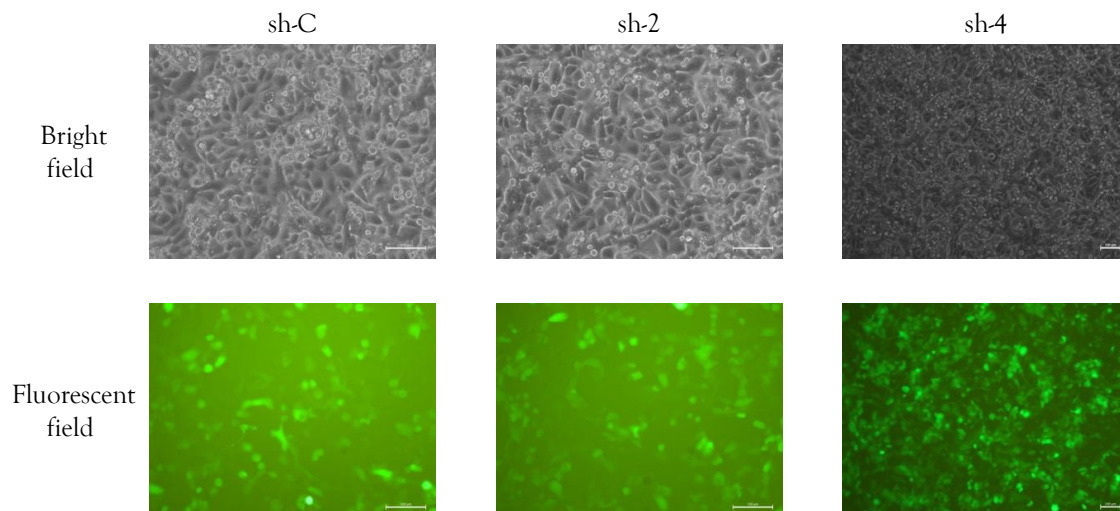


Figure 32. Lentivirus infection of PC3 PCa cell lines with the control and the *EIF3H* shRNA vectors. GFP expression 72 hours after starting puromycin selection on PC3 cells.

qPCR and western blot experiments were conducted to confirm silencing of *EIF3H* (Figure 33). Compared to the control, *EIF3H* mRNA levels were significantly decreased by

40% and 70% after silencing using sh-2 and sh-4, respectively (Figure 33A). EIF3H levels were also significantly reduced at the protein level (Figure 33B). In particular, EIF3H protein levels were decreased by 40% and 90% after inhibition with sh-2 and sh-4, respectively. Thus, these results indicated that shRNA silencing effectively inhibited EIF3H mRNA and protein level, and this inhibition was more efficient when using the sh-4 vector.

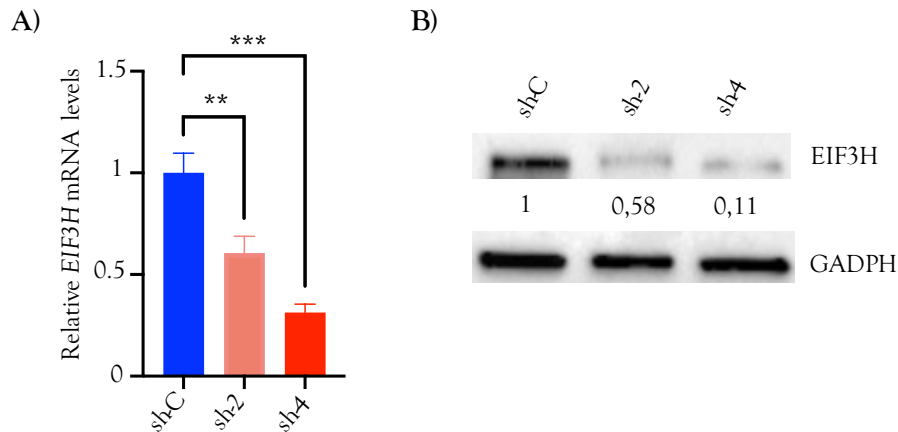


Figure 33. Silencing *EIF3H* expression in PC3 cell line using lentivirus-mediated shRNA. Representative A) qPCR and B) Western blot analysis of EIF3H after lentivirus infection. Results are expressed as mean \pm SEM in qPCR experiments. *** p-value < 0.001 and ** p-value < 0.01 vs sh-C group.

To evaluate the effect of EIF3H on PCa cell growth, proliferation and clonogenic assays were performed both in the control and knockdown cell lines. In the MTS assay, cell proliferation was markedly reduced at day 5 when inhibiting *EIF3H* expression with sh-2 and sh-4, respectively (Figure 34A). The MTS assay is a metabolic viability assay that measures mitochondrial activity, and it has been reported that external factors can influence the results of these tests (Ghasemi et al., 2021; Quent et al., 2010; Stockert et al., 2018; P. Wang et al., 2010). Thus, to confirm that the results were not affected by external conditions, a CyQUANT assay was conducted using the sh-C and sh-4. Similar to the MTS, the CyQUANT assay also showed a significant reduction in PC3 proliferation after infecting cells with sh-4 vector (Figure 34B).

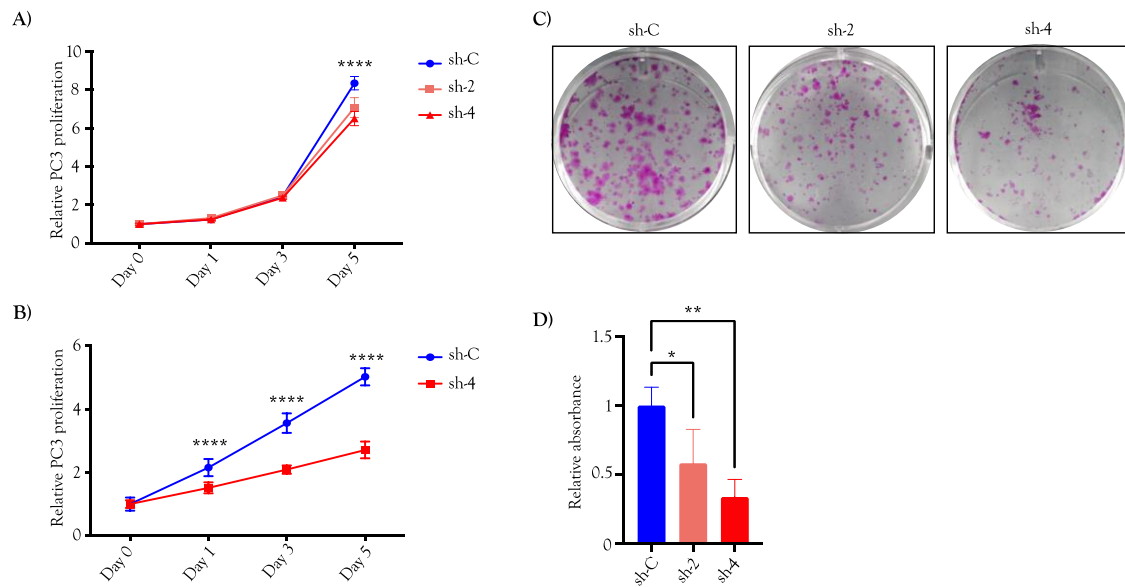


Figure 34. *EIF3H* knockdown inhibits the proliferation and colony formation of PC3 cells. A) MTS and B) CyQUANT proliferation assays showing that growth of PC3 cells was suppressed by down-regulation of *EIF3H*. C) Colony formation of PC3 cells was inhibited after infection of PC3 cells with sh-2 and sh-4 *EIF3H*. D) Relative absorbance after Sulforhodamine B solubilization. Results are expressed as mean \pm SEM in all experiments. **** p-value < 0.0001, ** p-value < 0.01 and * p-value < 0.05 vs sh-C group.

Similar results were observed in the clonogenic assay, where PC3 cells showed a significant 40% and 70% reduction in colony formation after *EIF3H* knockdown with sh-2 and sh-4, respectively (Figure 34C-D). Notably, as *EIF3H* inhibition was higher when using the sh-4, the proliferation and clonogenic capacity was lower in cells infected with this vector. These results were in agreement with previous studies, where proliferation and colony formation were reduced in PC3 cells after *EIF3H* knockdown (Zhang et al., 2008).

Moreover, to determine the effect of *EIF3H* down-regulation on cell migration, a wound-healing assay was performed in PCa cell models, and the width closure was measured at different times. As showed in Figure 35, cell migration capacity was significantly decreased after 8 h when silencing *EIF3H* with sh-2 and sh-4 vectors. This ability was also reduced at 24 h for the sh-4, that may be explained by the higher efficiency of sh-4 in reducing mRNA and protein levels of *EIF3H* compared to the sh-2.

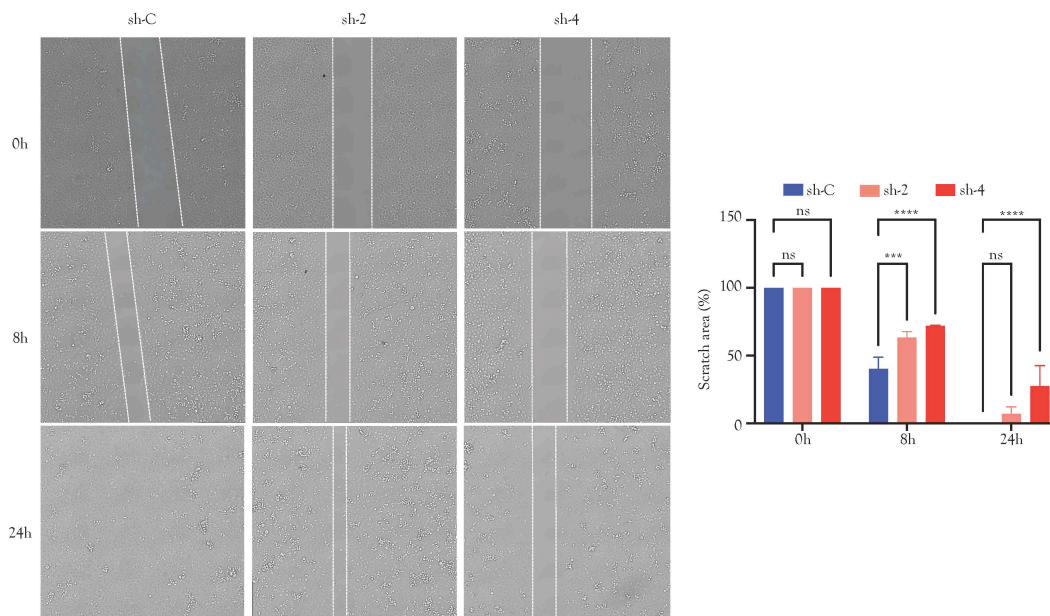


Figure 35. Silencing *EIF3H* expression has an effect on PC3 migration. Representative images of scratch wound healing assay taken at 0, 8 and 24 h comparing the migration rate between *EIF3H* sh-C, *EIF3H* sh and *EIF3H* sh-4 in PC3 cells. Results are expressed as mean \pm SEM. **** p-value < 0.0001 and *** p-value < 0.001 vs sh-C group.

Additionally, *EIF3H* knock-down models are currently being developed to confirm that the effect of *EIF3H* inhibition in cell proliferation and migration capacity is not cell line specific.

IV.2.8.3. EIF3H over-expression increases proliferation and migration in PCa cell lines

In addition, *EIF3H* was over-expressed in the PC3 cell line, using a plasmid containing Myc-*EIF3H* construct, to further validate its role in proliferation and migration in PCa cell lines. After confirming the efficiency of the lentivirus-mediated infection (Figure 36A), qPCR and western blot experiments were performed to confirm the over-expression of *EIF3H*. Compared to the control, the Myc-*EIF3H* infected cell line had 2.2-fold higher *EIF3H* mRNA levels (Figure 36B), and a 50% increase in protein levels (Figure 36C), therefore, confirming the efficiency of the *EIF3H* over-expression.

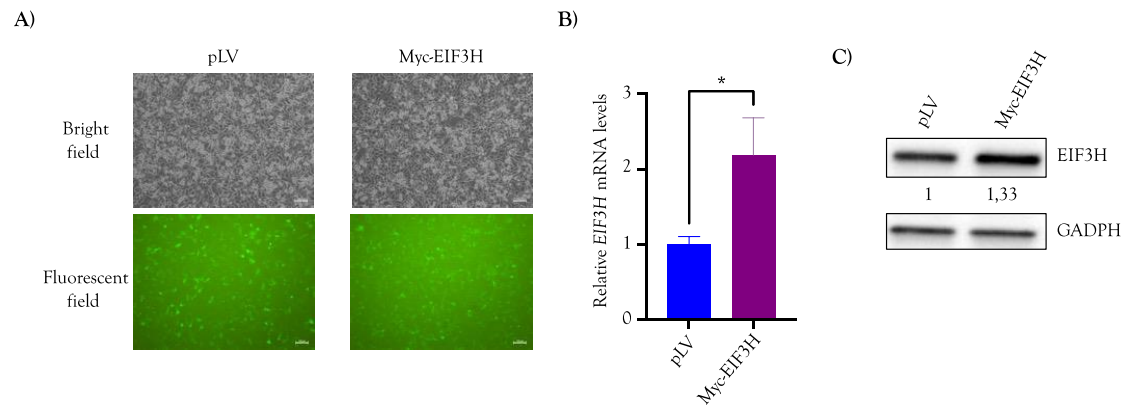


Figure 36. Over-expression of EIF3H in PC3 cell line using lentivirus-mediated shRNA. A) GFP expression 72 hours after starting puromycin selection on PC3 cells. Representative B) qPCR and C) Western blot analysis of EIF3H after lentivirus infection. Results are expressed as mean \pm SEM in qPCR experiments. * p-value $<$ 0.01 vs control group.

The effect of *EIF3H* over-expression on PCa cell growth was also evaluated by conducting a proliferation assay on the pLV and the Myc-EIF3H over-expressed cell line. In the MTS assay, cell proliferation was markedly increased from day 3 after *EIF3H* over-expression (Figure 37A). Notably, similar results were observed in the clonogenic assay, where PC3 cells showed a 44% increase in colony formation after *EIF3H* over-expression (Figure 34B-C).

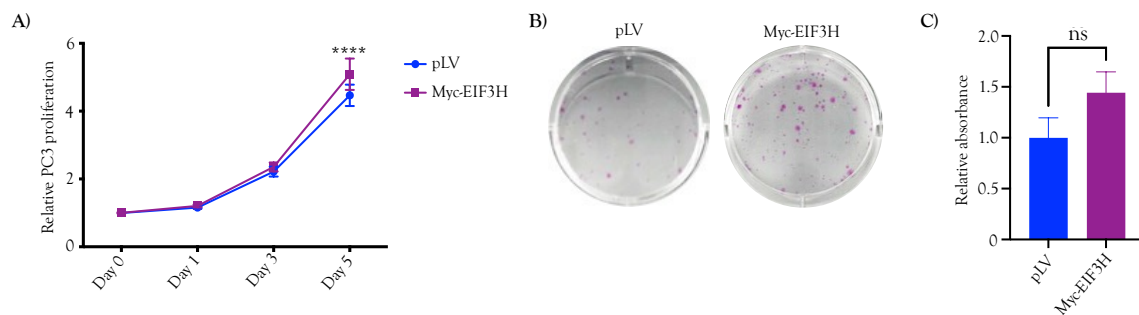


Figure 37. *EIF3H* over-expression enhances the proliferation and colony formation of PC3 cells. A) MTS proliferation assay showing that growth of PC3 cells was increased by over-expression of EIF3H. B) Colony formation of PC3 cells was enhanced when EIF3H was over-expressed. C) Relative absorbance after Sulforhodamine B solubilization. Results are expressed as mean \pm SEM in all experiments. **** p-value $<$ 0.0001 vs control group.

Finally, the effect of *EIF3H* over-expression on cell migration was also evaluated by conducting a wound-healing assay. After measuring the closure width, it was observed that,

after 8 h, cell migration capacity was significantly increased in the EIF3H over-expressing cell line model (Figure 38).

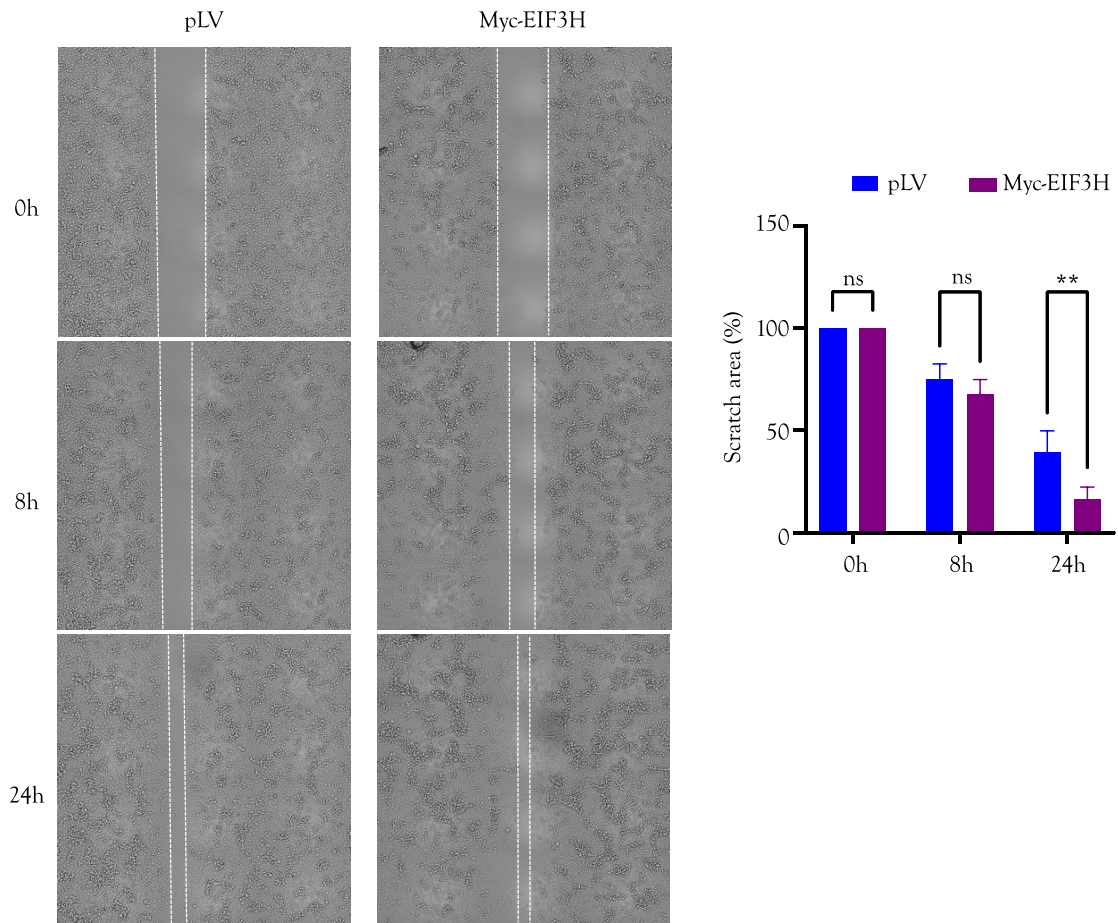


Figure 38. Over-expression of *EIF3H* expression has an effect on PC3 migration. Representative images of scratch wound healing assay taken at 0, 8 and 24 h comparing the migration rate between pLV and Myc-EIF3H in PC3 cells. Results are expressed as mean \pm SEM. ** p-value < 0.001 vs control group.

IV.2.8.4. Changes in *EIF3H* levels promote epithelial-mesenchymal transition

Finally, since cells need to promote the EMT to enhance cell invasion and migration, and contribute to cell growth and survival (Jung et al., 2015; Rafael et al., 2015), several EMT markers were examined following inhibition and over-expression of EIF3H in the PC3 cell line. During the EMT, the epithelial marker E-cadherin is down-regulated, while the mesenchymal marker vimentin is up-regulated (Thiery et al., 2009). Thus, the protein levels of E-cadherin and vimentin were evaluated by western blot analysis. This analysis revealed that E-cadherin protein levels were increased while vimentin levels were

decreased after inhibiting EIF3H expression, whereas increased E-cadherin protein levels and decreased vimentin levels were obtained when the gene was over-expressed (Figure 39). Although this experiment should be repeated with more biological replicates to confirm the results, these findings suggest a potential role of EIF3H in regulating EMT in PC3 cells.

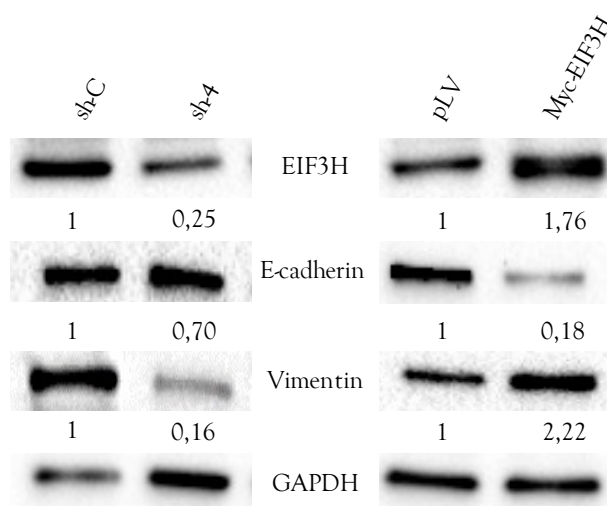


Figure 39. EIF3H induces epithelial-mesenchymal transition in PC3 cells. Western blot analysis showing changes in the protein levels of E-cadherin, Vimentin and EIF3H in PC3 cells after the inhibition or over-expression of EIF3H.

Taken all together, these results suggest that EIF3H is involved in proliferation and migration of PCa cell lines. Interestingly, although previous publications have reported that EIF3H plays a role in maintaining the malignant phenotype of PCa and it may inhibit Myc-dependent induction of apoptosis (Zhang et al., 2008), the detailed molecular mechanism underlying these changes in this disease has not been described. Several studies have attempted to elucidate the significance of EIF3H in different tumor types. Thus, in esophageal squamous cell carcinoma, EIF3H deubiquitination activity was reported to promote tumor aggressiveness by stabilization of SNAIL and subsequent induction of EMT signaling pathway (Guo et al., 2020). In another study, EIF3H was found to deubiquitinate and stabilize YAP, thus modulating the Hippo cascade and promoting tumor invasion and metastasis in breast cancer models (Zhou et al., 2020). A different study using colorectal cancer cells showed that EIF3H knockdown induced apoptosis through Bcl-2 and caspase-dependent way (G. Yu et al., 2018). Furthermore, it was reported that an interaction between EIF3H and METTL3 was required for enhanced translation and oncogenic transformation in lung cancer models (Choe et al., 2018). As little information is available regarding the specific role of EIF3H in PCa progression and aggressiveness, the

identification of EIF3H effector proteins in PCa models would be of interest in order to elucidate its function and understand the mechanism underlying the relevance of EIF3H in this disease.

IV.2.9. Identification of potential EIF3H-effector proteins

IV.2.9.1. EIF3H directly interacts with STAU1 in PCa cell lines

To identify the proteins interacting with EIF3H, a co-immunoprecipitation (Co-IP) assay was performed after infecting PC3 cells with the pLV empty vector or the Myc-EIF3H vector. To select the most relevant candidates, the list of proteins identified by MS was filtered and only proteins identified in all three replicates over-expressing EIF3H and not in the replicates infected with the pLV empty vector were considered. This analysis allowed to identify a total of 6 proteins that directly interacted with EIF3H in the samples. Among them, Staufen1 (STAU1) was further investigated due to its role in oncogenesis (Almasi & Jasmin, 2021).

STAU1 is a multi-functional, double-stranded RNA-binding protein (RBP) involved in critical steps of RNA metabolism, including splicing, cell cycling and translation (reviewed in Gerstberger et al., 2014). Given the relevance of RBPs in regulating multiple steps of RNA metabolism, the role of these proteins in controlling different cell aspects (e.g., growth, migration or apoptosis) has been widely studied (reviewed in Gerstberger et al., 2014). Notably, due to the significance of RBPs in regulating several cellular functions, their dysregulation contributes to the pathophysiology of several diseases, including cancer (Wurth, 2012). In this context, various studies have explored the role of STAU1 in the onset and progression of different tumor types, highlighting its role in tumor promotion (Crawford Parks et al., 2017; Gong & Maquat, 2011; Ruan et al., 2020; T.-P. Xu et al., 2015). Particularly, in PCa, STAU1 expression levels have been shown to be increased in PCa cells, and has been reported to play a critical role in regulating growth, migration and invasion capacities of different PCa cellular models (Marcellus et al., 2021).

Notably, when classifying PCa patients into high and low *STAU1* expression according to a specific cut-off value, the Human Protein Atlas database (<https://humantumoratlas.org>; Uhlen et al., 2017) shows a significant correlation between

higher *STAU1* expression and poor overall survival, suggesting *STAU1* as an unfavorable prognostic factor of PCa. In addition, based on the differential expression analysis conducted in this study, this gene showed higher expression in PCa vs healthy tissues (Figure 40A), and in aggressive (Figure 40C) and metastatic (Figure 40D) samples when compared to indolent and primary tissues, respectively. Furthermore, *STAU1* expression is significantly correlated with the GS variable (Figure 40B) and with shorter BCR-free time (Figure 40E-F).

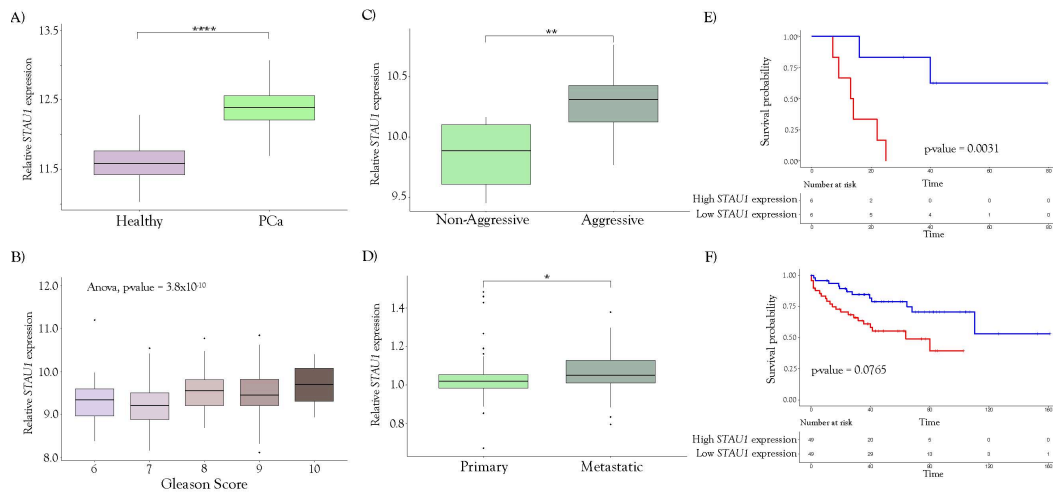


Figure 40. *STAU1* is over-expressed in PCa and associated with PCa progression. A) Relative expression in PCa and normal tissues based on publicly available data from the TCGA and GTXe (n = 548 PCa patients vs 100 healthy individuals) databases. B) Relative expression in different PCa samples from the TCGA dataset classified based on their Gleason Score (n = 497). Relative expression in different PCa stages and Kaplan-Meier curves based on publicly available data from C and E) gse46602 and, D and F) gse21035 GEO studies. **** p-value < 0.0001, ** p-value < 0.01 and * p-value < 0.05 vs reference group.

According to the literature, *STAU1* protein can be ubiquitinated and degraded by the ubiquitin-proteasome system (UPS) (Boulay et al., 2014; Gonzalez Quesada & DesGroseillers, 2022). Given that EIF3H functions as a deubiquitinating enzyme, it could be possible that, in our PCa cellular model, the interaction seen between EIF3H and *STAU1* could lead to *STAU1* deubiquitination, therefore, contributing to its stabilization and promotion of tumor aggressiveness.

IV.2.9.2. *STAU1* is a druggable target

From a drug development point of view, in terms of its chemical and molecular characteristics, the *STAU* protein is located in the cytoplasm, its molecular weight is 63.182 Da and has a sequence of 577 amino acids (UniProt Consortium, 2021). Based on the

information available on the PDB database, there is information available of 4 different 3D structures for human STAU1 with a resolution below 3.0 Å. Figure 41 illustrates STAU1 protein in complex with an RNA molecule. In addition, the recombinant protein, expressed and purified in various host, including *E. coli*, yeast and Baculovirus, with a purity above 85% is commercially available (<https://www.mybiosource.com>).



Figure 41. 3D structure of the PDB ID 6HTU. Structure of STAU1 in complex with RNA, where the STAU1 is represented in purple. The image was obtained from the PDB.

On the other, there are none reported inhibitors and the canSAR database has not predicted any potential ligandable cavities in the structure. Nevertheless, STAU1 has been reported to be a substrate of the E3 ubiquitin ligase anaphase-promoting complex/cyclosome (APC/C) (Boulay et al., 2014) and of the E3 ubiquitin ligase TRIM25 (Gonzalez Quesada & DesGroseillers, 2022) and, subsequently, being polyubiquitinated and degraded by the UPS. Interestingly, proteolysis-targeting chimeras (PROTACs) have emerged as a promising approach to target cancer-related proteins, an especially those considered to be undruggable, defined as proteins lacking of targetable cavities, such as DNA- and RNA-binding proteins or transcription factors (Buckley & Crews, 2014). Unlike small molecule inhibitors, PROTACs do not need an active site to modulate the biological activity of the protein to target. Briefly, PROTACs are heterobifunctional small molecules consisting of a ligand for a protein of interest (POI) that is to be targeted for its degradation, a ligand for recruiting an E3 ubiquitin ligase, and a linker connecting them (Buckley & Crews, 2014). When the complex is formed, the ligase induces the ubiquitination of the POI and its subsequent degradation by the UPS. Then, once the POI is degraded, the

the PROTAC is recycled to target another copy of the POI (Békés et al., 2022). Thus, given that PROTACs can be recycled, their dosage, administration frequency and toxicity is lower than those of the small molecule inhibitors (X. Li et al., 2022).

In the PCa field, several PROTAC have been developed to target the AR for degradation, and three AR-targeting molecules have entered phase I/II clinical trials to treat patients with mCRPC (reviewed in Avgeris et al., 2022). Thus, the development of new PROTACs targeting STAU1 for degradation could represent a promising novel approach for the development of new treatments for advanced PCa patients.

V. FUTURE PERSPECTIVES

The results presented in this thesis point out the potential of combining different omics data for the identification of new clinically relevant PCa biomarkers. In the first objective presented in this work, a multi-omics-based approach enabled the identification of a group of metabolites and metabolic pathways significantly dysregulated in high-GS patients. Thus, to increase the robustness of the reported findings, future analyses should include the validation in larger and independent cohorts of patients, and the use of *in vitro* and *in vivo* models to mechanistically understand the significance of these metabolic changes in the context of PCa.

Furthermore, the strategy followed to pursue the second objective included in this thesis, based on the calculation of essentiality scores and transcriptomics analyses, has been proved to be an effective approach for the identification of novel potential therapeutic targets in the oncology area. Among the 16 most promising candidates identified following this strategy, we have validated the role of EIF3H as a potential target in advanced PCa stages. Following experiments are focused on validating the role of EIF3H in other *in vitro* and *in vivo* models. Also, given the potential relevance of the observed interaction between EIF3H and STAU1 proteins in PCa cellular model, future steps will be focused on deciphering the biological significance of this interaction, together with the assessment of its potential towards the development of novel treatments for advanced PCa patients.

Finally, also derived from the results generated in this thesis, future projects will examine the potential role of LSM4 and SNRPE in PCa tumorigenesis, and explore the mechanism by which they could be regulating tumor proliferation and progression.

VI. CONCLUSIONS

The main conclusions that can be extracted from this doctoral thesis are summarized as follows:

1. The combined analysis of metabolic and transcriptomic data represents a valuable strategy to characterize metabolic alterations underlying PCa progression and identify non-invasive biomarkers with clinical potential for the management of PCa patients.
2. The metabolic changes observed in samples from PCa patients have revealed dysregulations in the nucleotide synthesis and energy metabolism of high-GS PCa patients.
3. At the transcriptomic level, high-GS PCa patients have showed increased purine biosynthesis resulted from an enhanced folate cycle, together with a slow glycolysis rate that may be balanced by an enhanced OXPHOS activity. These alterations are reflected, at the systemic level, by elevated serum levels of glycine and glucose and increased urine concentrations of 1-methylnicotinamide in high-GS PCa patients.
4. The combination of essentiality gene data, based on results from functional screenings, together with the analysis of differential expression and correlation analyses with disease progression, represent a promising approach to discover valuable genetic vulnerabilities for the identification of novel therapeutic targets for advanced PCa patients.
5. The genetic vulnerabilities specifically identified for advanced PCa are mainly associated with mRNA translation initiation and spliceosome assembly processes.
6. EIF3H, LSM4 and SNRPE represent potential novel therapeutic targets for drug development to treat advanced PCa patients.
7. Changes in EIF3H expression are significantly correlated with cell proliferation, colony formation and migration capacity in the evaluated PCa cellular models.

Conclusions

8. There exists a correlation between EIF3H expression and the expression levels of different EMT markers in the evaluated PCa cellular models, suggesting a potential role of EIF3H in EMT progression.

VII. REFERENCES

- Agrotis, A., & Ketteler, R. (2015). A new age in functional genomics using CRISPR/Cas9 in arrayed library screening. *Frontiers in Genetics*, 6, 300. <https://doi.org/10.3389/fgene.2015.00300>
- Alaiya, A. A., Al-Mohanna, M., Aslam, M., Shinwari, Z., Al-Mansouri, L., Al-Rodayan, M., Al-Eid, M., Ahmad, I., Hanash, K., Tulbah, A., Bin Mahfooz, A., & Adra, C. (2011). Proteomics-based signature for human benign prostate hyperplasia and prostate adenocarcinoma. *International Journal of Oncology*, 38(4), 1047–1057. <https://doi.org/10.3892/ijo.2011.937>
- Ali, M. U., Ur Rahman, M. S., Jia, Z., & Jiang, C. (2017). Eukaryotic translation initiation factors and cancer. *Tumour Biology: The Journal of the International Society for Oncodevelopmental Biology and Medicine*, 39(6), 1010428317709805. <https://doi.org/10.1177/1010428317709805>
- Almasi, S., & Jasmin, B. J. (2021). The multifunctional RNA-binding protein Staufen1: An emerging regulator of oncogenesis through its various roles in key cellular events. *Cellular and Molecular Life Sciences: CMLS*, 78(23), 7145–7160. <https://doi.org/10.1007/s00018-021-03965-w>
- Anchi, T., Tamura, K., Furihata, M., Satake, H., Sakoda, H., Kawada, C., Kamei, M., Shimamoto, T., Fukuhara, H., Fukata, S., Ashida, S., Karashima, T., Yamasaki, I., Yasuda, M., Kamada, M., Inoue, K., & Shuin, T. (2012). SNRPE is involved in cell proliferation and progression of high-grade prostate cancer through the regulation of androgen receptor expression. *Oncology Letters*, 3(2), 264–268. <https://doi.org/10.3892/ol.2011.505>
- Andersen, M. K., Rise, K., Giskeødegård, G. F., Richardsen, E., Bertilsson, H., Størkersen, Ø., Bathen, T. F., Rye, M., & Tessem, M.-B. (2018). Integrative metabolic and transcriptomic profiling of prostate cancer tissue containing reactive stroma. *Scientific Reports*, 8(1), 14269. <https://doi.org/10.1038/s41598-018-32549-1>
- Andreoiu, M., & Cheng, L. (2010). Multifocal prostate cancer: Biologic, prognostic, and therapeutic implications. *Human Pathology*, 41(6), 781–793. <https://doi.org/10.1016/j.humpath.2010.02.011>
- Antonarakis, E. S., Lu, C., Wang, H., Luber, B., Nakazawa, M., Roeser, J. C., Chen, Y., Mohammad, T. A., Chen, Y., Fedor, H. L., Lotan, T. L., Zheng, Q., De Marzo, A. M., Isaacs, J. T., Isaacs, W. B., Nadal, R., Paller, C. J., Denmeade, S. R., Carducci, M. A., ... Luo, J. (2014). AR-V7 and resistance to enzalutamide and abiraterone in prostate cancer. *The New England Journal of Medicine*, 371(11), 1028–1038. <https://doi.org/10.1056/NEJMoa1315815>
- Apaolaza, I., San José-Eneriz, E., Tobalina, L., Miranda, E., Garate, L., Agirre, X., Prósper, F., & Planes, F. J. (2017). An in-silico approach to predict and exploit synthetic lethality in cancer metabolism. *Nature Communications*, 8(1), 459. <https://doi.org/10.1038/s41467-017-00555-y>
- Arora, V. K., Schenkein, E., Murali, R., Subudhi, S. K., Wongvipat, J., Balbas, M. D., Shah, N., Cai, L., Efstathiou, E., Logothetis, C., Zheng, D., & Sawyers, C. L. (2013). Glucocorticoid receptor confers resistance to antiandrogens by bypassing androgen receptor blockade. *Cell*, 155(6), 1309–1322. <https://doi.org/10.1016/j.cell.2013.11.012>
- Ashton, T. M., McKenna, W. G., Kunz-Schughart, L. A., & Higgins, G. S. (2018). Oxidative Phosphorylation as an Emerging Target in Cancer Therapy. *Clinical Cancer Research: An Official Journal of the American*

References

- Association for Cancer Research, 24(11), 2482–2490. <https://doi.org/10.1158/1078-0432.CCR-17-3070>
- Avgeris, I., Pliatsika, D., Nikolaropoulos, S. S., & Foustieris, M. A. (2022). Targeting androgen receptor for prostate cancer therapy: From small molecules to PROTACs. *Bioorganic Chemistry*, 128, 106089. <https://doi.org/10.1016/j.bioorg.2022.106089>
- Azzouni, F., & Mohler, J. (2012). Biology of castration-recurrent prostate cancer. *The Urologic Clinics of North America*, 39(4), 435–452. <https://doi.org/10.1016/j.ucl.2012.07.002>
- Bai, R., Wan, R., Wang, L., Xu, K., Zhang, Q., Lei, J., & Shi, Y. (2021). Structure of the activated human minor spliceosome. *Science (New York, N.Y.)*, 371(6535), eabg0879. <https://doi.org/10.1126/science.abg0879>
- Banerjee, J., Mishra, N., & Dhas, Y. (2015). Metagenomics: A new horizon in cancer research. *Meta Gene*, 5, 84–89. <https://doi.org/10.1016/j.mgene.2015.05.005>
- Barfeld, S. J., Fazli, L., Persson, M., Marjavaara, L., Urbanucci, A., Kaukonen, K. M., Rennie, P. S., Ceder, Y., Chabes, A., Visakorpi, T., & Mills, I. G. (2015). Myc-dependent purine biosynthesis affects nucleolar stress and therapy response in prostate cancer. *Oncotarget*, 6(14), 12587–12602. <https://doi.org/10.18632/oncotarget.3494>
- Beckonert, O., Keun, H. C., Ebbels, T. M. D., Bundy, J., Holmes, E., Lindon, J. C., & Nicholson, J. K. (2007). Metabolic profiling, metabolomic and metabonomic procedures for NMR spectroscopy of urine, plasma, serum and tissue extracts. *Nature Protocols*, 2(11), 2692–2703. <https://doi.org/10.1038/nprot.2007.376>
- Behan, F. M., Iorio, F., Picco, G., Gonçalves, E., Beaver, C. M., Migliardi, G., Santos, R., Rao, Y., Sassi, F., Pinnelli, M., Ansari, R., Harper, S., Jackson, D. A., McRae, R., Pooley, R., Wilkinson, P., van der Meer, D., Dow, D., Buser-Doepner, C., ... Garnett, M. J. (2019). Prioritization of cancer therapeutic targets using CRISPR-Cas9 screens. *Nature*, 568(7753), 511–516. <https://doi.org/10.1038/s41586-019-1103-9>
- Beirnaert, C., Meysman, P., Vu, T. N., Hermans, N., Apers, S., Pieters, L., Covaci, A., & Laukens, K. (2018). speaq 2.0: A complete workflow for high-throughput 1D NMR spectra processing and quantification. *PLoS Computational Biology*, 14(3), e1006018. <https://doi.org/10.1371/journal.pcbi.1006018>
- Békés, M., Langley, D. R., & Crews, C. M. (2022). PROTAC targeted protein degraders: The past is prologue. *Nature Reviews. Drug Discovery*, 21(3), 181–200. <https://doi.org/10.1038/s41573-021-00371-6>
- Berman, H. M., Westbrook, J., Feng, Z., Gilliland, G., Bhat, T. N., Weissig, H., Shindyalov, I. N., & Bourne, P. E. (2000). The Protein Data Bank. *Nucleic Acids Research*, 28(1), 235–242. <https://doi.org/10.1093/nar/28.1.235>
- Bertram, K., Agafonov, D. E., Dybkov, O., Haselbach, D., Leelaram, M. N., Will, C. L., Urlaub, H., Kastner, B., Lührmann, R., & Stark, H. (2017). Cryo-EM Structure of a Pre-catalytic Human Spliceosome Primed for Activation. *Cell*, 170(4), 701–713.e11. <https://doi.org/10.1016/j.cell.2017.07.011>

- Beznosková, P., Cuchalová, L., Wagner, S., Shoemaker, C. J., Gunišová, S., von der Haar, T., & Valášek, L. S. (2013). Translation initiation factors eIF3 and HCR1 control translation termination and stop codon read-through in yeast cells. *PLoS Genetics*, 9(11), e1003962. <https://doi.org/10.1371/journal.pgen.1003962>
- Beznosková, P., Wagner, S., Jansen, M. E., von der Haar, T., & Valášek, L. S. (2015). Translation initiation factor eIF3 promotes programmed stop codon readthrough. *Nucleic Acids Research*, 43(10), 5099–5111. <https://doi.org/10.1093/nar/gkv421>
- Bhat, M., Robichaud, N., Hulea, L., Sonenberg, N., Pelletier, J., & Topisirovic, I. (2015). Targeting the translation machinery in cancer. *Nature Reviews. Drug Discovery*, 14(4), 261–278. <https://doi.org/10.1038/nrd4505>
- Biamonti, G., Catillo, M., Pignataro, D., Montecucco, A., & Ghigna, C. (2014). The alternative splicing side of cancer. *Seminars in Cell & Developmental Biology*, 32, 30–36. <https://doi.org/10.1016/j.semcdb.2014.03.016>
- Bitting, R. L., & Armstrong, A. J. (2013). Targeting the PI3K/Akt/mTOR pathway in castration-resistant prostate cancer. *Endocrine-Related Cancer*, 20(3), R83-99. <https://doi.org/10.1530/ERC-12-0394>
- Bjurlin, M. A., & Taneja, S. S. (2014). Standards for prostate biopsy. *Current Opinion in Urology*, 24(2), 155–161. <https://doi.org/10.1097/MOU.0000000000000031>
- Boesen, L. (2019). Magnetic resonance imaging-transrectal ultrasound image fusion guidance of prostate biopsies: Current status, challenges and future perspectives. *Scandinavian Journal of Urology*, 53(2–3), 89–96. <https://doi.org/10.1080/21681805.2019.1600581>
- Boettcher, M., & Hoheisel, J. D. (2010). Pooled RNAi Screens—Technical and Biological Aspects. *Current Genomics*, 11(3), 162–167. <https://doi.org/10.2174/138920210791110988>
- Bonnal, S., Vigevani, L., & Valcárcel, J. (2012). The spliceosome as a target of novel antitumour drugs. *Nature Reviews. Drug Discovery*, 11(11), 847–859. <https://doi.org/10.1038/nrd3823>
- Bose, S., Allen, A. E., & Locasale, J. W. (2020). The Molecular Link from Diet to Cancer Cell Metabolism. *Molecular Cell*, 78(6), 1034–1044. <https://doi.org/10.1016/j.molcel.2020.05.018>
- Boulay, K., Ghram, M., Viranaicken, W., Trépanier, V., Mollet, S., Fréchina, C., & DesGroseillers, L. (2014). Cell cycle-dependent regulation of the RNA-binding protein Staufen1. *Nucleic Acids Research*, 42(12), 7867–7883. <https://doi.org/10.1093/nar/gku506>
- Boysen, G., Barbieri, C. E., Prandi, D., Blattner, M., Chae, S.-S., Dahija, A., Nataraj, S., Huang, D., Marotz, C., Xu, L., Huang, J., Lecca, P., Chhangawala, S., Liu, D., Zhou, P., Sboner, A., de Bono, J. S., Demichelis, F., Houvras, Y., & Rubin, M. A. (2015). SPOP mutation leads to genomic instability in prostate cancer. *ELife*, 4, e09207. <https://doi.org/10.7554/eLife.09207>
- Braadland, P. R., Giskeødegård, G., Sandsmark, E., Bertilsson, H., Euceda, L. R., Hansen, A. F., Guldvik, I. J., Selnaes, K. M., Grytli, H. H., Katz, B., Svindland, A., Bathen, T. F., Eri, L. M., Nygård, S., Berge, V., Taskén, K. A., & Tessem, M.-B. (2017). Ex vivo metabolic fingerprinting identifies biomarkers predictive of prostate cancer recurrence following radical prostatectomy. *British Journal of Cancer*, 117(11), 1656–1664. <https://doi.org/10.1038/bjc.2017.346>

References

- Brito Querido, J., Sokabe, M., Kraatz, S., Gordiyenko, Y., Skehel, J. M., Fraser, C. S., & Ramakrishnan, V. (2020). Structure of a human 48S translational initiation complex. *Science (New York, N.Y.)*, 369(6508), 1220–1227. <https://doi.org/10.1126/science.aba4904>
- Brooks, J. D., Wei, W., Hawley, S., Auman, H., Newcomb, L., Boyer, H., Fazli, L., Simko, J., Hurtado-Coll, A., Troyer, D. A., Carroll, P. R., Gleave, M., Lance, R., Lin, D. W., Nelson, P. S., Thompson, I. M., True, L. D., Feng, Z., & McKenney, J. K. (2015). Evaluation of ERG and SPINK1 by Immunohistochemical Staining and Clinicopathological Outcomes in a Multi-Institutional Radical Prostatectomy Cohort of 1067 Patients. *PloS One*, 10(7), e0132343. <https://doi.org/10.1371/journal.pone.0132343>
- Brown, K. K., Hann, M. M., Lakdawala, A. S., Santos, R., Thomas, P. J., & Todd, K. (2018). Approaches to target tractability assessment—A practical perspective. *MedChemComm*, 9(4), 606–613. <https://doi.org/10.1039/c7md00633k>
- Brummelkamp, T. R., & Bernards, R. (2003). New tools for functional mammalian cancer genetics. *Nature Reviews. Cancer*, 3(10), 781–789. <https://doi.org/10.1038/nrc1191>
- Bruzzone, C., Loizaga-Iriarte, A., Sánchez-Mosquera, P., Gil-Redondo, R., Astobiza, I., Diercks, T., Cortazar, A. R., Ugalde-Olano, A., Schäfer, H., Blanco, F. J., Unda, M., Cannet, C., Spraul, M., Mato, J. M., Embade, N., Carracedo, A., & Millet, O. (2020). 1H NMR-Based Urine Metabolomics Reveals Signs of Enhanced Carbon and Nitrogen Recycling in Prostate Cancer. *Journal of Proteome Research*, 19(6), 2419–2428. <https://doi.org/10.1021/acs.jproteome.0c00091>
- Buckley, D. L., & Crews, C. M. (2014). Small-molecule control of intracellular protein levels through modulation of the ubiquitin proteasome system. *Angewandte Chemie (International Ed. in English)*, 53(9), 2312–2330. <https://doi.org/10.1002/anie.201307761>
- Buyyounouski, M. K., Choyke, P. L., McKenney, J. K., Sartor, O., Sandler, H. M., Amin, M. B., Kattan, M. W., & Lin, D. W. (2017). Prostate cancer—Major changes in the American Joint Committee on Cancer eighth edition cancer staging manual. *CA: A Cancer Journal for Clinicians*, 67(3), 245–253. <https://doi.org/10.3322/caac.21391>
- Cancer Genome Atlas Research Network. (2015). The Molecular Taxonomy of Primary Prostate Cancer. *Cell*, 163(4), 1011–1025. <https://doi.org/10.1016/j.cell.2015.10.025>
- Cancer.Net. (2012, June 25). *Prostate Cancer—Statistics*. Cancer.Net. <https://www.cancer.net/cancer-types/prostate-cancer/statistics>
- Cappuzzo, F., Varella-Garcia, M., Rossi, E., Gajapathy, S., Valente, M., Drabkin, H., & Gemmill, R. (2009). MYC and EIF3H Coamplification significantly improve response and survival of non-small cell lung cancer patients (NSCLC) treated with gefitinib. *Journal of Thoracic Oncology: Official Publication of the International Association for the Study of Lung Cancer*, 4(4), 472–478. <https://doi.org/10.1097/JTO.0b013e31819a5767>
- Carver, B. S., Chapinski, C., Wongvipat, J., Hieronymus, H., Chen, Y., Chandarlapaty, S., Arora, V. K., Le, C., Koutcher, J., Scher, H., Scardino, P. T., Rosen, N., & Sawyers, C. L. (2011). Reciprocal feedback

- regulation of PI3K and androgen receptor signaling in PTEN-deficient prostate cancer. *Cancer Cell*, 19(5), 575–586. <https://doi.org/10.1016/j.ccr.2011.04.008>
- Ceder, Y., Bjartell, A., Culig, Z., Rubin, M. A., Tomlins, S., & Visakorpi, T. (2016). The Molecular Evolution of Castration-resistant Prostate Cancer. *European Urology Focus*, 2(5), 506–513. <https://doi.org/10.1016/j.euf.2016.11.012>
- Chabot, B., & Shkreta, L. (2016). Defective control of pre-messenger RNA splicing in human disease. *The Journal of Cell Biology*, 212(1), 13–27. <https://doi.org/10.1083/jcb.201510032>
- Chan, S. C., & Dehm, S. M. (2014). Constitutive activity of the androgen receptor. *Advances in Pharmacology (San Diego, Calif.)*, 70, 327–366. <https://doi.org/10.1016/B978-0-12-417197-8.00011-0>
- Chandran, U. R., Ma, C., Dhir, R., Bisceglia, M., Lyons-Weiler, M., Liang, W., Michalopoulos, G., Becich, M., & Monzon, F. A. (2007). Gene expression profiles of prostate cancer reveal involvement of multiple molecular pathways in the metastatic process. *BMC Cancer*, 7, 64. <https://doi.org/10.1186/1471-2407-7-64>
- Chang, L., Ruiz, P., Ito, T., & Sellers, W. R. (2021). Targeting pan-essential genes in cancer: Challenges and opportunities. *Cancer Cell*, 39(4), 466–479. <https://doi.org/10.1016/j.ccell.2020.12.008>
- Chen, F. K., de Castro Abreu, A. L., & Palmer, S. L. (2016). Utility of Ultrasound in the Diagnosis, Treatment, and Follow-up of Prostate Cancer: State of the Art. *Journal of Nuclear Medicine: Official Publication, Society of Nuclear Medicine*, 57(Suppl 3), 13S-18S. <https://doi.org/10.2967/jnumed.116.177196>
- Chen, L., Lin, Y.-H., Liu, G.-Q., Huang, J.-E., Wei, W., Yang, Z.-H., Hu, Y.-M., Xie, J.-H., & Yu, H.-Z. (2021). Clinical Significance and Potential Role of LSM4 Overexpression in Hepatocellular Carcinoma: An Integrated Analysis Based on Multiple Databases. *Frontiers in Genetics*, 12, 804916. <https://doi.org/10.3389/fgene.2021.804916>
- Chen, Y., Clegg, N. J., & Scher, H. I. (2009). Anti-androgens and androgen-depleting therapies in prostate cancer: New agents for an established target. *The Lancet. Oncology*, 10(10), 981–991. [https://doi.org/10.1016/S1470-2045\(09\)70229-3](https://doi.org/10.1016/S1470-2045(09)70229-3)
- Chen, Y., Wang, K., Liu, T., Chen, J., Lv, W., Yang, W., Xu, S., Wang, X., & Li, L. (2020). Decreased glucose bioavailability and elevated aspartate metabolism in prostate cancer cells undergoing epithelial-mesenchymal transition. *Journal of Cellular Physiology*, 235(7–8), 5602–5612. <https://doi.org/10.1002/jcp.29490>
- Cheng, H. H., Pritchard, C. C., Boyd, T., Nelson, P. S., & Montgomery, B. (2016). Biallelic Inactivation of BRCA2 in Platinum-sensitive Metastatic Castration-resistant Prostate Cancer. *European Urology*, 69(6), 992–995. <https://doi.org/10.1016/j.eururo.2015.11.022>
- Chistiakov, D. A., Myasoedova, V. A., Grechko, A. V., Melnichenko, A. A., & Orekhov, A. N. (2018). New biomarkers for diagnosis and prognosis of localized prostate cancer. *Seminars in Cancer Biology*, 52(Pt 1), 9–16. <https://doi.org/10.1016/j.semcancer.2018.01.012>
- Choe, J., Lin, S., Zhang, W., Liu, Q., Wang, L., Ramirez-Moya, J., Du, P., Kim, W., Tang, S., Sliz, P., Santisteban, P., George, R. E., Richards, W. G., Wong, K.-K., Locker, N., Slack, F. J., & Gregory,

References

- R. I. (2018). mRNA circularization by METTL3-eIF3h enhances translation and promotes oncogenesis. *Nature*, *561*(7724), 556–560. <https://doi.org/10.1038/s41586-018-0538-8>
- Christenson, M., Song, C.-S., Liu, Y.-G., & Chatterjee, B. (2022). Precision Targets for Intercepting the Lethal Progression of Prostate Cancer: Potential Avenues for Personalized Therapy. *Cancers*, *14*(4), 892. <https://doi.org/10.3390/cancers14040892>
- Coker, E. A., Mitsopoulos, C., Tym, J. E., Komianou, A., Kannas, C., Di Micco, P., Villasclaras Fernandez, E., Ozer, B., Antolin, A. A., Workman, P., & Al-Lazikani, B. (2019). canSAR: Update to the cancer translational research and drug discovery knowledgebase. *Nucleic Acids Research*, *47*(D1), D917–D922. <https://doi.org/10.1093/nar/gky1129>
- Cookson, M. S., Aus, G., Burnett, A. L., Canby-Hagino, E. D., D'Amico, A. V., Dmochowski, R. R., Eton, D. T., Forman, J. D., Goldenberg, S. L., Hernandez, J., Higano, C. S., Kraus, S. R., Moul, J. W., Tangen, C., Thrasher, J. B., & Thompson, I. (2007). Variation in the definition of biochemical recurrence in patients treated for localized prostate cancer: The American Urological Association Prostate Guidelines for Localized Prostate Cancer Update Panel report and recommendations for a standard in the reporting of surgical outcomes. *The Journal of Urology*, *177*(2), 540–545. <https://doi.org/10.1016/j.juro.2006.10.097>
- Cornford, P., Bellmunt, J., Bolla, M., Briers, E., De Santis, M., Gross, T., Henry, A. M., Joniau, S., Lam, T. B., Mason, M. D., van der Poel, H. G., van der Kwast, T. H., Rouvière, O., Wiegel, T., & Mottet, N. (2017). EAU-ESTRO-SIOG Guidelines on Prostate Cancer. Part II: Treatment of Relapsing, Metastatic, and Castration-Resistant Prostate Cancer. *European Urology*, *71*(4), 630–642. <https://doi.org/10.1016/j.eururo.2016.08.002>
- Cowley, G. S., Weir, B. A., Vazquez, F., Tamayo, P., Scott, J. A., Rusin, S., East-Seletsky, A., Ali, L. D., Gerath, W. F., Pantel, S. E., Lizotte, P. H., Jiang, G., Hsiao, J., Tsherniak, A., Dwinell, E., Aoyama, S., Okamoto, M., Harrington, W., Gelfand, E., ... Hahn, W. C. (2014). Parallel genome-scale loss of function screens in 216 cancer cell lines for the identification of context-specific genetic dependencies. *Scientific Data*, *1*, 140035. <https://doi.org/10.1038/sdata.2014.35>
- Crawford Parks, T. E., Marcellus, K. A., Langill, J., Ravel-Chapuis, A., Michaud, J., Cowan, K. N., Côté, J., & Jasmin, B. J. (2017). Novel Roles for Stauf1 in Embryonal and Alveolar Rhabdomyosarcoma via c-myc-dependent and -independent events. *Scientific Reports*, *7*, 42342. <https://doi.org/10.1038/srep42342>
- Cui, T., Kovell, R. C., & Terlecki, R. P. (2016). Is it time to abandon the digital rectal examination? Lessons from the PLCO Cancer Screening Trial and peer-reviewed literature. *Current Medical Research and Opinion*, *32*(10), 1663–1669. <https://doi.org/10.1080/03007995.2016.1198312>
- D'Abronzio, L. S., & Ghosh, P. M. (2018). EIF4E Phosphorylation in Prostate Cancer. *Neoplasia*, *20*(6), 563–573. <https://doi.org/10.1016/j.neo.2018.04.003>
- Dall'Era, M. A., Albertsen, P. C., Bangma, C., Carroll, P. R., Carter, H. B., Cooperberg, M. R., Freedland, S. J., Klotz, L. H., Parker, C., & Soloway, M. S. (2012). Active surveillance for prostate cancer: A

- systematic review of the literature. *European Urology*, 62(6), 976–983. <https://doi.org/10.1016/j.eururo.2012.05.072>
- D'Amico, A. V., Whittington, R., Malkowicz, S. B., Schultz, D., Blank, K., Broderick, G. A., Tomaszewski, J. E., Renshaw, A. A., Kaplan, I., Beard, C. J., & Wein, A. (1998). Biochemical outcome after radical prostatectomy, external beam radiation therapy, or interstitial radiation therapy for clinically localized prostate cancer. *JAMA*, 280(11), 969–974. <https://doi.org/10.1001/jama.280.11.969>
- Davalieva, K., Kostovska, I. M., Kiprijanovska, S., Markoska, K., Kubelka-Sabit, K., Filipovski, V., Stavridis, S., Stankov, O., Komina, S., Petrussevska, G., & Polenakovic, M. (2015). Proteomics analysis of malignant and benign prostate tissue by 2D DIGE/MS reveals new insights into proteins involved in prostate cancer. *The Prostate*, 75(14), 1586–1600. <https://doi.org/10.1002/pros.23034>
- Davoli, T., Mengwasser, K. E., Duan, J., Chen, T., Christensen, C., Wooten, E. C., Anselmo, A. N., Li, M. Z., Wong, K.-K., Kahle, K. T., & Elledge, S. J. (2016). Functional genomics reveals that tumors with activating phosphoinositide 3-kinase mutations are dependent on accelerated protein turnover. *Genes & Development*, 30(24), 2684–2695. <https://doi.org/10.1101/gad.290122.116>
- De Nunzio, C., Pastore, A. L., Lombardo, R., Simone, G., Leonardo, C., Mastroianni, R., Collura, D., Muto, G., Gallucci, M., Carbone, A., Fuschi, A., Dutto, L., Witt, J. H., De Dominicis, C., & Tubaro, A. (2018). The new Epstein gleason score classification significantly reduces upgrading in prostate cancer patients. *European Journal of Surgical Oncology*, 44(6), 835–839. <https://doi.org/10.1016/j.ejso.2017.12.003>
- Dell'Atti, L. (2016). Prognostic significance of perineural invasion in patients who underwent radical prostatectomy for localized prostate cancer. *Journal of B.U.ON.: Official Journal of the Balkan Union of Oncology*, 21(5), 1219–1223.
- Dereziński, P., Klupczynska, A., Sawicki, W., Pałka, J. A., & Kokot, Z. J. (2017). Amino Acid Profiles of Serum and Urine in Search for Prostate Cancer Biomarkers: A Pilot Study. *International Journal of Medical Sciences*, 14(1), 1–12. <https://doi.org/10.7150/ijms.15783>
- des Georges, A., Dhote, V., Kuhn, L., Hellen, C. U. T., Pestova, T. V., Frank, J., & Hashem, Y. (2015). Structure of mammalian eIF3 in the context of the 43S preinitiation complex. *Nature*, 525(7570), 491–495. <https://doi.org/10.1038/nature14891>
- Dieterle, F., Ross, A., Schlotterbeck, G., & Senn, H. (2006). Probabilistic quotient normalization as robust method to account for dilution of complex biological mixtures. Application in ¹H NMR metabonomics. *Analytical Chemistry*, 78(13), 4281–4290. <https://doi.org/10.1021/ac051632c>
- Dolfi, S. C., Chan, L. L.-Y., Qiu, J., Tedeschi, P. M., Bertino, J. R., Hirshfield, K. M., Oltvai, Z. N., & Vazquez, A. (2013). The metabolic demands of cancer cells are coupled to their size and protein synthesis rates. *Cancer & Metabolism*, 1(1), 20. <https://doi.org/10.1186/2049-3002-1-20>
- Drake, J. M., Graham, N. A., Lee, J. K., Stoyanova, T., Faltermeier, C. M., Sud, S., Titz, B., Huang, J., Pienta, K. J., Graeber, T. G., & Witte, O. N. (2013). Metastatic castration-resistant prostate cancer reveals inpatient similarity and interpatient heterogeneity of therapeutic kinase targets. *Proceedings of the*

References

- National Academy of Sciences of the United States of America, 110(49), E4762-4769. <https://doi.org/10.1073/pnas.1319948110>
- Drake, R. R. (2015). Glycosylation and cancer: Moving glycomics to the forefront. *Advances in Cancer Research*, 126, 1–10. <https://doi.org/10.1016/bs.acr.2014.12.002>
- Dvinge, H., Kim, E., Abdel-Wahab, O., & Bradley, R. K. (2016). RNA splicing factors as oncoproteins and tumour suppressors. *Nature Reviews. Cancer*, 16(7), 413–430. <https://doi.org/10.1038/nrc.2016.51>
- Emwas, A.-H. M. (2015). The Strengths and Weaknesses of NMR Spectroscopy and Mass Spectrometry with Particular Focus on Metabolomics Research. In J. T. Bjerrum (Ed.), *Metabolomics* (Vol. 1277, pp. 161–193). Springer New York. https://doi.org/10.1007/978-1-4939-2377-9_13
- Emwas, A.-H., Roy, R., McKay, R. T., Tenori, L., Saccenti, E., Gowda, G. A. N., Raftery, D., Alahmari, F., Jaremko, L., Jaremko, M., & Wishart, D. S. (2019). NMR Spectroscopy for Metabolomics Research. *Metabolites*, 9(7), E123. <https://doi.org/10.3390/metabo9070123>
- Enchev, R. I., Schreiber, A., Beuron, F., & Morris, E. P. (2010). Structural insights into the COP9 signalosome and its common architecture with the 26S proteasome lid and eIF3. *Structure (London, England: 1993)*, 18(4), 518–527. <https://doi.org/10.1016/j.str.2010.02.008>
- Endoh, K., Nishi, M., Ishiguro, H., Uemura, H., Miyagi, Y., Aoki, I., Hirano, H., Kubota, Y., & Ryo, A. (2012). Identification of phosphorylated proteins involved in the oncogenesis of prostate cancer via Pin1-proteomic analysis. *The Prostate*, 72(6), 626–637. <https://doi.org/10.1002/pros.21466>
- Epstein, J. I. (2016). Prostate cancer: Urology journals recommend new prostate cancer grade groups. *Nature Reviews. Urology*, 13(7), 374–375. <https://doi.org/10.1038/nrurol.2016.96>
- Epstein, J. I., Egevad, L., Amin, M. B., Delahunt, B., Srigley, J. R., Humphrey, P. A., & Grading Committee. (2016). The 2014 International Society of Urological Pathology (ISUP) Consensus Conference on Gleason Grading of Prostatic Carcinoma: Definition of Grading Patterns and Proposal for a New Grading System. *The American Journal of Surgical Pathology*, 40(2), 244–252. <https://doi.org/10.1097/PAS.0000000000000530>
- Epstein, J. I., Zelefsky, M. J., Sjoberg, D. D., Nelson, J. B., Egevad, L., Magi-Galluzzi, C., Vickers, A. J., Parwani, A. V., Reuter, V. E., Fine, S. W., Eastham, J. A., Wiklund, P., Han, M., Reddy, C. A., Cizek, J. P., Nyberg, T., & Klein, E. A. (2016). A Contemporary Prostate Cancer Grading System: A Validated Alternative to the Gleason Score. *European Urology*, 69(3), 428–435. <https://doi.org/10.1016/j.eururo.2015.06.046>
- Eriksson, L., Johansson, E., Kettaneh-Wold, N., Trygg, J., Wikstrom, C., & Wold, S. (2013). *Multi- and megavariable data analysis. 1: Basic principles and applications* (Third revised edition). MKS Umetrics AB.
- Erzberger, J. P., Stengel, F., Pellarin, R., Zhang, S., Schaefer, T., Aylett, C. H. S., Cimermančič, P., Boehringer, D., Sali, A., Aebersold, R., & Ban, N. (2014). Molecular architecture of the 40S-eIF1-eIF3 translation initiation complex. *Cell*, 158(5), 1123–1135. <https://doi.org/10.1016/j.cell.2014.07.044>

- Etzioni, R., Penson, D. F., Legler, J. M., di Tommaso, D., Boer, R., Gann, P. H., & Feuer, E. J. (2002). Overdiagnosis due to prostate-specific antigen screening: Lessons from U.S. prostate cancer incidence trends. *Journal of the National Cancer Institute*, 94(13), 981–990. <https://doi.org/10.1093/jnci/94.13.981>
- Fabrizio, P., Dannenberg, J., Dube, P., Kastner, B., Stark, H., Urlaub, H., & Lührmann, R. (2009). The evolutionarily conserved core design of the catalytic activation step of the yeast spliceosome. *Molecular Cell*, 36(4), 593–608. <https://doi.org/10.1016/j.molcel.2009.09.040>
- Fan, L., Zhang, F., Xu, S., Cui, X., Hussain, A., Fazli, L., Gleave, M., Dong, X., & Qi, J. (2018). Histone demethylase JMJD1A promotes alternative splicing of AR variant 7 (AR-V7) in prostate cancer cells. *Proceedings of the National Academy of Sciences of the United States of America*, 115(20), E4584–E4593. <https://doi.org/10.1073/pnas.1802415115>
- Fei, T., Chen, Y., Xiao, T., Li, W., Cato, L., Zhang, P., Cotter, M. B., Bowden, M., Lis, R. T., Zhao, S. G., Wu, Q., Feng, F. Y., Loda, M., He, H. H., Liu, X. S., & Brown, M. (2017). Genome-wide CRISPR screen identifies HNRNPL as a prostate cancer dependency regulating RNA splicing. *Proceedings of the National Academy of Sciences of the United States of America*, 114(26), E5207–E5215. <https://doi.org/10.1073/pnas.1617467114>
- Ferlay, J., Laversanne, M., Ervik, M., Lam, F., Colombet, D. M., Piñeros, M., Znaor, A., Soerjomataram, I., & Bray, F. (2020). *Global Cancer Observatory: Cancer Tomorrow*. Lyon, France: International Agency for Research on Cancer. <https://gco.iarc.fr/tomorrow>
- Fizazi, K., Scher, H. I., Molina, A., Logothetis, C. J., Chi, K. N., Jones, R. J., Staffurth, J. N., North, S., Vogelzang, N. J., Saad, F., Mainwaring, P., Harland, S., Goodman, O. B., Sternberg, C. N., Li, J. H., Kheoh, T., Haqq, C. M., de Bono, J. S., & COU-AA-301 Investigators. (2012). Abiraterone acetate for treatment of metastatic castration-resistant prostate cancer: Final overall survival analysis of the COU-AA-301 randomised, double-blind, placebo-controlled phase 3 study. *The Lancet. Oncology*, 13(10), 983–992. [https://doi.org/10.1016/S1470-2045\(12\)70379-0](https://doi.org/10.1016/S1470-2045(12)70379-0)
- Frantzi, M., Hupe, M. C., Merseburger, A. S., Schanstra, J. P., Mischak, H., & Latosinska, A. (2020). Omics Derived Biomarkers and Novel Drug Targets for Improved Intervention in Advanced Prostate Cancer. *Diagnostics (Basel, Switzerland)*, 10(9), E658. <https://doi.org/10.3390/diagnostics10090658>
- Fraser, M., & Rouette, A. (2019). Prostate Cancer Genomic Subtypes. *Advances in Experimental Medicine and Biology*, 1210, 87–110. https://doi.org/10.1007/978-3-030-32656-2_5
- Fujita, K., Kume, H., Matsuzaki, K., Kawashima, A., Ujike, T., Nagahara, A., Uemura, M., Miyagawa, Y., Tomonaga, T., & Nonomura, N. (2017). Proteomic analysis of urinary extracellular vesicles from high Gleason score prostate cancer. *Scientific Reports*, 7, 42961. <https://doi.org/10.1038/srep42961>
- Furic, L., Rong, L., Larsson, O., Koumakpayi, I. H., Yoshida, K., Brueschke, A., Petroulakis, E., Robichaud, N., Pollak, M., Gaboury, L. A., Pandolfi, P. P., Saad, F., & Sonenberg, N. (2010). EIF4E phosphorylation promotes tumorigenesis and is associated with prostate cancer progression. *Proceedings of the National Academy of Sciences of the United States of America*, 107(32), 14134–14139. <https://doi.org/10.1073/pnas.1005320107>

References

- Fütterer, J. J., Briganti, A., De Visschere, P., Emberton, M., Giannarini, G., Kirkham, A., Taneja, S. S., Thoeny, H., Villeirs, G., & Villers, A. (2015). Can Clinically Significant Prostate Cancer Be Detected with Multiparametric Magnetic Resonance Imaging? A Systematic Review of the Literature. *European Urology*, 68(6), 1045–1053. <https://doi.org/10.1016/j.eururo.2015.01.013>
- Gao, B., Lue, H.-W., Podolak, J., Fan, S., Zhang, Y., Serawat, A., Alumkal, J. J., Fiehn, O., & Thomas, G. V. (2019). Multi-Omics Analyses Detail Metabolic Reprogramming in Lipids, Carnitines, and Use of Glycolytic Intermediates between Prostate Small Cell Neuroendocrine Carcinoma and Prostate Adenocarcinoma. *Metabolites*, 9(5), E82. <https://doi.org/10.3390/metabo9050082>
- Gashaw, I., Ellinghaus, P., Sommer, A., & Asadullah, K. (2012). What makes a good drug target? *Drug Discovery Today*, 17 Suppl, S24-30. <https://doi.org/10.1016/j.drudis.2011.12.008>
- Gautier, L., Cope, L., Bolstad, B. M., & Irizarry, R. A. (2004). affy—Analysis of Affymetrix GeneChip data at the probe level. *Bioinformatics (Oxford, England)*, 20(3), 307–315. <https://doi.org/10.1093/bioinformatics/btg405>
- Geisler, C., Gaisa, N. T., Pfister, D., Fuessel, S., Kristiansen, G., Braunschweig, T., Gostek, S., Beine, B., Diehl, H. C., Jackson, A. M., Borchers, C. H., Heidenreich, A., Meyer, H. E., Knüchel, R., & Henkel, C. (2015). Identification and validation of potential new biomarkers for prostate cancer diagnosis and prognosis using 2D-DIGE and MS. *BioMed Research International*, 2015, 454256. <https://doi.org/10.1155/2015/454256>
- Geng, C., He, B., Xu, L., Barbieri, C. E., Eedunuri, V. K., Chew, S. A., Zimmermann, M., Bond, R., Shou, J., Li, C., Blattner, M., Lonard, D. M., Demichelis, F., Coarfa, C., Rubin, M. A., Zhou, P., O'Malley, B. W., & Mitsiades, N. (2013). Prostate cancer-associated mutations in speckle-type POZ protein (SPOP) regulate steroid receptor coactivator 3 protein turnover. *Proceedings of the National Academy of Sciences of the United States of America*, 110(17), 6997–7002. <https://doi.org/10.1073/pnas.1304502110>
- Gerstberger, S., Hafner, M., & Tuschl, T. (2014). A census of human RNA-binding proteins. *Nature Reviews Genetics*, 15(12), 829–845. <https://doi.org/10.1038/nrg3813>
- Ghasemi, M., Turnbull, T., Sebastian, S., & Kempson, I. (2021). The MTT Assay: Utility, Limitations, Pitfalls, and Interpretation in Bulk and Single-Cell Analysis. *International Journal of Molecular Sciences*, 22(23), 12827. <https://doi.org/10.3390/ijms222312827>
- Gleason, D. F., & Mellinger, G. T. (1974). Prediction of prognosis for prostatic adenocarcinoma by combined histological grading and clinical staging. *The Journal of Urology*, 111(1), 58–64. [https://doi.org/10.1016/s0022-5347\(17\)59889-4](https://doi.org/10.1016/s0022-5347(17)59889-4)
- Gómez-Cebrián, N., Poveda, J. L., Pineda-Lucena, A., & Puchades-Carrasco, L. (2022). Metabolic Phenotyping in Prostate Cancer Using Multi-Omics Approaches. *Cancers*, 14(3), 596. <https://doi.org/10.3390/cancers14030596>
- Goncalves, M. D., Lu, C., Tutnauer, J., Hartman, T. E., Hwang, S.-K., Murphy, C. J., Pauli, C., Morris, R., Taylor, S., Bosch, K., Yang, S., Wang, Y., Van Riper, J., Lekaye, H. C., Roper, J., Kim, Y., Chen, Q., Gross, S. S., Rhee, K. Y., ... Yun, J. (2019). High-fructose corn syrup enhances intestinal tumor

- growth in mice. *Science (New York, N.Y.)*, 363(6433), 1345–1349. <https://doi.org/10.1126/science.aat8515>
- Gong, C., & Maquat, L. E. (2011). LncRNAs transactivate STAU1-mediated mRNA decay by duplexing with 3' UTRs via Alu elements. *Nature*, 470(7333), 284–288. <https://doi.org/10.1038/nature09701>
- Gonzalez Quesada, Y., & DesGroseillers, L. (2022). A Degradation Motif in STAU1 Defines a Novel Family of Proteins Involved in Inflammation. *International Journal of Molecular Sciences*, 23(19), 11588. <https://doi.org/10.3390/ijms231911588>
- Gordetsky, J., & Epstein, J. (2016). Grading of prostatic adenocarcinoma: Current state and prognostic implications. *Diagnostic Pathology*, 11, 25. <https://doi.org/10.1186/s13000-016-0478-2>
- Goto, T., Terada, N., Inoue, T., Kobayashi, T., Nakayama, K., Okada, Y., Yoshikawa, T., Miyazaki, Y., Uegaki, M., Utsunomiya, N., Makino, Y., Sumiyoshi, S., Yamasaki, T., Kamba, T., & Ogawa, O. (2015). Decreased expression of lysophosphatidylcholine (16:0/OH) in high resolution imaging mass spectrometry independently predicts biochemical recurrence after surgical treatment for prostate cancer. *The Prostate*, 75(16), 1821–1830. <https://doi.org/10.1002/pros.23088>
- Gowda, G. N., Zhang, S., Gu, H., Asiago, V., Shanaiah, N., & Raftery, D. (2008). Metabolomics-based methods for early disease diagnostics. *Expert Review of Molecular Diagnostics*, 8(5), 617–633. <https://doi.org/10.1586/14737159.8.5.617>
- Graf, R. P., Fisher, V., Mateo, J., Gjoerup, O. V., Madison, R. W., Raskina, K., Tukachinsky, H., Creeden, J., Cunningham, R., Huang, R. S. P., Mata, D. A., Ross, J. S., Oxnard, G. R., Venstrom, J. M., & Zurita, A. J. (2022). Predictive Genomic Biomarkers of Hormonal Therapy Versus Chemotherapy Benefit in Metastatic Castration-resistant Prostate Cancer. *European Urology*, 81(1), 37–47. <https://doi.org/10.1016/j.eururo.2021.09.030>
- Graff, J. R., Konicek, B. W., Lynch, R. L., Dumstorf, C. A., Dowless, M. S., McNulty, A. M., Parsons, S. H., Brail, L. H., Colligan, B. M., Koop, J. W., Hurst, B. M., Deddens, J. A., Neubauer, B. L., Stancato, L. F., Carter, H. W., Douglass, L. E., & Carter, J. H. (2009). EIF4E activation is commonly elevated in advanced human prostate cancers and significantly related to reduced patient survival. *Cancer Research*, 69(9), 3866–3873. <https://doi.org/10.1158/0008-5472.CAN-08-3472>
- Grasso, C. S., Wu, Y.-M., Robinson, D. R., Cao, X., Dhanasekaran, S. M., Khan, A. P., Quist, M. J., Jing, X., Lonigro, R. J., Brenner, J. C., Asangani, I. A., Ateeq, B., Chun, S. Y., Siddiqui, J., Sam, L., Anstett, M., Mehra, R., Prensner, J. R., Palanisamy, N., ... Tomlins, S. A. (2012). The mutational landscape of lethal castration-resistant prostate cancer. *Nature*, 487(7406), 239–243. <https://doi.org/10.1038/nature11125>
- Gravis, G., Boher, J.-M., Joly, F., Soulié, M., Albiges, L., Priou, F., Latorzeff, I., Delva, R., Krakowski, I., Laguerre, B., Rolland, F., Théodore, C., Deplanque, G., Ferrero, J.-M., Culine, S., Mourey, L., Beuzebec, P., Habibian, M., Oudard, S., ... GETUG. (2016). Androgen Deprivation Therapy (ADT) Plus Docetaxel Versus ADT Alone in Metastatic Non castrate Prostate Cancer: Impact of Metastatic Burden and Long-term Survival Analysis of the Randomized Phase 3 GETUG-AFU15 Trial. *European Urology*, 70(2), 256–262. <https://doi.org/10.1016/j.eururo.2015.11.005>

References

- Guertin, D. A., Stevens, D. M., Saitoh, M., Kinkel, S., Crosby, K., Sheen, J.-H., Mullholland, D. J., Magnuson, M. A., Wu, H., & Sabatini, D. M. (2009). mTOR complex 2 is required for the development of prostate cancer induced by Pten loss in mice. *Cancer Cell*, *15*(2), 148–159. <https://doi.org/10.1016/j.ccr.2008.12.017>
- Guo, X., Zhu, R., Luo, A., Zhou, H., Ding, F., Yang, H., & Liu, Z. (2020). EIF3H promotes aggressiveness of esophageal squamous cell carcinoma by modulating Snail stability. *Journal of Experimental & Clinical Cancer Research: CR*, *39*(1), 175. <https://doi.org/10.1186/s13046-020-01678-9>
- Hanahan, D. (2022). Hallmarks of Cancer: New Dimensions. *Cancer Discovery*, *12*(1), 31–46. <https://doi.org/10.1158/2159-8290.CD-21-1059>
- Hanahan, D., & Weinberg, R. A. (2000). The hallmarks of cancer. *Cell*, *100*(1), 57–70. [https://doi.org/10.1016/s0092-8674\(00\)81683-9](https://doi.org/10.1016/s0092-8674(00)81683-9)
- Hanahan, D., & Weinberg, R. A. (2011). Hallmarks of cancer: The next generation. *Cell*, *144*(5), 646–674. <https://doi.org/10.1016/j.cell.2011.02.013>
- Hansen, A. F., Sandsmark, E., Rye, M. B., Wright, A. J., Bertilsson, H., Richardsen, E., Viset, T., Bofin, A. M., Angelsen, A., Selnæs, K. M., Bathen, T. F., & Tessem, M.-B. (2016). Presence of TMPRSS2-ERG is associated with alterations of the metabolic profile in human prostate cancer. *Oncotarget*, *7*(27), 42071–42085. <https://doi.org/10.18632/oncotarget.9817>
- Hart, T., Brown, K. R., Sircoulomb, F., Rottapel, R., & Moffat, J. (2014). Measuring error rates in genomic perturbation screens: Gold standards for human functional genomics. *Molecular Systems Biology*, *10*, 733. <https://doi.org/10.15252/msb.20145216>
- Hart, T., & Moffat, J. (2016). BAGEL: A computational framework for identifying essential genes from pooled library screens. *BMC Bioinformatics*, *17*, 164. <https://doi.org/10.1186/s12859-016-1015-8>
- Harvey, C. J., Pilcher, J., Richenberg, J., Patel, U., & Frauscher, F. (2012). Applications of transrectal ultrasound in prostate cancer. *The British Journal of Radiology*, *85 Spec No 1*(Spec Iss 1), S3-17. <https://doi.org/10.1259/bjr/56357549>
- Hasin, Y., Seldin, M., & Lusis, A. (2017). Multi-omics approaches to disease. *Genome Biology*, *18*(1), 83. <https://doi.org/10.1186/s13059-017-1215-1>
- Heidenreich, A., Bastian, P. J., Bellmunt, J., Bolla, M., Joniau, S., van der Kwast, T., Mason, M., Matveev, V., Wiegand, T., Zattoni, F., Mottet, N., & European Association of Urology. (2014). EAU guidelines on prostate cancer. Part II: Treatment of advanced, relapsing, and castration-resistant prostate cancer. *European Urology*, *65*(2), 467–479. <https://doi.org/10.1016/j.eururo.2013.11.002>
- Henzler, C., Li, Y., Yang, R., McBride, T., Ho, Y., Sprenger, C., Liu, G., Coleman, I., Lakely, B., Li, R., Ma, S., Landman, S. R., Kumar, V., Hwang, T. H., Raj, G. V., Higano, C. S., Morrissey, C., Nelson, P. S., Plymate, S. R., & Dehm, S. M. (2016). Truncation and constitutive activation of the androgen receptor by diverse genomic rearrangements in prostate cancer. *Nature Communications*, *7*, 13668. <https://doi.org/10.1038/ncomms13668>

- Hernández, G., Ramírez, J. L., Pedroza-Torres, A., Herrera, L. A., & Jiménez-Ríos, M. A. (2019). The Secret Life of Translation Initiation in Prostate Cancer. *Frontiers in Genetics*, *10*, 14. <https://doi.org/10.3389/fgene.2019.00014>
- Hoang, L. T., Domingo-Sabugo, C., Starren, E. S., Willis-Owen, S. A. G., Morris-Rosendahl, D. J., Nicholson, A. G., Cookson, W. O. C. M., & Moffatt, M. F. (2019). Metabolomic, transcriptomic and genetic integrative analysis reveals important roles of adenosine diphosphate in haemostasis and platelet activation in non-small-cell lung cancer. *Molecular Oncology*, *13*(11), 2406–2421. <https://doi.org/10.1002/1878-0261.12568>
- Hong, S., Liu, Y., Xiong, H., Cai, D., & Fan, Q. (2018). Eukaryotic translation initiation factor 3H suppression inhibits osteocarcinoma cell growth and tumorigenesis. *Experimental and Therapeutic Medicine*, *15*(6), 4925–4931. <https://doi.org/10.3892/etm.2018.6031>
- Hoogland, A. M., Kweldam, C. F., & van Leenders, G. J. L. H. (2014). Prognostic histopathological and molecular markers on prostate cancer needle-biopsies: A review. *BioMed Research International*, *2014*, 341324. <https://doi.org/10.1155/2014/341324>
- Hou, W., & Zhang, Y. (2021). Circ_0025033 promotes the progression of ovarian cancer by activating the expression of LSM4 via targeting miR-184. *Pathology, Research and Practice*, *217*, 153275. <https://doi.org/10.1016/j.prp.2020.153275>
- Hsieh, A. C., Nguyen, H. G., Wen, L., Edlind, M. P., Carroll, P. R., Kim, W., & Ruggero, D. (2015). Cell type-specific abundance of 4EBP1 primes prostate cancer sensitivity or resistance to PI3K pathway inhibitors. *Science Signaling*, *8*(403), ra116. <https://doi.org/10.1126/scisignal.aad5111>
- Hu, Y., Wei, X., Lv, Y., Xie, X., Yang, L., He, J., Tao, X., Ma, Y., Su, Y., Wu, L., Fang, W., & Liu, Z. (2020). EIF3H interacts with PDCD4 enhancing lung adenocarcinoma cell metastasis. *American Journal of Cancer Research*, *10*(1), 179–195.
- Huang, J., Mondul, A. M., Weinstein, S. J., Karoly, E. D., Sampson, J. N., & Albanes, D. (2017). Prospective serum metabolomic profile of prostate cancer by size and extent of primary tumor. *Oncotarget*, *8*(28), 45190–45199. <https://doi.org/10.18632/oncotarget.16775>
- Hübner, N., Shariat, S., & Remzi, M. (2018). Prostate biopsy: Guidelines and evidence. *Current Opinion in Urology*, *28*(4), 354–359. <https://doi.org/10.1097/MOU.0000000000000510>
- Hussain, M., Mateo, J., Fizazi, K., Saad, F., Shore, N., Sandhu, S., Chi, K. N., Sartor, O., Agarwal, N., Olmos, D., Thiery-Vuillemin, A., Twardowski, P., Roubaud, G., Özgüroğlu, M., Kang, J., Burgents, J., Gresty, C., Corcoran, C., Adelman, C. A., ... PROfound Trial Investigators. (2020). Survival with Olaparib in Metastatic Castration-Resistant Prostate Cancer. *The New England Journal of Medicine*, *383*(24), 2345–2357. <https://doi.org/10.1056/NEJMoa2022485>
- Hutter, C. M., Chang-Claude, J., Slattery, M. L., Pflugeisen, B. M., Lin, Y., Duggan, D., Nan, H., Lemire, M., Rangrej, J., Figueiredo, J. C., Jiao, S., Harrison, T. A., Liu, Y., Chen, L. S., Stelling, D. L., Warnick, G. S., Hoffmeister, M., Küry, S., Fuchs, C. S., ... Peters, U. (2012). Characterization of gene-environment interactions for colorectal cancer susceptibility loci. *Cancer Research*, *72*(8), 2036–2044. <https://doi.org/10.1158/0008-5472.CAN-11-4067>

References

- Iglesias-Gato, D., Wikström, P., Tyanova, S., Lavalley, C., Thysell, E., Carlsson, J., Hägglöf, C., Cox, J., Andrén, O., Stattin, P., Egevad, L., Widmark, A., Bjartell, A., Collins, C. C., Bergh, A., Geiger, T., Mann, M., & Flores-Morales, A. (2016). The Proteome of Primary Prostate Cancer. *European Urology*, 69(5), 942–952. <https://doi.org/10.1016/j.eururo.2015.10.053>
- Ilic, N., Birsoy, K., Aguirre, A. J., Kory, N., Pacold, M. E., Singh, S., Moody, S. E., DeAngelo, J. D., Spardy, N. A., Freinkman, E., Weir, B. A., Tsherniak, A., Cowley, G. S., Root, D. E., Asara, J. M., Vazquez, F., Widlund, H. R., Sabatini, D. M., & Hahn, W. C. (2017). PIK3CA mutant tumors depend on oxoglutarate dehydrogenase. *Proceedings of the National Academy of Sciences of the United States of America*, 114(17), E3434–E3443. <https://doi.org/10.1073/pnas.1617922114>
- Ingolia, N. T., Ghaemmighami, S., Newman, J. R. S., & Weissman, J. S. (2009). Genome-wide analysis in vivo of translation with nucleotide resolution using ribosome profiling. *Science (New York, N.Y.)*, 324(5924), 218–223. <https://doi.org/10.1126/science.1168978>
- Iremashvili, V., Manoharan, M., Rosenberg, D. L., Acosta, K., & Soloway, M. S. (2012). Pathological findings at radical prostatectomy in patients initially managed by active surveillance: A comparative analysis. *The Prostate*, 72(14), 1573–1579. <https://doi.org/10.1002/pros.22507>
- Jain, M., Nilsson, R., Sharma, S., Madhusudhan, N., Kitami, T., Souza, A. L., Kafri, R., Kirschner, M. W., Clish, C. B., & Mootha, V. K. (2012). Metabolite profiling identifies a key role for glycine in rapid cancer cell proliferation. *Science (New York, N.Y.)*, 336(6084), 1040–1044. <https://doi.org/10.1126/science.1218595>
- Jaiswal, P. K., Koul, S., Shanmugam, P. S. T., & Koul, H. K. (2018). Eukaryotic Translation Initiation Factor 4 Gamma 1 (eIF4G1) is upregulated during Prostate cancer progression and modulates cell growth and metastasis. *Scientific Reports*, 8(1), 7459. <https://doi.org/10.1038/s41598-018-25798-7>
- Jamaspishvili, T., Berman, D. M., Ross, A. E., Scher, H. I., De Marzo, A. M., Squire, J. A., & Lotan, T. L. (2018). Clinical implications of PTEN loss in prostate cancer. *Nature Reviews. Urology*, 15(4), 222–234. <https://doi.org/10.1038/nrurol.2018.9>
- Jones, D., Friend, C., Dreher, A., Allgar, V., & Macleod, U. (2018). The diagnostic test accuracy of rectal examination for prostate cancer diagnosis in symptomatic patients: A systematic review. *BMC Family Practice*, 19(1), 79. <https://doi.org/10.1186/s12875-018-0765-y>
- Joseph, J. D., Lu, N., Qian, J., Sensintaffar, J., Shao, G., Brigham, D., Moon, M., Maneval, E. C., Chen, L., Darimont, B., & Hager, J. H. (2013). A clinically relevant androgen receptor mutation confers resistance to second-generation antiandrogens enzalutamide and ARN-509. *Cancer Discovery*, 3(9), 1020–1029. <https://doi.org/10.1158/2159-8290.CD-13-0226>
- Joshi, M., Kim, J., D'Alessandro, A., Monk, E., Bruce, K., Elajaili, H., Nozik-Grayck, E., Goodspeed, A., Costello, J. C., & Schlaepfer, I. R. (2020). CPT1A Over-Expression Increases Reactive Oxygen Species in the Mitochondria and Promotes Antioxidant Defenses in Prostate Cancer. *Cancers*, 12(11), E3431. <https://doi.org/10.3390/cancers12113431>

- Jung, H.-Y., Fattet, L., & Yang, J. (2015). Molecular pathways: Linking tumor microenvironment to epithelial-mesenchymal transition in metastasis. *Clinical Cancer Research: An Official Journal of the American Association for Cancer Research*, 21(5), 962–968. <https://doi.org/10.1158/1078-0432.CCR-13-3173>
- Kanehisa, M. (2019). Toward understanding the origin and evolution of cellular organisms. *Protein Science: A Publication of the Protein Society*, 28(11), 1947–1951. <https://doi.org/10.1002/pro.3715>
- Kanehisa, M., & Goto, S. (2000). KEGG: Kyoto encyclopedia of genes and genomes. *Nucleic Acids Research*, 28(1), 27–30. <https://doi.org/10.1093/nar/28.1.27>
- Kanehisa, M., Sato, Y., Furumichi, M., Morishima, K., & Tanabe, M. (2019). New approach for understanding genome variations in KEGG. *Nucleic Acids Research*, 47(D1), D590–D595. <https://doi.org/10.1093/nar/gky962>
- Karantanos, T., Corn, P. G., & Thompson, T. C. (2013). Prostate cancer progression after androgen deprivation therapy: Mechanisms of castrate resistance and novel therapeutic approaches. *Oncogene*, 32(49), 5501–5511. <https://doi.org/10.1038/onc.2013.206>
- Karczewski, K. J., & Snyder, M. P. (2018). Integrative omics for health and disease. *Nature Reviews. Genetics*, 19(5), 299–310. <https://doi.org/10.1038/nrg.2018.4>
- Kassambara, A., & Mundt, F. (2020). *Extract and Visualize the Results of Multivariate Data Analyses [R package factoextra version 1.0.7]*.
- Kawachi, M. H., Bahnson, R. R., Barry, M., Busby, J. E., Carroll, P. R., Carter, H. B., Catalona, W. J., Cookson, M. S., Epstein, J. I., Etzioni, R. B., Giri, V. N., Hemstreet, G. P., Howe, R. J., Lange, P. H., Lilja, H., Loughlin, K. R., Mohler, J., Moul, J., Nadler, R. B., ... Wei, J. T. (2010). NCCN clinical practice guidelines in oncology: Prostate cancer early detection. *Journal of the National Comprehensive Cancer Network: JNCCN*, 8(2), 240–262. <https://doi.org/10.6004/jnccn.2010.0016>
- Kelly, R. S., Sinnott, J. A., Rider, J. R., Ebot, E. M., Gerke, T., Bowden, M., Pettersson, A., Loda, M., Sesso, H. D., Kantoff, P. W., Martin, N. E., Giovannucci, E. L., Tyekucheva, S., Heiden, M. V., & Mucci, L. A. (2016). The role of tumor metabolism as a driver of prostate cancer progression and lethal disease: Results from a nested case-control study. *Cancer & Metabolism*, 4, 22. <https://doi.org/10.1186/s40170-016-0161-9>
- Kenner, L. R., Anand, A. A., Nguyen, H. C., Myasnikov, A. G., Klose, C. J., McGeever, L. A., Tsai, J. C., Miller-Vedam, L. E., Walter, P., & Frost, A. (2019). EIF2B-catalyzed nucleotide exchange and phosphoregulation by the integrated stress response. *Science (New York, N.Y.)*, 364(6439), 491–495. <https://doi.org/10.1126/science.aaw2922>
- Keyes, M., Crook, J., Morton, G., Vigneault, E., Usmani, N., & Morris, W. J. (2013). Treatment options for localized prostate cancer. *Canadian Family Physician Medecin De Famille Canadien*, 59(12), 1269–1274.
- Khamis, Z. I., Iczkowski, K. A., Sahab, Z. J., & Sang, Q.-X. A. (2010). Protein profiling of isolated leukocytes, myofibroblasts, epithelial, Basal, and endothelial cells from normal, hyperplastic, cancerous, and inflammatory human prostate tissues. *Journal of Cancer*, 1, 70–79. <https://doi.org/10.7150/jca.1.70>
- Kiebish, M. A., Cullen, J., Mishra, P., Ali, A., Milliman, E., Rodrigues, L. O., Chen, E. Y., Tolstikov, V., Zhang, L., Panagopoulos, K., Shah, P., Chen, Y., Petrovics, G., Rosner, I. L., Sesterhenn, I. A.,

References

- McLeod, D. G., Granger, E., Sarangarajan, R., Akmaev, V., ... Dobi, A. (2020). Multi-omic serum biomarkers for prognosis of disease progression in prostate cancer. *Journal of Translational Medicine*, 18(1), 10. <https://doi.org/10.1186/s12967-019-02185-y>
- Klotz, L., & Toren, P. (2012). Androgen deprivation therapy in advanced prostate cancer: Is intermittent therapy the new standard of care? *Current Oncology (Toronto, Ont.)*, 19(Suppl 3), S13-21. <https://doi.org/10.3747/co.19.1298>
- Kodama, M., Oshikawa, K., Shimizu, H., Yoshioka, S., Takahashi, M., Izumi, Y., Bamba, T., Tateishi, C., Tomonaga, T., Matsumoto, M., & Nakayama, K. I. (2020). A shift in glutamine nitrogen metabolism contributes to the malignant progression of cancer. *Nature Communications*, 11(1), 1320. <https://doi.org/10.1038/s41467-020-15136-9>
- Kumar, D., Gupta, A., Mandhani, A., & Sankhwar, S. N. (2015). Metabolomics-derived prostate cancer biomarkers: Fact or fiction? *Journal of Proteome Research*, 14(3), 1455-1464. <https://doi.org/10.1021/pr5011108>
- Kumar, D., Gupta, A., Mandhani, A., & Sankhwar, S. N. (2016). NMR spectroscopy of filtered serum of prostate cancer: A new frontier in metabolomics. *The Prostate*, 76(12), 1106-1119. <https://doi.org/10.1002/pros.23198>
- Labuschagne, C. F., van den Broek, N. J. F., Mackay, G. M., Vousden, K. H., & Maddocks, O. D. K. (2014). Serine, but not glycine, supports one-carbon metabolism and proliferation of cancer cells. *Cell Reports*, 7(4), 1248-1258. <https://doi.org/10.1016/j.celrep.2014.04.045>
- Lajis, N., Maulidiani, M., Abas, F., & Ismail, I. S. (2017). Metabolomics Approach in Pharmacognosy. In *Pharmacognosy* (pp. 597-616). Elsevier. <https://doi.org/10.1016/B978-0-12-802104-0.00030-5>
- Lam, J. S., Leppert, J. T., Vemulapalli, S. N., Shvarts, O., & Belldegrün, A. S. (2006). Secondary hormonal therapy for advanced prostate cancer. *The Journal of Urology*, 175(1), 27-34. [https://doi.org/10.1016/S0022-5347\(05\)00034-0](https://doi.org/10.1016/S0022-5347(05)00034-0)
- Lamb, A. D., Massie, C. E., & Neal, D. E. (2014). The transcriptional programme of the androgen receptor (AR) in prostate cancer. *BJU International*, 113(3), 358-366. <https://doi.org/10.1111/bju.12415>
- Latonen, L., Afyounian, E., Jylhä, A., Nättinen, J., Aapola, U., Annala, M., Kivinummi, K. K., Tammela, T. T. L., Beuerman, R. W., Uusitalo, H., Nykter, M., & Visakorpi, T. (2018). Integrative proteomics in prostate cancer uncovers robustness against genomic and transcriptomic aberrations during disease progression. *Nature Communications*, 9(1), 1176. <https://doi.org/10.1038/s41467-018-03573-6>
- Lê, S., Josse, J., & Husson, F. (2008). FactoMineR: An R Package for Multivariate Analysis. *Journal of Statistical Software*, 25(1). <https://doi.org/10.18637/jss.v025.i01>
- Lee, S. C.-W., & Abdel-Wahab, O. (2016). Therapeutic targeting of splicing in cancer. *Nature Medicine*, 22(9), 976-986. <https://doi.org/10.1038/nm.4165>
- Lee, Y., & Rio, D. C. (2015). Mechanisms and Regulation of Alternative Pre-mRNA Splicing. *Annual Review of Biochemistry*, 84, 291-323. <https://doi.org/10.1146/annurev-biochem-060614-034316>

- Lewis, J. E., & Kemp, M. L. (2021). Integration of machine learning and genome-scale metabolic modeling identifies multi-omics biomarkers for radiation resistance. *Nature Communications*, *12*(1), 2700. <https://doi.org/10.1038/s41467-021-22989-1>
- Li, C., Han, J., Yao, Q., Zou, C., Xu, Y., Zhang, C., Shang, D., Zhou, L., Zou, C., Sun, Z., Li, J., Zhang, Y., Yang, H., Gao, X., & Li, X. (2013). Subpathway-GM: Identification of metabolic subpathways via joint power of interesting genes and metabolites and their topologies within pathways. *Nucleic Acids Research*, *41*(9), e101. <https://doi.org/10.1093/nar/gkt161>
- Li, H., Wang, Z., Tang, K., Zhou, H., Liu, H., Yan, L., Guan, W., Chen, K., Xu, H., & Ye, Z. (2018). Prognostic Value of Androgen Receptor Splice Variant 7 in the Treatment of Castration-resistant Prostate Cancer with Next generation Androgen Receptor Signal Inhibition: A Systematic Review and Meta-analysis. *European Urology Focus*, *4*(4), 529–539. <https://doi.org/10.1016/j.euf.2017.01.004>
- Li, J., Song, Y., Zhang, C., Wang, R., Hua, L., Guo, Y., Gan, D., Zhu, L., Li, S., Ma, P., Yang, C., Li, H., Yang, J., Shi, J., Liu, X., & Su, H. (2022). TMEM43 promotes pancreatic cancer progression by stabilizing PRPF3 and regulating RAP2B/ERK axis. *Cellular & Molecular Biology Letters*, *27*(1), 24. <https://doi.org/10.1186/s11658-022-00321-z>
- Li, M., Zhang, Q., & Yang, K. (2021). Role of MRI-Based Functional Imaging in Improving the Therapeutic Index of Radiotherapy in Cancer Treatment. *Frontiers in Oncology*, *11*, 645177. <https://doi.org/10.3389/fonc.2021.645177>
- Li, X., Pu, W., Zheng, Q., Ai, M., Chen, S., & Peng, Y. (2022). Proteolysis-targeting chimeras (PROTACs) in cancer therapy. *Molecular Cancer*, *21*(1), 99. <https://doi.org/10.1186/s12943-021-01434-3>
- Li, Y., Zhuang, H., Zhang, X., Li, Y., Liu, Y., Yi, X., Qin, G., Wei, W., & Chen, R. (2018). Multiomics Integration Reveals the Landscape of Prometastasis Metabolism in Hepatocellular Carcinoma. *Molecular & Cellular Proteomics: MCP*, *17*(4), 607–618. <https://doi.org/10.1074/mcp.RA118.000586>
- Lian, X., Gu, J., Gao, B., Li, Y., Damodaran, C., Wei, W., Fu, Y., & Cai, L. (2018). Fenofibrate inhibits mTOR-p70S6K signaling and simultaneously induces cell death in human prostate cancer cells. *Biochemical and Biophysical Research Communications*, *496*(1), 70–75. <https://doi.org/10.1016/j.bbrc.2017.12.168>
- Liang, H., Ding, X., Zhou, C., Zhang, Y., Xu, M., Zhang, C., & Xu, L. (2012). Knockdown of eukaryotic translation initiation factors 3B (EIF3B) inhibits proliferation and promotes apoptosis in glioblastoma cells. *Neurological Sciences: Official Journal of the Italian Neurological Society and of the Italian Society of Clinical Neurophysiology*, *33*(5), 1057–1062. <https://doi.org/10.1007/s10072-011-0894-8>
- Lima, A. R., Carvalho, M., Aveiro, S. S., Melo, T., Domingues, M. R., Macedo-Silva, C., Coimbra, N., Jerónimo, C., Henrique, R., Bastos, M. de L., Guedes de Pinho, P., & Pinto, J. (2021). Comprehensive Metabolomics and Lipidomics Profiling of Prostate Cancer Tissue Reveals

References

- Metabolic Dysregulations Associated with Disease Development. *Journal of Proteome Research*, acs.jproteome.1c00754. <https://doi.org/10.1021/acs.jproteome.1c00754>
- Lima, A. R., Pinto, J., Azevedo, A. I., Barros-Silva, D., Jerónimo, C., Henrique, R., de Lourdes Bastos, M., Guedes de Pinho, P., & Carvalho, M. (2019). Identification of a biomarker panel for improvement of prostate cancer diagnosis by volatile metabolic profiling of urine. *British Journal of Cancer*, 121(10), 857–868. <https://doi.org/10.1038/s41416-019-0585-4>
- Lin, A., & Sheltzer, J. M. (2020). Discovering and validating cancer genetic dependencies: Approaches and pitfalls. *Nature Reviews. Genetics*, 21(11), 671–682. <https://doi.org/10.1038/s41576-020-0247-7>
- Liu, F., Dai, M., Xu, Q., Zhu, X., Zhou, Y., Jiang, S., Wang, Y., Ai, Z., Ma, L., Zhang, Y., Hu, L., Yang, Q., Li, J., Zhao, S., Zhang, Z., & Teng, Y. (2018). SRSF10-mediated IL1RAP alternative splicing regulates cervical cancer oncogenesis via mIL1RAP-NF- κ B-CD47 axis. *Oncogene*, 37(18), 2394–2409. <https://doi.org/10.1038/s41388-017-0119-6>
- Liu, J., & Li, T. (2019). CRISPR-Cas9-mediated loss-of-function screens. *Frontiers in Life Science*, 12(1), 1–13. <https://doi.org/10.1080/21553769.2019.1670739>
- Liu, L., & Dong, X. (2014). Complex impacts of PI3K/AKT inhibitors to androgen receptor gene expression in prostate cancer cells. *PLoS One*, 9(10), e108780. <https://doi.org/10.1371/journal.pone.0108780>
- Liu, W., Bai, X., Liu, Y., Wang, W., Han, J., Wang, Q., Xu, Y., Zhang, C., Zhang, S., Li, X., Ren, Z., Zhang, J., & Li, C. (2015). Topologically inferring pathway activity toward precise cancer classification via integrating genomic and metabolomic data: Prostate cancer as a case. *Scientific Reports*, 5, 13192. <https://doi.org/10.1038/srep13192>
- Liu, Y. (2006). Fatty acid oxidation is a dominant bioenergetic pathway in prostate cancer. *Prostate Cancer and Prostatic Diseases*, 9(3), 230–234. <https://doi.org/10.1038/sj.pcan.4500879>
- Liu, Y., Yang, Y., Luo, Y., Wang, J., Lu, X., Yang, Z., & Yang, J. (2020). Prognostic potential of PRPF3 in hepatocellular carcinoma. *Aging*, 12(1), 912–930. <https://doi.org/10.18632/aging.102665>
- Liu, Y., Zuckier, L. S., & Ghesani, N. V. (2010). Dominant uptake of fatty acid over glucose by prostate cells: A potential new diagnostic and therapeutic approach. *Anticancer Research*, 30(2), 369–374.
- Liu, Z., Wang, S., Dong, D., Wei, J., Fang, C., Zhou, X., Sun, K., Li, L., Li, B., Wang, M., & Tian, J. (2019). The Applications of Radiomics in Precision Diagnosis and Treatment of Oncology: Opportunities and Challenges. *Theranostics*, 9(5), 1303–1322. <https://doi.org/10.7150/thno.30309>
- Loeb, S., & Catalona, W. J. (2009). What is the role of digital rectal examination in men undergoing serial screening of serum PSA levels? *Nature Clinical Practice. Urology*, 6(2), 68–69. <https://doi.org/10.1038/ncpuro1294>
- Luo, X., Yu, H., Song, Y., & Sun, T. (2019). Integration of metabolomic and transcriptomic data reveals metabolic pathway alteration in breast cancer and impact of related signature on survival. *Journal of Cellular Physiology*, 234(8), 13021–13031. <https://doi.org/10.1002/jcp.27973>
- Lv, M., Zhu, X., Wang, H., Wang, F., & Guan, W. (2014). Roles of caloric restriction, ketogenic diet and intermittent fasting during initiation, progression and metastasis of cancer in animal models: A

- systematic review and meta-analysis. *PloS One*, 9(12), e115147. <https://doi.org/10.1371/journal.pone.0115147>
- Lv, Y., Wang, X., Li, X., Xu, G., Bai, Y., Wu, J., Piao, Y., Shi, Y., Xiang, R., & Wang, L. (2020). Nucleotide de novo synthesis increases breast cancer stemness and metastasis via cGMP-PKG-MAPK signaling pathway. *PLOS Biology*, 18(11), e3000872. <https://doi.org/10.1371/journal.pbio.3000872>
- Madhu, B., Shaw, G. L., Warren, A. Y., Neal, D. E., & Griffiths, J. R. (2016). Response of Degarelix treatment in human prostate cancer monitored by HR-MAS 1H NMR spectroscopy. *Metabolomics: Official Journal of the Metabolomic Society*, 12, 120. <https://doi.org/10.1007/s11306-016-1055-0>
- Mahal, B. A., Butler, S., Franco, I., Spratt, D. E., Rebbeck, T. R., D'Amico, A. V., & Nguyen, P. L. (2019). Use of Active Surveillance or Watchful Waiting for Low-Risk Prostate Cancer and Management Trends Across Risk Groups in the United States, 2010-2015. *JAMA*, 321(7), 704-706. <https://doi.org/10.1001/jama.2018.19941>
- Mahmood, S. F., Gruel, N., Chapeaublanc, E., Lescure, A., Jones, T., Reyat, F., Vincent-Salomon, A., Raynal, V., Pierron, G., Perez, F., Camonis, J., Del Nery, E., Delattre, O., Radvanyi, F., & Bernard-Pierrot, I. (2014). A siRNA screen identifies RAD21, EIF3H, CHRAC1 and TANC2 as driver genes within the 8q23, 8q24.3 and 17q23 amplicons in breast cancer with effects on cell growth, survival and transformation. *Carcinogenesis*, 35(3), 670-682. <https://doi.org/10.1093/carcin/bgt351>
- Marcellus, K. A., Crawford Parks, T. E., Almasi, S., & Jasmin, B. J. (2021). Distinct roles for the RNA-binding protein Stauf1 in prostate cancer. *BMC Cancer*, 21(1), 120. <https://doi.org/10.1186/s12885-021-07844-2>
- Mateo, J., Carreira, S., Sandhu, S., Miranda, S., Mossop, H., Perez-Lopez, R., Nava Rodrigues, D., Robinson, D., Omlin, A., Tunariu, N., Boysen, G., Porta, N., Flohr, P., Gillman, A., Figueiredo, I., Paulding, C., Seed, G., Jain, S., Ralph, C., ... de Bono, J. S. (2015). DNA-Repair Defects and Olaparib in Metastatic Prostate Cancer. *The New England Journal of Medicine*, 373(18), 1697-1708. <https://doi.org/10.1056/NEJMoa1506859>
- McDunn, J. E., Li, Z., Adam, K.-P., Neri, B. P., Wolfert, R. L., Milburn, M. V., Lotan, Y., & Wheeler, T. M. (2013). Metabolomic signatures of aggressive prostate cancer. *The Prostate*, 73(14), 1547-1560. <https://doi.org/10.1002/pros.22704>
- McFarland, J. M., Ho, Z. V., Kugener, G., Dempster, J. M., Montgomery, P. G., Bryan, J. G., Krill-Burger, J. M., Green, T. M., Vazquez, F., Boehm, J. S., Golub, T. R., Hahn, W. C., Root, D. E., & Tsherniak, A. (2018). Improved estimation of cancer dependencies from large-scale RNAi screens using model-based normalization and data integration. *Nature Communications*, 9(1), 4610. <https://doi.org/10.1038/s41467-018-06916-5>
- Meng, J., Lu, X., Jin, C., Zhou, Y., Ge, Q., Zhou, J., Hao, Z., Yan, F., Zhang, M., & Liang, C. (2021). Integrated multi-omics data reveals the molecular subtypes and guides the androgen receptor signalling inhibitor treatment of prostate cancer. *Clinical and Translational Medicine*, 11(12), e655. <https://doi.org/10.1002/ctm2.655>

References

- Meyers, R. M., Bryan, J. G., McFarland, J. M., Weir, B. A., Sizemore, A. E., Xu, H., Dharia, N. V., Montgomery, P. G., Cowley, G. S., Pantel, S., Goodale, A., Lee, Y., Ali, L. D., Jiang, G., Lubonja, R., Harrington, W. F., Strickland, M., Wu, T., Hawes, D. C., ... Tsherniak, A. (2017). Computational correction of copy number effect improves specificity of CRISPR-Cas9 essentiality screens in cancer cells. *Nature Genetics*, *49*(12), 1779–1784. <https://doi.org/10.1038/ng.3984>
- Mohler, J. L., Antonarakis, E. S., Armstrong, A. J., D'Amico, A. V., Davis, B. J., Dorff, T., Eastham, J. A., Enke, C. A., Farrington, T. A., Higano, C. S., Horwitz, E. M., Hurwitz, M., Ippolito, J. E., Kane, C. J., Kuettel, M. R., Lang, J. M., McKenney, J., Netto, G., Penson, D. F., ... Freedman-Cass, D. A. (2019). Prostate Cancer, Version 2.2019, NCCN Clinical Practice Guidelines in Oncology. *Journal of the National Comprehensive Cancer Network*, *17*(5), 479–505. <https://doi.org/10.6004/jnccn.2019.0023>
- Mondul, A. M., Moore, S. C., Weinstein, S. J., Karoly, E. D., Sampson, J. N., & Albanes, D. (2015). Metabolomic analysis of prostate cancer risk in a prospective cohort: The alpha-tocopherol, beta-carotene cancer prevention (ATBC) study. *International Journal of Cancer*, *137*(9), 2124–2132. <https://doi.org/10.1002/ijc.29576>
- Montaner, D., & Dopazo, J. (2010). Multidimensional gene set analysis of genomic data. *PLoS One*, *5*(4), e10348. <https://doi.org/10.1371/journal.pone.0010348>
- Mortensen, M. M., Høyer, S., Lynnerup, A.-S., Ørntoft, T. F., Sørensen, K. D., Borre, M., & Dyrskjøt, L. (2015). Expression profiling of prostate cancer tissue delineates genes associated with recurrence after prostatectomy. *Scientific Reports*, *5*, 16018. <https://doi.org/10.1038/srep16018>
- Mottet, N., Bellmunt, J., Bolla, M., Briers, E., Cumberbatch, M. G., De Santis, M., Fossati, N., Gross, T., Henry, A. M., Joniau, S., Lam, T. B., Mason, M. D., Matveev, V. B., Moldovan, P. C., van den Bergh, R. C. N., Van den Broeck, T., van der Poel, H. G., van der Kwast, T. H., Rouvière, O., ... Cornford, P. (2017). EAU-ESTRO-SIOG Guidelines on Prostate Cancer. Part 1: Screening, Diagnosis, and Local Treatment with Curative Intent. *European Urology*, *71*(4), 618–629. <https://doi.org/10.1016/j.eururo.2016.08.003>
- Nadiminty, N., Tummala, R., Liu, C., Lou, W., Evans, C. P., & Gao, A. C. (2015). NF-κB2/p52:c-Myc:hnRNPA1 Pathway Regulates Expression of Androgen Receptor Splice Variants and Enzalutamide Sensitivity in Prostate Cancer. *Molecular Cancer Therapeutics*, *14*(8), 1884–1895. <https://doi.org/10.1158/1535-7163.MCT-14-1057>
- Nakagawa, T., Kollmeyer, T. M., Morlan, B. W., Anderson, S. K., Bergstralh, E. J., Davis, B. J., Asmann, Y. W., Klee, G. G., Ballman, K. V., & Jenkins, R. B. (2008). A tissue biomarker panel predicting systemic progression after PSA recurrence post-definitive prostate cancer therapy. *PLoS One*, *3*(5), e2318. <https://doi.org/10.1371/journal.pone.0002318>
- Narayan, M., Seeley, K. W., & Jinwal, U. K. (2016). Identification of Apo B48 and other novel biomarkers in amyotrophic lateral sclerosis patient fibroblasts. *Biomarkers in Medicine*, *10*(5), 453–462. <https://doi.org/10.2217/bmm-2016-0025>

- Nayak, A. P., Kapur, A., Barroilhet, L., & Patankar, M. S. (2018). Oxidative Phosphorylation: A Target for Novel Therapeutic Strategies Against Ovarian Cancer. *Cancers*, *10*(9), E337. <https://doi.org/10.3390/cancers10090337>
- Neurauter, G., Grahmann, A. V., Klieber, M., Zeimet, A., Ledochowski, M., Sperner-Unterweger, B., & Fuchs, D. (2008). Serum phenylalanine concentrations in patients with ovarian carcinoma correlate with concentrations of immune activation markers and of isoprostane-8. *Cancer Letters*, *272*(1), 141–147. <https://doi.org/10.1016/j.canlet.2008.07.002>
- Nguyen, H. G., Conn, C. S., Kye, Y., Xue, L., Forester, C. M., Cowan, J. E., Hsieh, A. C., Cunningham, J. T., Truillet, C., Tameire, F., Evans, M. J., Evans, C. P., Yang, J. C., Hann, B., Koumenis, C., Walter, P., Carroll, P. R., & Ruggero, D. (2018). Development of a stress response therapy targeting aggressive prostate cancer. *Science Translational Medicine*, *10*(439), eaar2036. <https://doi.org/10.1126/scitranslmed.aar2036>
- Nguyen, Q.-H., Nguyen, H., Nguyen, T., & Le, D.-H. (2020). Multi-Omics Analysis Detects Novel Prognostic Subgroups of Breast Cancer. *Frontiers in Genetics*, *11*, 574661. <https://doi.org/10.3389/fgene.2020.574661>
- Nielsen, N.-P. V., Carstensen, J. M., & Smedsgaard, J. (1998). Aligning of single and multiple wavelength chromatographic profiles for chemometric data analysis using correlation optimised warping. *Journal of Chromatography A*, *805*(1–2), 17–35. [https://doi.org/10.1016/S0021-9673\(98\)00021-1](https://doi.org/10.1016/S0021-9673(98)00021-1)
- Nupponen, N. N., Porkka, K., Kakkola, L., Tanner, M., Persson, K., Borg, A., Isola, J., & Visakorpi, T. (1999). Amplification and overexpression of p40 subunit of eukaryotic translation initiation factor 3 in breast and prostate cancer. *The American Journal of Pathology*, *154*(6), 1777–1783. [https://doi.org/10.1016/S0002-9440\(10\)65433-8](https://doi.org/10.1016/S0002-9440(10)65433-8)
- Oberhuber, M., Pecoraro, M., Ruzs, M., Oberhuber, G., Wieselberg, M., Haslinger, P., Gurnhofer, E., Schlederer, M., Limberger, T., Lagger, S., Pencik, J., Kodajova, P., Högler, S., Stockmaier, G., Grund-Gröschke, S., Aberger, F., Bolis, M., Theurillat, J.-P., Wiebringhaus, R., ... Kenner, L. (2020). STAT3-dependent analysis reveals PDK4 as independent predictor of recurrence in prostate cancer. *Molecular Systems Biology*, *16*(4), e9247. <https://doi.org/10.15252/msb.20199247>
- Okamoto, H., Yasui, K., Zhao, C., Arie, S., & Inazawa, J. (2003). PTK2 and EIF3S3 genes may be amplification targets at 8q23-q24 and are associated with large hepatocellular carcinomas. *Hepatology (Baltimore, Md.)*, *38*(5), 1242–1249. <https://doi.org/10.1053/jhep.2003.50457>
- Olivier, M., Asmis, R., Hawkins, G. A., Howard, T. D., & Cox, L. A. (2019). The Need for Multi-Omics Biomarker Signatures in Precision Medicine. *International Journal of Molecular Sciences*, *20*(19), E4781. <https://doi.org/10.3390/ijms20194781>
- Parker, C., Castro, E., Fizazi, K., Heidenreich, A., Ost, P., Procopio, G., Tombal, B., Gillessen, S., & ESMO Guidelines Committee. Electronic address: clinicalguidelines@esmo.org. (2020). Prostate cancer: ESMO Clinical Practice Guidelines for diagnosis, treatment and follow-up. *Annals of Oncology: Official Journal of the European Society for Medical Oncology*, *31*(9), 1119–1134. <https://doi.org/10.1016/j.annonc.2020.06.011>

References

- Paronetto, M. P., Cappellari, M., Busà, R., Pedrotti, S., Vitali, R., Comstock, C., Hyslop, T., Knudsen, K. E., & Sette, C. (2010). Alternative splicing of the cyclin D1 proto-oncogene is regulated by the RNA-binding protein Sam68. *Cancer Research*, *70*(1), 229–239. <https://doi.org/10.1158/0008-5472.CAN-09-2788>
- Paschalis, A., Sharp, A., Welti, J. C., Neeb, A., Raj, G. V., Luo, J., Plymate, S. R., & de Bono, J. S. (2018). Alternative splicing in prostate cancer. *Nature Reviews. Clinical Oncology*, *15*(11), 663–675. <https://doi.org/10.1038/s41571-018-0085-0>
- Pelletier, J., Graff, J., Ruggero, D., & Sonenberg, N. (2015). Targeting the eIF4F translation initiation complex: A critical nexus for cancer development. *Cancer Research*, *75*(2), 250–263. <https://doi.org/10.1158/0008-5472.CAN-14-2789>
- Pena, V., Liu, S., Bujnicki, J. M., Lührmann, R., & Wahl, M. C. (2007). Structure of a multipartite protein-protein interaction domain in splicing factor prp8 and its link to retinitis pigmentosa. *Molecular Cell*, *25*(4), 615–624. <https://doi.org/10.1016/j.molcel.2007.01.023>
- Penney, K. L., Sinnott, J. A., Fall, K., Pawitan, Y., Hoshida, Y., Kraft, P., Stark, J. R., Fiorentino, M., Perner, S., Finn, S., Calza, S., Flavin, R., Freedman, M. L., Setlur, S., Sesso, H. D., Andersson, S.-O., Martin, N., Kantoff, P. W., Johansson, J.-E., ... Mucci, L. A. (2011). MRNA expression signature of Gleason grade predicts lethal prostate cancer. *Journal of Clinical Oncology: Official Journal of the American Society of Clinical Oncology*, *29*(17), 2391–2396. <https://doi.org/10.1200/JCO.2010.32.6421>
- Percival, B., Gibson, M., Leenders, J., Wilson, P. B., & Grootveld, M. (2020). Chapter 1. Univariate and Multivariate Statistical Approaches to the Analysis and Interpretation of NMR-based Metabolomics Datasets of Increasing Complexity. In P. B. Wilson & M. Grootveld (Eds.), *Theoretical and Computational Chemistry Series* (pp. 1–40). Royal Society of Chemistry. <https://doi.org/10.1039/9781788015882-00001>
- Pérez-Rambla, C., Puchades-Carrasco, L., García-Flores, M., Rubio-Briones, J., López-Guerrero, J. A., & Pineda-Lucena, A. (2017). Non-invasive urinary metabolomic profiling discriminates prostate cancer from benign prostatic hyperplasia. *Metabolomics: Official Journal of the Metabolomic Society*, *13*(5), 52. <https://doi.org/10.1007/s11306-017-1194-y>
- Petrylak, D. P., Tangen, C. M., Hussain, M. H. A., Lara, P. N., Jones, J. A., Taplin, M. E., Burch, P. A., Berry, D., Moinpour, C., Kohli, M., Benson, M. C., Small, E. J., Raghavan, D., & Crawford, E. D. (2004). Docetaxel and estramustine compared with mitoxantrone and prednisone for advanced refractory prostate cancer. *The New England Journal of Medicine*, *351*(15), 1513–1520. <https://doi.org/10.1056/NEJMoa041318>
- Philip, J., Dutta Roy, S., Ballal, M., Foster, C. S., & Javál, P. (2005). Is a digital rectal examination necessary in the diagnosis and clinical staging of early prostate cancer? *BJU International*, *95*(7), 969–971. <https://doi.org/10.1111/j.1464-410X.2005.05449.x>
- Pierorazio, P. M., Walsh, P. C., Partin, A. W., & Epstein, J. I. (2013). Prognostic Gleason grade grouping: Data based on the modified Gleason scoring system. *BJU International*, *111*(5), 753–760. <https://doi.org/10.1111/j.1464-410X.2012.11611.x>

- Pisarev, A. V., Hellen, C. U. T., & Pestova, T. V. (2007). Recycling of eukaryotic posttermination ribosomal complexes. *Cell*, *131*(2), 286–299. <https://doi.org/10.1016/j.cell.2007.08.041>
- Pittman, A. M., Naranjo, S., Jalava, S. E., Twiss, P., Ma, Y., Olver, B., Lloyd, A., Vijayakrishnan, J., Qureshi, M., Broderick, P., van Wezel, T., Morreau, H., Tuupanen, S., Aaltonen, L. A., Alonso, M. E., Manzanares, M., Gavilán, A., Visakorpi, T., Gómez-Skarmeta, J. L., & Houlston, R. S. (2010). Allelic variation at the 8q23.3 colorectal cancer risk locus functions as a cis-acting regulator of EIF3H. *PLoS Genetics*, *6*(9), e1001126. <https://doi.org/10.1371/journal.pgen.1001126>
- Pokorny, M. R., de Rooij, M., Duncan, E., Schröder, F. H., Parkinson, R., Barentsz, J. O., & Thompson, L. C. (2014). Prospective study of diagnostic accuracy comparing prostate cancer detection by transrectal ultrasound-guided biopsy versus magnetic resonance (MR) imaging with subsequent MR-guided biopsy in men without previous prostate biopsies. *European Urology*, *66*(1), 22–29. <https://doi.org/10.1016/j.eururo.2014.03.002>
- Postma, R., & Schröder, F. H. (2005). Screening for prostate cancer. *European Journal of Cancer (Oxford, England: 1990)*, *41*(6), 825–833. <https://doi.org/10.1016/j.ejca.2004.12.029>
- Pourmand, G., Ziaee, A.-A., Abedi, A. R., Mehraei, A., Alavi, H. A., Ahmadi, A., & Saadati, H. R. (2007). Role of PTEN gene in progression of prostate cancer. *Urology Journal*, *4*(2), 95–100.
- Proud, C. G. (2019). Phosphorylation and Signal Transduction Pathways in Translational Control. *Cold Spring Harbor Perspectives in Biology*, *11*(7), a033050. <https://doi.org/10.1101/cshperspect.a033050>
- Qi, L., Wang, W., Wu, T., Zhu, L., He, L., & Wang, X. (2021). Multi-Omics Data Fusion for Cancer Molecular Subtyping Using Sparse Canonical Correlation Analysis. *Frontiers in Genetics*, *12*, 607817. <https://doi.org/10.3389/fgene.2021.607817>
- Quent, V. M. C., Loessner, D., Friis, T., Reichert, J. C., & Huttmacher, D. W. (2010). Discrepancies between metabolic activity and DNA content as tool to assess cell proliferation in cancer research. *Journal of Cellular and Molecular Medicine*, *14*(4), 1003–1013. <https://doi.org/10.1111/j.1582-4934.2010.01013.x>
- Quidville, V., Alsafadi, S., Goubar, A., Commo, F., Scott, V., Pioche-Durieu, C., Girault, I., Baconnais, S., Le Cam, E., Lazar, V., Delalogue, S., Saghatchian, M., Pautier, P., Morice, P., Dessen, P., Vagner, S., & André, F. (2013). Targeting the deregulated spliceosome core machinery in cancer cells triggers mTOR blockade and autophagy. *Cancer Research*, *73*(7), 2247–2258. <https://doi.org/10.1158/0008-5472.CAN-12-2501>
- Rafael, D., Doktorovová, S., Florindo, H. F., Gener, P., Abasolo, I., Schwartz, S., & Videira, M. A. (2015). EMT blockage strategies: Targeting Akt dependent mechanisms for breast cancer metastatic behaviour modulation. *Current Gene Therapy*, *15*(3), 300–312. <https://doi.org/10.2174/1566523215666150126123642>
- Ramsden, D. B., Waring, R. H., Barlow, D. J., & Parsons, R. B. (2017). Nicotinamide N-Methyltransferase in Health and Cancer. *International Journal of Tryptophan Research*, *10*, 117864691769173. <https://doi.org/10.1177/1178646917691739>

References

- Rebello, R. J., Oing, C., Knudsen, K. E., Loeb, S., Johnson, D. C., Reiter, R. E., Gillissen, S., Van der Kwast, T., & Bristow, R. G. (2021). Prostate cancer. *Nature Reviews. Disease Primers*, 7(1), 9. <https://doi.org/10.1038/s41572-020-00243-0>
- Ren, H., Mai, G., Liu, Y., Xiang, R., Yang, C., & Su, W. (2021). Eukaryotic Translation Initiation Factor 3 Subunit B Is a Promoter in the Development and Progression of Pancreatic Cancer. *Frontiers in Oncology*, 11, 644156. <https://doi.org/10.3389/fonc.2021.644156>
- Richter, J. A., Rodríguez, M., Rioja, J., Peñuelas, I., Martí-Climent, J., Garrastachu, P., Quincoces, G., Zudaire, J., & García-Velloso, M. J. (2010). Dual tracer 11C-choline and FDG-PET in the diagnosis of biochemical prostate cancer relapse after radical treatment. *Molecular Imaging and Biology*, 12(2), 210–217. <https://doi.org/10.1007/s11307-009-0243-y>
- Ritch, C. R., & Cookson, M. S. (2016). Advances in the management of castration resistant prostate cancer. *BMJ (Clinical Research Ed.)*, 355, i4405. <https://doi.org/10.1136/bmj.i4405>
- Ritchie, M. E., Phipson, B., Wu, D., Hu, Y., Law, C. W., Shi, W., & Smyth, G. K. (2015). Limma powers differential expression analyses for RNA-sequencing and microarray studies. *Nucleic Acids Research*, 43(7), e47. <https://doi.org/10.1093/nar/gkv007>
- Roach, M., Hanks, G., Thames, H., Schellhammer, P., Shipley, W. U., Sokol, G. H., & Sandler, H. (2006). Defining biochemical failure following radiotherapy with or without hormonal therapy in men with clinically localized prostate cancer: Recommendations of the RTOG-ASTRO Phoenix Consensus Conference. *International Journal of Radiation Oncology, Biology, Physics*, 65(4), 965–974. <https://doi.org/10.1016/j.ijrobp.2006.04.029>
- Roberts, L. D., Souza, A. L., Gerszten, R. E., & Clish, C. B. (2012). Targeted metabolomics. *Current Protocols in Molecular Biology*, Chapter 30, Unit 30.2.1-24. <https://doi.org/10.1002/0471142727.mb3002s98>
- Robichaud, N., Sonenberg, N., Ruggero, D., & Schneider, R. J. (2019). Translational Control in Cancer. *Cold Spring Harbor Perspectives in Biology*, 11(7), a032896. <https://doi.org/10.1101/cshperspect.a032896>
- Robins, D. M. (2012). Androgen receptor gene polymorphisms and alterations in prostate cancer: Of humanized mice and men. *Molecular and Cellular Endocrinology*, 352(1–2), 26–33. <https://doi.org/10.1016/j.mce.2011.06.003>
- Robinson, D., Van Allen, E. M., Wu, Y.-M., Schultz, N., Lonigro, R. J., Mosquera, J.-M., Montgomery, B., Taplin, M.-E., Pritchard, C. C., Attard, G., Beltran, H., Abida, W., Bradley, R. K., Vinson, J., Cao, X., Vats, P., Kunju, L. P., Hussain, M., Feng, F. Y., ... Chinnaiyan, A. M. (2015). Integrative clinical genomics of advanced prostate cancer. *Cell*, 161(5), 1215–1228. <https://doi.org/10.1016/j.cell.2015.05.001>
- Rose, M. L., Madren, J., Bunzendahl, H., & Thurman, R. G. (1999). Dietary glycine inhibits the growth of B16 melanoma tumors in mice. *Carcinogenesis*, 20(5), 793–798. <https://doi.org/10.1093/carcin/20.5.793>
- Ross, H. M., Kryvenko, O. N., Cowan, J. E., Simko, J. P., Wheeler, T. M., & Epstein, J. I. (2012). Do adenocarcinomas of the prostate with Gleason score (GS) ≤6 have the potential to metastasize to

- lymph nodes? *The American Journal of Surgical Pathology*, 36(9), 1346–1352. <https://doi.org/10.1097/PAS.0b013e3182556dcd>
- Ross-Adams, H., Lamb, A. D., Dunning, M. J., Halim, S., Lindberg, J., Massie, C. M., Egevad, L. A., Russell, R., Ramos-Montoya, A., Vowler, S. L., Sharma, N. L., Kay, J., Whitaker, H., Clark, J., Hurst, R., Gnanapragasam, V. J., Shah, N. C., Warren, A. Y., Cooper, C. S., ... CamCaP Study Group. (2015). Integration of copy number and transcriptomics provides risk stratification in prostate cancer: A discovery and validation cohort study. *EBioMedicine*, 2(9), 1133–1144. <https://doi.org/10.1016/j.ebiom.2015.07.017>
- Roux, P. P., & Topisirovic, I. (2018). Signaling Pathways Involved in the Regulation of mRNA Translation. *Molecular and Cellular Biology*, 38(12), e00070-18. <https://doi.org/10.1128/MCB.00070-18>
- Ruan, X., Zheng, J., Liu, X., Liu, Y., Liu, L., Ma, J., He, Q., Yang, C., Wang, D., Cai, H., Li, Z., Liu, J., & Xue, Y. (2020). LncRNA LINC00665 Stabilized by TAF15 Impeded the Malignant Biological Behaviors of Glioma Cells via STAU1-Mediated mRNA Degradation. *Molecular Therapy. Nucleic Acids*, 20, 823–840. <https://doi.org/10.1016/j.omtn.2020.05.003>
- Ruggero, D. (2013). Translational control in cancer etiology. *Cold Spring Harbor Perspectives in Biology*, 5(2), a012336. <https://doi.org/10.1101/cshperspect.a012336>
- Salman, J. W., Schoots, I. G., Carlsson, S. V., Jenster, G., & Roobol, M. J. (2015). Prostate Specific Antigen as a Tumor Marker in Prostate Cancer: Biochemical and Clinical Aspects. *Advances in Experimental Medicine and Biology*, 867, 93–114. https://doi.org/10.1007/978-94-017-7215-0_7
- Sandsmark, E., Andersen, M. K., Bofin, A. M., Bertilsson, H., Drabløs, F., Bathen, T. F., Rye, M. B., & Tessem, M.-B. (2017). SFRP4 gene expression is increased in aggressive prostate cancer. *Scientific Reports*, 7(1), 14276. <https://doi.org/10.1038/s41598-017-14622-3>
- Sanhueza, C., & Kohli, M. (2018). Clinical and Novel Biomarkers in the Management of Prostate Cancer. *Current Treatment Options in Oncology*, 19(2), 8. <https://doi.org/10.1007/s11864-018-0527-z>
- Saramäki, O., Willi, N., Bratt, O., Gasser, T. C., Koivisto, P., Nupponen, N. N., Bubendorf, L., & Visakorpi, T. (2001). Amplification of EIF3S3 gene is associated with advanced stage in prostate cancer. *The American Journal of Pathology*, 159(6), 2089–2094. [https://doi.org/10.1016/S0002-9440\(10\)63060-X](https://doi.org/10.1016/S0002-9440(10)63060-X)
- Sathianathan, N. J., Konety, B. R., Crook, J., Saad, F., & Lawrentschuk, N. (2018). Landmarks in prostate cancer. *Nature Reviews. Urology*, 15(10), 627–642. <https://doi.org/10.1038/s41585-018-0060-7>
- Savinainen, K. J., Helenius, M. A., Lehtonen, H. J., & Visakorpi, T. (2006). Overexpression of EIF3S3 promotes cancer cell growth. *The Prostate*, 66(11), 1144–1150. <https://doi.org/10.1002/pros.20452>
- Savir-Baruch, B., Zanoni, L., & Schuster, D. M. (2017). Imaging of Prostate Cancer Using Fluciclovine. *PET Clinics*, 12(2), 145–157. <https://doi.org/10.1016/j.cpet.2016.11.005>
- Savorani, F., Tomasi, G., & Engelsens, S. B. (2010). icoshift: A versatile tool for the rapid alignment of 1D NMR spectra. *Journal of Magnetic Resonance*, 202(2), 190–202. <https://doi.org/10.1016/j.jmr.2009.11.012>

References

- Sboner, A., Demichelis, F., Calza, S., Pawitan, Y., Setlur, S. R., Hoshida, Y., Perner, S., Adami, H.-O., Fall, K., Mucci, L. A., Kantoff, P. W., Stampfer, M., Andersson, S.-O., Varenhorst, E., Johansson, J.-E., Gerstein, M. B., Golub, T. R., Rubin, M. A., & Andrén, O. (2010). Molecular sampling of prostate cancer: A dilemma for predicting disease progression. *BMC Medical Genomics*, 3, 8. <https://doi.org/10.1186/1755-8794-3-8>
- Scher, H. I., Fizazi, K., Saad, F., Taplin, M.-E., Sternberg, C. N., Miller, K., de Wit, R., Mulders, P., Chi, K. N., Shore, N. D., Armstrong, A. J., Flaig, T. W., Fléchon, A., Mainwaring, P., Fleming, M., Hainsworth, J. D., Hirmand, M., Selby, B., Seely, L., ... AFFIRM Investigators. (2012). Increased survival with enzalutamide in prostate cancer after chemotherapy. *The New England Journal of Medicine*, 367(13), 1187–1197. <https://doi.org/10.1056/NEJMoa1207506>
- Schmidt, D. R., Patel, R., Kirsch, D. G., Lewis, C. A., Vander Heiden, M. G., & Locasale, J. W. (2021). Metabolomics in cancer research and emerging applications in clinical oncology. *CA: A Cancer Journal for Clinicians*, 71(4), 333–358. <https://doi.org/10.3322/caac.21670>
- Schmidt, J. A., Fensom, G. K., Rinaldi, S., Scalbert, A., Appleby, P. N., Achaintre, D., Gicquiau, A., Gunter, M. J., Ferrari, P., Kaaks, R., Kühn, T., Floegel, A., Boeing, H., Trichopoulou, A., Lagiou, P., Anifantis, E., Agnoli, C., Palli, D., Trevisan, M., ... Travis, R. C. (2017). Pre-diagnostic metabolite concentrations and prostate cancer risk in 1077 cases and 1077 matched controls in the European Prospective Investigation into Cancer and Nutrition. *BMC Medicine*, 15(1), 122. <https://doi.org/10.1186/s12916-017-0885-6>
- Shalem, O., Sanjana, N. E., & Zhang, F. (2015). High-throughput functional genomics using CRISPR-Cas9. *Nature Reviews. Genetics*, 16(5), 299–311. <https://doi.org/10.1038/nrg3899>
- Shao, D. D., Tsherniak, A., Gopal, S., Weir, B. A., Tamayo, P., Stransky, N., Schumacher, S. E., Zack, T. I., Beroukhi, R., Garraway, L. A., Margolin, A. A., Root, D. E., Hahn, W. C., & Mesirov, J. P. (2013). ATARiS: Computational quantification of gene suppression phenotypes from multisample RNAi screens. *Genome Research*, 23(4), 665–678. <https://doi.org/10.1101/gr.143586.112>
- Sharma, D. K., Bressler, K., Patel, H., Balasingam, N., & Thakor, N. (2016). Role of Eukaryotic Initiation Factors during Cellular Stress and Cancer Progression. *Journal of Nucleic Acids*, 2016, 8235121. <https://doi.org/10.1155/2016/8235121>
- Sheils, T. K., Mathias, S. L., Kelleher, K. J., Siramshetty, V. B., Nguyen, D.-T., Bologna, C. G., Jensen, L. J., Vidović, D., Koletić, A., Schürer, S. C., Waller, A., Yang, J. J., Holmes, J., Bocci, G., Southall, N., Dharkar, P., Mathé, E., Simeonov, A., & Oprea, T. I. (2021). TCRD and Pharos 2021: Mining the human proteome for disease biology. *Nucleic Acids Research*, 49(D1), D1334–D1346. <https://doi.org/10.1093/nar/gkaa993>
- Sheng, J., Zhao, Q., Zhao, J., Zhang, W., Sun, Y., Qin, P., Lv, Y., Bai, L., Yang, Q., Chen, L., Qi, Y., Zhang, G., Zhang, L., Gu, C., Deng, X., Liu, H., Meng, S., Gu, H., Liu, Q., ... Wang, Y. (2018). SRSF1 modulates PTPMT1 alternative splicing to regulate lung cancer cell radioresistance. *EBioMedicine*, 38, 113–126. <https://doi.org/10.1016/j.ebiom.2018.11.007>

- Shur, J. D., Doran, S. J., Kumar, S., Ap Dafydd, D., Downey, K., O'Connor, J. P. B., Papanikolaou, N., Messiou, C., Koh, D.-M., & Orton, M. R. (2021). Radiomics in Oncology: A Practical Guide. *Radiographics: A Review Publication of the Radiological Society of North America, Inc*, 41(6), 1717–1732. <https://doi.org/10.1148/rg.2021210037>
- Sica, V., Bravo-San Pedro, J. M., Stoll, G., & Kroemer, G. (2020). Oxidative phosphorylation as a potential therapeutic target for cancer therapy. *International Journal of Cancer*, 146(1), 10–17. <https://doi.org/10.1002/ijc.32616>
- Silvera, D., Formenti, S. C., & Schneider, R. J. (2010). Translational control in cancer. *Nature Reviews. Cancer*, 10(4), 254–266. <https://doi.org/10.1038/nrc2824>
- Simonetti, A., Brito Querido, J., Myasnikov, A. G., Mancera-Martinez, E., Renaud, A., Kuhn, L., & Hashem, Y. (2016). EIF3 Peripheral Subunits Rearrangement after mRNA Binding and Start-Codon Recognition. *Molecular Cell*, 63(2), 206–217. <https://doi.org/10.1016/j.molcel.2016.05.033>
- Singh, B., & Eyraş, E. (2017). The role of alternative splicing in cancer. *Transcription*, 8(2), 91–98. <https://doi.org/10.1080/21541264.2016.1268245>
- Sirniö, P., Väyrynen, J. P., Klintrup, K., Mäkelä, J., Karhu, T., Herzig, K.-H., Minkkinen, I., Mäkinen, M. J., Karttunen, T. J., & Tuomisto, A. (2019). Alterations in serum amino-acid profile in the progression of colorectal cancer: Associations with systemic inflammation, tumour stage and patient survival. *British Journal of Cancer*, 120(2), 238–246. <https://doi.org/10.1038/s41416-018-0357-6>
- Sokół, E., Kędzierska, H., Czuby, A., Rybicka, B., Rodzik, K., Tański, Z., Bogusławska, J., & Piekiełko-Witkowska, A. (2018). MicroRNA-mediated regulation of splicing factors SRSF1, SRSF2 and hnRNP A1 in context of their alternatively spliced 3'UTRs. *Experimental Cell Research*, 363(2), 208–217. <https://doi.org/10.1016/j.yexcr.2018.01.009>
- Sosnowski, R., Zagrodzka, M., & Borkowski, T. (2016). The limitations of multiparametric magnetic resonance imaging also must be borne in mind. *Central European Journal of Urology*, 69(1), 22–23. <https://doi.org/10.5173/cej.2016.e113>
- Spilka, R., Ernst, C., Mehta, A. K., & Haybaeck, J. (2013). Eukaryotic translation initiation factors in cancer development and progression. *Cancer Letters*, 340(1), 9–21. <https://doi.org/10.1016/j.canlet.2013.06.019>
- Sridhar, S. S., Freedland, S. J., Gleave, M. E., Higano, C., Mulders, P., Parker, C., Sartor, O., & Saad, F. (2014). Castration-resistant prostate cancer: From new pathophysiology to new treatment. *European Urology*, 65(2), 289–299. <https://doi.org/10.1016/j.eururo.2013.08.008>
- Stockert, J. C., Horobin, R. W., Colombo, L. L., & Blázquez-Castro, A. (2018). Tetrazolium salts and formazan products in Cell Biology: Viability assessment, fluorescence imaging, and labeling perspectives. *Acta Histochemica*, 120(3), 159–167. <https://doi.org/10.1016/j.acthis.2018.02.005>
- Struck-Lewicka, W., Kordalewska, M., Bujak, R., Yumba Mpanga, A., Markuszewski, M., Jacyna, J., Matuszewski, M., Kaliszan, R., & Markuszewski, M. J. (2015). Urine metabolic fingerprinting using LC-MS and GC-MS reveals metabolite changes in prostate cancer: A pilot study. *Journal of Pharmaceutical and Biomedical Analysis*, 111, 351–361. <https://doi.org/10.1016/j.jpba.2014.12.026>

References

- Sugie, S., Mukai, S., Yamasaki, K., Kamibeppu, T., Tsukino, H., & Kamoto, T. (2015). Significant Association of Caveolin-1 and Caveolin-2 with Prostate Cancer Progression. *Cancer Genomics & Proteomics*, *12*(6), 391–396.
- Sullivan, M. R., Danai, L. V., Lewis, C. A., Chan, S. H., Gui, D. Y., Kunchok, T., Dennstedt, E. A., Vander Heiden, M. G., & Muir, A. (2019). Quantification of microenvironmental metabolites in murine cancers reveals determinants of tumor nutrient availability. *ELife*, *8*, e44235. <https://doi.org/10.7554/eLife.44235>
- Sun, Q., Zhao, W., Wang, L., Guo, F., Song, D., Zhang, Q., Zhang, D., Fan, Y., & Wang, J. (2019). Integration of metabolomic and transcriptomic profiles to identify biomarkers in serum of lung cancer. *Journal of Cellular Biochemistry*. <https://doi.org/10.1002/jcb.28482>
- Sung, H., Ferlay, J., Siegel, R. L., Laversanne, M., Soerjomataram, I., Jemal, A., & Bray, F. (2021). Global cancer statistics 2020: GLOBOCAN estimates of incidence and mortality worldwide for 36 cancers in 185 countries. *CA: A Cancer Journal for Clinicians*, caac.21660. <https://doi.org/10.3322/caac.21660>
- Szklarczyk, D., Gable, A. L., Nastou, K. C., Lyon, D., Kirsch, R., Pyysalo, S., Doncheva, N. T., Legeay, M., Fang, T., Bork, P., Jensen, L. J., & von Mering, C. (2021). The STRING database in 2021: Customizable protein-protein networks, and functional characterization of user-uploaded gene/measurement sets. *Nucleic Acids Research*, *49*(D1), D605–D612. <https://doi.org/10.1093/nar/gkaa1074>
- Ta, H. D. K., Wang, W.-J., Phan, N. N., An Ton, N. T., Anuraga, G., Ku, S.-C., Wu, Y.-F., Wang, C.-Y., & Lee, K.-H. (2021). Potential Therapeutic and Prognostic Values of LSM Family Genes in Breast Cancer. *Cancers*, *13*(19), 4902. <https://doi.org/10.3390/cancers13194902>
- Takayama, K.-I., Suzuki, T., Fujimura, T., Yamada, Y., Takahashi, S., Homma, Y., Suzuki, Y., & Inoue, S. (2017). Dysregulation of spliceosome gene expression in advanced prostate cancer by RNA-binding protein PSF. *Proceedings of the National Academy of Sciences of the United States of America*, *114*(39), 10461–10466. <https://doi.org/10.1073/pnas.1706076114>
- Tamura, K., Furihata, M., Tsunoda, T., Ashida, S., Takata, R., Obara, W., Yoshioka, H., Daigo, Y., Nasu, Y., Kumon, H., Konaka, H., Namiki, M., Tozawa, K., Kohri, K., Tanji, N., Yokoyama, M., Shimazui, T., Akaza, H., Mizutani, Y., ... Nakagawa, H. (2007). Molecular features of hormone-refractory prostate cancer cells by genome-wide gene expression profiles. *Cancer Research*, *67*(11), 5117–5125. <https://doi.org/10.1158/0008-5472.CAN-06-4040>
- Tannock, I. F., de Wit, R., Berry, W. R., Horti, J., Pluzanska, A., Chi, K. N., Oudard, S., Théodore, C., James, N. D., Turesson, I., Rosenthal, M. A., Eisenberger, M. A., & TAX 327 Investigators. (2004). Docetaxel plus prednisone or mitoxantrone plus prednisone for advanced prostate cancer. *The New England Journal of Medicine*, *351*(15), 1502–1512. <https://doi.org/10.1056/NEJMoa040720>
- Taylor, B. S., Schultz, N., Hieronymus, H., Gopalan, A., Xiao, Y., Carver, B. S., Arora, V. K., Kaushik, P., Cerami, E., Reva, B., Antipin, Y., Mitsiades, N., Landers, T., Dolgalev, I., Major, J. E., Wilson, M.,

- Socci, N. D., Lash, A. E., Heguy, A., ... Gerald, W. L. (2010). Integrative genomic profiling of human prostate cancer. *Cancer Cell*, *18*(1), 11–22. <https://doi.org/10.1016/j.ccr.2010.05.026>
- Thiery, J. P., Acloque, H., Huang, R. Y. J., & Nieto, M. A. (2009). Epithelial-mesenchymal transitions in development and disease. *Cell*, *139*(5), 871–890. <https://doi.org/10.1016/j.cell.2009.11.007>
- Tomlins, S. A., Rhodes, D. R., Yu, J., Varambally, S., Mehra, R., Perner, S., Demichelis, F., Helgeson, B. E., Laxman, B., Morris, D. S., Cao, Q., Cao, X., Andr n, O., Fall, K., Johnson, L., Wei, J. T., Shah, R. B., Al-Ahmadie, H., Eastham, J. A., ... Chinnaiyan, A. M. (2008). The role of SPINK1 in ETS rearrangement-negative prostate cancers. *Cancer Cell*, *13*(6), 519–528. <https://doi.org/10.1016/j.ccr.2008.04.016>
- Triba, M. N., Le Moyec, L., Amathieu, R., Goossens, C., Bouchemal, N., Nahon, P., Rutledge, D. N., & Savarin, P. (2015). PLS/OPLS models in metabolomics: The impact of permutation of dataset rows on the K-fold cross-validation quality parameters. *Molecular BioSystems*, *11*(1), 13–19. <https://doi.org/10.1039/C4MB00414K>
- Truitt, M. L., & Ruggero, D. (2016). New frontiers in translational control of the cancer genome. *Nature Reviews. Cancer*, *16*(5), 288–304. <https://doi.org/10.1038/nrc.2016.27>
- Tsherniak, A., Vazquez, F., Montgomery, P. G., Weir, B. A., Kryukov, G., Cowley, G. S., Gill, S., Harrington, W. F., Pantel, S., Krill-Burger, J. M., Meyers, R. M., Ali, L., Goodale, A., Lee, Y., Jiang, G., Hsiao, J., Gerath, W. F. J., Howell, S., Merkel, E., ... Hahn, W. C. (2017). Defining a Cancer Dependency Map. *Cell*, *170*(3), 564–576.e16. <https://doi.org/10.1016/j.cell.2017.06.010>
- Uhlen, M., Zhang, C., Lee, S., Sj stedt, E., Fagerberg, L., Bidkhor, G., Benfeitas, R., Arif, M., Liu, Z., Edfors, F., Sanli, K., von Feilitzen, K., Oksvold, P., Lundberg, E., Hober, S., Nilsson, P., Mattsson, J., Schwenk, J. M., Brunnstr m, H., ... Ponten, F. (2017). A pathology atlas of the human cancer transcriptome. *Science (New York, N.Y.)*, *357*(6352), eaan2507. <https://doi.org/10.1126/science.aan2507>
- Umbehr, M. H., M ntener, M., Hany, T., Sulser, T., & Bachmann, L. M. (2013). The role of 11C-choline and 18F-fluorocholine positron emission tomography (PET) and PET/CT in prostate cancer: A systematic review and meta-analysis. *European Urology*, *64*(1), 106–117. <https://doi.org/10.1016/j.eururo.2013.04.019>
- Ummanni, R., Mundt, F., Pospisil, H., Venz, S., Scharf, C., Barrett, C., F lth, M., K llermann, J., Walther, R., Schlomm, T., Sauter, G., Bokemeyer, C., S ltmann, H., Schuppert, A., Br ummendorf, T. H., & Balabanov, S. (2011). Identification of clinically relevant protein targets in prostate cancer with 2D-DIGE coupled mass spectrometry and systems biology network platform. *PloS One*, *6*(2), e16833. <https://doi.org/10.1371/journal.pone.0016833>
- UniProt Consortium. (2021). UniProt: The universal protein knowledgebase in 2021. *Nucleic Acids Research*, *49*(D1), D480–D489. <https://doi.org/10.1093/nar/gkaa1100>
- Vainio, P., Mpindi, J.-P., Kohonen, P., Fey, V., Mirtti, T., Alanen, K. A., Per l , M., Kallioniemi, O., & Iljin, K. (2012). High-throughput transcriptomic and RNAi analysis identifies AIM1, ERGIC1, TMED3

References

- and TPX2 as potential drug targets in prostate cancer. *PLoS One*, 7(6), e39801. <https://doi.org/10.1371/journal.pone.0039801>
- Valásek, L. S. (2012). 'Ribozomin'—Translation initiation from the perspective of the ribosome-bound eukaryotic initiation factors (eIFs). *Current Protein & Peptide Science*, 13(4), 305–330. <https://doi.org/10.2174/138920312801619385>
- van der Steen, T., Tindall, D. J., & Huang, H. (2013). Posttranslational modification of the androgen receptor in prostate cancer. *International Journal of Molecular Sciences*, 14(7), 14833–14859. <https://doi.org/10.3390/ijms140714833>
- Varisli, L. (2013). Identification of new genes downregulated in prostate cancer and investigation of their effects on prognosis. *Genetic Testing and Molecular Biomarkers*, 17(7), 562–566. <https://doi.org/10.1089/gtmb.2012.0524>
- Verma, R., Aravind, L., Oania, R., McDonald, W. H., Yates, J. R., Koonin, E. V., & Deshaies, R. J. (2002). Role of Rpn11 metalloprotease in deubiquitination and degradation by the 26S proteasome. *Science (New York, N.Y.)*, 298(5593), 611–615. <https://doi.org/10.1126/science.1075898>
- von Rundstedt, F.-C., Rajapakshe, K., Ma, J., Arnold, J. M., Gohlke, J., Putluri, V., Krishnapuram, R., Piyarathna, D. B., Lotan, Y., Gödde, D., Roth, S., Störkel, S., Levitt, J. M., Michailidis, G., Sreekumar, A., Lerner, S. P., Coarfa, C., & Putluri, N. (2016). Integrative Pathway Analysis of Metabolic Signature in Bladder Cancer: A Linkage to The Cancer Genome Atlas Project and Prediction of Survival. *The Journal of Urology*, 195(6), 1911–1919. <https://doi.org/10.1016/j.juro.2016.01.039>
- Vu, T. N., Valkenburg, D., Smets, K., Verwaest, K. A., Dommissie, R., Lemièrre, F., Verschoren, A., Goethals, B., & Laukens, K. (2011). An integrated workflow for robust alignment and simplified quantitative analysis of NMR spectrometry data. *BMC Bioinformatics*, 12(1), 405. <https://doi.org/10.1186/1471-2105-12-405>
- Wang, H., Ru, Y., Sanchez-Carbayo, M., Wang, X., Kieft, J. S., & Theodorescu, D. (2013). Translation initiation factor eIF3b expression in human cancer and its role in tumor growth and lung colonization. *Clinical Cancer Research: An Official Journal of the American Association for Cancer Research*, 19(11), 2850–2860. <https://doi.org/10.1158/1078-0432.CCR-12-3084>
- Wang, H., Zhang, N., Wu, X., Zheng, X., Ling, Y., & Gong, Y. (2019). Prognostic value of U2AF1 mutant in patients with de novo myelodysplastic syndromes: A meta-analysis. *Annals of Hematology*, 98(12), 2629–2639. <https://doi.org/10.1007/s00277-019-03843-3>
- Wang, P., Henning, S. M., & Heber, D. (2010). Limitations of MTT and MTS-based assays for measurement of antiproliferative activity of green tea polyphenols. *PLoS One*, 5(4), e10202. <https://doi.org/10.1371/journal.pone.0010202>
- Wang, X., Bao, J., Ping, X., Hu, C., Hou, J., Dong, F., & Guo, L. (2018). The diagnostic value of PI-RADS V1 and V2 using multiparametric MRI in transition zone prostate clinical cancer. *Oncology Letters*, 16(3), 3201–3206. <https://doi.org/10.3892/ol.2018.9038>

- Wang, X., Li, Y., He, M., Kong, X., Jiang, P., Liu, X., Diao, L., Zhang, X., Li, H., Ling, X., Xia, S., Liu, Z., Liu, Y., Cui, C.-P., Wang, Y., Tang, L., Zhang, L., He, F., & Li, D. (2022). UbiBrowser 2.0: A comprehensive resource for proteome-wide known and predicted ubiquitin ligase/deubiquitinase-substrate interactions in eukaryotic species. *Nucleic Acids Research*, *50*(D1), D719–D728. <https://doi.org/10.1093/nar/gkab962>
- Wang, X., Wang, H., Zhao, S., Sun, P., Wen, D., Liu, T., Liu, H., Yang, Z., & Ma, Z. (2018). Eukaryotic translation initiation factor EIF3H potentiates gastric carcinoma cell proliferation. *Tissue & Cell*, *53*, 23–29. <https://doi.org/10.1016/j.tice.2018.05.006>
- Wang, Z., Chen, J., Sun, J., Cui, Z., & Wu, H. (2012). RNA interference-mediated silencing of eukaryotic translation initiation factor 3, subunit B (EIF3B) gene expression inhibits proliferation of colon cancer cells. *World Journal of Surgical Oncology*, *10*, 119. <https://doi.org/10.1186/1477-7819-10-119>
- Wei, F., Ding, L., Wei, Z., Zhang, Y., Li, Y., Qinghua, L., Ma, Y., Guo, L., Lv, G., & Liu, Y. (2016). Ribosomal protein L34 promotes the proliferation, invasion and metastasis of pancreatic cancer cells. *Oncotarget*, *7*(51), 85259–85272. <https://doi.org/10.18632/oncotarget.13269>
- Westerhuis, J. A., Hoefsloot, H. C. J., Smit, S., Vis, D. J., Smilde, A. K., van Velzen, E. J. J., van Duijnhoven, J. P. M., & van Dorsten, F. A. (2008). Assessment of PLS-DA cross validation. *Metabolomics*, *4*(1), 81–89. <https://doi.org/10.1007/s11306-007-0099-6>
- Witwicki, R. M., Ekram, M. B., Qiu, X., Janiszewska, M., Shu, S., Kwon, M., Trinh, A., Frias, E., Ramadan, N., Hoffman, G., Yu, K., Xie, Y., McAllister, G., McDonald, R., Golji, J., Schlabach, M., deWeck, A., Keen, N., Chan, H. M., ... Polyak, K. (2018). TRPS1 Is a Lineage-Specific Transcriptional Dependency in Breast Cancer. *Cell Reports*, *25*(5), 1255–1267.e5. <https://doi.org/10.1016/j.celrep.2018.10.023>
- Wright, J. L., Plymate, S. R., Porter, M. P., Gore, J. L., Lin, D. W., Hu, E., & Zeliadt, S. B. (2013). Hyperglycemia and prostate cancer recurrence in men treated for localized prostate cancer. *Prostate Cancer and Prostatic Diseases*, *16*(2), 204–208. <https://doi.org/10.1038/pcan.2013.5>
- Wu, X., Daniels, G., Lee, P., & Monaco, M. E. (2014). Lipid metabolism in prostate cancer. *American Journal of Clinical and Experimental Urology*, *2*(2), 111–120.
- Wulaningsih, W., Holmberg, L., Garmo, H., Zethelius, B., Wigertz, A., Carroll, P., Lambe, M., Hammar, N., Walldius, G., Jungner, I., & Van Hemelrijck, M. (2013). Serum glucose and fructosamine in relation to risk of cancer. *PloS One*, *8*(1), e54944. <https://doi.org/10.1371/journal.pone.0054944>
- Wurth, L. (2012). Versatility of RNA-Binding Proteins in Cancer. *Comparative and Functional Genomics*, *2012*, 178525. <https://doi.org/10.1155/2012/178525>
- Xiang, P., Sun, Y., Fang, Z., Yan, K., & Fan, Y. (2020). Eukaryotic translation initiation factor 3 subunit b is a novel oncogenic factor in prostate cancer. *Mammalian Genome: Official Journal of the International Mammalian Genome Society*, *31*(7–8), 197–204. <https://doi.org/10.1007/s00335-020-09842-4>
- Xie, G., & Xu, X. (2020). Amplification of SNRPE promotes tumor proliferation and invasion in triple-negative breast cancer by activating mTOR signaling. *European Journal of Cancer*, *138*, S31–S32. [https://doi.org/10.1016/S0959-8049\(20\)31153-9](https://doi.org/10.1016/S0959-8049(20)31153-9)

References

- Xie, J., Kusnadi, E. P., Furic, L., & Selth, L. A. (2021). Regulation of mRNA Translation by Hormone Receptors in Breast and Prostate Cancer. *Cancers*, 13(13), 3254. <https://doi.org/10.3390/cancers13133254>
- Xie, R., Chen, X., Chen, Z., Huang, M., Dong, W., Gu, P., Zhang, J., Zhou, Q., Dong, W., Han, J., Wang, X., Li, H., Huang, J., & Lin, T. (2019). Polypyrimidine tract binding protein 1 promotes lymphatic metastasis and proliferation of bladder cancer via alternative splicing of MEIS2 and PKM. *Cancer Letters*, 449, 31–44. <https://doi.org/10.1016/j.canlet.2019.01.041>
- Xie, X., Yu, H., Wang, Y., Zhou, Y., Li, G., Ruan, Z., Li, F., Wang, X., Liu, H., & Zhang, J. (2014). Nicotinamide N-methyltransferase enhances the capacity of tumorigenesis associated with the promotion of cell cycle progression in human colorectal cancer cells. *Archives of Biochemistry and Biophysics*, 564, 52–66. <https://doi.org/10.1016/j.abb.2014.08.017>
- Xu, J., & Qiu, Y. (2016). Role of androgen receptor splice variants in prostate cancer metastasis. *Asian Journal of Urology*, 3(4), 177–184. <https://doi.org/10.1016/j.ajur.2016.08.003>
- Xu, N., Wu, Y.-P., Yin, H.-B., Chen, S.-H., Li, X.-D., Xue, X.-Y., & Gou, X. (2020). SHCBP1 promotes tumor cell proliferation, migration, and invasion, and is associated with poor prostate cancer prognosis. *Journal of Cancer Research and Clinical Oncology*, 146(8), 1953–1969. <https://doi.org/10.1007/s00432-020-03247-1>
- Xu, T.-P., Liu, X.-X., Xia, R., Yin, L., Kong, R., Chen, W.-M., Huang, M.-D., & Shu, Y.-Q. (2015). SP1-induced upregulation of the long noncoding RNA TINCR regulates cell proliferation and apoptosis by affecting KLF2 mRNA stability in gastric cancer. *Oncogene*, 34(45), 5648–5661. <https://doi.org/10.1038/onc.2015.18>
- Xue, R., Hua, L., Xu, W., Gao, Y., Pang, Y., & Hao, J. (2018). Derivation and Validation of the Potential Core Genes in Pancreatic Cancer for Tumor-Stroma Crosstalk. *BioMed Research International*, 2018, 4283673. <https://doi.org/10.1155/2018/4283673>
- Yan, M., Qi, H., Li, J., Ye, G., Shao, Y., Li, T., Liu, J., Piao, H.-L., & Xu, G. (2017). Identification of SPOP related metabolic pathways in prostate cancer. *Oncotarget*, 8(61), 103032–103046. <https://doi.org/10.18632/oncotarget.21460>
- Yang, K., & Han, X. (2016). Lipidomics: Techniques, Applications, and Outcomes Related to Biomedical Sciences. *Trends in Biochemical Sciences*, 41(11), 954–969. <https://doi.org/10.1016/j.tibs.2016.08.010>
- Yang, Q., Fung, K.-M., Day, W. V., Kropp, B. P., & Lin, H.-K. (2005). Androgen receptor signaling is required for androgen-sensitive human prostate cancer cell proliferation and survival. *Cancer Cell International*, 5(1), 8. <https://doi.org/10.1186/1475-2867-5-8>
- Yi, C., Wan, X., Zhang, Y., Fu, F., Zhao, C., Qin, R., Wu, H., Li, Y., & Huang, Y. (2018). SNORA42 enhances prostate cancer cell viability, migration and EMT and is correlated with prostate cancer poor prognosis. *The International Journal of Biochemistry & Cell Biology*, 102, 138–150. <https://doi.org/10.1016/j.biocel.2018.07.009>

- Yin, J., Lin, C., Jiang, M., Tang, X., Xie, D., Chen, J., & Ke, R. (2021). CENPL, ISG20L2, LSM4, MRPL3 are four novel hub genes and may serve as diagnostic and prognostic markers in breast cancer. *Scientific Reports*, 11(1), 15610. <https://doi.org/10.1038/s41598-021-95068-6>
- Yu, G., Liao, J., Wu, J., Ding, J., & Zhang, L. (2018). The proliferation of colorectal cancer cells is suppressed by silencing of EIF3H. *Bioscience, Biotechnology, and Biochemistry*, 82(10), 1694–1701. <https://doi.org/10.1080/09168451.2018.1484271>
- Yu, K.-H., & Snyder, M. (2016). Omics Profiling in Precision Oncology. *Molecular & Cellular Proteomics: MCP*, 15(8), 2525–2536. <https://doi.org/10.1074/mcp.O116.059253>
- Yu, Y. P., Landsittel, D., Jing, L., Nelson, J., Ren, B., Liu, L., McDonald, C., Thomas, R., Dhir, R., Finkelstein, S., Michalopoulos, G., Becich, M., & Luo, J.-H. (2004). Gene expression alterations in prostate cancer predicting tumor aggression and preceding development of malignancy. *Journal of Clinical Oncology: Official Journal of the American Society of Clinical Oncology*, 22(14), 2790–2799. <https://doi.org/10.1200/JCO.2004.05.158>
- Zaragozá, P., Ruiz-Cerdá, J. L., Quintás, G., Gil, S., Costero, A. M., León, Z., Vivancos, J.-L., & Martínez-Mañez, R. (2014). Towards the potential use of 1H NMR spectroscopy in urine samples for prostate cancer detection. *The Analyst*, 139(16), 3875–3878. <https://doi.org/10.1039/C4AN00690A>
- Zhan, X., Yan, C., Zhang, X., Lei, J., & Shi, Y. (2018). Structures of the human pre-catalytic spliceosome and its precursor spliceosome. *Cell Research*, 28(12), 1129–1140. <https://doi.org/10.1038/s41422-018-0094-7>
- Zhang, H., Zeng, J., Tan, Y., Lu, L., Sun, C., Liang, Y., Zou, H., Yang, X., & Tan, Y. (2018). Subgroup analysis reveals molecular heterogeneity and provides potential precise treatment for pancreatic cancers. *OncoTargets and Therapy*, 11, 5811–5819. <https://doi.org/10.2147/OTT.S163139>
- Zhang, J., & Manley, J. L. (2013). Misregulation of pre-mRNA alternative splicing in cancer. *Cancer Discovery*, 3(11), 1228–1237. <https://doi.org/10.1158/2159-8290.CD-13-0253>
- Zhang, L., Pan, X., & Hershey, J. W. B. (2007). Individual overexpression of five subunits of human translation initiation factor eIF3 promotes malignant transformation of immortal fibroblast cells. *The Journal of Biological Chemistry*, 282(8), 5790–5800. <https://doi.org/10.1074/jbc.M606284200>
- Zhang, L., Smit-McBride, Z., Pan, X., Rheinhardt, J., & Hershey, J. W. B. (2008). An oncogenic role for the phosphorylated h-subunit of human translation initiation factor eIF3. *The Journal of Biological Chemistry*, 283(35), 24047–24060. <https://doi.org/10.1074/jbc.M800956200>
- Zhang, P., Gao, H., Ye, C., Yan, R., Yu, L., Xia, C., & Yang, D. (2022). Large-Scale Transcriptome Data Analysis Identifies KIF2C as a Potential Therapeutic Target Associated With Immune Infiltration in Prostate Cancer. *Frontiers in Immunology*, 13, 905259. <https://doi.org/10.3389/fimmu.2022.905259>
- Zhang, X., Xu, L., Shen, J., Cao, B., Cheng, T., Zhao, T., Liu, X., & Zhang, H. (2013). Metabolic signatures of esophageal cancer: NMR-based metabolomics and UHPLC-based focused metabolomics of blood serum. *Biochimica Et Biophysica Acta*, 1832(8), 1207–1216. <https://doi.org/10.1016/j.bbadis.2013.03.009>

References

- Zhang, X., Yan, C., Zhan, X., Li, L., Lei, J., & Shi, Y. (2018). Structure of the human activated spliceosome in three conformational states. *Cell Research*, 28(3), 307–322. <https://doi.org/10.1038/cr.2018.14>
- Zhou, Z., Zhou, H., Ponzoni, L., Luo, A., Zhu, R., He, M., Huang, Y., Guan, K.-L., Bahar, I., Liu, Z., & Wan, Y. (2020). EIF3H Orchestrates Hippo Pathway-Mediated Oncogenesis via Catalytic Control of YAP Stability. *Cancer Research*, 80(12), 2550–2563. <https://doi.org/10.1158/0008-5472.CAN-19-3718>
- Zhu, Q., Qiao, G.-L., Zeng, X.-C., Li, Y., Yan, J.-J., Duan, R., & Du, Z.-Y. (2016). Elevated expression of eukaryotic translation initiation factor 3H is associated with proliferation, invasion and tumorigenicity in human hepatocellular carcinoma. *Oncotarget*, 7(31), 49888–49901. <https://doi.org/10.18632/oncotarget.10222>

VIII. APPENDICES

Appendix 1. Metabolites identified in PCa biofluid samples

Serum			Urine		
Metabolite	Left limit (ppm)	Right limit (ppm)	Metabolite	Left limit (ppm)	Right limit (ppm)
Leucine	0.959	0.943	Leucine	0.970	0.960
Isoleucine	1.038	1.026	Valine	1.011	0.985
Valine	1.074	1.041	Isoleucine	1.026	1.017
Methylsuccinate	1.099	1.075	Isobutyrate	1.090	1.063
Propylene Glycol	1.147	1.124	3-methyl-2-oxovalerate	1.124	1.098
Lactate	1.360	1.328	Methylmalonate	1.247	1.226
Alanine	1.515	1.482	3-hydroxyisovalerate	1.282	1.269
Arginine/Lysine	1.809	1.650	Lactate	1.355	1.322
Acetate	1.938	1.926	Alanine	1.506	1.474
Acetoacetate	2.302	2.288	Acetoacetate	2.284	2.267
Succinate	2.391	2.380	Citrate	2.576	2.510
Glutamine	2.499	2.446	Carnitine	3.239	3.223
Citrate	2.580	2.528	Scyllo-inositol	3.374	3.359
Trimethylamine	2.906	2.895	Taurine	3.457	3.412
N,N-dimethylglycine	2.923	2.909	Glycine	3.583	3.569
Scyllo-inositol	3.378	3.371	Creatinine	4.089	4.037
Glycine	3.581	3.572	2-furoylglycine	6.661	6.633
Glucose	3.815	3.705	Phenylalanine	7.448	7.405
Fumarate	6.787	6.712	4-Py	7.831	7.821
Tyrosine	6.944	6.891	Formate	8.456	8.475
Histidine	7.098	7.057	Trigonelline	9.143	9.103
Phenylalanine	7.473	7.316	1-methylnicotinamide	9.295	9.251
Formate	8.484	8.464			

4-Py: N1-Methyl-4-pyridone-5-carboxamide.

Appendix 2. Protocol followed for plasmid purification

1. Transfer bacteria cultures to a 500 mL centrifuge bottle and spin down at 4500 rpm for 10 min at RT.
2. Discard supernatants, resuspend the pellet in 5 mL of 50 mM Glucose, 10.5 mM Tris, 12.73 mM EDTA cold solution, and transfer it to a 50 ml tube.
3. Add 25 mg of lysozyme to the suspension and left incubating for 8 min at RT.
4. Add 10 mL of freshly made solution (1% SDS, 0.2 mM NaOH) and incubate on ice for 10 min, regularly mixing by hand.
5. When the solution looks syrupy with no ribbons of milky solution, add 7.5 mL of 3 M $\text{CH}_3\text{CO}_2\text{K}$, 57.5 mL of acetic glacial solution and left tubes incubating on ice for 10 min.
6. After incubation, spin tubes at 12.000 rpm at 4°C for 20 min.
7. Transfer supernatants to a new tube, adding 14 ml of RT isopropanol and incubating at RT for 30 min.
8. Spin tubes at 9000 rpm at 4°C for 20 min, discard supernatants and airdry pellets for 10 min.
9. Resuspend pellets in 4 ml 1X TE buffer (10 mM Tris, 1mM EDTA, pH = 8), leaving them on a rocking platform for 10 min.
10. When resuspended, add 2 mL of cold 7.5 mM ammonium acetate, incubate pellets on ice for 30 min and spin at 10.000 rpm at 4°C for 10 min.
11. After centrifugation, transfer supernatants to a new tube, and incubate at -20°C overnight after adding 12 mL of ice cold 100% ethanol (EtOH).
12. Next day, spin tubes at 10.000 rpm at 4°C for 10 min, discard supernatants and airdry pellets for 10 min.
13. Once dried, resuspend pellets in 500 μl of 1X TE buffer, using a rocking platform, and transfer the solution to a 1.5 mL Eppendorf tube.
14. Add 1 μl of 10 mg/ml RNase to each solution and left incubating at 37°C for 30 min.
15. After incubation, add a mix solution of 250 μl of cold phenol and 250 μl of cold chloroform (CHCl_3) to each sample, and vortex Eppendorfs for 30 sec at maximum speed at RT for 5 min.
16. Transfer the upper aqueous phase to a new microtube, add 250 μl of CHCl_3 to the aqueous phase, and vortex samples again for 30 sec at maximum speed at RT for 5 min.

17. Repeat this step one more time.
18. After transferring the upper phase, add 50 μ l 3M sodium acetate to the aqueous phase and mix the solution well.
19. Then, add 1 mL of ice cold 100% EtOH to each microtube, mix sample by inversion, and spool and transfer precipitated DNA to an Eppendorf tube containing 70% EtOH.
20. Spin microtubes at maximum speed at 4°C for 5 min, remove supernatants and airdry pellets overnight.
21. Finally, resuspend pellets on 1X TE buffer and quantify them using a nanodrop.

Appendix 3. PCA generated for each transcriptomic study to evaluate sample heterogeneity and detect potential outliers. A) gse16560, B) gse46602 and C) gse70768. Blue and green colors represent low- and high-GS patients, respectively.



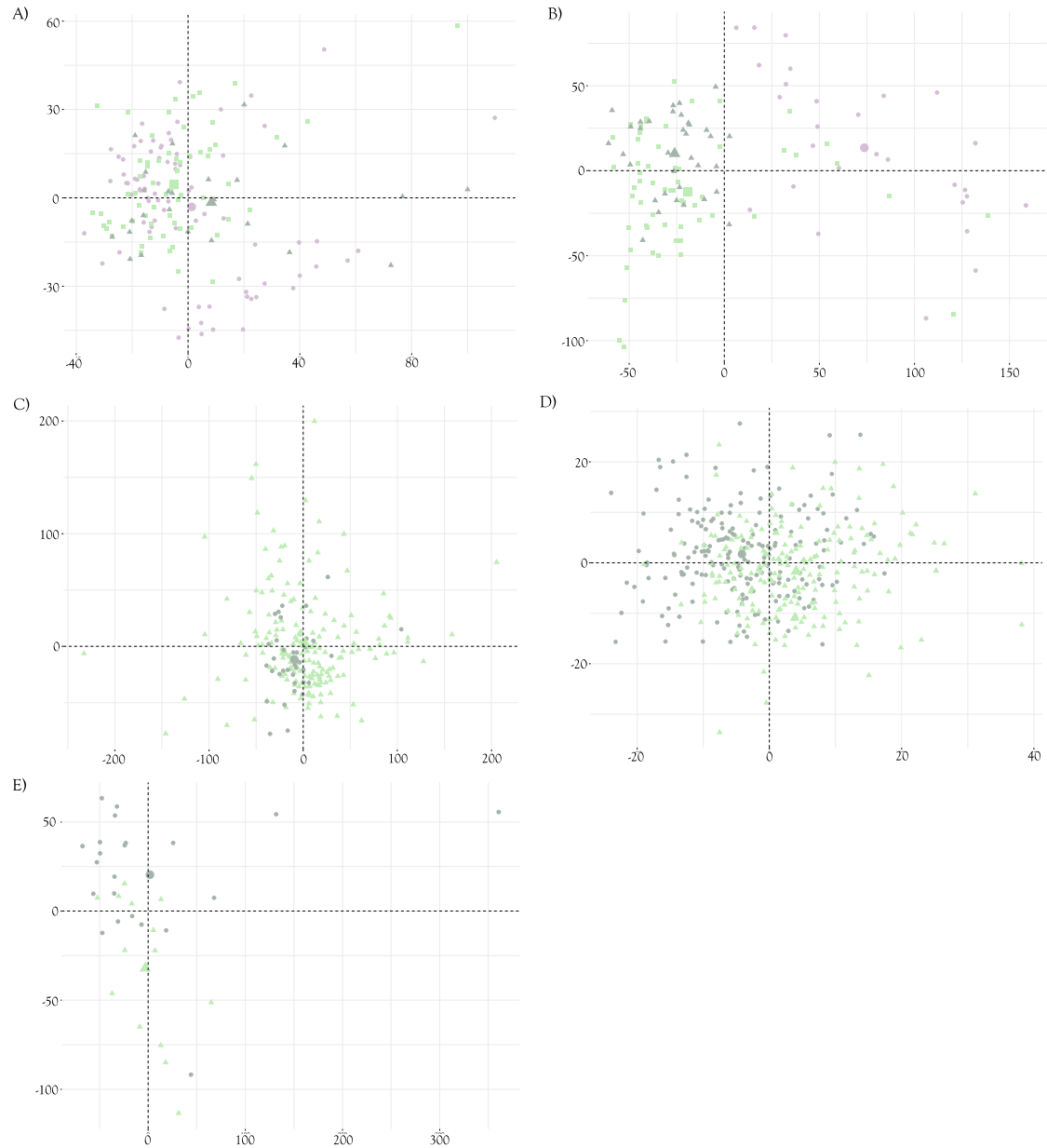
Appendix 4. Gene set enrichment analysis of transcriptomics datasets included in this study

ID KEGG	Pathway name	ID dataset	LOR ^a	p-value ^b	FDR
hsa00010	Glycolysis / Gluconeogenesis	GSE16560	-0,4197	0,0052	0,3537
hsa00020	Citrate cycle (TCA cycle)	GSE46602	0,5167	0,0071	0,2692
hsa00040	Pentose and glucuronate interconversions	GSE16560	-0,7404	0,0072	0,4189
hsa00051	Fructose and mannose metabolism	GSE16560	-0,5106	0,0096	0,4369
hsa00100	Steroid biosynthesis	GSE46602	0,6657	0,0127	0,3497
hsa00140	Steroid hormone biosynthesis	GSE16560	-0,6065	0,0002	0,0432
hsa00190	Oxidative phosphorylation	GSE16560	0,2993	0,0136	0,5574
		GSE46602	0,8950	1,33E-18	5,14E-16
		GSE70768	0,5294	1,08E-08	4,35E-06
hsa00220	Arginine biosynthesis	GSE16560	-0,5581	0,0325	1,0000
hsa00230	Purine metabolism	GSE46602	0,4492	4,04E-08	5,19E-06
		GSE70768	0,2416	0,0027	0,1797
hsa00240	Pyrimidine metabolism	GSE16560	0,4899	0,0021	0,2106
		GSE46602	0,6645	2,57E-09	4,94E-07
		GSE70768	0,4265	0,0001	0,0109
hsa00270	Cysteine and methionine metabolism	GSE46602	0,3250	0,0420	0,8525
hsa00280	Valine, leucine and isoleucine degradation	GSE46602	0,3786	0,0120	0,3497
		GSE70768	0,2970	0,0424	1,0000
hsa00340	Histidine metabolism	GSE70768	-0,7859	0,0010	0,0970
hsa00350	Tyrosine metabolism	GSE16560	-0,6329	0,0007	0,0942
hsa00440	Phosphonate and phosphinate metabolism	GSE70768	-0,8034	0,0479	1,0000
hsa00480	Glutathione metabolism	GSE70768	-0,3903	0,0043	0,2177
hsa00510	N-Glycan biosynthesis	GSE46602	0,4407	0,0053	0,2692
		GSE70768	0,3647	0,0112	0,4534
hsa00532	Glycosaminoglycan biosynthesis - chondroitin sulfate / dermatan sulfate	GSE46602	0,4911	0,0258	0,5846
hsa00562	Inositol phosphate metabolism	GSE46602	0,3210	0,0077	0,2692
		GSE70768	-0,2400	0,0416	1,0000
hsa00563	Glycosylphosphatidylinositol (GPI)-anchor biosynthesis	GSE70768	0,5903	0,0031	0,1797
hsa00590	Arachidonic acid metabolism	GSE16560	-0,4476	0,0180	0,6708
hsa00591	Linoleic acid metabolism	GSE16560	-0,7716	0,0051	0,3537
hsa00600	Sphingolipid metabolism	GSE46602	0,4516	0,0047	0,2692
hsa00601	Glycosphingolipid biosynthesis - lacto and neolacto series	GSE16560	-0,6162	0,0206	0,7013
		GSE70768	-0,5601	0,0053	0,2388
hsa00620	Pyruvate metabolism	GSE46602	0,4262	0,0181	0,4351
hsa00630	Glyoxylate and dicarboxylate metabolism	GSE70768	0,6608	0,0014	0,1095
hsa00640	Propanoate metabolism	GSE70768	0,3969	0,0256	0,9374
hsa00670	One carbon pool by folate	GSE16560	0,7281	0,0091	0,4369
hsa00740	Riboflavin metabolism	GSE46602	0,8734	0,0101	0,3241
hsa00760	Nicotinate and nicotinamide metabolism	GSE70768	-0,4459	0,0463	1,0000
hsa00830	Retinol metabolism	GSE16560	-0,8751	3,90E-06	0,0016
		GSE46602	-0,3993	0,0068	0,2692
hsa00860	Porphyrin and chlorophyll metabolism	GSE46602	0,3946	0,0302	0,6464
hsa00900	Terpenoid backbone biosynthesis	GSE46602	0,7854	0,0003	0,0228
hsa01200	Carbon metabolism	GSE46602	0,2926	0,0072	0,2692
		GSE70768	0,3306	0,0005	0,0722

Appendices

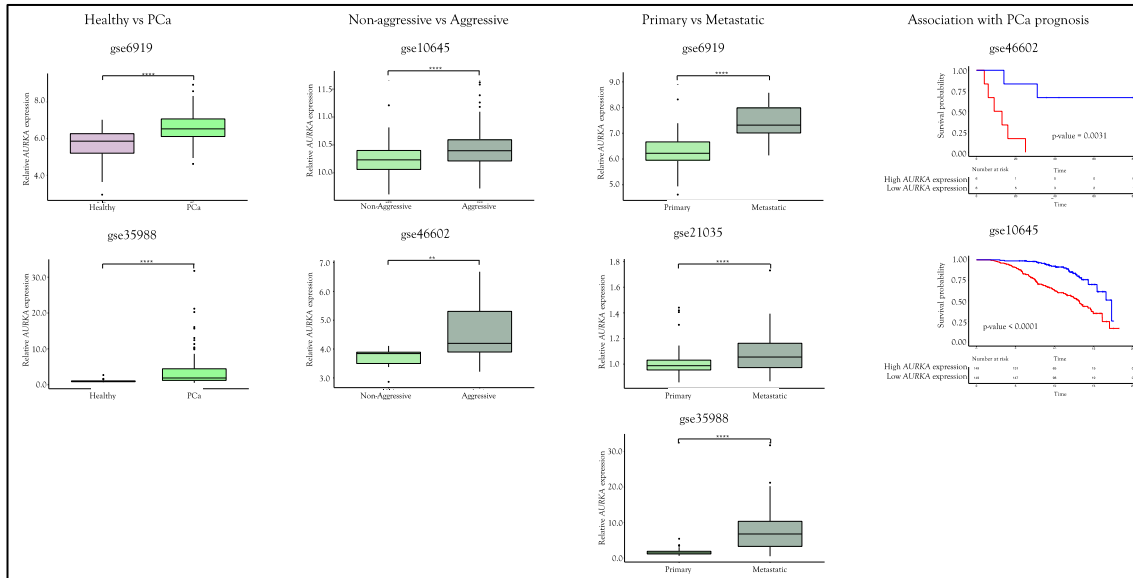
hsa01210	2-Oxocarboxylic acid metabolism	GSE46602	0,6212	0,0144	0,3705
hsa01230	Biosynthesis of amino acids	GSE46602	0,5104	0,0002	0,0155

Appendix 5. PCA generated for each transcriptomic study to evaluate sample heterogeneity and detect potential outliers. A) gse6919, B) gse35988, C) gse21035, D) gse10645 and E) gse46602. Pink, light green and dark green colors represent healthy, indolent/primary, and aggressive/metastatic individuals, respectively.

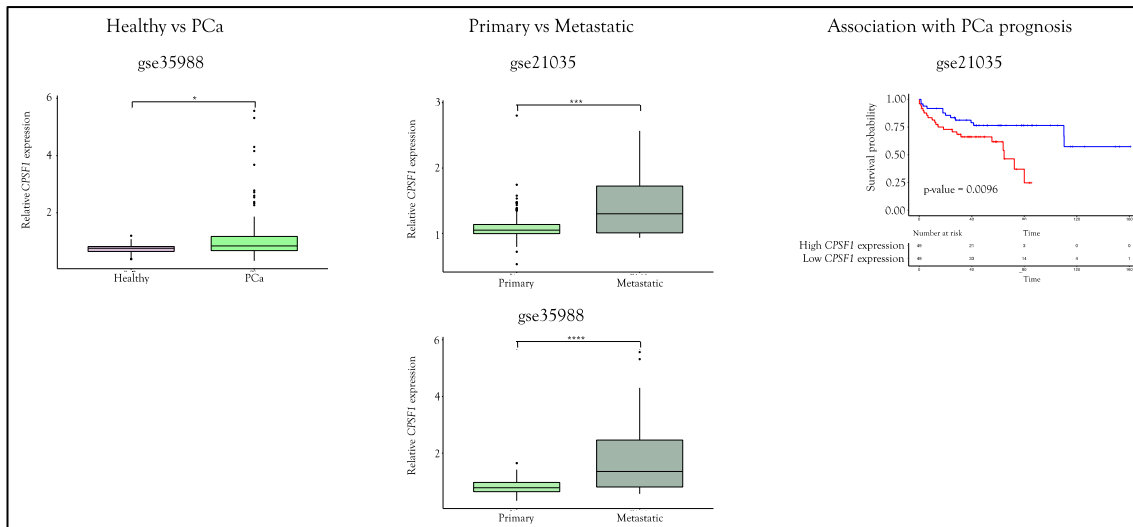


Appendix 6. Differential expression and survival analyses of the sixteen potential therapeutic targets

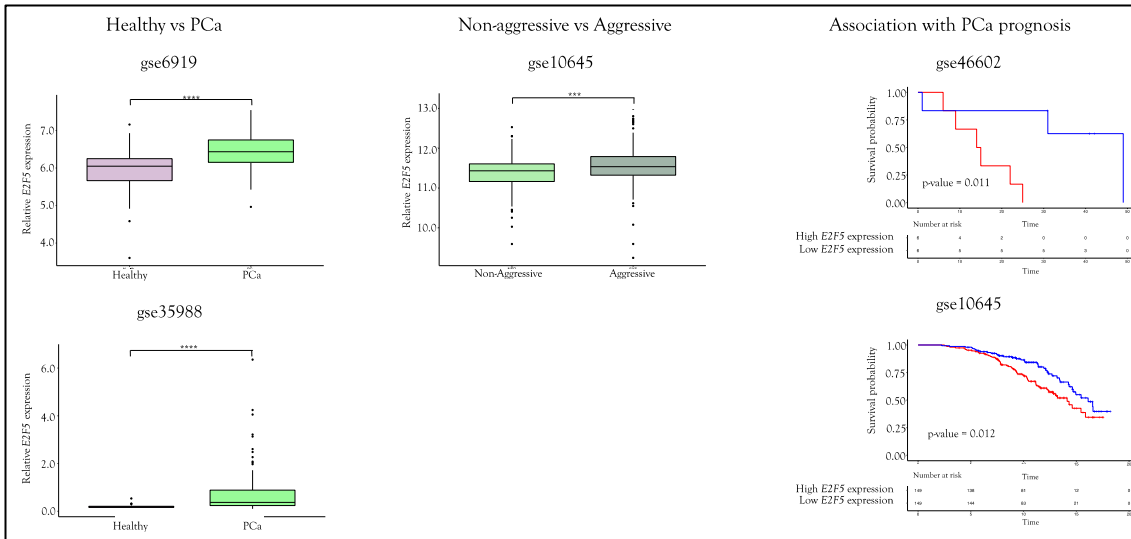
AURKA



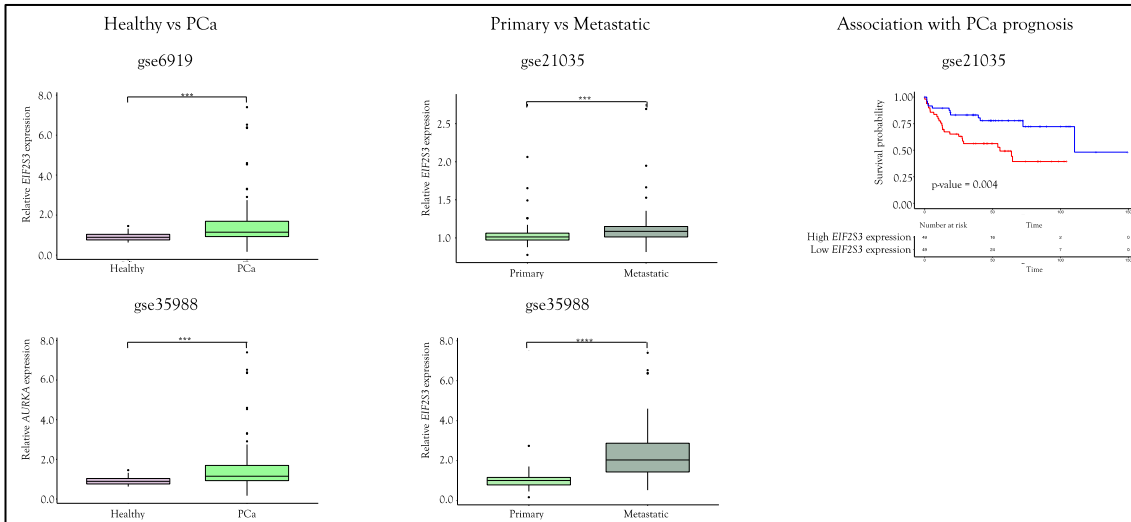
CPSF1



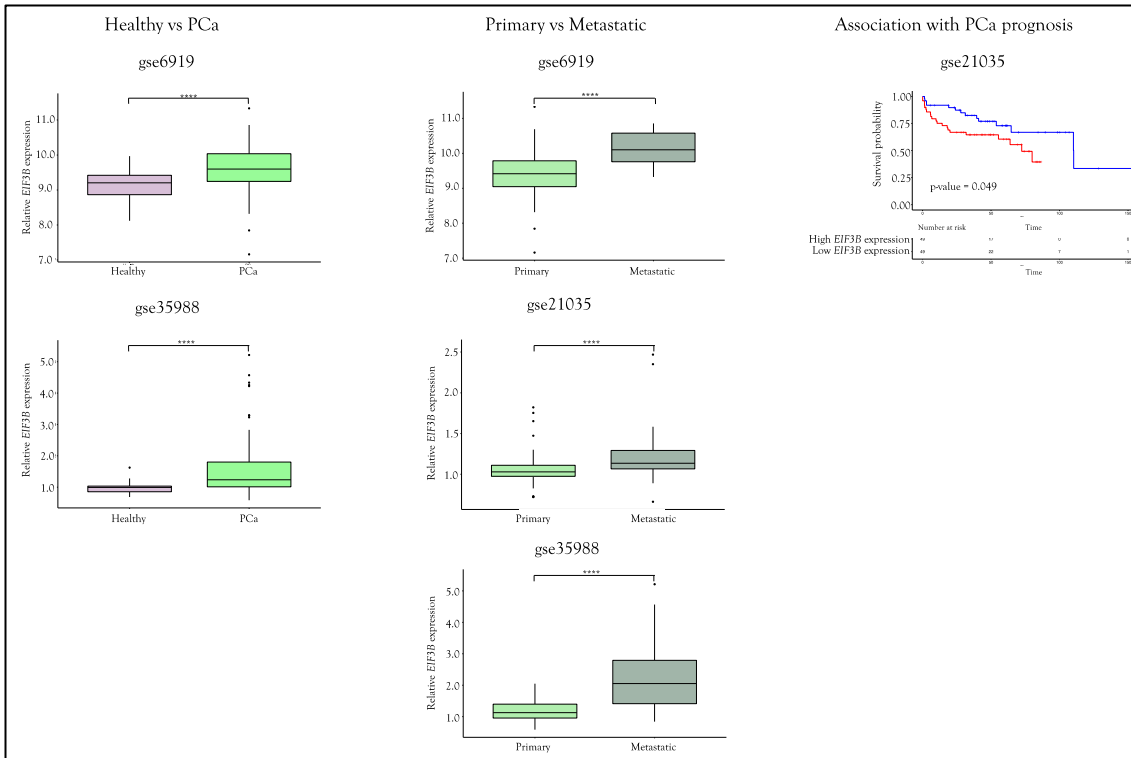
E2F5



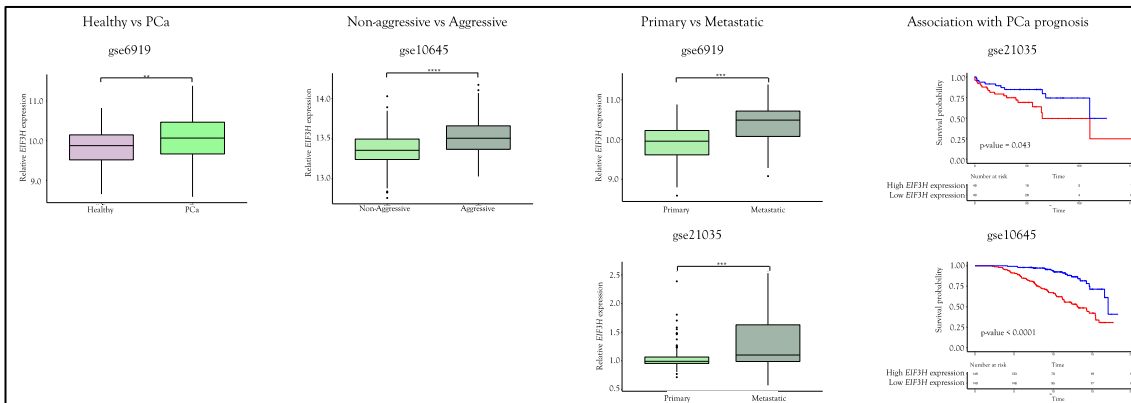
EIF2S3



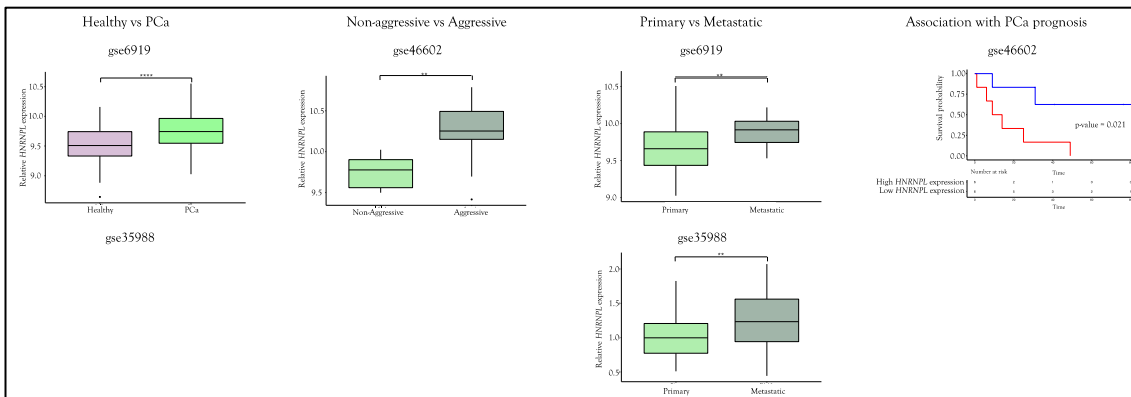
EIF3B



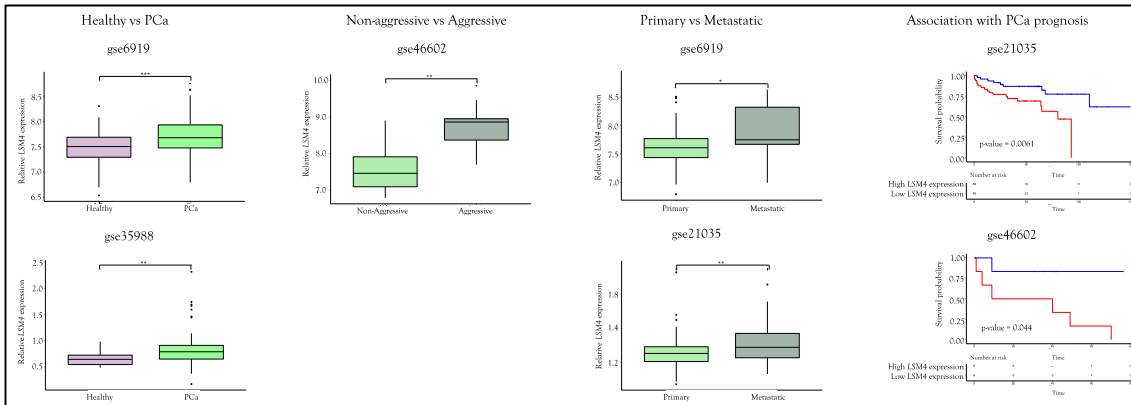
EIF3H



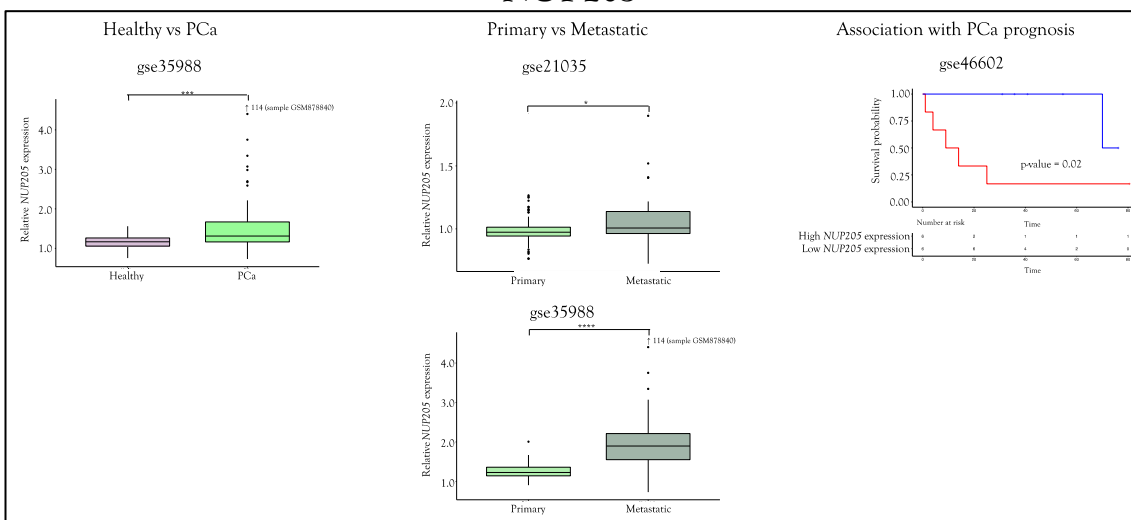
HNRNPL



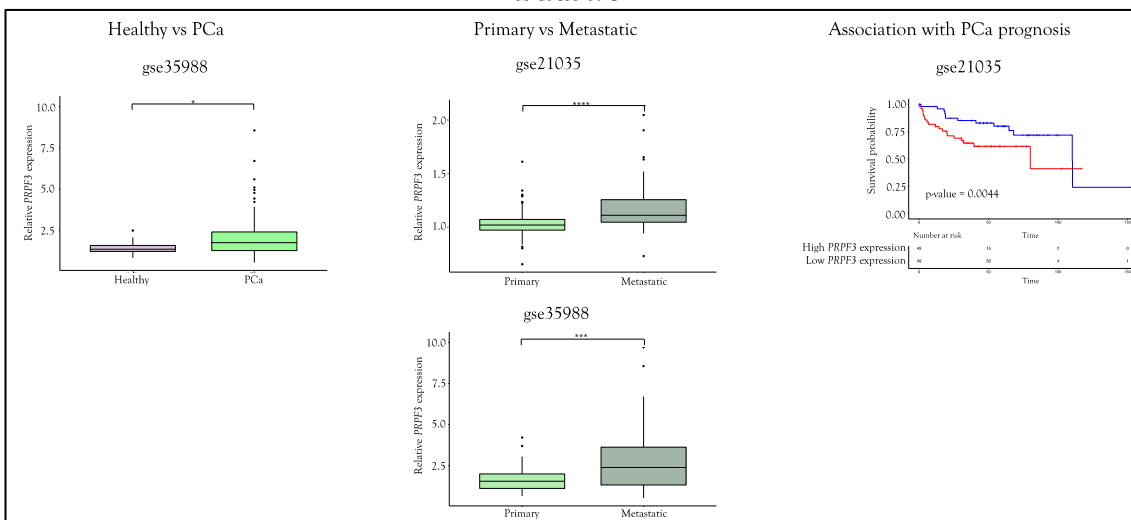
LSM4



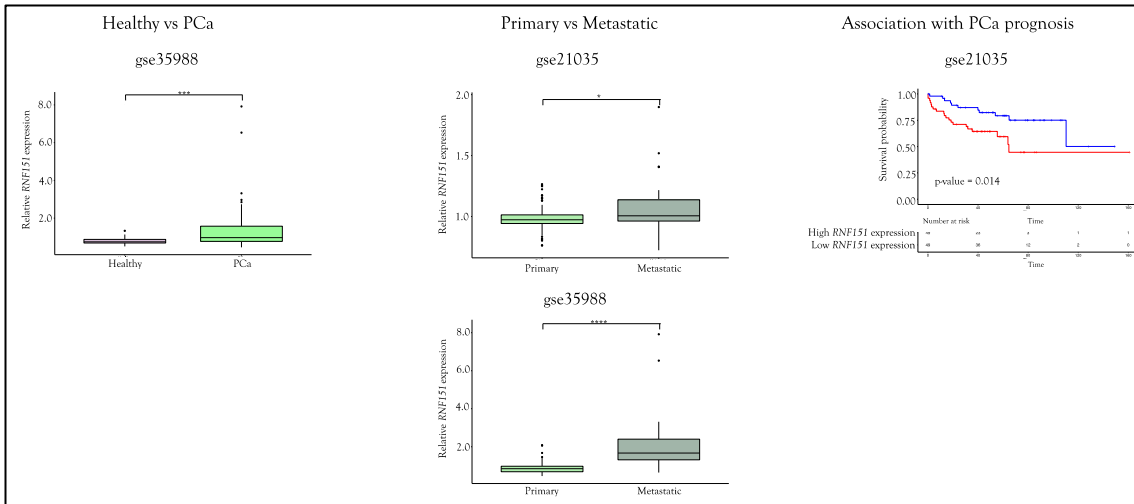
NUP205



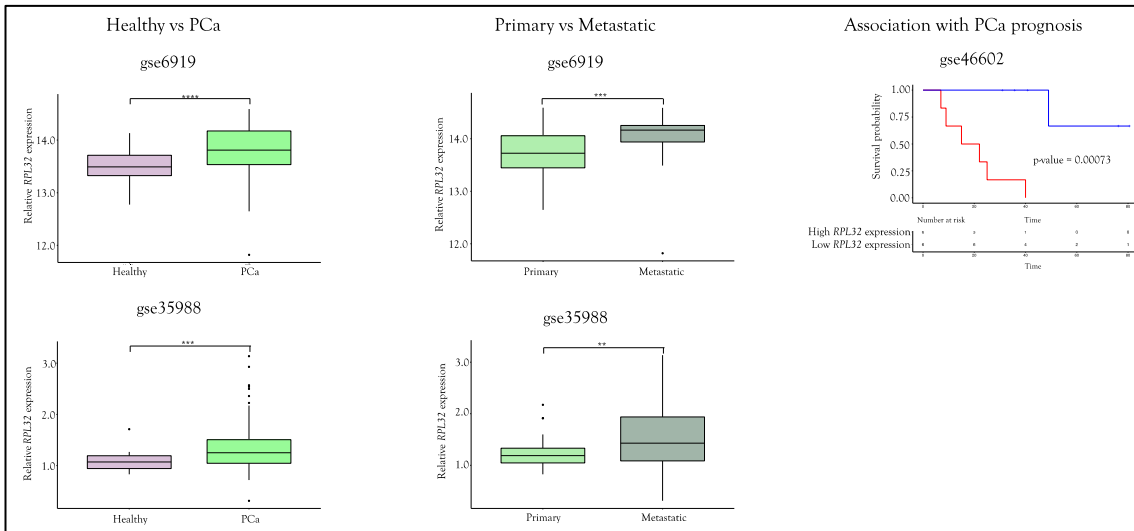
PRPF3



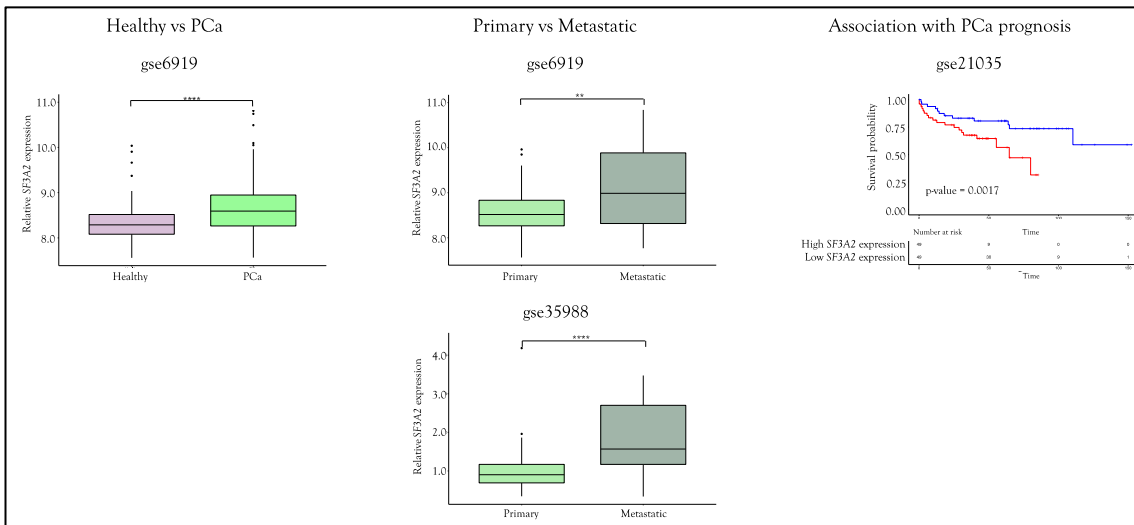
RNF151



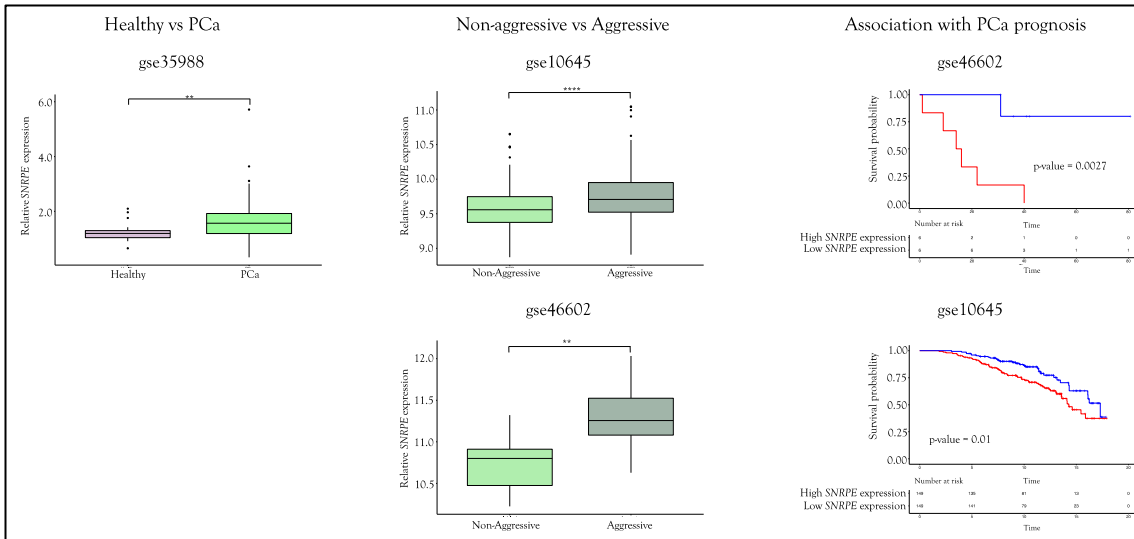
RPL32



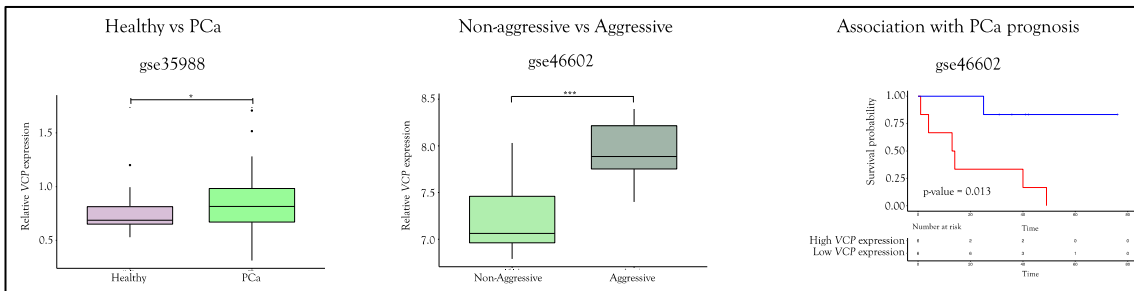
SF3A2



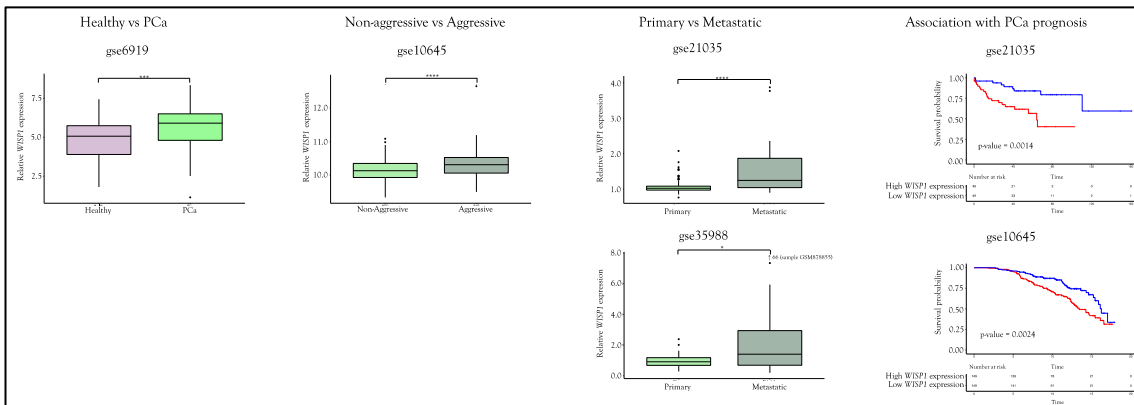
SNRPE



VCP



WISP1



IX. PUBLICATIONS

Review

Metabolomics Contributions to the Discovery of Prostate Cancer Biomarkers

Nuria Gómez-Cebrián ^{1,2,3}, Ayelén Rojas-Benedicto ^{1,2}, Arturo Albors-Vaquero ^{1,2}, José Antonio López-Guerrero ³, Antonio Pineda-Lucena ^{1,2} and Leonor Puchades-Carrasco ^{2,*}

¹ Drug Discovery Unit, Instituto de Investigación Sanitaria La Fe, Valencia 46026, Spain; ngomez@cipf.es (N.G.-C.); ayelen_rojas@iislafe.es (A.R.-B.); arturo_albors@iislafe.es (A.A.-V.); pineda_ant@gva.es (A.P.-L.)

² Joint Research Unit in Clinical Metabolomics, Centro de Investigación Príncipe Felipe/Instituto de Investigación Sanitaria La Fe, Valencia 46012, Spain

³ Laboratory of Molecular Biology, Fundación Instituto Valenciano de Oncología, Valencia 46009, Spain; jalopez@fivo.org

* Correspondence: leonor.puchadescarrasco@icr.ac.uk; Tel.: +34-96-124-6713

Received: 31 January 2019; Accepted: 4 March 2019; Published: 8 March 2019



Abstract: Prostate cancer (PCa) is one of the most frequently diagnosed cancers and a leading cause of death among men worldwide. Despite extensive efforts in biomarker discovery during the last years, currently used clinical biomarkers are still lacking enough specificity and sensitivity for PCa early detection, patient prognosis, and monitoring. Therefore, more precise biomarkers are required to improve the clinical management of PCa patients. In this context, metabolomics has shown to be a promising and powerful tool to identify novel PCa biomarkers in biofluids. Thus, changes in polyamines, tricarboxylic acid (TCA) cycle, amino acids, and fatty acids metabolism have been reported in different studies analyzing PCa patients' biofluids. The review provides an up-to-date summary of the main metabolic alterations that have been described in biofluid-based studies of PCa patients, as well as a discussion regarding their potential to improve clinical PCa diagnosis and prognosis. Furthermore, a summary of the most significant findings reported in these studies and the connections and interactions between the different metabolic changes described has also been included, aiming to better describe the specific metabolic signature associated to PCa.

Keywords: metabolomics; metabolism; prostate cancer; biomarker; early diagnosis; prognosis

1. Introduction

Prostate cancer (PCa) is the second most frequently diagnosed cancer and represents the fifth leading cause of death in men [1]. In 2018, new cases of PCa were estimated to account for over 1.3 million, and 359,000 PCa-associated deaths were expected worldwide [1]. PCa is a hormone-dependent tumor characterized by an extremely variable clinical course, ranging from an indolent condition to a rapid progression into an aggressive phenotype that disseminates and metastasizes to the lymph nodes and bones. Moreover, there is a current lack of reliable and reproducible assays to identify tumors destined to remain indolent. Thus, stratifying PCa patients into different risk phenotypes at time of diagnosis is still a major clinical challenge.

Nowadays, PCa screening tests rely on the determination of prostate-specific antigen (PSA) serum levels and digital rectal examination (DRE). Based on the results of these screening tests, trans-rectal ultrasound (TRUS)-guided prostate biopsy is performed to confirm diagnosis when necessary. However, these tests suffer from a number of limitations and do not provide enough information to enable a precise discrimination between indolent and aggressive tumors. While PSA

provides high sensitivity and low specificity for PCa diagnosis, (TRUS)-guided prostate biopsy has been associated with high false negative rates due to the high degree of PCa inter- and intra-heterogeneity [2]. Moreover, even the recently updated histopathology-based estimation of the Gleason Score (GS), the current clinical gold standard for assessing the risk of PCa metastasis and prognosis, exhibits limitations [3]. During the last years, many research studies have focused on the identification of molecular biomarkers that could help to improve early diagnosis and risk stratification of PCa patients [4–7]. Among them, a potential biomarker, that has been evaluated in combination with PSA levels, is the non-coding transcript PCA3 (overexpressed in >95% of PCa). The quantification of PCA3 levels in urine has shown improvement, when combined with PSA, in PCa detection [8], although no optimal cut-off for urinary PCA3 levels has been established for maximizing clinical benefit while avoiding overdiagnosis [9]. Another potential biomarker is the TMPRSS2:ERG fusion transcript [10], that is being evaluated as a potential diagnostic and therapeutic target associated with PCa invasion [11]. Despite being 100% indicative of PCa [12], it is only detected in 50% of PCa cases [13]. In summary, although intense efforts have been devoted to the discovery and development of new PCa biomarkers, there still exists an unmet clinical need to identify accurate PCa biomarkers for early diagnosis, prognosis and monitoring of PCa patients, both in terms of sensitivity and specificity [14,15].

Moreover, additional clinically robust biomarkers able to differentiate between indolent and aggressive PCa are urgently needed. In this context, several metabolomics studies have been carried out to attempt the characterization of a specific PCa metabolic profile, with the ultimate goal of identifying potential metabolic biomarkers that could improve the clinical management of PCa patients [16–19].

2. Cancer and Metabolic Reprogramming: Metabolomics Opportunities

The metabolic profile is closely associated with the pathophysiological condition of an individual. In particular, the metabolic composition can be strongly influenced, both from a qualitative and quantitative point of view, as a result of pathological processes or in the presence of specific drug treatments [20]. These changes can provide useful clues for the characterization of biomarkers associated with the onset and progression of diseases, as well as with the prediction of the response to therapeutic interventions.

Different studies, linking significant metabolic alterations and cancer onset and progression, have been extensively described since Warburg's pioneering studies [21]. The metabolic rewiring associated with the neoplastic processes is the result of mutations in specific oncogenes and tumor suppressors, leading to the activation of different signaling pathways and transcriptional networks [22]. Furthermore, it is well known that neoplastic processes have a strong influence on gene expression, cellular differentiation and tumor microenvironment [23,24]. Metabolites represent the end products of biochemical pathways, and the concentrations of these compounds are extremely sensitive to different alterations. At the molecular level, the progression of cancer involves multiple alterations in metabolic pathways that are specifically required for cancer cells to survive [23]. Interestingly, cancer cells exhibit different metabolic phenotypes [25,26]. Thus, some tumors preferentially use aerobic glycolysis to proliferate [27], while others rely on glutaminolysis [28], or one-carbon metabolism [29]. There are also tumors that benefit from the utilization of several of these metabolic routes at the same time [25,26,28].

In this context, metabolomics, that relies on the systematic analysis of low-molecular-weight metabolites present in biological samples, provides an accurate and complementary approach for getting a better understanding of the biochemical alterations responsible for the onset and progression of neoplastic processes, thus offering new opportunities for biomarker discovery in complex diseases [30]. Metabolomics studies offer a holistic view of the biochemical processes that could contribute to getting a deeper insight into the molecular alterations underlying pathological processes. This information could significantly improve the opportunities to identify clinically relevant biomarkers for the diagnosis and prognosis of different pathological processes, including PCa.

3. Metabolomics and PCa

The ultimate goal of metabolomics is to measure and identify as many metabolites as possible, ideally obtaining a complete overview of the metabolome. Metabolomics can provide an accurate description of the phenotype of an individual because it represents the final step of the omics cascade. The analysis of metabolic changes associated with specific biochemical pathways offers unprecedented opportunities for identifying the molecular mechanisms of complex diseases. Taken into consideration the limitations of current diagnostic procedures, this information could result in the characterization of specific and novel disease biomarkers [31].

At the analytical level, these studies are extremely challenging [32,33]. The complexity of the matrix to be examined (e.g., osmolarity, the presence of proteins, and inorganic salt concentration), the dynamic range of metabolites concentrations, and the vast chemical diversity of metabolite types (e.g., acidic, neutral, basic, lyophilic, and hydrophilic) greatly complicate the choice of analytical modality. However, a number of technical improvements have been introduced over the last few years. This has led to the development of a wide variety of analytical platforms that are currently used to characterize the metabolic content of biological samples [34–36]. The selection of the appropriate approach usually depends on the experimental objectives and the biological matrix. The detection of metabolites in cells, tissues or biofluids is usually carried out by either Nuclear Magnetic Resonance (NMR) spectroscopy or mass spectrometry (MS). In general, NMR spectroscopy, mostly ¹H-NMR, and MS, particularly liquid chromatography (LC)-MS, are the two most important analytical platforms used in metabolomics studies.

PCa is a disease of great interest from a metabolomics perspective. A number of studies, focused on the characterization of the specific PCa metabolic phenotype using different experimental approaches, have been reported recently [37–61]. These studies have shown that healthy prostate cells are characterized by a decreased citrate oxidation and metabolism within the tricarboxylic acid (TCA) cycle, resulting in citrate accumulation [62] and the reliance on glucose oxidation for energy production [63]. Benign prostate cells accumulate zinc, resulting in the inhibition of the m-aconitase (ACO), the enzyme that catalyzes the isomerization of citrate in the TCA cycle [62]. However, when prostate cells undergo malignant transformation, their characteristic ability to accumulate zinc is lost, leading to the TCA activation. Furthermore, it has been shown that early PCa does not exhibit the Warburg effect [64], relying on lipids and other energetic molecules for energy production, but not on aerobic respiration [65,66]. In this context, it should be noted that several metabolic alterations have also been identified in PCa tissue compared with normal tissue, including an increase of choline [67] and sarcosine [68], and a decrease of polyamine and citrate levels [69,70]. Nevertheless, the clinical relevance of some of these changes remains controversial due to the contradictory results reported in different studies (e.g., alterations in sarcosine levels—further discussed in the following section).

Overall, the possibility to directly evaluate the metabolic phenotype of PCa patients offers a great potential from a clinical perspective. To this end, many metabolomics projects, based on the analysis of different biological samples, have been conducted over the last few years with a focus on the discovery of new biomarkers that could improve the clinical management of PCa patients (Table 1).

4. PCa Metabolic Biomarkers in Biofluids

Changes in the concentration of metabolites in biofluids are reflective of alterations in the physiological status of an individual. The metabolome, that is, the set of all metabolites present on a particular biological sample, represents the downstream end product of the omics cascade, and a closer approach to the phenotype. Therefore, metabolite signatures obtained from biofluids can be a useful approach for identifying non-invasive biomarkers and characterizing the molecular mechanisms associated with pathological conditions. The most widely used biofluids in PCa studies have been urine, serum and seminal fluid.

4.1. Urine Biomarkers

Urine samples offer some advantages for carrying out metabolomics studies since they can be collected non-invasively and have a less complex composition compared with other biofluids, thus facilitating the discovery of novel biomarkers [71]. However, the analysis of this biofluid has several limitations, including the presence of diluted urinary constituents and interferences between molecules [37,71], that can result in failing to detect underrepresented metabolites or to correctly identify the molecules. Despite these problems, different studies have discovered metabolic alterations in urine samples from PCa patients and evaluated their clinical utility as biomarkers for this neoplastic process.

Urine is anatomically close to the prostate, which explains why it has been extensively studied for metabolic biomarker discovery in PCa [37]. As shown in Table 1, most of these studies have aimed to identify metabolic dysregulations that could provide clinically relevant PCa biomarkers. Most of these studies focused on the characterization of the metabolic differences between urine samples from healthy individuals [38–43] or benign prostate hyperplasia (BPH) patients [37,44,45] and PCa patients. In general, they were performed using mass spectrometry (MS)-based metabolomics as an analytical platform ($n = 8$), and only one study was performed using NMR spectroscopy for the analysis of urine samples [44].

The study conducted by Liang et al., including the analysis of 233 healthy individuals and 236 PCa patients, highlighted the clinical utility of three metabolites: 5-hydroxy-L-tryptophan, hippurate, and glycocholic acid, as potential metabolic biomarkers for the early diagnosis of PCa (area under the curve, (AUC) > 0.95) [38]. A metabolite called 5-hydroxy-L-tryptophan is involved in tryptophan metabolism, a pathway that has been associated with the ability of several tumors to evade the antitumor immune response [72,73]. Another metabolite involved in this pathway, kynurenic acid, also exhibited a moderate diagnostic value (AUC = 0.62) in a study conducted by Gkotsos et al. for the detection of PCa using urine samples obtained after prostatic massage [39].

Another metabolite that has been extensively investigated as a potential biomarker of PCa is sarcosine. Sarcosine is an intermediate product in the synthesis and degradation of glycine. In 2009, Sreekumar et al. identified sarcosine as a promising PCa biomarker, being highly correlated with PCa progression and more detectable in the urine of PCa patients when compared with healthy individuals [68]. Similarly, Khan et al. reported in 2013 markedly elevated sarcosine levels in the urine sediments of PCa patients compared with controls [74]. In serum, Kumar et al. [46,47] also found increased sarcosine levels in PCa samples compared with healthy individuals. In these studies, it was shown that sarcosine, in combination with other metabolites, could accurately differentiate PCa patients from healthy individuals (accuracy = 90.2%) [47] and PCa from BPH patients (87.7% sensitivity and 85.5% specificity) [46]. Furthermore, the authors showed that metabolomics provided better predictions than serum PSA levels for the discrimination between PCa patients and healthy individuals as well as between PCa and BPH patients. However, the role of sarcosine as a metabolic biomarker for PCa diagnosis and prognosis remains controversial due to the contradictory results reported in further studies. In a case-control study conducted by Ankerst et al., the use of sarcosine as a biomarker for early PCa detection was investigated in serum samples of matched-age controls and PCa patients [75]. These authors reported no differences in sarcosine levels when comparing both groups. Furthermore, in another pilot study by Dereziński et al., where higher serum sarcosine levels were found in PCa patients when compared with the control group, no statistically significant differences were observed in urine samples [76]. Similarly, Pérez-Rambla et al. found elevated sarcosine levels in PCa patients when compared with BPH patients, although these alterations were not found to be statistically significant [44].

Beyond the alteration in sarcosine levels, Pérez-Rambla et al. also identified alterations in the urine levels of six metabolites that facilitated the discrimination of the metabolomic profile of PCa and BPH patients [44]. Among the characteristic changes, PCa patients showed decreased concentration of glycine, a metabolite involved in one-carbon metabolism and associated with cell transformation

and tumorigenesis [77]. Interestingly, Struck-Lewicka et al. reported lower levels of this metabolite in urine samples from PCa patients when compared with a control group [40]. The overall results of this study showed alterations in the urine levels of metabolites associated with TCA cycle, purine, glucose, amino acid and urea metabolism in PCa patients. These findings are in agreement with those obtained by Fernández-Peralbo et al., where variations in the levels of 28 metabolites involved in amino acid, purine and pyrimidine, and tryptophan metabolism were also identified [41] when comparing PCa patients and healthy individuals. The results of this study led to a predictive model of high quality for the discrimination of these two groups (sensitivity = 88.4% sensitivity, specificity = 92.9%).

Metabolic changes have also been identified when comparing urine samples from low and high risk PCa patients. Heger et al. performed a study focused on the characterization of differences in protein expression levels between two different risk groups of PCa patients after radical prostatectomy (RP) [48]. The two experimental cohorts were divided based on the presence of positive ($n = 15$) or negative ($n = 15$) surgical margins. The analysis led to the identification of three proteins with different expression levels. Among them, the glycolytic enzyme lactate dehydrogenase C (LDHC), that plays a key role in metabolism, was detected at higher expression levels in PCa patients with positive surgical margins [48]. Beyond PCa, increased LDHC expression has also been observed in melanoma, lung and breast cancer [78]. Moreover, this enzyme has been shown to be involved in tumor invasion and migration in breast cancer [79].

A complementary approach, that has also been the focus of recent studies in the context of urinary alterations associated with PCa, is the analysis of extracellular vesicles (EV). The analysis of these particles still requires the optimization of methods for isolation and storage of urinary EV, as well as for the normalization of metabolite levels [80]. Nevertheless, in a preliminary study, Puhka et al. analyzed urine EV samples from three controls and three PCa patients, obtained before and after prostatectomy [42]. After normalization tests, decreased levels of glucuronate, D-ribose 5-phosphate and isobutyryl-L-carnitine were observed in pre-prostatectomy samples when compared with the healthy individuals and post-prostatectomy samples. In agreement with these results, Clos-García et al. also reported variations in carnitine-related metabolites when comparing urine EV samples from PCa ($n = 31$) and BPH ($n = 14$) patients [37]. In this study, changes in the expression levels of seven enzymes related to fatty acid, steroid biosynthesis, creatine, and cAMP metabolism were also observed [37]. Increased levels of another enzyme involved in fatty acid metabolism (fatty acid binding protein 5, FABP5) were also found in urinary EVs from PCa patients collected after prostatic massage [43]. In this study, the AUC for the prediction of PCa with GS ≥ 6 based on FABP5 was 0.757 (confidence interval 0.570–0.994, p -value = 0.027), whereas the AUC value for the prediction based on serum PSA was 0.593 (confidence interval 0.372–0.815, p -value = 0.42). FABP5 is an enzyme involved in the uptake and transport of fatty acids, that has been previously found to be overexpressed in PCa tissues [81]. Increased levels of this enzyme have been described in serum and tissue samples from PCa patients with lymph node metastasis [82].

Overall, these studies show that the urine metabolic phenotype of PCa patients is significantly different from that of healthy individuals and BPH patients. Taken together, alterations in the levels of metabolites involved in TCA cycle, tryptophan, amino acid, fatty acid, nucleotide, and carbon metabolism have been reported. In general, a significant limitation of these studies has been the sample size, except for the study carried out by Liang et al. where a total of 469 urine samples were analyzed [38]. Therefore, further analyses and validation studies will be necessary to assess the clinical utility of these findings.

4.2. Serum Biomarkers

Metabolic dysregulations in TCA cycle, fatty acid, amino acid, purine, histidine, creatine, glycine, and serine, and threonine metabolism have been described when analyzing serum metabolic profile of PCa patients. Particularly, a study conducted by Giskeødegård et al., comparing the serum metabolic profile of 21 BPH and 29 PCa patients, revealed significant changes in fatty acid, choline and amino

acid metabolism [49]. In this study, different metabolomics analytical platforms were used to perform the analysis. The combination of the most relevant metabolites identified using the different platforms provided the best classification results, enabling the discrimination of PCa patients and BPH controls with a sensitivity and specificity of 81.5% and 75.2%, respectively. In a different study, Kumar et al. reported a metabolic signature of three metabolites (pyruvate, glycine, and sarcosine) that classified 90.2% of PCa samples ($n = 70$) with 84.8% sensitivity and 92.9% specificity compared with healthy controls ($n = 32$) [47]. Furthermore, Kumar et al., using filtered serum samples ($n = 210$), obtained a model based on five metabolites (alanine, sarcosine, creatinine, glycine, and citrate) that enabled the discrimination of BPH and PCa patients with high accuracy (88.3%) [46]. Finally, Zhao et al., analyzing the metabolic profile of plasma samples from 32 control cases and 32 PCa patients, reported alterations in different metabolic pathways, including amino acid, propanoate, butanoate, and nucleotide metabolism [50]. After evaluation of the predictive value of individual changes, a predictive model combining sarcosine, acetylglycine, and coreximine was reported. However, although a discrete increase in the diagnostic performance (AUC = 0.941; confidence interval 0.812–1) was found when compared with PSA levels (AUC = 0.926; confidence interval 0.851–0.978), this model partially relied on changes in the levels of coreximine, a compound belonging to a family of alkaloids and derivatives, probably from exogenous origin.

Regarding PCa biomarkers associated with disease progression and outcome, different studies, focused on the analysis of PCa serum samples, have been performed trying to identify metabolic alterations that could be useful from this clinical perspective [47,51]. These studies revealed alterations in TCA cycle, lipids, and amino acids metabolism. Lin et al. investigated the correlation between the plasma lipidome and the outcome of 96 castration-resistant PCa (CRPC) patients [51]. A three-lipid signature, comprising ceramide d18:1/24:1, sphingomyelin d18:2/16:0 and phosphatidylcholine 16:0/16:0, was found to be associated with poor prognosis in this study and further validated in an independent cohort of 63 CRPC patients. The results also revealed an association between the lipid signature in the serum of the patients and the overall survival time. Eleven out of the 63 patients of the validation cohort exhibited the three-lipid signature, and their median overall survival time was significantly shorter than those not displaying that signature (11.3 vs. 21.4 months). In another study performed in serum samples, Kumar et al. described a model consisting of three metabolites (alanine, pyruvate and glycine) that allowed the discrimination of low- ($n = 40$) from high-grade ($n = 30$) PCa serum samples with 92.5% sensitivity and 93.3% specificity [47]. Alanine and glycine can be metabolized to a common end product, pyruvate. Increased levels of these two metabolites have also been observed in urine [83] and tissue [84] from PCa patients. Tissue levels of both metabolites have also shown a statistically significant correlation with the GS [85]. Finally, in a study performed by Mondul et al., 200 matched-controls and 200 PCa patients (100 aggressive) were analyzed [52]. The authors reported inverse associations between the risk of aggressive PCa and the levels of glycerophospholipids and fatty acids, inositol-1-phosphate showing the strongest inverse association. On the contrary, aggressive PCa risk was correlated with the levels of α -ketoglutarate, thyroxine, TMAO, and erucoyl-sphingomyelin, while metabolites involved in the metabolism of nucleotides, steroid hormones and tobacco were associated with non-aggressive PCa [52]. In this particular study, although levels of two known nicotine-derived metabolites (cotinine and hydroxycotinine) were found to be associated with non-aggressive PCa, the authors argued that it was unlikely that these changes were related to tobacco smoking as all individuals included in the study were smokers at the time of sample collection. Furthermore, results remained unchanged when adjusting for cigarettes smoked per day, suggesting that cigarette smoking did not strongly influence the results.

Additionally, some of the most recent PCa metabolomics studies based on the analysis of serum samples have aimed to identify metabolic alterations that could provide insights into the risk of developing PCa. These studies were carried out with a significant number of samples in each experimental cohort compared with those focused on the identification of biomarkers for PCa diagnosis and/or prognosis. Thus, Kühn et al. evaluated the association between the levels of pre-diagnostic

metabolites and the risk of developing different cancers, including PCa [53]. Serum samples of 310 PCa patients with a median follow-up of 6.83 years were included in the study. High levels of lysophosphatidylcholines were found to be positively correlated to lower PCa risk, while high levels of phosphatidylcholines were associated with increased risk of developing the disease [53]. Schmidt et al. analyzed 1077 healthy and PCa serum samples to assess the risk of developing PCa [54]. In this study, higher citrulline levels were associated with a 27% decreased risk of PCa in the first five years of follow-up but not after longer periods of time [54]. The authors also reported inverse associations between 12 glycerophospholipids and advanced stage disease. In another study, Huang et al. analyzed serum samples from controls ($n = 200$) and PCa patients classified according to their tumor stage (T2: $n = 71$, T3: $n = 51$, T4: $n = 15$), and identified metabolites associated with the risk of being diagnosed with each stage [55]. Histidine and uridine-related metabolites were associated with risk of T2 stage. Glycerophospholipids and primary bile acid lipids showed inverse correlations with T3 stage, while sphingomyelins were positively associated with risk of T3. Secondary bile acid, sex steroids, histamine, and BCAA were associated with T4 risk, while citrate and fumarate were inversely correlated. Finally, a recent study carried out by Andras et al. used serum samples to identify variations in the metabolite levels that could be useful for predicting PCa before biopsy [56]. These authors analyzed 90 samples from patients with suspicion of PCa and derived a predictive score based on six metabolites, that was validated using a subgroup of patients. A cut-off value of 0.528 for the derived score showed good accuracy for PCa prediction before biopsy (AUC = 0.779; confidence interval 0.625–0.876), although not statistically significantly higher than the predictive ability of PSA levels (AUC = 0.793; confidence interval 0.665–0.889). In PCa patients with PSA levels < 10 ng/mL, this score had 80.95% sensitivity and 64.52% specificity for PCa detection at biopsy.

4.3. Seminal Fluid Biomarkers

Seminal fluid has a number of advantages over blood and urine in terms of its potential as a source of PCa specific biomarkers. Prostatic constituents are highly enriched in seminal fluid compared with other biofluids. In the last few years, several metabolomics studies have been performed aiming to analyze the metabolic profile of seminal fluid samples from either healthy individuals [57–59] or BPH patients [60] and PCa patients to discover metabolic alterations that could be useful for discriminating between both groups. In general, these studies were performed using NMR spectroscopy ($n = 4$) and the sample size of the different cohorts was relatively small. Most of the metabolic alterations identified included changes in the TCA cycle, amino acid, and lipid metabolism. In a preliminary study, Aversa et al. found decreased concentrations of citrate in PCa ($n = 3$) compared to BPH ($n = 1$) samples [60]. Similarly, Kline et al. also observed lower citrate levels in PCa samples both when analyzing seminal fluid samples and expressed prostatic secretions (EPS) from 33 healthy volunteers and 28 PCa patients [57]. In this study, authors reported good values for predicting PCa in patients (AUC = 0.81 in seminal fluid, confidence interval 0.60–0.92 and AUC = 0.73 in EPS, confidence interval 0.38–0.90), outperforming the predictive ability of PSA (AUC = 0.61, confidence interval 0.44–0.74) in these samples. Furthermore, using an ELISA assay, Etheridge et al. identified alpha methylacyl A coenzyme racemase (AMACR) as a promising biomarker for PCa diagnosis [58]. Higher levels of this enzyme were detected in seminal fluid samples of PCa patients ($n = 28$) compared with age-matched controls ($n = 15$). AMACR, a key regulator of lipid metabolism, is involved in the peroxisomal and mitochondrial β -oxidation of branched-chain fatty acids. This enzyme had been previously described as an immunohistological marker for PCa diagnosis [86,87], associated with poor prognosis in patients with localized PCa [88] and found to be overexpressed in PCa tissues [89]. Interestingly, AMACR has also been identified as a promising prognostic indicator in other cancer types, including gastric cancer [90] and hepatocellular [91] and nasopharyngeal [92] carcinomas.

Besides seminal fluid, EPS is another biofluid enriched in prostatic material that has shown potential utility for the identification of new PCa disease-specific biomarkers. EPS is obtained in the first void following vigorous DRE or prostatic massage. Given the nature of this biofluid, metabolites

present in EPS are usually found at lower concentrations than in seminal fluid, thus requiring the use of highly sensitive detection methods. In 2008, Serkova et al. analyzed EPS samples from 26 healthy volunteers and 52 PCa patients aiming to identify potential metabolites that could contribute to PCa risk assessment [59]. This study revealed that concentrations of citrate, myo-inositol, and spermine were inversely correlated with PCa risk (AUC values of 0.89, 0.87 and 0.79, respectively). However, in a more recent study attempting to validate the role of these metabolites as biomarkers for assessing PCa risk, Roberts et al. found that citrate, spermine, and myo-inositol had minimal predictive ability when analyzing seminal fluid samples [61]. Therefore, further studies using larger cohorts will be required to confirm the utility of seminal fluid and EPS derived biomarkers for PCa diagnosis and prognosis.

Table 1. Metabolomics studies focused on the analysis of biofluids to identify clinically relevant prostate cancer (PCa) biomarkers.

Article	Sample	Experimental Approach	Research Aim	Sample Cohort	Main Findings	Validation Cohort
Clos-Garcia et al., 2018 [37]	Urine EVs	UHPLC-MS	Diagnosis	31 × PCa; 14 × BPH	Statistically significant changes in 76 metabolites and 7 enzymes related to urea cycle, TCA cycle, and metabolism of steroid hormone biosynthesis, leukotriene, and prostaglandin, linoleate and purine, glycerophospholipid and tryptophan	No
Liang et al., 2017 [38]	Urine	FPLC-MS/MS	Diagnosis	236 × PCa; 233 × HV	↑ glycocholic acid; hippurate; chenodeoxycholic acid: PCa > HV ↓ taurocholic acid; 5-hydroxy-L-tryptophan: PCa < HV	No
Gkotsos et al., 2017 [39]	Urine	UPLC-MS/MS	Diagnosis	52 × PCa, 49 × HV	↓ kynurenic acid: PCa < HV	No
Struck-Lewicka et al., 2015 [40]	Urine	HPLC-TOF-MS; GC-QqQ-MS	Diagnosis	32 × PCa; 32 × HV	Statistically significant changes in 82 metabolites related to amino acid, organic acids, sphingolipids, fatty acids, and carbohydrates metabolism	No
Fernández-Peralbo et al., 2016 [41]	Urine	LC-QTOF-MS/MS	Diagnosis	43 × PCa; 29 × HV	↑ 7-methylguanaine: PCa > HV ↓ Statistically significant changes in 27 metabolites related to amino acid metabolism: PCa < HV	19 × PCa; 13 × HV
Puhka et al., 2017 [42]	Urine EVs; Plasma EVs	UPLC-MS/MS	Diagnosis	3 × PCa pre-prostatectomy; 3 × PCa post-prostatectomy; 3 × HV	↓ glucoronate; isobutyryl-L-carnitine; D-Ribose-5-phosphate: pre- < post-prostatectomy and HV	No
Fujita et al., 2017 [43]	Urine EVs	iTRAQ; LC-MS/MS	Diagnosis and prognosis	12 × PCa (6 × HG PCa; 6 × LG PCa); 6 × HV	↑ FABP5: PCa > HV ↑ FABP5; GRN; AMBP; CHMP4A; CHMP4C associated with higher GS	18 × PCa (6 × HG; 12 × LG); 11 × HV
Perez-Rambla et al., 2017 [44]	Urine	¹ H-NMR	Diagnosis	64 × PCa; 51 × BPH	↑ BCAAs; glutamate; pseudouridine: PCa > BPH ↓ glycine; dimethylglycine; fumarate; 4-imidazole-acetate: PCa < BPH	No
Davalieva et al., 2015 [45]	Urine	2D-DIGE-MS	Diagnosis	8 × PCa; 16 × BPH	↑ AMBP: PCa > BPH ↓ HP: PCa < BPH	16 × PCa; 16 × BPH
Heger et al., 2015 [46]	Urine	2D-DIGE; MALDI-TOF-MS	Diagnosis	15 × HG PCa; 15 × LG PCa	↑ CDK6; M2BP; LDHC: HG PCa > LG PCa	No
Kumar et al., 2016 [46]	Serum	¹ H-NMR	Diagnosis	75 × PCa; 70 × BPH; 65 × HV	↑ alanine; sarcosine; creatine; creatinine: PCa > BPH and HV ↑ pyruvate; 3-methylhistidine; xanthine; hypoxanthine: BPH and PCa > HV ↓ glycine: PCa < HV ↓ citrate: PCa < BPH and HV	No

Table 1. Contd.

Article	Sample	Experimental Approach	Research Aim	Sample Cohort	Main Findings	Validation Cohort
Kumar et al., 2015 [47]	Serum	¹ H-NMR	Diagnosis and prognosis	21 × HG PCa; 28 × LG PCa; 22 × HV	↑ alanine; sarcosine; LG PCa > HG PCa and HV ↑ pyruvate; LG PCa and HG PCa > HV ↓ glycine; LG PCa and HG PCa < HV	9 × HG PCa; 12 × LG PCa; 12 × HV
Giskeoedgård et al., 2015 [49]	Plasma/Serum	¹ H-NMR; UPLC-MS/MS; GC-MS	Diagnosis	29 × PCa; 21 × BPH	↑ decanoyl carnitine (c10); tetradecenoyl carnitine (c14:1); octanoyl carnitine (c8); dimethylsulfone; phenylalanine; lysine; PCa > BPH ↓ phosphatidylcholine diacyl (c34:4); lipid -(CH2) _n -CH2-CH2-CO: PCa < BPH	No
Zhao et al., 2017 [50]	Plasma	UPLC-MS/MS	Diagnosis	32 × PCa; 32 × HV	Statistically significant changes in 19 metabolites related to amino acid, nucleotide, butanoate and propionate metabolism	No
Lin et al., 2017 [51]	Plasma	LC-MS/MS	Prognosis	96 × CRPC	↑ ceramide d18:1/24:1; sphingomyelin d18:2/16:0; phosphatidylcholine 16:0/16:0 correlated with shorter overall survival	63 × CRPC
Mondul et al., 2015 [52]	Serum	UHPLC-MS; GC-MS	PCa risk Prognosis	100 × HG PCa; 100 × LG PCa; 200 × HV	Statistically significant changes in 22 metabolites related to lipid and amino acid metabolism associated with overall PCa risk Statistically significant changes in 14 metabolites related to TCA cycle and lipid metabolism associated with HG PCa Statistically significant changes in 34 metabolites related to lipid, amino acid and nucleotide metabolism associated with LG PCa	No
Kühn et al., 2016 [53]	Plasma	LC-MS/MS; FIA-MS/MS	PCa risk	310 × PCa; 774 × HV	↑ Phosphatidylcholine (PC) associated with higher risk of PCa ↑ lysoPC associated with lower risk of PCa	No
Schmidt et al., 2017 [54]	Plasma	QqQ-MS	PCa risk Prognosis	1077 × PCa; 1077 × HV 208 × advanced PCa; 456 × localized PCa	Statistically significant changes in 14 metabolites related to lipid and amino acid metabolism associated with overall PCa risk 12 glycerophospholipids inversely associated with risk of advanced PCa	No No

Table 1. Cont.

Article	Sample	Experimental Approach	Research Aim	Sample Cohort	Main Findings	Validation Cohort
Huang et al., 2017 [55]	Serum	UHPLC-MS; GC-MS	PCa risk	71 × PCa T2 stage; 51 × PCa T3 stage; 15 × PCa T4 stage; 200 × HV	Statistically significant changes in 8 metabolites related to histidine and uridine metabolism associated with PCa T2 risk. Statistically significant changes in 12 metabolites related to fatty acid and primary bile acid metabolism associated with PCa T3 risk Statistically significant changes in 16 metabolites related to TCA, BCAA secondary bile acid, sex steroids and histamine metabolism associated with PCa T4 risk.	No
Andras et al., 2017 [56]	Serum	HPLC-ESI-QTOF-MS	Prediction	59 × patients with high PSA levels	6 metabolites involved in lipid, purine and tryptophan metabolism predictive for prostate biopsy outcome	31 × patients with high PSA levels
Kline et al., 2006 [57]	Seminal fluid; Prostatic secretion	¹ H-NMR	Diagnosis	28 × PCa; 33 × HV	↓ citrate: PCa < HV	No
Etheridge et al., 2018 [58]	Seminal fluid	ELISA	Diagnosis	28 × PCa; 15 × HV	↑ AMACR: PCa > HV	No
Serkova et al., 2008 [59]	Prostatic secretion	¹ H-NMR	Prediction PCa risk	52 × PCa; 26 × HV	↓ citrate; myo-inositol; spermine shown highly predictive of PCa and inversely associated with PCa risk	No
Averna et al., 2005 [60]	Seminal fluid	¹ H-NMR	Diagnosis	3 × PCa; 1 × BPH; 4 × HV	↓ citrate: PCa < BPH	No
Roberts et al., 2017 [61]	Seminal fluid	¹ H-NMR	Prediction	98 × PCa; 53 × HV	Statistically significant changes in choline, valine and leucine.	No

¹H-NMR: Proton nuclear magnetic resonance spectroscopy; 2D-DIGE-MS: Two dimensional-difference gel electrophoresis-mass spectrometry; BCAA: Branched-chain amino acids; BPH: Benign Prostatic Hyperplasia; CRPC: Metastatic castration-resistant prostate cancer; ELISA: Enzyme-linked immunosorbent assay; EV: Extracellular vesicles; FIA-MS/MS: Flow injection analysis-tandem mass spectrometry; FPLC-MS: Fast ultra-high performance liquid chromatography-mass spectrometry; GC-MS: Gas chromatography-mass spectrometry; GC-QqQ-MS: Gas chromatography-triple quadrupole-mass spectrometry; HG: High-grade (GS ≥ 8); HPLC-ESI-QTOF-MS: High performance liquid chromatography-electrospray ionization-quadrupole time of flight-mass spectrometry; HPLC-TOF-MS: High performance liquid chromatography-time of flight-mass spectrometry; HV: Healthy Volunteers; iTRAQ: Isobaric tag for relative and absolute quantification; LC-MS: Liquid chromatography-mass spectrometry; LC-MS/MS: Liquid chromatography-tandem mass spectrometry; LG: Low-grade (GS ≤ 7); MALDI-TOF-MS: Matrix-assisted laser desorption ionization-time of flight-mass spectrometry; PCa: Prostate Cancer; PM: Prostatic massage; QqQ-MS: Triple quadrupole-mass spectrometry; T: Stage; TCA: Tricarboxylic acid; UHPLC-MS: Ultra high performance liquid chromatography-mass spectrometry; UPLC-MS/MS: Ultra performance liquid chromatography-tandem mass spectrometry.

5. Conclusions and Future Perspectives

The identification and characterization of the metabolic changes accompanying the transformation of benign into malignant prostate cells has led to an increased interest, over the last few years, in the application of metabolomics for identifying clinically relevant biomarkers in this field. Omics approaches, including genomics, proteomics, transcriptomics, and metabolomics, are highly innovative areas of research. One of the major advantages of the omics approaches is their ability to provide information using unbiased large-scale approaches. Among them, metabolomics provides an unprecedented opportunity for understanding the pathophysiological condition of an individual. Metabolites represent the end products of biochemical pathways, and the concentrations of these compounds are extremely sensitive to different alterations. Thus, these metabolic fingerprints can provide useful clues for the characterization of biomarkers associated with the onset and progression of diseases. Furthermore, as metabolomics studies can be performed using biological fluids that could be easily accessible (e.g., serum, plasma, urine, and seminal fluid), it offers a high potential for clinical translatability when compared with other omics approaches.

In this manuscript, we aimed to review the main findings described in recent PCa metabolomics studies focused on the analysis of different biofluids (Table 1). Furthermore, a summary of the most significant findings reported in these studies and the connections and interactions between the different metabolic changes described has also been included, aiming to better describe the specific metabolic signature associated to PCa (Figure 1).

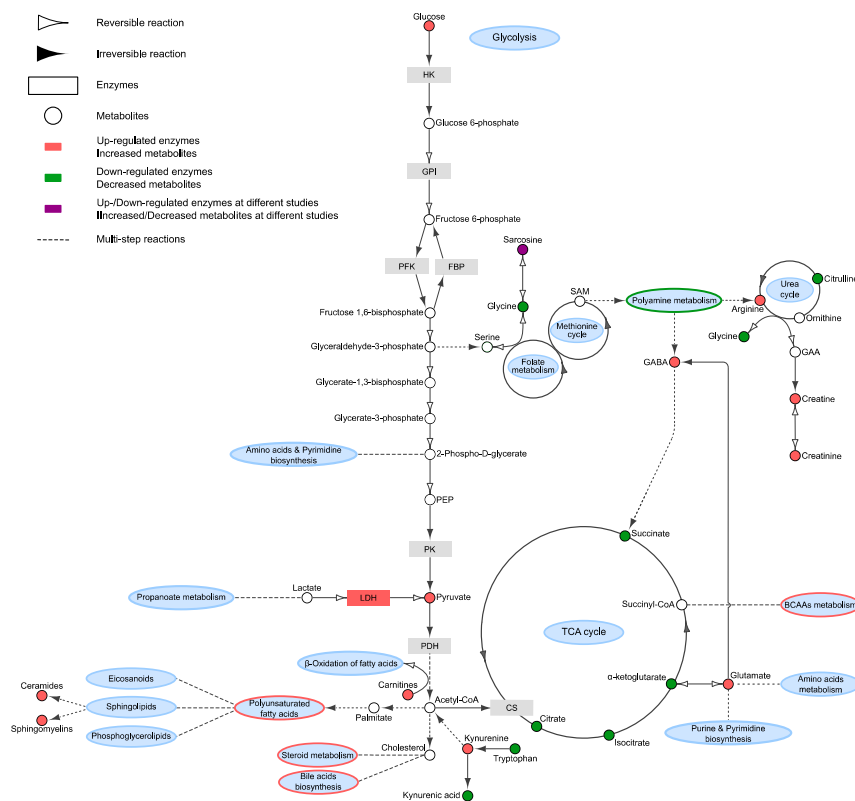


Figure 1. Overview of main metabolic changes described in metabolic-related studies of human biofluids applied to PCa biomarker discovery. BCAA: Branched-chain amino acids; CS: Citrate synthase; FBP1: Fructose-bisphosphatase; GAA: Guanidinoacetate; GABA: Gamma-aminobutyric acid; GPI: Glucose-6-phosphate isomerase; HK2: Hexokinase 2; LDH: Lactate dehydrogenase; PDH: Pyruvate dehydrogenase; PEP: Phosphoenolpyruvate; PFK: Phosphofructokinase; PK: Pyruvate kinase; SAM: S-Adenosyl methionine.

Most of the studies included in this review were based on the analysis of blood or urine samples, probably due to their easy accessibility and non-invasiveness. NMR and MS are the two most commonly used analytical platforms in these studies, though other analytical techniques have also been applied to the identification of PCa-related metabolic changes [58,93–95]. Although a significant number of studies focused on the identification of biomarkers for PCa diagnosis, some of them also explored the potential of metabolic biomarkers for patient prognosis and PCa risk evaluation.

Overall, these studies have revealed that alterations in TCA cycle, polyamines, glycolysis, one-carbon metabolism, nucleotide synthesis, amino acid, fatty acid, and lipid metabolism are associated with PCa onset and progression. Figure 1 illustrates the main alterations, in terms of metabolic pathways and metabolites, associated with PCa based on current literature.

The results of the different studies provide compelling evidence of the potential of metabolomics strategies for identifying new PCa biomarkers in biofluids that could be of interest from a clinical perspective. The potential of this approach for routine clinical diagnostics is significant since only minimal biological preparation is necessary. Despite the advances achieved in the field of PCa biomarker discovery, intense efforts are still required before metabolite profiling can be implemented in the clinic. So far, the variability in the metabolic alterations reported precludes consistent, universal signatures to be established, showing that a long path is still to be thread toward the full validation and clinical approval of putative new metabolic biomarkers. In this context, it is worth noting that although most of the reviewed studies included the internal validation of the statistical models developed during the study, either for PCa diagnosis or prognosis, a limited number of them included the assessment of the clinical utility of these findings using an external validation cohort of patients. Thus, future studies should include larger sample cohorts from adequately defined and matched groups of samples. In addition, statistical validation of multivariate models would benefit from full external validation. Finally, increased knowledge on the biological significance of potential PCa biomarkers should be assessed through the integration of metabolomics with other biochemical/biological approaches.

Author Contributions: Conceptualization, N.G.-C., A.P.-L. and L.P.-C.; Writing—Original Draft Preparation, N.G.-C. with input from L.P.-C.; Writing—Figure 1, A.R.-B.; Writing—Table 1, A.A.-V.; Clinical aspects and interpretation of literature data, J.A.L.-G.; Writing—Review and Editing, A.P.-L. and L.P.-C. All authors critically commented on and approved the final submitted version of the paper.

Funding: This research was funded by the Ministerio de Economía y Competitividad grant number [SAF2017-89229-R] and the Conselleria de Educació, Investigació, Cultura y Deporte grant number [GVA, PROMETEO/2016/103].

Conflicts of Interest: The authors declare no conflict of interest.

Abbreviations

The following abbreviations are used in this manuscript:

¹ H-NMR	Proton nuclear magnetic resonance spectroscopy
2D-DIGE-MS	Two dimensional–difference gel electrophoresis–mass spectrometry
AUC	Area under the curve
BCAA	Branched-chain amino acids
BPH	Benign prostatic hyperplasia
CRPC	Castration-resistant prostate cancer
CS	Citrate synthase
DRE	Digital rectal examination
ELISA	Enzyme-linked immunosorbent assay
EPS	Expressed prostatic secretions
EV	Extracellular vesicles

¹ H-NMR	Proton nuclear magnetic resonance spectroscopy
FBP	Fructose-bisphosphatase
FIA-MS/MS	Flow injection analysis–tandem mass spectrometry
FPLC-MS	Fast ultra-high-performance liquid chromatography–mass spectrometry
GAA	Guanidinoacetate
GABA	Gamma-aminobutyric acid
GPI	Glucose-6-phosphate isomerase
GS	Gleason Score
GC-MS	Gas chromatography–mass spectrometry
GC-QqQ-MS	Gas chromatography–triple quadrupole–mass spectrometry
HG	High-grade (GS ≥ 8)
HK2	Hexokinase 2
HPLC-ESI-QTOF-MS	High performance liquid chromatography–electrospray ionization–quadrupole time of flight–mass spectrometry
HPLC-TOF-MS	High performance liquid chromatography–time of flight–mass spectrometry
HV	Healthy Volunteers
iTRAQ	Isobaric tag for relative and absolute quantification
LC-MS	Liquid chromatography–mass spectrometry
LC-MS/MS	Liquid chromatography–tandem mass spectrometry
LDH	Lactate dehydrogenase
LG	Low-grade (GS ≤ 7)
MALDI-TOF-MS	Matrix-assisted laser desorption ionization–time of flight–mass spectrometry
MS	Mass spectroscopy
NMR	Nuclear magnetic resonance
QqQ-MS:	Triple quadrupole–mass spectrometry
PCa	Prostate cancer
PDH	Pyruvate dehydrogenase
PEP	Phosphoenolpyruvate
PFK	Phosphofructokinase
PK	Pyruvate kinase
PM	Prostatic massage
PSA	Prostate specific antigen
SAM	S-Adenosyl methionine
T	Stage
TCA	Tricarboxylic acid
TMAO	Trimethylamine N-oxide
TRUS	Trans-rectal ultrasound
UHPLC-MS	Ultra-high-performance liquid chromatography–mass spectrometry
UPLC-MS/MS	Ultra performance liquid chromatography–tandem mass spectrometry

References

1. Bray, F.; Ferlay, J.; Soerjomataram, I.; Siegel, R.L.; Torre, L.A.; Jemal, A. Global cancer statistics 2018: GLOBOCAN estimates of incidence and mortality worldwide for 36 cancers in 185 countries. *CA Cancer J. Clin.* **2018**, *68*, 394–424. [[CrossRef](#)] [[PubMed](#)]
2. Schoenfield, L.; Jones, J.S.; Zippe, C.D.; Reuther, A.M.; Klein, E.; Zhou, M.; Magi-Galluzzi, C. The incidence of high-grade prostatic intraepithelial neoplasia and atypical glands suspicious for carcinoma on first-time saturation needle biopsy, and the subsequent risk of cancer. *BJU Int.* **2007**, *99*, 770–774. [[CrossRef](#)] [[PubMed](#)]
3. Offermann, A.; Hohensteiner, S.; Kuempers, C.; Ribbat-Idel, J.; Schneider, F.; Becker, F.; Hupe, M.C.; Duensing, S.; Merseburger, A.S.; Kirfel, J.; et al. Prognostic Value of the New Prostate Cancer International Society of Urological Pathology Grade Groups. *Front. Med.* **2017**, *4*, 157. [[CrossRef](#)] [[PubMed](#)]

4. Chistiakov, D.A.; Myasoedova, V.A.; Grechko, A.V.; Melnichenko, A.A.; Orekhov, A.N. New biomarkers for diagnosis and prognosis of localized prostate cancer. *Semin. Cancer Biol.* **2018**, *52*, 9–16. [[CrossRef](#)] [[PubMed](#)]
5. Gordetsky, J.; Epstein, J. Grading of prostatic adenocarcinoma: Current state and prognostic implications. *Diagn. Pathol.* **2016**, *11*, 25. [[CrossRef](#)] [[PubMed](#)]
6. Foley, R.W.; Maweni, R.M.; Gorman, L.; Murphy, K.; Lundon, D.J.; Durkan, G.; Power, R.; O'Brien, F.; O'Malley, K.J.; Galvin, D.J.; et al. European Randomised Study of Screening for Prostate Cancer (ERSPC) risk calculators significantly outperform the Prostate Cancer Prevention Trial (PCPT) 2.0 in the prediction of prostate cancer: A multi-institutional study. *BJU Int.* **2016**, *118*, 706–713. [[CrossRef](#)]
7. Nam, R.K.; Satkunasivam, R.; Chin, J.L.; Izawa, J.; Trachtenberg, J.; Rendon, R.; Bell, D.; Singal, R.; Sherman, C.; Sugar, L.; et al. Next-generation prostate cancer risk calculator for primary care physicians. *Can. Urol. Assoc. J.* **2017**, *12*, E64–E70. [[CrossRef](#)]
8. Loeb, S.; Partin, A.W. Review of the Literature: PCA3 for Prostate Cancer Risk Assessment and Prognostication. *Rev. Urol.* **2011**, *13*, 191–195. [[CrossRef](#)]
9. Sanhueza, C.; Kohli, M. Clinical and Novel Biomarkers in the Management of Prostate Cancer. *Curr. Treat. Options Oncol.* **2018**, *19*. [[CrossRef](#)]
10. Biomarkers PCA3 and TMPRSS2-ERG: Better together: Prostate cancer. *Nat. Rev. Urol.* **2014**, *11*, 129. [[CrossRef](#)]
11. Perner, S.; Mosquera, J.-M.; Demichelis, F.; Hofer, M.D.; Paris, P.L.; Simko, J.; Collins, C.; Bismar, T.A.; Chinnaiyan, A.M.; De Marzo, A.M.; et al. TMPRSS2-ERG Fusion Prostate Cancer: An Early Molecular Event Associated with Invasion. *Am. J. Surg. Pathol.* **2007**, *31*, 882–888. [[CrossRef](#)] [[PubMed](#)]
12. Barbieri, C.E.; Demichelis, F.; Rubin, M.A. Molecular genetics of prostate cancer: Emerging appreciation of genetic complexity. *Histopathology* **2012**, *60*, 187–198. [[CrossRef](#)] [[PubMed](#)]
13. Tomlins, S.A. Recurrent Fusion of TMPRSS2 and ETS Transcription Factor Genes in Prostate. *Cancer Sci.* **2005**, *310*, 644–648. [[CrossRef](#)] [[PubMed](#)]
14. Ferro, M.; Buonerba, C.; Terracciano, D.; Lucarelli, G.; Cosimato, V.; Bottero, D.; Deliu, V.M.; Ditonno, P.; Perdonà, S.; Autorino, R.; et al. Biomarkers in localized prostate cancer. *Future Oncol.* **2016**, *12*, 399–411. [[CrossRef](#)] [[PubMed](#)]
15. Hendriks, R.J.; van Oort, I.M.; Schalken, J.A. Blood-based and urinary prostate cancer biomarkers: A review and comparison of novel biomarkers for detection and treatment decisions. *Prostate Cancer Prostatic Dis.* **2017**, *20*, 12–19. [[CrossRef](#)] [[PubMed](#)]
16. Khan, A.; Choi, S.A.; Na, J.; Pamungkas, A.D.; Jung, K.J.; Jee, S.H.; Park, Y.H. Non-invasive Serum Metabolomic Profiling Reveals Elevated Kynurenine Pathway's Metabolites in Humans with Prostate Cancer. *J. Proteome Res.* **2019**. [[CrossRef](#)] [[PubMed](#)]
17. Andersen, M.K.; Rise, K.; Giskeødegård, G.F.; Richardsen, E.; Bertilsson, H.; Størkersen, Ø.; Bathen, T.F.; Rye, M.; Tessem, M.-B. Integrative metabolic and transcriptomic profiling of prostate cancer tissue containing reactive stroma. *Sci. Rep.* **2018**, *8*, 14269. [[CrossRef](#)] [[PubMed](#)]
18. Fujita, K.; Nonomura, N. Urinary biomarkers of prostate cancer. *Int. J. Urol.* **2018**, *25*, 770–779. [[CrossRef](#)] [[PubMed](#)]
19. Kumar, D.; Gupta, A.; Nath, K. NMR-based metabolomics of prostate cancer: A protagonist in clinical diagnostics. *Expert Rev. Mol. Diagn.* **2016**, *16*, 651–661. [[CrossRef](#)] [[PubMed](#)]
20. Holmes, E.; Wilson, I.D.; Nicholson, J.K. Metabolic phenotyping in health and disease. *Cell* **2008**, *134*, 714–717. [[CrossRef](#)] [[PubMed](#)]
21. Warburg, O. On the origin of cancer cells. *Science* **1956**, *123*, 309–314. [[CrossRef](#)] [[PubMed](#)]
22. Vander Heiden, M.G.; DeBerardinis, R.J. Understanding the Intersections between Metabolism and Cancer Biology. *Cell* **2017**, *168*, 657–669. [[CrossRef](#)] [[PubMed](#)]
23. Hanahan, D.; Weinberg, R.A. Hallmarks of cancer: The next generation. *Cell* **2011**, *144*, 646–674. [[CrossRef](#)] [[PubMed](#)]
24. Pavlova, N.N.; Thompson, C.B. The Emerging Hallmarks of Cancer Metabolism. *Cell Metab.* **2016**, *23*, 27–47. [[CrossRef](#)]
25. Levine, A.J.; Puzio-Kuter, A.M. The control of the metabolic switch in cancers by oncogenes and tumor suppressor genes. *Science* **2010**, *330*, 1340–1344. [[CrossRef](#)] [[PubMed](#)]

26. Ward, P.S.; Patel, J.; Wise, D.R.; Abdel-Wahab, O.; Bennett, B.D.; Collier, H.A.; Cross, J.R.; Fantin, V.R.; Hedvat, C.V.; Perl, A.E.; et al. The common feature of leukemia-associated IDH1 and IDH2 mutations is a neomorphic enzyme activity converting alpha-ketoglutarate to 2-hydroxyglutarate. *Cancer Cell* **2010**, *17*, 225–234. [[CrossRef](#)] [[PubMed](#)]
27. Hipp, S.J.; Steffen-Smith, E.A.; Patronas, N.; Herscovitch, P.; Solomon, J.M.; Bent, R.S.; Steinberg, S.M.; Warren, K.E. Molecular imaging of pediatric brain tumors: Comparison of tumor metabolism using 18F-FDG-PET and MRSI. *J. Neurooncol.* **2012**, *109*, 521–527. [[CrossRef](#)]
28. Zhan, H.; Ciano, K.; Dong, K.; Zucker, S. Targeting glutamine metabolism in myeloproliferative neoplasms. *Blood Cells Mol. Dis.* **2015**, *55*, 241–247. [[CrossRef](#)]
29. Sutinen, E.; Nurmi, M.; Roivainen, A.; Varpula, M.; Tolvanen, T.; Lehtikoinen, P.; Minn, H. Kinetics of [(11)C]choline uptake in prostate cancer: A PET study. *Eur. J. Nuclear Med. Mol. Imaging* **2004**, *31*, 317–324. [[CrossRef](#)]
30. Srivastava, A.; Creek, D.J. Discovery and Validation of Clinical Biomarkers of Cancer: A Review Combining Metabolomics and Proteomics. *Proteomics* **2018**, 1700448. [[CrossRef](#)]
31. Zhang, A.; Sun, H.; Yan, G.; Wang, P.; Wang, X. Metabolomics for Biomarker Discovery: Moving to the Clinic. *Biomed. Res. Int.* **2015**, *2015*, 354671. [[CrossRef](#)] [[PubMed](#)]
32. Mirnaghi, F.S.; Caudy, A.A. Challenges of analyzing different classes of metabolites by a single analytical method. *Bioanalysis* **2014**, *6*, 3393–3416. [[CrossRef](#)] [[PubMed](#)]
33. Wolfender, J.-L.; Marti, G.; Thomas, A.; Bertrand, S. Current approaches and challenges for the metabolite profiling of complex natural extracts. *J. Chromatogr. A* **2015**, *1382*, 136–164. [[CrossRef](#)] [[PubMed](#)]
34. Alonso, A.; Marsal, S.; Julià, A. Analytical methods in untargeted metabolomics: State of the art in 2015. *Front. Bioeng. Biotechnol.* **2015**, *3*, 23. [[CrossRef](#)] [[PubMed](#)]
35. Bingol, K.; Brüschweiler, R. Two elephants in the room: New hybrid nuclear magnetic resonance and mass spectrometry approaches for metabolomics. *Curr. Opin. Clin. Nutr. Metab. Care* **2015**, *18*, 471–477. [[CrossRef](#)] [[PubMed](#)]
36. Fuhrer, T.; Zamboni, N. High-throughput discovery metabolomics. *Curr. Opin. Biotechnol.* **2015**, *31*, 73–78. [[CrossRef](#)] [[PubMed](#)]
37. Clos-Garcia, M.; Loizaga-Iriarte, A.; Zuñiga-Garcia, P.; Sánchez-Mosquera, P.; Rosa Cortazar, A.; González, E.; Torrano, V.; Alonso, C.; Pérez-Cormenzana, M.; Ugalde-Olano, A.; et al. Metabolic alterations in urine extracellular vesicles are associated to prostate cancer pathogenesis and progression. *J. Extracell. Vesicles* **2018**, *7*, 1470442. [[CrossRef](#)]
38. Liang, Q.; Liu, H.; Xie, L.; Li, X.; Zhang, A.-H. High-throughput metabolomics enables biomarker discovery in prostate cancer. *RSC Adv.* **2017**, *7*, 2587–2593. [[CrossRef](#)]
39. Gkotsos, G.; Virgiliou, C.; Lagoudaki, I.; Sardeli, C.; Raikos, N.; Theodoridis, G.; Dimitriadis, G. The Role of Sarcosine, Uracil, and Kynurenic Acid Metabolism in Urine for Diagnosis and Progression Monitoring of Prostate Cancer. *Metabolites* **2017**, *7*, 9. [[CrossRef](#)]
40. Struck-Lewicka, W.; Kordalewska, M.; Bujak, R.; Yumba Mpanga, A.; Markuszewski, M.; Jacyna, J.; Matuszewski, M.; Kalisz, R.; Markuszewski, M.J. Urine metabolic fingerprinting using LC-MS and GC-MS reveals metabolite changes in prostate cancer: A pilot study. *J. Pharm. Biomed. Anal.* **2015**, *111*, 351–361. [[CrossRef](#)]
41. Fernández-Peralbo, M.A.; Gómez-Gómez, E.; Calderón-Santiago, M.; Carrasco-Valiente, J.; Ruiz-García, J.; Requena-Tapia, M.J.; Luque de Castro, M.D.; Priego-Capote, F. Prostate Cancer Patients–Negative Biopsy Controls Discrimination by Untargeted Metabolomics Analysis of Urine by LC-QTOF: Upstream Information on Other Omics. *Sci. Rep.* **2016**, *6*. [[CrossRef](#)] [[PubMed](#)]
42. Puhka, M.; Takatalo, M.; Nordberg, M.-E.; Valkonen, S.; Nandania, J.; Aatonen, M.; Yliperttula, M.; Laitinen, S.; Velagapudi, V.; Mirtti, T.; et al. Metabolomic Profiling of Extracellular Vesicles and Alternative Normalization Methods Reveal Enriched Metabolites and Strategies to Study Prostate Cancer-Related Changes. *Theranostics* **2017**, *7*, 3824–3841. [[CrossRef](#)] [[PubMed](#)]
43. Fujita, K.; Kume, H.; Matsuzaki, K.; Kawashima, A.; Ujike, T.; Nagahara, A.; Uemura, M.; Miyagawa, Y.; Tomonaga, T.; Nonomura, N. Proteomic analysis of urinary extracellular vesicles from high Gleason score prostate cancer. *Sci. Rep.* **2017**, *7*, 42961. [[CrossRef](#)] [[PubMed](#)]

44. Pérez-Rambla, C.; Puchades-Carrasco, L.; García-Flores, M.; Rubio-Briones, J.; López-Guerrero, J.A.; Pineda-Lucena, A. Non-invasive urinary metabolomic profiling discriminates prostate cancer from benign prostatic hyperplasia. *Metabolomics* **2017**, *13*. [[CrossRef](#)]
45. Davaliev, K.; Kostovska, I.M.; Kiprijanovska, S.; Markoska, K.; Kubelka-Sabit, K.; Filipovski, V.; Stavridis, S.; Stankov, O.; Komina, S.; Petrusevska, G.; et al. Proteomics analysis of malignant and benign prostate tissue by 2D DIGE/MS reveals new insights into proteins involved in prostate cancer: Proteomics Analysis of Prostate Cancer. *Prostate* **2015**, *75*, 1586–1600. [[CrossRef](#)] [[PubMed](#)]
46. Kumar, D.; Gupta, A.; Mandhani, A.; Sankhwar, S.N. NMR spectroscopy of filtered serum of prostate cancer: A new frontier in metabolomics: Metabolomics of Prostate Cancer. *Prostate* **2016**, *76*, 1106–1119. [[CrossRef](#)] [[PubMed](#)]
47. Kumar, D.; Gupta, A.; Mandhani, A.; Sankhwar, S.N. Metabolomics-Derived Prostate Cancer Biomarkers: Fact or Fiction? *J. Proteome Res.* **2015**, *14*, 1455–1464. [[CrossRef](#)] [[PubMed](#)]
48. Heger, Z.; Michalek, P.; Guran, R.; Cernei, N.; Duskova, K.; Vesely, S.; Anyz, J.; Stepankova, O.; Zitka, O.; Adam, V.; et al. Differences in urinary proteins related to surgical margin status after radical prostatectomy. *Oncol. Rep.* **2015**, *34*, 3247–3255. [[CrossRef](#)] [[PubMed](#)]
49. Giskeødegård, G.F.; Hansen, A.F.; Bertilsson, H.; Gonzalez, S.V.; Kristiansen, K.A.; Bruheim, P.; Mjøs, S.A.; Angelsen, A.; Bathen, T.F.; Tessem, M.-B. Metabolic markers in blood can separate prostate cancer from benign prostatic hyperplasia. *Br. J. Cancer* **2015**, *113*, 1712–1719. [[CrossRef](#)] [[PubMed](#)]
50. Zhao, Y.; Lv, H.; Qiu, S.; Gao, L.; Ai, H. Plasma metabolic profiling and novel metabolite biomarkers for diagnosing prostate cancer. *RSC Adv.* **2017**, *7*, 30060–30069. [[CrossRef](#)]
51. Lin, H.-M.; Mahon, K.L.; Weir, J.M.; Mundra, P.A.; Spielman, C.; Briscoe, K.; Gurney, H.; Mallesara, G.; Marx, G.; Stockler, M.R.; et al. A distinct plasma lipid signature associated with poor prognosis in castration-resistant prostate cancer: Prognostic lipid signature in metastatic prostate cancer. *Int. J. Cancer* **2017**, *141*, 2112–2120. [[CrossRef](#)] [[PubMed](#)]
52. Mondul, A.M.; Moore, S.C.; Weinstein, S.J.; Karoly, E.D.; Sampson, J.N.; Albanes, D. Metabolomic analysis of prostate cancer risk in a prospective cohort: The alpha-tocopherol, beta-carotene cancer prevention (ATBC) study: Serum Metabolomics Profiling of Prostate Cancer Risk. *Int. J. Cancer* **2015**, *137*, 2124–2132. [[CrossRef](#)] [[PubMed](#)]
53. Kühn, T.; Floegel, A.; Sookthai, D.; Johnson, T.; Rolle-Kampczyk, U.; Otto, W.; von Bergen, M.; Boeing, H.; Kaaks, R. Higher plasma levels of lysophosphatidylcholine 18:0 are related to a lower risk of common cancers in a prospective metabolomics study. *BMC Med.* **2016**, *14*. [[CrossRef](#)] [[PubMed](#)]
54. Schmidt, J.A.; Fensom, G.K.; Rinaldi, S.; Scalbert, A.; Appleby, P.N.; Achaintre, D.; Gicquiau, A.; Gunter, M.J.; Ferrari, P.; Kaaks, R.; et al. Pre-diagnostic metabolite concentrations and prostate cancer risk in 1077 cases and 1077 matched controls in the European Prospective Investigation into Cancer and Nutrition. *BMC Med.* **2017**, *15*. [[CrossRef](#)] [[PubMed](#)]
55. Huang, J.; Mondul, A.M.; Weinstein, S.J.; Karoly, E.D.; Sampson, J.N.; Albanes, D. Prospective serum metabolomic profile of prostate cancer by size and extent of primary tumor. *Oncotarget* **2017**, *8*. [[CrossRef](#)]
56. Andras, I.; Crisan, N.; Vesa, S.; Rahota, R.; Romanciuc, F.; Lazar, A.; Socaciu, C.; Matei, D.-V.; de Cobelli, O.; Bocsan, I.-S.; et al. Serum metabolomics can predict the outcome of first systematic transrectal prostate biopsy in patients with PSA <10 ng/mL. *Future Oncol.* **2017**, *13*, 1793–1800. [[CrossRef](#)]
57. Kline, E.E.; Treat, E.G.; Averna, T.A.; Davis, M.S.; Smith, A.Y.; Sillerud, L.O. Citrate Concentrations in Human Seminal Fluid and Expressed Prostatic Fluid Determined via ¹H Nuclear Magnetic Resonance Spectroscopy Outperform Prostate Specific Antigen in Prostate Cancer Detection. *J. Urol.* **2006**, *176*, 2274–2279. [[CrossRef](#)]
58. Etheridge, T.; Straus, J.; Ritter, M.A.; Jarrard, D.F.; Huang, W. Semen AMACR protein as a novel method for detecting prostate cancer. *Urol. Oncol.* **2018**. [[CrossRef](#)]
59. Serkova, N.J.; Gamito, E.J.; Jones, R.H.; O'Donnell, C.; Brown, J.L.; Green, S.; Sullivan, H.; Hedlund, T.; Crawford, E.D. The metabolites citrate, myo-inositol, and spermine are potential age-independent markers of prostate cancer in human expressed prostatic secretions. *Prostate* **2008**, *68*, 620–628. [[CrossRef](#)]
60. Averna, T.; Kline, E.; Smith, A.; Sillerud, L. A decrease in ¹H nuclear magnetic resonance spectroscopically determined citrate in human seminal fluid accompanies the development of prostate adenocarcinoma. *J. Urol.* **2005**, *173*, 433–438. [[CrossRef](#)]

61. Roberts, M.J.; Richards, R.S.; Chow, C.W.K.; Buck, M.; Yaxley, J.; Lavin, M.F.; Schirra, H.J.; Gardiner, R.A. Seminal plasma enables selection and monitoring of active surveillance candidates using nuclear magnetic resonance-based metabolomics: A preliminary investigation. *Prostate Int.* **2017**, *5*, 149–157. [[CrossRef](#)] [[PubMed](#)]
62. Eidelman, E.; Twum-Ampofo, J.; Ansari, J.; Siddiqui, M.M. The Metabolic Phenotype of Prostate Cancer. *Front. Oncol.* **2017**, *7*. [[CrossRef](#)] [[PubMed](#)]
63. Lima, A.; Araújo, A.; Pinto, J.; Jerónimo, C.; Henrique, R.; Bastos, M.; Carvalho, M.; Guedes de Pinho, P. GC-MS-Based Endometabolome Analysis Differentiates Prostate Cancer from Normal Prostate Cells. *Metabolites* **2018**, *8*, 23. [[CrossRef](#)] [[PubMed](#)]
64. Giunchi, F.; Fiorentino, M.; Loda, M. The Metabolic Landscape of Prostate Cancer. *Eur. Urol. Oncol.* **2018**, *2*, 28–36. [[CrossRef](#)]
65. Sadeghi, R.N.; Karami-Tehrani, F.; Salami, S. Targeting prostate cancer cell metabolism: Impact of hexokinase and CPT-1 enzymes. *Tumour Biol.* **2015**, *36*, 2893–2905. [[CrossRef](#)] [[PubMed](#)]
66. Twum-Ampofo, J.; Fu, D.-X.; Passaniti, A.; Hussain, A.; Siddiqui, M.M. Metabolic targets for potential prostate cancer therapeutics. *Curr. Opin. Oncol.* **2016**, *28*, 241–247. [[CrossRef](#)] [[PubMed](#)]
67. Awwad, H.M.; Geisel, J.; Obeid, R. The role of choline in prostate cancer. *Clin. Biochem.* **2012**, *45*, 1548–1553. [[CrossRef](#)] [[PubMed](#)]
68. Sreekumar, A.; Poisson, L.M.; Rajendiran, T.M.; Khan, A.P.; Cao, Q.; Yu, J.; Laxman, B.; Mehra, R.; Lonigro, R.J.; Li, Y.; et al. Metabolomic profiles delineate potential role for sarcosine in prostate cancer progression. *Nature* **2009**, *457*, 910–914. [[CrossRef](#)] [[PubMed](#)]
69. Giskeødegård, G.F.; Bertilsson, H.; Selnaes, K.M.; Wright, A.J.; Bathen, T.F.; Viset, T.; Halgunset, J.; Angelsen, A.; Gribbestad, I.S.; Tessem, M.-B. Spermine and Citrate as Metabolic Biomarkers for Assessing Prostate Cancer Aggressiveness. *PLoS ONE* **2013**, *8*, e62375. [[CrossRef](#)]
70. Zabala-Letona, A.; Arruabarrena-Aristorena, A.; Martín-Martín, N.; Fernandez-Ruiz, S.; Sutherland, J.D.; Clasquin, M.; Tomas-Cortazar, J.; Jimenez, J.; Torres, I.; Quang, P.; et al. mTORC1-dependent AMD1 regulation sustains polyamine metabolism in prostate cancer. *Nature* **2017**, *547*, 109–113. [[CrossRef](#)] [[PubMed](#)]
71. Wu, D.; Ni, J.; Beretov, J.; Cozzi, P.; Willcox, M.; Wasinger, V.; Walsh, B.; Graham, P.; Li, Y. Urinary biomarkers in prostate cancer detection and monitoring progression. *Crit. Rev. Oncol. Hematol.* **2017**, *118*, 15–26. [[CrossRef](#)] [[PubMed](#)]
72. Amobi, A.; Qian, F.; Lugade, A.A.; Odunsi, K. Tryptophan Catabolism and Cancer Immunotherapy Targeting IDO Mediated Immune Suppression. *Adv. Exp. Med. Biol.* **2017**, *1036*, 129–144. [[PubMed](#)]
73. Santhanam, S.; Alvarado, D.M.; Ciorba, M.A. Therapeutic targeting of inflammation and tryptophan metabolism in colon and gastrointestinal cancer. *Transl. Res.* **2016**, *167*, 67–79. [[CrossRef](#)] [[PubMed](#)]
74. Khan, A.P.; Rajendiran, T.M.; Bushra, A.; Asangani, I.A.; Athanikar, J.N.; Yocum, A.K.; Mehra, R.; Siddiqui, J.; Palapattu, G.; Wei, J.T.; et al. The Role of Sarcosine Metabolism in Prostate Cancer Progression. *Neoplasia* **2013**, *15*, 491–501. [[CrossRef](#)] [[PubMed](#)]
75. Ankerst, D.P.; Liss, M.; Zapata, D.; Hoefler, J.; Thompson, I.M.; Leach, R.J. A case control study of sarcosine as an early prostate cancer detection biomarker. *BMC Urol.* **2015**, *15*, 99. [[CrossRef](#)] [[PubMed](#)]
76. Dereziński, P.; Klupczynska, A.; Sawicki, W.; Pałka, J.A.; Kokot, Z.J. Amino Acid Profiles of Serum and Urine in Search for Prostate Cancer Biomarkers: A Pilot Study. *Int. J. Med. Sci.* **2017**, *14*, 1–12. [[CrossRef](#)] [[PubMed](#)]
77. Locasale, J.W. Serine, glycine and one-carbon units: Cancer metabolism in full circle. *Nat. Rev. Cancer* **2013**, *13*, 572–583. [[CrossRef](#)] [[PubMed](#)]
78. Koslowski, M.; Türeci, O.; Bell, C.; Krause, P.; Lehr, H.-A.; Brunner, J.; Seitz, G.; Nestle, F.O.; Huber, C.; Sahin, U. Multiple splice variants of lactate dehydrogenase C selectively expressed in human cancer. *Cancer Res.* **2002**, *62*, 6750–6755. [[PubMed](#)]
79. Kong, L.; Du, W.; Cui, Z.; Wang, L.; Yang, Z.; Zhang, H.; Lin, D. Expression of lactate dehydrogenase C in MDA-MB-231 cells and its role in tumor invasion and migration. *Mol. Med. Rep.* **2016**, *13*, 3533–3538. [[CrossRef](#)]
80. Merchant, M.L.; Rood, I.M.; Deegens, J.K.J.; Klein, J.B. Isolation and characterization of urinary extracellular vesicles: Implications for biomarker discovery. *Nat. Rev. Nephrol.* **2017**, *13*, 731–749. [[CrossRef](#)]
81. Myers, J.S.; von Lersner, A.K.; Sang, Q.-X.A. Proteomic Upregulation of Fatty Acid Synthase and Fatty Acid Binding Protein 5 and Identification of Cancer- and Race-Specific Pathway Associations in Human Prostate Cancer Tissues. *J. Cancer* **2016**, *7*, 1452–1464. [[CrossRef](#)] [[PubMed](#)]

82. Pang, J.; Liu, W.-P.; Liu, X.-P.; Li, L.-Y.; Fang, Y.-Q.; Sun, Q.-P.; Liu, S.-J.; Li, M.-T.; Su, Z.-L.; Gao, X. Profiling protein markers associated with lymph node metastasis in prostate cancer by DIGE-based proteomics analysis. *J. Proteome Res.* **2010**, *9*, 216–226. [[CrossRef](#)] [[PubMed](#)]
83. Wu, H.; Liu, T.; Ma, C.; Xue, R.; Deng, C.; Zeng, H.; Shen, X. GC/MS-based metabolomic approach to validate the role of urinary sarcosine and target biomarkers for human prostate cancer by microwave-assisted derivatization. *Anal. Bioanal. Chem.* **2011**, *401*, 635–646. [[CrossRef](#)] [[PubMed](#)]
84. Kami, K.; Fujimori, T.; Sato, H.; Sato, M.; Yamamoto, H.; Ohashi, Y.; Sugiyama, N.; Ishihama, Y.; Onozuka, H.; Ochiai, A.; et al. Metabolomic profiling of lung and prostate tumor tissues by capillary electrophoresis time-of-flight mass spectrometry. *Metabolomics* **2013**, *9*, 444–453. [[CrossRef](#)] [[PubMed](#)]
85. McDunn, J.E.; Li, Z.; Adam, K.-P.; Neri, B.P.; Wolfert, R.L.; Milburn, M.V.; Lotan, Y.; Wheeler, T.M. Metabolomic signatures of aggressive prostate cancer. *Prostate* **2013**, *73*, 1547–1560. [[CrossRef](#)] [[PubMed](#)]
86. Jiang, Z.; Woda, B.A. Diagnostic utility of alpha-methylacyl CoA racemase (P504S) on prostate needle biopsy. *Adv. Anat. Pathol.* **2004**, *11*, 316–321. [[CrossRef](#)]
87. Zhou, M.; Jiang, Z.; Epstein, J.I. Expression and diagnostic utility of alpha-methylacyl-CoA-racemase (P504S) in foamy gland and pseudohyperplastic prostate cancer. *Am. J. Surg. Pathol.* **2003**, *27*, 772–778. [[CrossRef](#)]
88. Box, A.; Alshalalfa, M.; Hegazy, S.A.; Donnelly, B.; Bismar, T.A. High alpha-methylacyl-CoA racemase (AMACR) is associated with ERG expression and with adverse clinical outcome in patients with localized prostate cancer. *Tumour Biol.* **2016**, *37*, 12287–12299. [[CrossRef](#)]
89. Alinezhad, S.; Väänänen, R.-M.; Ochoa, N.T.; Vertosick, E.A.; Bjartell, A.; Boström, P.J.; Taimen, P.; Pettersson, K. Global expression of AMACR transcripts predicts risk for prostate cancer—A systematic comparison of AMACR protein and mRNA expression in cancerous and noncancerous prostate. *BMC Urol.* **2016**, *16*, 10. [[CrossRef](#)]
90. Mroz, A.; Kiedrowski, M.; Lewandowski, Z. α -Methylacyl-CoA racemase (AMACR) in gastric cancer: Correlation with clinicopathologic data and disease-free survival. *Appl. Immunohistochem. Mol. Morphol.* **2013**, *21*, 313–317. [[CrossRef](#)]
91. Xu, B.; Cai, Z.; Zeng, Y.; Chen, L.; Du, X.; Huang, A.; Liu, X.; Liu, J. α -Methylacyl-CoA racemase (AMACR) serves as a prognostic biomarker for the early recurrence/metastasis of HCC. *J. Clin. Pathol.* **2014**, *67*, 974–979. [[CrossRef](#)] [[PubMed](#)]
92. Lee, Y.-E.; He, H.-L.; Lee, S.-W.; Chen, T.-J.; Chang, K.-Y.; Hsing, C.-H.; Li, C.-F. AMACR overexpression as a poor prognostic factor in patients with nasopharyngeal carcinoma. *Tumour Biol.* **2014**, *35*, 7983–7991. [[CrossRef](#)] [[PubMed](#)]
93. Da Costa, I.A.; Hennenlotter, J.; Stühler, V.; Kühs, U.; Scharpf, M.; Todenhöfer, T.; Stenzl, A.; Bedke, J. Transketolase like 1 (TKTL1) expression alterations in prostate cancer tumorigenesis. *Urol. Oncol.* **2018**, *36*, 472.e21–472.e27. [[CrossRef](#)] [[PubMed](#)]
94. Kojima, Y.; Yoneyama, T.; Hatakeyama, S.; Mikami, J.; Sato, T.; Mori, K.; Hashimoto, Y.; Koie, T.; Ohyama, C.; Fukuda, M.; et al. Detection of Core2 β -1,6-N-Acetylglucosaminyltransferase in Post-Digital Rectal Examination Urine Is a Reliable Indicator for Extracapsular Extension of Prostate Cancer. *PLoS ONE* **2015**, *10*, e0138520. [[CrossRef](#)] [[PubMed](#)]
95. Sato, T.; Yoneyama, T.; Tobisawa, Y.; Hatakeyama, S.; Yamamoto, H.; Kojima, Y.; Mikami, J.; Mori, K.; Hashimoto, Y.; Koie, T.; et al. Core 2 β -1, 6-N-acetylglucosaminyltransferase-1 expression in prostate biopsy specimen is an indicator of prostate cancer aggressiveness. *Biochem. Biophys. Res. Commun.* **2016**, *470*, 150–156. [[CrossRef](#)] [[PubMed](#)]



Targeted Metabolomics Analyses Reveal Specific Metabolic Alterations in High-Grade Prostate Cancer Patients

Nuria Gómez-Cebrián, María García-Flores, José Rubio-Briones, José Antonio López-Guerrero, Antonio Pineda-Lucena, and Leonor Puchades-Carrasco*

Cite This: *J. Proteome Res.* 2020, 19, 4082–4092

Read Online

ACCESS |

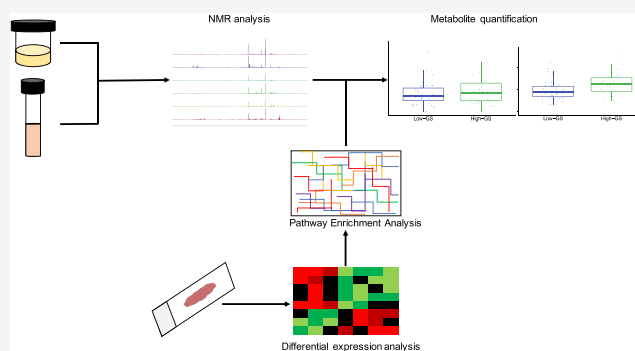
Metrics & More

Article Recommendations

Supporting Information

ABSTRACT: Prostate cancer (PCa) is a hormone-dependent tumor characterized by an extremely heterogeneous prognosis. Despite recent advances in partially uncovering some of the biological processes involved in its progression, there is still an urgent need for identifying more accurate and specific prognostic procedures to differentiate between disease stages. In this context, targeted approaches, focused on mapping dysregulated metabolic pathways, could play a critical role in identifying the mechanisms driving tumorigenesis and metastasis. In this study, a targeted analysis of the nuclear magnetic resonance-based metabolomic profile of PCa patients with different tumor grades, guided by transcriptomics profiles associated with their stages, was performed. Serum and urine samples were collected from 73 PCa patients. Samples were classified according to their Gleason score (GS) into low-GS (GS < 7) and high-GS PCa (GS ≥ 7) groups. A total of 36 metabolic pathways were found to be dysregulated in the comparison between different PCa grades. Particularly, the levels of glucose, glycine and 1-methylpyridinium, metabolites involved in energy metabolism and nucleotide synthesis were significantly altered between both groups of patients. These results underscore the potential of targeted metabolomic profiling to characterize relevant metabolic changes involved in the progression of this neoplastic process.

KEYWORDS: biomarker, tumour metabolism, metabolomics, prostate cancer, nuclear magnetic resonance



INTRODUCTION

Prostate cancer (PCa) is the second most prevalent cancer and represents the fifth leading cause of cancer-related death in men worldwide.¹ Although the five-year survival rate for localized PCa is nearly 100%, once the tumors have spread beyond the prostate, it drops to 30%.² Moreover, PCa is characterized by an extremely clinical variable course. Patients with similar clinical features at diagnosis often have quite heterogeneous prognoses.

Nowadays, PCa diagnosis tests rely on prostate-specific antigen (PSA) blood test and digital rectal examination, followed by trans-rectal ultrasound-guided prostate biopsy, preferentially guided by multiparametric magnetic resonance imaging. The gold standard test for evaluating PCa prognosis is the histopathology-based estimation of the Gleason score (GS).³ However, treatment outcome is very variable within each GS group and between patients with the same PSA serum levels and pathological state at the time of diagnosis. During the last years, research has focused on the identification of molecular biomarkers to improve early diagnosis and risk stratification of PCa patients. Although many attempts have been made to improve the PCa grading system in the last three decades, there remains no classification scheme that enables

discrimination between indolent and aggressive PCa phenotypes.⁴ Hence, while the Gleason scoring system has been of critical importance, the development of precise and robust PCa biomarkers able to accurately stratify PCa patients into different risk phenotypes at the time of diagnosis remains a major clinical challenge.

In this scenario, metabolomics, defined as the comprehensive analysis of metabolites in a defined biological compartment, represents a powerful and promising approach for the identification of noninvasive biomarkers.^{5–9} The term metabolite encompasses various and diverse endogenous molecules, as well as exogenous molecules belonging to different chemical and biochemical classes (e.g., amino acids, sugars, fatty acids, lipids, nucleotides, drugs, and drug metabolites). Furthermore, a number of studies have demonstrated the strong correlation that exists between the

Received: July 2, 2020

Published: September 14, 2020



metabolic changes observed in different biofluids and changes in the metabolic machinery in various tumors.^{10–15} In recent years, a number of studies have focused on the characterization of the metabolic profile of PCa cells, aiming for a better understanding of the biological processes occurring during disease progression. Some of the results of these studies have revealed that healthy prostate cells exhibit decreased citrate oxidation rate and a slower tricarboxylic acid cycle metabolism because of the effect of high zinc concentrations on *m*-aconitase, the enzyme that catalyzes the oxidation of citrate.¹⁶ This metabolic phenotype results in citrate accumulation and reliance on the glycolytic pathway as the main energy source in healthy prostate cells.^{16,17} However, during malignant transformation, PCa cells lose their ability to accumulate zinc, leading to reactivation of the TCA cycle.¹⁶ Several studies have also focused on the identification of metabolic alterations that could be used as promising PCa biomarkers for improving diagnosis and prognosis of PCa patients.^{18–22} However, the complexity of human metabolome and its regulation at multiple levels make the translation of consistent metabolic signatures to the clinic difficult, showing that there is still a long way toward the validation of potential new metabolic biomarkers.^{23,24} In this context, targeted analysis of the metabolic profile, based on other biochemical/biological approaches could provide better translational outcomes.

In addition to metabolomics, other omics-based approaches, such as transcriptomics that aims to identify genes differentially expressed among predefined groups of samples, have shown a great potential in the identification of new clinically relevant PCa biomarkers.^{25–28} Furthermore, it has been shown that the integration of different omics approaches provides relevant insights into the onset and progression of the diseases, more than any of these methodologies on their own.^{29–31} In PCa, the integration of metabolomics and transcriptomics for the analysis of tissue samples has already revealed significant enrichment of genes and accumulation of metabolites involved in the TCA cycle,³² as well as other metabolic alterations, including cysteine and methionine metabolism, nicotinamide adenine dinucleotide metabolism, and hexosamine biosynthesis, when comparing PCa and benign prostatic hyperplasia (BPH) tissues.³³ Recent studies have demonstrated the potential of combining metabolomics and transcriptomics analyses for the identification and validation of clinically relevant metabolic changes in different cancer patients' biofluids.^{29,34–36} In this context, the analysis of changes in the expression of metabolism-related genes in tumor tissues could provide a powerful strategy for the identification of metabolic biomarkers in different biofluids.³⁷

Recent studies based on the analysis of tissues and biofluids of PCa patients have shown different metabolic alterations.^{38,39} However, the combination of these approaches has not been extensively used so far for the identification of new metabolic biomarkers that could potentially improve PCa patients' management using noninvasive biofluids. Hence, the main goal of this study was to evaluate the potential of the metabolomics-targeted analysis, driven by the characterization of transcriptomic changes in tumor samples, for the identification of specific metabolic changes that could be detected in easily accessible biofluids (urine and serum) in high-GS PCa patients. Overall, this strategy could facilitate a better understanding of the biochemical changes involved in the progression of PCa and, potentially, pave the way for the identification of new PCa prognostic biomarkers.

MATERIALS AND METHODS

Sample Collection

Patient recruitment was performed at the Urology Department and the Biobank of the Instituto Valenciano de Oncología (Valencia, Spain). Patient recruitment and sampling procedures were carried out following all applicable local regulatory requirements and laws, in accordance with the Declaration of Helsinki, and after approval from the Ethics Committee of the Instituto Valenciano de Oncología (CAPROSIVO, GVA, PROMETEO/2016/103) on May 2015. Before being included in the study, a written informed consent from each participant was obtained.

Serum and/or urine samples were collected, following specific standard operating procedures,^{40–42} from 73 PCa patients without any other disease at the time of sample collection. Samples were classified according to patients' GS into low-GS (<7) and high-GS PCa (≥7) groups. Urine and serum samples were frozen after collection and stored in liquid nitrogen until analysis using nuclear magnetic resonance (NMR) spectroscopy.

NMR Sample Preparation

At the time of ¹H NMR analysis, urine samples were thawed on ice and centrifuged at 6000 rpm for 10 min. After centrifugation, 60 μL of buffer (1.5 M KH₂PO₄, 0.1% trimethylsilylpropionic acid-*d*₄ sodium salt (TSP) and 0.05% NaN₃, pH = 7.4, in D₂O) was added to 540 μL of the urine sample supernatant. Serum samples were also thawed on ice at the time of ¹H NMR analysis. Then, 300 μL of serum was added to 300 μL of buffer (75 mM of Na₂HPO₄, 4.6 mM of TSP, and 0.04% NaN₃, pH = 7.4, in D₂O). Finally, 550 μL of each sample was transferred to a 5 mm NMR tube for analysis.

NMR Measurements

NMR measurements were acquired using a Bruker AVANCE II 500 MHz spectrometer. For urine samples, the acquisition temperature was set at 300 K. A one-dimensional nuclear Overhauser effect spectroscopy pulse sequence⁴³ was collected for each sample with 256 scans and 65 K data points over a spectral width of 29 ppm. A 4 s relaxation delay was included between free induction decays (FIDs). For serum samples, Carr–Purcell–Meiboom–Gill spin-echo pulse sequence⁴⁴ were collected for each sample, with an acquisition temperature of 310 K. The ¹H NMR spectra were acquired for a total of 256 scans and 61 K data points over a spectral width of 20 ppm and a relaxation delay of 4 s between FIDs. Then, urine and serum spectra were multiplied by a line-broadening factor of 1 Hz and Fourier-transformed. Finally, all spectra were automatically phased, baseline-corrected, and referenced to the methyl group signal of TSP at 0.00 ppm using TopSpin 3.5 (Bruker Biospin).

NMR Data Processing

After acquisition, urine spectra were binned using AMIX 3.9.7 (Bruker Biospin) into 0.001 ppm wide rectangular buckets over the spectral region δ 9.38–0.07 ppm. The residual water (δ 4.86–4.72 ppm) and urea (δ 6.10–5.45 ppm) signal regions were excluded from further analyses to avoid interferences. Spectra were then aligned using the “speaq” R package,⁴⁵ normalized to the total area of the corresponding spectra and by probabilistic quotient normalization.⁴⁶ On the other hand, serum spectra were also binned using AMIX into 0.01 ppm wide rectangular buckets over the spectral region δ 8.5–0.5 ppm, excluding the water (δ 4.87–4.51 ppm) and urea (δ

Table 1. Clinical Characteristics of PCa Patients Included in the Study^a

	serum (<i>n</i> = 66)			urine (<i>n</i> = 73)		
	low-GS	high-GS	<i>p</i> -value ^b	low-GS	high-GS	<i>p</i> -value ^b
number of patients (%)	36 (54.5%)	30 (45.5%)		41 (56.16%)	32 (43.84%)	
age (years)	65.69 ± 6.61	64.33 ± 11.60	0.70	65.66 ± 6.95	64.47 ± 11.23	0.79
BMI (kg/m ²)	25.02 ± 2.87	26.68 ± 7.66	0.33	26.43 ± 3.08	26.73 ± 7.34	0.61
prostate volume (mL)	44.26 ± 22.71	44.18 ± 23.71	0.95	43.71 ± 22.46	42.42 ± 23.83	0.97
PSA (ng/mL)	5.93 ± 3.65	70.70 ± 179.19	<0.001	5.78 ± 3.48	66.68 ± 174.04	<0.001

^aBMI, body mass index; GS, Gleason score; PSA, prostate-specific antigen; SD, standard deviation. Values expressed as mean ± SD. ^b*p*-value calculated using the Mann–Whitney *U* test (*p*-value < 0.05).

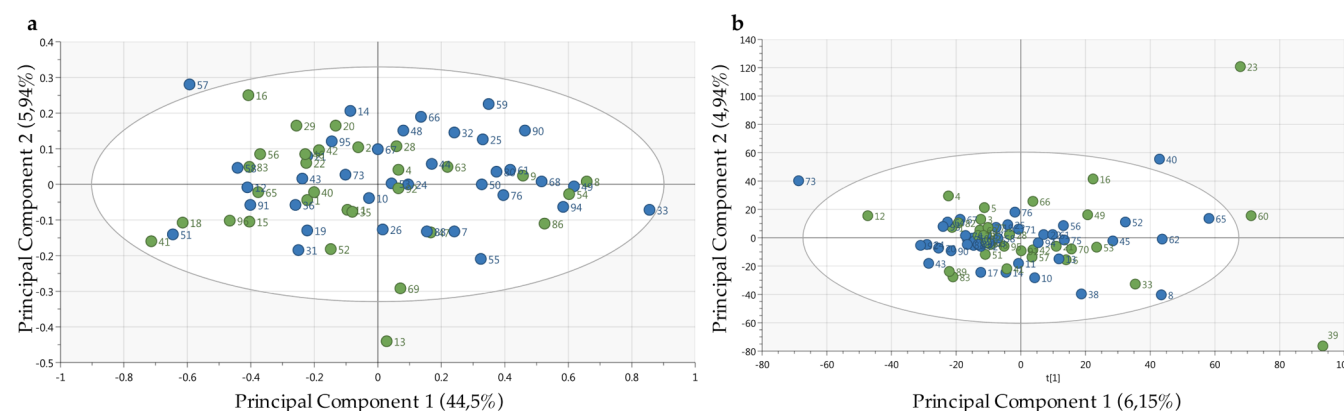


Figure 1. PCA score plots of (a) serum and (b) urine global metabolic profile of low-GS (blue ●) and high-GS (green ●) PCa patients.

6.65–5.53 ppm) signal regions. Spectra were finally normalized to the total area of the corresponding spectra.

Untargeted Metabolomics Analysis

Multivariate statistical analyses were performed using SIMCA-P 14.0 (Umetrics AB). A nonsupervised approach based on principal component analysis (PCA) was performed for the identification of patterns, intergroup clusters, and potential outliers. A supervised analysis using orthogonal partial least squares discriminant analysis (OPLS-DA) was carried out to decrease the possible variability within group and further evaluate the discriminatory potential of the metabolic profile between both groups of study. The default method of sevenfold internal cross-validation was applied, from which Q^2Y (predictive ability parameter, estimated by cross-validation) and R^2Y (goodness of fit parameter) values were extracted. These parameters were used for the evaluation of the quality of the OPLS-DA models obtained.

Transcriptomics Analysis

Three PCA transcriptomic data sets (accession numbers: GSE16560,⁴⁷ GSE46602,⁴⁸ and GSE70769⁴⁹), were selected from the Gene Expression Omnibus (<https://www.ncbi.nlm.nih.gov/geo/>) database.

All statistical analyses were conducted using the R 3.6.0 version. If not previously performed, gene expression data were subjected to log 2 transformation, and samples were classified according to their GS into low-GS (GS < 7) and high-GS (GS ≥ 7) groups. The “mdgsa” package⁵⁰ was used to conduct a gene set enrichment analysis (GSEA), and the statistical significance of differential gene expression between the two groups was assessed applying the Mann–Whitney *U* test from the “stats” R package. The Mann–Whitney *U* test was used to rank all genes, which were then grouped using the metabolism-related pathways defined by the Kyoto Encyclopedia of Genes

and Genomes database.^{51–53} Metabolic pathways showing a *p*-value < 0.05 were defined as significantly dysregulated. The Venn diagram for the comparison of the results obtained in the different studies was created using the Venny online tool.⁵⁴

Targeted Metabolomics Analysis

Metabolites were assigned using publicly available databases (e.g., HMDB, BRMB) in combination with the Bruker NMR metabolic profiling database BBIORFECODE 2.0.0 (Bruker Biospin). Optimal metabolite signals were defined (Tables S1 and S2), integrated, and quantified in urine and serum samples using MestreNova 8.0. The statistical significance of the differences between the means of the two experimental groups was assessed using the Mann–Whitney *U* test. A *p*-value < 0.05 was considered as statistically significant.

RESULTS

Study Cohort

A total of 66 serum and 73 urine samples were included in the study. Clinical characteristics of the individuals included in the study are summarized in Table 1.

Untargeted Analysis of PCa Serum and Urine Metabolic Profiles

To explore sample heterogeneity, a nonsupervised analysis (PCA) of the ¹H NMR serum and urine spectra was carried out to evaluate the potential influence of different clinical variables (age, body mass index, metastatic disease, serum levels of PSA, and disease grade) on the metabolic profiles of samples. The nonsupervised analysis of the global serum and urine metabolic profiles of samples included in the study did not reveal any significant sample clustering according to any of these variables, including disease grade (Figure 1).

To better examine potential differences between the groups of study, OPLS-DA models aiming to discriminate the serum

and urinary profiles, respectively, from low- and high-GS PCa were generated. Although these OPLS-DA models showed a reasonable fitting of the data ($R^2Y = 0.227$ and 0.556 for serum and urine, respectively), these multivariate models did not exhibit any predictive power ($Q^2Y = 0.0231$ and -0.256 , for serum and urine, respectively).

GSEA of PCa Transcriptomics Studies

Data from three published PCa transcriptomic studies (Table 2) were used to carry out a GSEA focused on the identification of significantly altered metabolic pathways between both groups of PCa patients.

Table 2. Characteristics of PCa Transcriptomic Studies^a

study ID	analytical platform ID	number of genes	number of samples	experimental groups
GSE46602	GPL570	23,495	36	low-GS ($n = 17$); high-GS ($n = 19$)
GSE70768	GPL10558	30,947	122	low-GS ($n = 17$); high-GS ($n = 105$)
GSE16560	GPL5474	6100	281	low-GS ($n = 83$); high-GS ($n = 198$)

^aGS, Gleason score; ID, identification.

Using this approach, a total of 36 metabolic pathways were found to be significantly dysregulated (p -value < 0.05) between the two groups (Table S3). Table 3 summarizes the most significantly altered metabolic pathways.

Significant PCa-metabolism-related alterations were shared in all three studies. Moreover, additional specific alterations were identified in each different study, according to differences in the array size and the genes included in each array (Figure S1).

Targeted Analysis of PCa Serum and Urine Metabolic Profiles

Assignment of all metabolites involved in the metabolic pathways exhibiting significant alterations in the GSEA was performed for all metabolites detectable in PCa patients' serum and urine NMR metabolic profiles. All detectable NMR signals were integrated for further analysis. Using this approach, a total of 23 and 22 metabolite signals were integrated in serum and urine ¹H NMR, respectively. The statistical significance of the changes in the levels of these metabolites was evaluated for the comparison between the two groups of study (Tables 4 and 5). The relative quantifications of the metabolites showing higher

variations in intensity between the groups of study are illustrated in Figures 2 and 3. Specifically, the serum metabolic profile of high-GS PCa patients was characterized by statistically significant high concentrations of glucose and glycine, while the urine of those same patients was dominated by statistically significant increased levels of 1-methylnicotinamide (MNA). Interestingly, relevant alterations (over 7%), although nonstatistically significant, in the levels of phenylalanine were found in both biofluids for high-GS PCa patients.

DISCUSSION

A number of metabolic alterations have been associated with PCa disease onset and progression over the last few years.³⁹ However, the identification of PCa metabolic biomarkers that may contribute to a better understanding of the molecular mechanisms underlying the progression of this neoplastic process still remains a critical goal. In fact, in a recent study, based on the analysis of 650 urine samples, only univariate analysis of the data revealed significant metabolic differences between PCa and BPH patients, highlighting the modest impact of prostate alterations in biofluid composition and the multifactorial nature of PCa.²² Similarly, in our study, the results of the untargeted OPLS-DA analysis of PCa serum and urine metabolic profiles did not reveal significant differences, considering that more subtle changes would potentially be expected when comparing low- and high-GS PCa patients.

Integrative approaches including the combination of different omics strategies (i.e., genomics, transcriptomics, metabolomics, etc.) have shown to be a very valuable tool for the characterization of specific genetic and metabolic alterations involved in different diseases.^{25–28} In this study, a targeted analysis of the metabolic profile of serum and urine samples obtained from low-GS and high-GS PCa patients, based on the analysis of transcriptomic data obtained from tumor tissue, was performed. In this study, three publicly available transcriptomic studies focused on the analysis of the genetic expression profile of low- and high-GS PCa patients were included. A GSEA revealed statistically significant metabolic alterations in a total of 36 metabolic pathways when comparing tumor tissues from low- and high-GS PCa patients. Notably, some of the most significantly altered pathways, including purine and pyrimidine metabolism and oxidative phosphorylation (OXPHOS), had already been associated with PCa progression in previous studies, thus providing support to our findings. Purine and pyrimidine metabolism are known to be enhanced in order to

Table 3. Top Ten Most Significantly Enriched Metabolic Pathways^a

ID KEGG	pathway name	LOR ^b	p -value ^c	FDR
hsa00190	oxidative phosphorylation	0.8950	1.33×10^{-18}	5.14×10^{-16}
hsa00240	pyrimidine metabolism	0.6645	2.57×10^{-9}	4.94×10^{-7}
hsa00230	purine metabolism	0.4492	4.04×10^{-8}	5.19×10^{-6}
hsa00830	retinol metabolism	-0.8751	3.90×10^{-6}	0.0016
hsa01230	biosynthesis of amino acids	0.5104	0.0002	0.0155
hsa00140	steroid hormone biosynthesis	-0.6065	0.0002	0.0432
hsa00900	terpenoid backbone biosynthesis	0.7854	0.0003	0.0228
hsa01200	carbon metabolism	0.3306	0.0005	0.0722
hsa00350	tyrosine metabolism	-0.6329	0.0007	0.0942
hsa00340	histidine metabolism	-0.7859	0.0010	0.0970

^aFDR, false discovery rate; ID, identification; KEGG, Kyoto Encyclopedia of Genes and Genomes; LOR, log odds ratio. ^bPositive and negative LOR values indicate that the pathway is enriched with genes up- and down-regulated in the high-GS PCa group. ^c p -value corrected by the Benjamini–Yekutieli (BY) procedure.

Table 4. Mean Intensities and Variations for the Metabolites Identified in the Serum Samples of Low- and High-GS PCA Patients^a

metabolite	mean low-GS	SD low-GS	mean high-GS	SD high-GS	<i>p</i> -value ^b	FC	% variation ^c	direction ^d
glucose	485,827	78,779	536,112	78,767	150	11,035	103,504	↑
glycine	28,665	6326	30,893	5310	369	10,777	77,730	↑
phenylalanine	26,653	5504	28,567	4964	765	10,718	71,806	↑
scyllo-inositol	7631	1897	8178	1818	2457	10,717	71,655	↑
formate	630	157	659	154	3872	10,468	46,777	↑
acetate	10,986	2009	11,464	2149	4461	10,435	43,507	↑
citrate	21,463	4163	22,267	3693	3463	10,375	37,484	↑
acetoacetate	12,676	1825	13,125	2519	7443	10,354	35,441	↑
arginine/lysine	90,840	11,895	93,924	11,613	3732	10,339	33,944	↑
valine	38,874	7271	40,092	6068	3943	10,313	31,337	↑
glutamine	55,521	11,009	56,804	10,345	6133	10,231	23,116	↑
leucine	39,624	5109	40,243	4131	4616	10,156	15,617	↑
lactate	60,0575	104,254	592,342	86,205	9643	9863	13,708	↓
fumarate	5427	913	5498	992	6589	10,132	13,194	↑
trimethylamine	3561	528	3608	575	8429	10,131	13,053	↑
alanine	66,098	11,125	66,874	9480	5517	10,117	11,733	↑
<i>NN</i> -dimethylglycine	6652	1027	6723	1141	8629	10,107	10,683	↑
propylene glycol	12,123	679	12,005	482	2108	9902	9803	↓
isoleucine	10,214	1096	10,147	919	9847	9935	6549	↓
succinate	9430	2268	9485	1862	7154	10,059	5862	↑
tyrosine	8111	1758	8153	1461	6964	10,052	5168	↑
histidine	7557	1223	7596	1227	9643	10,052	5156	↑
methylsuccinate	9494	884	9511	734	9847	10,018	1816	↑

^aSD, standard deviation; FC, fold change. ^b*p*-value calculated using the Mann–Whitney *U* test (*p*-value <0.05). ^cMean signal intensity variation between groups (%). ^dDirection of the variation, considering the low-GS group as a reference.

Table 5. Mean Intensities and Variations for the Metabolites Identified in the Urine Samples of Low- and High-GS PCA Patients^a

metabolite	mean low-GS	SD low-GS	mean high-GS	SD high-GS	<i>p</i> -value ^b	FC	% variation ^c	direction ^d
phenylalanine	124,293	65,254	159,270	115,533	4098	12,814	281,407	↑
4-Py	138,703	97,431	114,132	96,532	1540	8229	177,146	↓
lactate	127,163	108,158	108,707	35,066	8727	8549	145,139	↓
MNA	2219	1915	2528	911	56	11,395	139,466	↑
methylmalonate	98,610	43,057	85,232	23,148	1355	8643	135,660	↓
acetoacetate	84,185	31,900	93,849	39,161	3384	11,148	114,792	↑
alanine	104,308	31,810	94,522	18,824	4226	9062	93,819	↓
3-hydroxyisovalerate	46,490	9309	42,404	10,895	707	9121	87,900	↓
2-furoylglycine	14,283	7950	13,033	6604	6013	9125	87,542	↓
isobutyrate	37,875	8659	34,973	7745	1348	9234	76,631	↓
citrate	444,248	166,546	478,244	238,925	9604	10,765	76,525	↑
formate	11,654	3651	12,270	4054	4757	10,528	52,847	↑
leucine	14,110	3517	13,486	2213	7445	9558	44,222	↓
carnitine	113,446	48,417	118,231	71,531	8727	10,422	42,179	↑
scyllo-inositol	62,374	19,472	59,919	11,823	9252	9606	39,356	↓
glycine	163,502	55,583	157,644	48,645	6624	9642	35,828	↓
valine	23,994	4984	23,369	3390	9164	9740	26,047	↓
trigonelline	12,269	11,233	11,966	9148	4688	9753	24,710	↓
creatinine	1,235,729	201,437	1,221,583	184,016	9956	9886	11,448	↓
isoleucine	6135	1442	6095	1145	9512	9934	6559	↓
3-methyl-2-oxovalerate	41,272	8293	41,458	12,483	5767	10,045	4500	↑
taurine	263,869	54,990	263,335	87,617	5322	9980	2023	↓

^aSD, standard deviation; FC, fold change; 4-Py, *N*1-methyl-4-pyridone-5-carboxamide. ^b*p*-value calculated using the Mann–Whitney *U* test (*p*-value <0.05). ^cMean signal intensity variation between groups (%). ^dDirection of the variation, considering the low-GS group as a reference.

maintain the biosynthesis of nucleotides that support tumor cell proliferation in PCA and other cancers.^{55,56} Particularly, in PCA, increased pyrimidine metabolism has been associated with high Gleason grade and more aggressive tumors.⁵⁷

Furthermore, OXPHOS is a major pathway in energy production and plays a key role in cancer progression, found to be activated in high-grade PCA.⁵⁶ This metabolic process has become an emerging target in cancer therapy owing to the

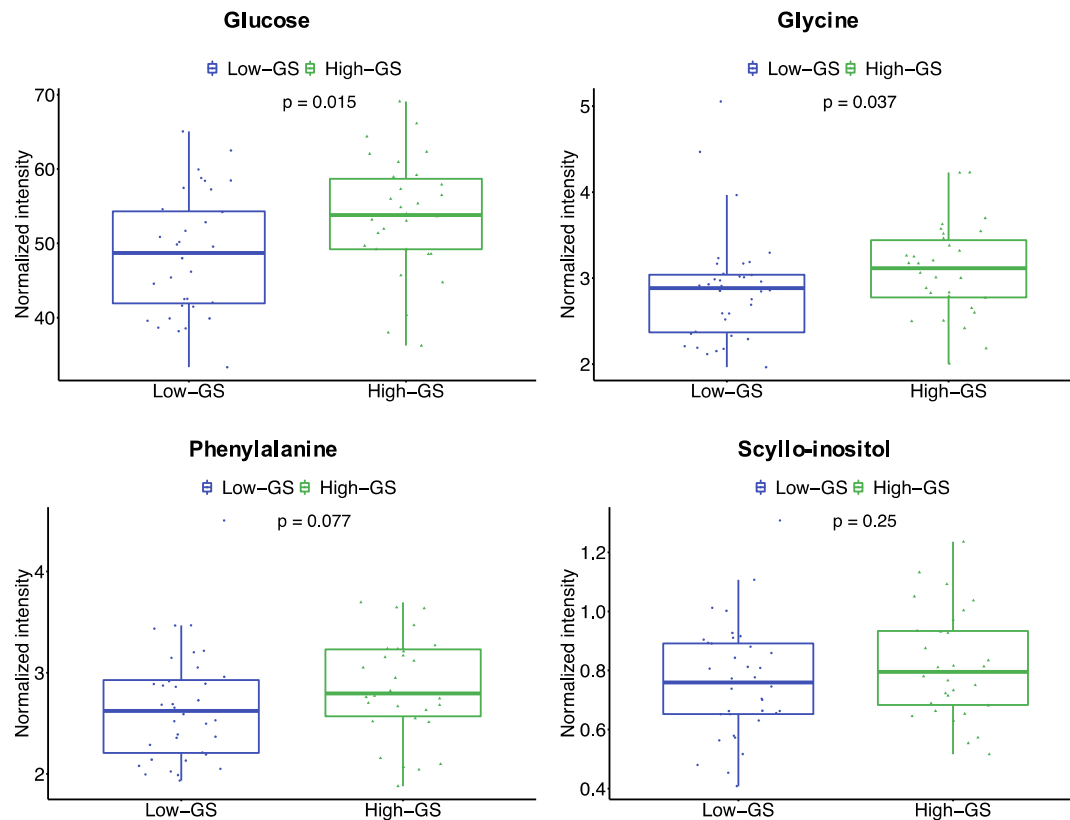


Figure 2. Box plot representing the normalized serum intensities of the metabolites showing higher variations in intensity between the groups of study (low-GS PCA: blue; high-GS PCA: green). For each box, the central line is the median, the edges of the box are the upper and lower quartiles, the whiskers extend the box by a further ± 1.5 the interquartile range, and samples are plotted as individual points. *p*-value represented above the box plots and calculated using the Mann–Whitney–Wilcoxon test.

heavy reliance of certain tumors on this pathway for ATP generation.^{58–60} Moreover, specific changes in the transcriptomic profile and metabolite levels involved in these pathways were further assessed. The most relevant genetic and metabolic alterations found in our study when comparing low- and high-GS PCA patients are illustrated in Figure 4.

Increased glucose serum levels and its correlation with tumor progression have been described in previous studies. Wright et al. observed that high glucose serum levels at the time of diagnosis in PCA patients were positively correlated with increased risk of recurrence.⁶¹ Additionally, serum levels of glucose were positively associated with increased risk of PCA in a different study.⁶² Glucose is involved in the glycolysis pathway, being transported through the cell membrane by glucose transporters (GLUT) and then converted to glucose-6-phosphate by hexokinase (HK). Most tumors exhibit high rates of glucose consumption to meet their energetic demands and biosynthesis requirements, which is the rationale for fluorodeoxyglucose (FDG)-positron emission tomography (PET) scanning. Nevertheless, other cancerous conditions, such as PCA, show low rates of glucose uptake and rely on alternative energy sources such as fatty acid oxidation.^{63–65} In line with these findings, the GSEA in this study revealed a decreased glycolysis activity in the high-GS PCA group. This specific characteristic of high-GS tumors could be behind the limitations of FDG-PET scanning and the higher sensitivity observed in choline-PET scans.⁶⁶ An in-depth analysis of the levels of enzymes involved in this pathway, determined in the transcriptomics studies included in this analysis, showed a significant down-regulation of the expression of GLUT and

HK. These results support the idea that glucose is not being used as the main energy source in high-GS PCA patients and is accumulated as a result of the down-regulation of two main glycolytic enzymes and the subsequent slow glycolysis rate.

The role of glycine in tumor proliferation is controversial. While some studies have reported decreased glycine levels in the serum of high-grade PCA,²¹ and shown that glycine uptake is associated with rapid tumor proliferation,⁶⁷ others have shown that excess glycine has an inhibitory effect on tumorigenesis.^{68,69} Glycine and serine can be interconverted by the serine hydroxymethyl transferase (SHMT). Thus, it has been argued that glycine may be released in order to limit intracellular glycine levels and maintain an activated nucleotide biosynthesis and further cell proliferation.⁶⁹ In the present study, the GSEA revealed an enhanced activity of the one-carbon pool by folate and purine biosynthesis, with higher expression levels of SHMT. These results, together with the higher expression levels of PHGDH, PSAT, and PSPH and all genes involved in the serine synthesis pathway, suggest that high-GS PCA patients might be using serine, but not glycine, to support one-carbon metabolism. Higher serum levels of glycine found in high-GS PCA patients in this study would be a consequence of this metabolite being produced from serine through the up-regulation SHMT. Also, these results are in accordance with metabolic alterations described in previous NMR-based metabolomic studies performed in tissue and serum samples^{70,71} from PCA patients.

In urine, we observed increased concentrations of MNA in high-GS PCA patients. Increased MNA levels have previously been associated with cancer progression. Xie et al. showed that

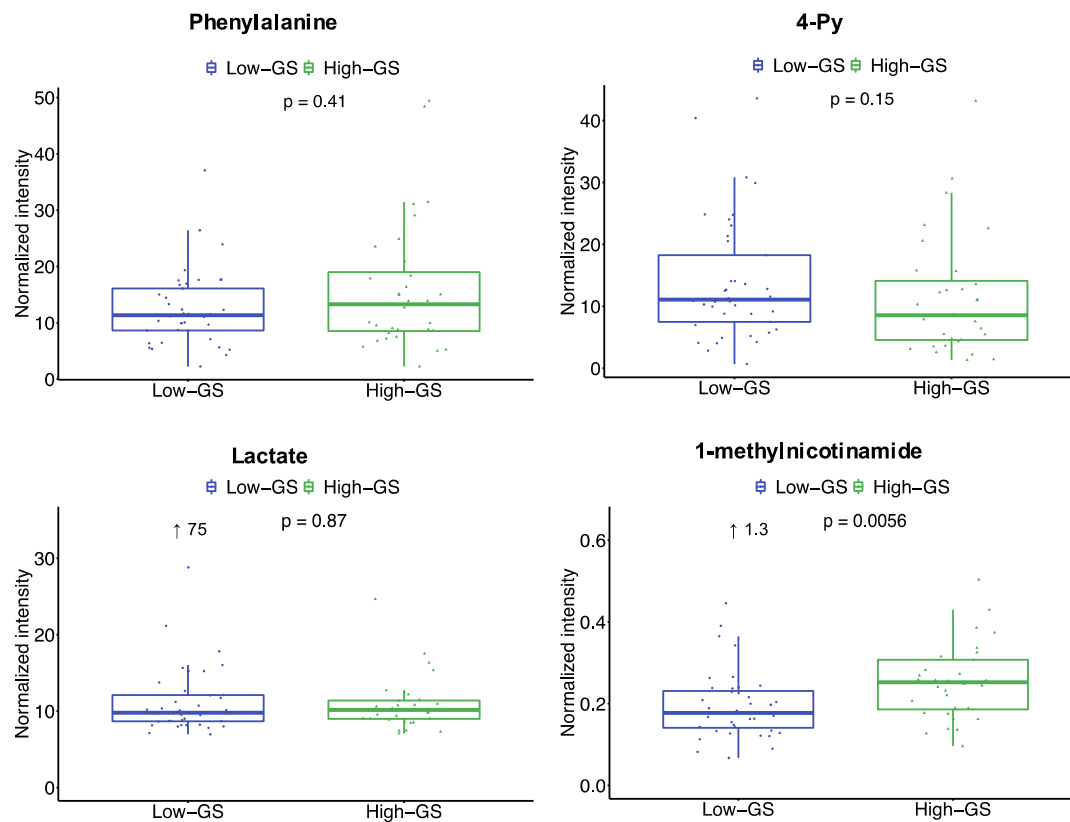


Figure 3. Box plot representing the normalized urine intensities of the metabolites showing higher variations in intensity between the groups of study (low-GS PCA: blue; high-GS PCA: green). For each box, the central line is the median, the edges of the box are the upper and lower quartiles, the whiskers extend the box by a further ± 1.5 interquartile range, and samples are plotted as individual points. *p*-value represented above the box plots and calculated using the Mann–Whitney–Wilcoxon test. 4-Py, N1-methyl-4-pyridone-5-carboxamide.

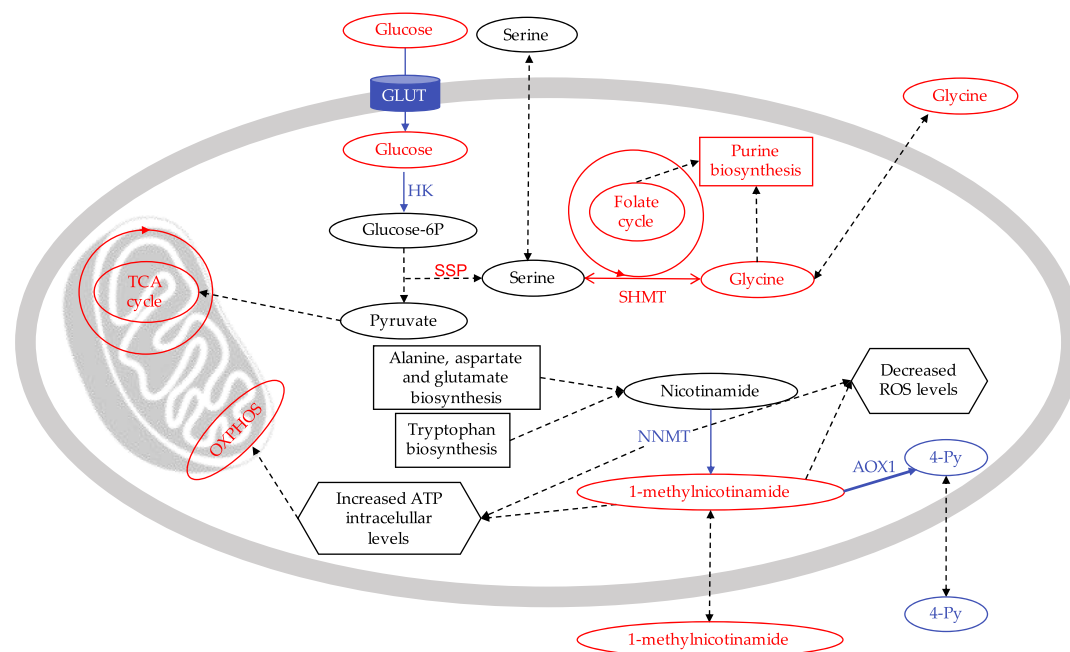


Figure 4. Schematic representation of the genetic and metabolic alterations found for the comparison between low- and high-GS PCA patients. Red and blue fonts indicate increases and decreases, respectively, in high-GS PCA patients. Noncolored font represents nonavailable data. Solid and dashed arrows are for direct and multistep reactions, respectively. 4-Py, N1-methyl-4-pyridone-5-carboxamide; AOX1, aldehyde oxidase 1; ATP, adenosine triphosphate; glucose-6P, glucose 6-phosphate; GLUT, glucose transporter; HK, hexokinase; NNMT, nicotinamide N-methyltransferase; OXPHOS, oxidative phosphorylation; ROS, reactive oxygen species; SHMT, serine hydroxymethyl transferase; SSP, serine synthesis pathway; TCA, tricarboxylic acid cycle.

MNA can accelerate cell growth, inhibit apoptosis, promote cell cycle progression, limit ROS production, and increase ATP production in colorectal cancer cells.⁷² In addition, another study reported that high levels of MNA can contribute to maintain enhanced OXPHOS activity in rapidly dividing cells, avoiding their metabolic shift toward glycolysis.⁷³ Notably, this finding perfectly correlates with the results obtained in the GSEA carried out in this study, as it was found that high-GS PCa patients were characterized by slow glycolysis and increased OXPHOS activities. Particularly, MNA is derived from nicotinamide by nicotinamide N-methyltransferase (NNMT) and then further catabolized to pyridones (2-Py and 4-Py) through aldehyde oxidase (AOX1). Interestingly, the AOX1 expression level has previously been shown to be lower in high-GS and in metastatic PCa samples.⁷⁴ In our study, although both NNMT and AOX1 were found to be down-regulated in the high-GS PCa group, the ratio NNMT/AOX1 was higher in this group of patients. Thus, we hypothesized that, in the high-GS PCa group, metabolism of MNA to pyridones might be lower than its synthesis from nicotinamide, resulting in its accumulation. This idea is also supported by the decreased levels of 4-Py observed in the high-GS PCa group (Figure 3).

Finally, phenylalanine was the only metabolite in this study that exhibited high increased levels both in the serum and urine samples of the high-GS PCa patients included in this study. Phenylalanine is metabolized to tyrosine through the enzyme phenylalanine hydroxylase (PAH). Dysfunctional PAH has been observed in inflammatory and malignant diseases, and elevated phenylalanine levels have also been observed in other cancer types.^{75–77} In the present study, lower PAH expression levels observed in high-GS PCa patients could be explaining the accumulation of phenylalanine in both biofluids.

CONCLUSIONS

The multiomics analysis performed in this study provides further evidence to the hypothesis that the combination of data from different complementary approaches could offer a broader picture of the metabolic changes underlying PCa progression. Overall, in this study, the targeted analysis of the metabolomic profile from PCa patients at different stages, based on complementary transcriptomics profiles, allowed the identification of significant metabolic alterations in high-grade PCa patients. These metabolic alterations include increased serum levels of glucose and glycine, and high levels of MNA in urine. Further validation of the results, analyzing biofluids and tissue-paired samples, using complementary metabolomics experimental approaches in larger and independent cohorts of patients and/or models, would be necessary to confirm the clinical potential of these findings. Taken together, although several limitations still need to be addressed, the results from this study demonstrate the great potential that these targeted approaches could have for the identification of new clinically relevant biomarkers.

ASSOCIATED CONTENT

Supporting Information

The Supporting Information is available free of charge at <https://pubs.acs.org/doi/10.1021/acs.jproteome.0c00493>.

Integration regions for the metabolites identified in serum samples of PCa patients, integration regions for the metabolites identified in urine samples of PCa

patients, GSEA of transcriptomics data sets included in this study, Venn diagram representing the overlap between the results obtained for the GSEA of the different PCa transcriptomic data sets included in the analysis (PDF)

AUTHOR INFORMATION

Corresponding Author

Leonor Puchades-Carrasco – Drug Discovery Unit, Instituto de Investigación Sanitaria La Fe, Valencia 46026, Spain; orcid.org/0000-0003-0340-7458; Phone: +34-96-124-6713; Email: leonor_puchades@iislafe.es

Authors

Nuria Gómez-Cebrián – Drug Discovery Unit, Instituto de Investigación Sanitaria La Fe, Valencia 46026, Spain; Laboratory of Molecular Biology, Fundación Instituto Valenciano de Oncología (FIVO), Valencia 46009, Spain

María García-Flores – Laboratory of Molecular Biology, Fundación Instituto Valenciano de Oncología (FIVO), Valencia 46009, Spain; IVO-CIPF Joint Research Unit of Cancer, Príncipe Felipe Research Centre (CIPF), Valencia 46012, Spain

José Rubio-Briones – Department of Urology, Fundación Instituto Valenciano de Oncología (FIVO), Valencia 46009, Spain

José Antonio López-Guerrero – Laboratory of Molecular Biology, Fundación Instituto Valenciano de Oncología (FIVO), Valencia 46009, Spain; IVO-CIPF Joint Research Unit of Cancer, Príncipe Felipe Research Centre (CIPF), Valencia 46012, Spain; Department of Basic Medical Sciences, School of Medicine, Catholic University of Valencia ‘San Vicente Martir’, Valencia 46001, Spain

Antonio Pineda-Lucena – Drug Discovery Unit, Instituto de Investigación Sanitaria La Fe, Valencia 46026, Spain; Molecular Therapeutics Program, Centro de Investigación Médica Aplicada, Navarra 31008, Spain

Complete contact information is available at: <https://pubs.acs.org/10.1021/acs.jproteome.0c00493>

Author Contributions

Conceptualization, J.A.L.-G., J.R.-B., A.P.-L., and L.P.-C.; methodology, N.G.-C. and M.G.-F.; formal analysis, A.P.-L., L.P.-C., and N.G.-C.; writing—original draft preparation, N.G.-C. and L.P.-C.; writing—review and editing, J.A.L.-G., A.P.-L., and L.P.-C. All authors have read and agreed to the published version of the manuscript.

Funding

Funding for the present study was provided by the Ministerio de Economía y Competitividad (SAF2017-89229-R) and the Conselleria de Educación, Investigación, Cultura y Deporte (GVA, PROMETEO/2016/103). Part of the equipment used in this work was cofunded by the Generalitat Valenciana and European Regional Development Fund (FEDER) funds (PO FEDER of Comunitat Valenciana 2014–2020).

Notes

The authors declare no competing financial interest.
¶These authors share co-senior authorship.

ACKNOWLEDGMENTS

Authors thank to the Biobank of the Fundación Instituto Valenciano de Oncología, belonging to the Valencia Network

of Biobanks (RVB) and the Spanish Network of Biobanks (RNB) for providing the samples necessary for carrying out this study.

REFERENCES

- (1) Bray, F.; Ferlay, J.; Soerjomataram, I.; Siegel, R. L.; Torre, L. A.; Jemal, A. Global Cancer Statistics 2018: GLOBOCAN Estimates of Incidence and Mortality Worldwide for 36 Cancers in 185 Countries. *Ca-Cancer J. Clin.* **2018**, *68*, 394–424.
- (2) Howlader, N.; Noone, A.; Krapcho, M.; Miller, B.; Brest, A.; Yu, M.; Ruhl, J.; Tatalovich, Z.; Mariotto, A.; Lewis, D.; Chen, H.; Feuer, E.; Cronin, K. *SEER Cancer Statistics Review*; National Cancer Institute: Bethesda, MD, 2020 (accessed Jan 31, 2020).
- (3) Offermann, A.; Hohensteiner, S.; Kuempers, C.; Ribbat-Idel, J.; Schneider, F.; Becker, F.; Hupe, M. C.; Duensing, S.; Merseburger, A. S.; Kirfel, J.; Reischl, M.; Lubczyk, V.; Kuefer, R.; Perner, S. Prognostic Value of the New Prostate Cancer International Society of Urological Pathology Grade Groups. *Front. Med.* **2017**, *4*, 157.
- (4) Miles, B.; Ittmann, M.; Wheeler, T.; Sayeeduddin, M.; Cubilla, A.; Rowley, D.; Bu, P.; Ding, Y.; Gao, Y.; Lee, M.; Ayala, G. E. Moving Beyond Gleason Scoring. *Arch. Pathol. Lab. Med.* **2019**, *143*, S65–S70.
- (5) Puchades-Carrasco, L.; Pineda-Lucena, A. Metabolomics Applications in Precision Medicine: An Oncological Perspective. *Curr. Top. Med. Chem.* **2017**, *17*, 2740–2751.
- (6) Puchades-Carrasco, L.; Jantus-Lewintre, E.; Pérez-Rambla, C.; García-García, F.; Lucas, R.; Calabuig, S.; Blasco, A.; Dopazo, J.; Camps, C.; Pineda-Lucena, A. Serum Metabolomic Profiling Facilitates the Non-Invasive Identification of Metabolic Biomarkers Associated with the Onset and Progression of Non-Small Cell Lung Cancer. *Oncotarget* **2016**, *7*, 12904–12916.
- (7) Vicente-Muñoz, S.; Cobo, T.; Puchades-Carrasco, L.; Sánchez-García, A. B.; Agustí, N.; Palacio, M.; Pineda-Lucena, A.; Gratacós, E. Vaginal Metabolome: Towards a Minimally Invasive Diagnosis of Microbial Invasion of the Amniotic Cavity in Women with Preterm Labor. *Sci. Rep.* **2020**, *10*, 5465.
- (8) Albers-Vaquer, A.; Rizvi, A.; Matzapetakis, M.; Lamosa, P.; Coelho, A. V.; Patel, M.; Mande, S. C.; Gaddam, S.; Pineda-Lucena, A.; Banerjee, S.; Puchades-Carrasco, L. Active and Prospective Latent Tuberculosis Are Associated with Different Metabolomic Profiles: Clinical Potential for the Identification of Rapid and Non-Invasive Biomarkers. *Emerging Microbes Infect.* **2020**, *9*, 1131–1139.
- (9) Gholizadeh, N.; Pundavela, J.; Nagarajan, R.; Dona, A.; Quadrelli, S.; Biswas, T.; Greer, P. B.; Ramadan, S. Nuclear Magnetic Resonance Spectroscopy of Human Body Fluids and in Vivo Magnetic Resonance Spectroscopy: Potential Role in the Diagnosis and Management of Prostate Cancer. *Urol. Oncol.: Semin. Orig. Invest.* **2020**, *38*, 150–173.
- (10) Manna, S. K.; Tanaka, N.; Krausz, K. W.; Haznadar, M.; Xue, X.; Matsubara, T.; Bowman, E. D.; Fearon, E. R.; Harris, C. C.; Shah, Y. M.; Gonzalez, F. J. Biomarkers of Coordinate Metabolic Reprogramming in Colorectal Tumors in Mice and Humans. *Gastroenterology* **2014**, *146*, 1313–1324.
- (11) Loras, A.; Suárez-Cabrera, C.; Martínez-Bisbal, M. C.; Quintás, G.; Paramio, J. M.; Martínez-Mañez, R.; Gil, S.; Ruiz-Cerdá, J. L. Integrative Metabolomic and Transcriptomic Analysis for the Study of Bladder Cancer. *Cancers* **2019**, *11*, 686.
- (12) Nam, H.; Chung, B. C.; Kim, Y.; Lee, K.; Lee, D. Combining Tissue Transcriptomics and Urine Metabolomics for Breast Cancer Biomarker Identification. *Bioinformatics* **2009**, *25*, 3151–3157.
- (13) Dutta, M.; Singh, B.; Joshi, M.; Das, D.; Subramani, E.; Maan, M.; Jana, S. K.; Sharma, U.; Das, S.; Dasgupta, S.; Ray, C. D.; Chakravarty, B.; Chaudhury, K. Metabolomics Reveals Perturbations in Endometrium and Serum of Minimal and Mild Endometriosis. *Sci. Rep.* **2018**, *8*, 6466.
- (14) More, T. H.; RoyChoudhury, S.; Christie, J.; Taunk, K.; Mane, A.; Santra, M. K.; Chaudhury, K.; Rapole, S. Metabolomic Alterations in Invasive Ductal Carcinoma of Breast: A Comprehensive Metabolomic Study Using Tissue and Serum Samples. *Oncotarget* **2018**, *9*, 2678–2696.
- (15) Liesenfeld, D. B.; Grapov, D.; Fahrman, J. F.; Salou, M.; Scherer, D.; Toth, R.; Habermann, N.; Böhm, J.; Schrotz-King, P.; Gigic, B.; Schneider, M.; Ulrich, A.; Herpel, E.; Schirmacher, P.; Fiehn, O.; Lampe, J. W.; Ulrich, C. M. Metabolomics and Transcriptomics Identify Pathway Differences between Visceral and Subcutaneous Adipose Tissue in Colorectal Cancer Patients: The ColoCare Study. *Am. J. Clin. Nutr.* **2015**, *102*, 433–443.
- (16) Eidelman, E.; Twum-Ampofo, J.; Ansari, J.; Siddiqui, M. M. The Metabolic Phenotype of Prostate Cancer. *Front. Oncol.* **2017**, *7*, 131.
- (17) Lima, A.; Araújo, A.; Pinto, J.; Jerónimo, C.; Henrique, R.; Bastos, M.; Carvalho, M.; Guedes de Pinho, P. GC-MS-Based Endometabolome Analysis Differentiates Prostate Cancer from Normal Prostate Cells. *Metabolites* **2018**, *8*, 23.
- (18) Struck-Lewicka, W.; Kordalewska, M.; Bujak, R.; Yumba Mpanga, A.; Markuszewski, M.; Jacyna, J.; Matuszewski, M.; Kaliszan, R.; Markuszewski, M. J. Urine metabolic fingerprinting using LC-MS and GC-MS reveals metabolite changes in prostate cancer: A pilot study. *J. Pharm. Biomed. Anal.* **2015**, *111*, 351–361.
- (19) Pérez-Rambla, C.; Puchades-Carrasco, L.; García-Flores, M.; Rubio-Briones, J.; López-Guerrero, J. A.; Pineda-Lucena, A. Non-Invasive Urinary Metabolomic Profiling Discriminates Prostate Cancer from Benign Prostatic Hyperplasia. *Metabolomics* **2017**, *13*, 52.
- (20) Sreekumar, A.; Poisson, L. M.; Rajendiran, T. M.; Khan, A. P.; Cao, Q.; Yu, J.; Laxman, B.; Mehra, R.; Lonigro, R. J.; Li, Y.; Nyati, M. K.; Ahsan, A.; Kalyana-Sundaram, S.; Han, B.; Cao, X.; Byun, J.; Omenn, G. S.; Ghosh, D.; Pennathur, S.; Alexander, D. C.; Berger, A.; Shuster, J. R.; Wei, J. T.; Varambally, S.; Beecher, C.; Chinnaiyan, A. M. Metabolomic Profiles Delineate Potential Role for Sarcosine in Prostate Cancer Progression. *Nature* **2009**, *457*, 910–914.
- (21) Kumar, D.; Gupta, A.; Mandhani, A.; Sankhwar, S. N. Metabolomics-Derived Prostate Cancer Biomarkers: Fact or Fiction? *J. Proteome Res.* **2015**, *14*, 1455–1464.
- (22) Bruzzzone, C.; Loizaga-Iriarte, A.; Sánchez-Mosquera, P.; Gil-Redondo, R.; Astobiza, I.; Diercks, T.; Cortazar, A. R.; Ugalde-Olano, A.; Schäfer, H.; Blanco, F. J.; Unda, M.; Cagnet, C.; Spraul, M.; Mato, J. M.; Embade, N.; Carracedo, A.; Millet, O. 1H NMR-Based Urine Metabolomics Reveals Signs of Enhanced Carbon and Nitrogen Recycling in Prostate Cancer. *J. Proteome Res.* **2020**, *19*, 2419–2428.
- (23) Jelonek, K.; Widlak, P. Metabolome-Based Biomarkers: Their Potential Role in the Early Detection of Lung Cancer. *Contemp. Oncol.* **2018**, *22*, 135–140.
- (24) Khamis, M. M.; Adamko, D. J.; El-Aneed, A. Strategies and Challenges in Method Development and Validation for the Absolute Quantification of Endogenous Biomarker Metabolites Using Liquid Chromatography-tandem Mass Spectrometry. *Mass Spectrom. Rev.* **2019**, *39*, 1–22.
- (25) Ros, S.; Santos, C. R.; Moco, S.; Baenke, F.; Kelly, G.; Howell, M.; Zamboni, N.; Schulze, A. Functional Metabolic Screen Identifies 6-Phosphofructo-2-Kinase/Fructose-2,6-Biphosphatase 4 as an Important Regulator of Prostate Cancer Cell Survival. *Cancer Discovery* **2012**, *2*, 328–343.
- (26) Sandsmark, E.; Andersen, M. K.; Bofin, A. M.; Bertilsson, H.; Drabløs, F.; Bathen, T. F.; Rye, M. B.; Tessem, M.-B. SFRP4 Gene Expression Is Increased in Aggressive Prostate Cancer. *Sci. Rep.* **2017**, *7*, 14276.
- (27) Yi, C.; Wan, X.; Zhang, Y.; Fu, F.; Zhao, C.; Qin, R.; Wu, H.; Li, Y.; Huang, Y. SNORA42 Enhances Prostate Cancer Cell Viability, Migration and EMT and Is Correlated with Prostate Cancer Poor Prognosis. *Int. J. Biochem. Cell Biol.* **2018**, *102*, 138–150.
- (28) Etheridge, T.; Straus, J.; Ritter, M. A.; Jarrard, D. F.; Huang, W. Semen AMACR Protein as a Novel Method for Detecting Prostate Cancer. *Urol. Oncol.: Semin. Orig. Invest.* **2018**, *36*, S32.e1–S32.e7.
- (29) Luo, X.; Yu, H.; Song, Y.; Sun, T. Integration of Metabolomic and Transcriptomic Data Reveals Metabolic Pathway Alteration in Breast Cancer and Impact of Related Signature on Survival. *J. Cell. Physiol.* **2019**, *234*, 13021–13031.

- (30) Hoang, L. T.; Domingo-Sabugo, C.; Starren, E. S.; Willis-Owen, S. A. G.; Morris-Rosendahl, D. J.; Nicholson, A. G.; Cookson, W. O. C. M.; Moffatt, M. F. Metabolomic, transcriptomic and genetic integrative analysis reveals important roles of adenosine diphosphate in haemostasis and platelet activation in non-small-cell lung cancer. *Mol. Oncol.* **2019**, *13*, 2406–2421.
- (31) Hasin, Y.; Seldin, M.; Lusic, A. Multi-Omics Approaches to Disease. *Genome Biol.* **2017**, *18*, 83.
- (32) Shao, Y.; Ye, G.; Ren, S.; Piao, H.-L.; Zhao, X.; Lu, X.; Wang, F.; Ma, W.; Li, J.; Yin, P.; Xia, T.; Xu, C.; Yu, J. J.; Sun, Y.; Xu, G. Metabolomics and transcriptomics profiles reveal the dysregulation of the tricarboxylic acid cycle and related mechanisms in prostate cancer. *Int. J. Cancer* **2018**, *143*, 396–407.
- (33) Ren, S.; Shao, Y.; Zhao, X.; Hong, C. S.; Wang, F.; Lu, X.; Li, J.; Ye, G.; Yan, M.; Zhuang, Z.; Xu, C.; Xu, G.; Sun, Y. Integration of Metabolomics and Transcriptomics Reveals Major Metabolic Pathways and Potential Biomarker Involved in Prostate Cancer. *Mol. Cell. Proteomics* **2016**, *15*, 154–163.
- (34) Ruiying, C.; Zeyun, L.; Yongliang, Y.; Zijia, Z.; Ji, Z.; Xin, T.; Xiaojian, Z. A Comprehensive Analysis of Metabolomics and Transcriptomics in Non-Small Cell Lung Cancer. *PLoS One* **2020**, *15*, e0232272.
- (35) Yang, K.; Xia, B.; Wang, W.; Cheng, J.; Yin, M.; Xie, H.; Li, J.; Ma, L.; Yang, C.; Li, A.; Fan, X.; Dhillon, H. S.; Hou, Y.; Lou, G.; Li, K. A Comprehensive Analysis of Metabolomics and Transcriptomics in Cervical Cancer. *Sci. Rep.* **2017**, *7*, 43353.
- (36) Sun, Q.; Zhao, W.; Wang, L.; Guo, F.; Song, D.; Zhang, Q.; Zhang, D.; Fan, Y.; Wang, J. Integration of Metabolomic and Transcriptomic Profiles to Identify Biomarkers in Serum of Lung Cancer. *J. Cell. Biochem.* **2019**, *120*, 11981–11989.
- (37) Olivier, M.; Asmis, R.; Hawkins, G. A.; Howard, T. D.; Cox, L. A. The Need for Multi-Omics Biomarker Signatures in Precision Medicine. *Int. J. Mol. Sci.* **2019**, *20*, 4781.
- (38) Andersen, M. K.; Giskeødegård, G. F.; Tessem, M.-B. Metabolic Alterations in Tissues and Biofluids of Patients with Prostate Cancer. *Curr. Opin. Endocr. Metab. Res.* **2020**, *10*, 23–28.
- (39) Gómez-Cebrián, N.; Rojas-Benedicto, A.; Albors-Vaquer, A.; López-Guerrero, J.; Pineda-Lucena, A.; Puchades-Carrasco, L. Metabolomics Contributions to the Discovery of Prostate Cancer Biomarkers. *Metabolites* **2019**, *9*, 48.
- (40) Beckonert, O.; Keun, H. C.; Ebbels, T. M. D.; Bundy, J.; Holmes, E.; Lindon, J. C.; Nicholson, J. K. Metabolic Profiling, Metabolomic and Metabonomic Procedures for NMR Spectroscopy of Urine, Plasma, Serum and Tissue Extracts. *Nat. Protoc.* **2007**, *2*, 2692–2703.
- (41) Ghini, V.; Quaglio, D.; Luchinat, C.; Turano, P. NMR for Sample Quality Assessment in Metabolomics. *New Biotechnol.* **2019**, *52*, 25–34.
- (42) Dona, A. C.; Jiménez, B.; Schäfer, H.; Humpfer, E.; Spraul, M.; Lewis, M. R.; Pearce, J. T. M.; Holmes, E.; Lindon, J. C.; Nicholson, J. K. Precision High-Throughput Proton NMR Spectroscopy of Human Urine, Serum, and Plasma for Large-Scale Metabolic Phenotyping. *Anal. Chem.* **2014**, *86*, 9887–9894.
- (43) Nicholson, J. K.; Foxall, P. J. D.; Spraul, M.; Farrant, R. D.; Lindon, J. C. 750 MHz ¹H and ¹H-¹³C NMR Spectroscopy of Human Blood Plasma. *Anal. Chem.* **1995**, *67*, 793–811.
- (44) Meiboom, S.; Gill, D. Modified Spin-Echo Method for Measuring Nuclear Relaxation Times. *Rev. Sci. Instrum.* **1958**, *29*, 688–691.
- (45) Vu, T. N.; Valkenburg, D.; Smets, K.; Verwaest, K. A.; Dommissie, R.; Lemièr, F.; Verschoren, A.; Goethals, B.; Laukens, K. An Integrated Workflow for Robust Alignment and Simplified Quantitative Analysis of NMR Spectrometry Data. *BMC Bioinf.* **2011**, *12*, 405.
- (46) Dieterle, F.; Ross, A.; Schlotterbeck, G.; Senn, H. Probabilistic Quotient Normalization as Robust Method to Account for Dilution of Complex Biological Mixtures. Application in ¹H NMR Metabolomics. *Anal. Chem.* **2006**, *78*, 4281–4290.
- (47) Sboner, A.; Demichelis, F.; Calza, S.; Pawitan, Y.; Setlur, S. R.; Hoshida, Y.; Perner, S.; Adami, H.-O.; Fall, K.; Mucci, L. A.; Kantoff, P. W.; Stampfer, M.; Andersson, S.-O.; Varenhorst, E.; Johansson, J.-E.; Gerstein, M. B.; Golub, T. R.; Rubin, M. A.; Andrén, O. Molecular Sampling of Prostate Cancer: A Dilemma for Predicting Disease Progression. *BMC Med. Genomics* **2010**, *3*, 8.
- (48) Mortensen, M. M.; Høyer, S.; Lynnerup, A.-S.; Ørntoft, T. F.; Sørensen, K. D.; Borre, M.; Dyrskjødt, L. Expression Profiling of Prostate Cancer Tissue Delineates Genes Associated with Recurrence after Prostatectomy. *Sci. Rep.* **2015**, *5*, 16018.
- (49) Ross-Adams, H.; Lamb, A. D.; Dunning, M. J.; Halim, S.; Lindberg, J.; Massie, C. M.; Egevad, L. A.; Russell, R.; Ramos-Montoya, A.; Vowler, S. L.; Sharma, N. L.; Kay, J.; Whitaker, H.; Clark, J.; Hurst, R.; Gnanapragasam, V. J.; Shah, N. C.; Warren, A. Y.; Cooper, C. S.; Lynch, A. G.; Stark, R.; Mills, I. G.; Grönberg, H.; Neal, D. E.; CamCaP Study Group. Integration of Copy Number and Transcriptomics Provides Risk Stratification in Prostate Cancer: A Discovery and Validation Cohort Study. *EBioMedicine* **2015**, *2*, 1133–1144.
- (50) Montaner, D.; Dopazo, J. Multidimensional Gene Set Analysis of Genomic Data. *PLoS One* **2010**, *5*, e10348.
- (51) Kanehisa, M. KEGG: Kyoto Encyclopedia of Genes and Genomes. *Nucleic Acids Res.* **2000**, *28*, 27–30.
- (52) Kanehisa, M.; Sato, Y.; Furumichi, M.; Morishima, K.; Tanabe, M. New Approach for Understanding Genome Variations in KEGG. *Nucleic Acids Res.* **2019**, *47*, D590–D595.
- (53) Kanehisa, M. Toward Understanding the Origin and Evolution of Cellular Organisms. *Protein Sci.* **2019**, *28*, 1947–1951.
- (54) Oliveros, J. C. Venny. An Interactive Tool for Comparing Lists with Venn's Diagrams, 2007. Available: <https://bioinfogp.cnb.csic.es/tools/venny/>.
- (55) Barfeld, S. J.; Fazli, L.; Persson, M.; Marjavaara, L.; Urbanucci, A.; Kaukoniemi, K. M.; Rennie, P. S.; Ceder, Y.; Chabes, A.; Visakorpi, T.; Mills, I. G. Myc-Dependent Purine Biosynthesis Affects Nucleolar Stress and Therapy Response in Prostate Cancer. *Oncotarget* **2015**, *6*, 12587–12602.
- (56) Kelly, R. S.; Sinnott, J. A.; Rider, J. R.; Ebot, E. M.; Gerke, T.; Bowden, M.; Pettersson, A.; Loda, M.; Sesso, H. D.; Kantoff, P. W.; Martin, N. E.; Giovannucci, E. L.; Tyekuceva, S.; Heiden, M. V.; Mucci, L. A. The Role of Tumor Metabolism as a Driver of Prostate Cancer Progression and Lethal Disease: Results from a Nested Case-Control Study. *Cancer Metab.* **2016**, *4*, 22.
- (57) Penney, K. L.; Sinnott, J. A.; Fall, K.; Pawitan, Y.; Hoshida, Y.; Kraft, P.; Stark, J. R.; Fiorentino, M.; Perner, S.; Finn, S.; Calza, S.; Flavin, R.; Freedman, M. L.; Setlur, S.; Sesso, H. D.; Andersson, S.-O.; Martin, N.; Kantoff, P. W.; Johansson, J.-E.; Adami, H.-O.; Rubin, M. A.; Loda, M.; Golub, T. R.; Andrén, O.; Stampfer, M. J.; Mucci, L. A. MRNA Expression Signature of Gleason Grade Predicts Lethal Prostate Cancer. *J. Clin. Oncol.* **2011**, *29*, 2391–2396.
- (58) Ashton, T. M.; McKenna, W. G.; Kunz-Schughart, L. A.; Higgins, G. S. Oxidative Phosphorylation as an Emerging Target in Cancer Therapy. *Clin. Cancer Res.* **2018**, *24*, 2482–2490.
- (59) Nayak, A.; Kapur, A.; Barroilhet, L.; Patankar, M. Oxidative Phosphorylation: A Target for Novel Therapeutic Strategies Against Ovarian Cancer. *Cancers* **2018**, *10*, 337.
- (60) Sica, V.; Bravo-San Pedro, J. M.; Stoll, G.; Kroemer, G. Oxidative Phosphorylation as a Potential Therapeutic Target for Cancer Therapy. *Int. J. Cancer* **2020**, *146*, 10–17.
- (61) Wright, J. L.; Plymate, S. R.; Porter, M. P.; Gore, J. L.; Lin, D. W.; Hu, E.; Zeliadt, S. B. Hyperglycemia and Prostate Cancer Recurrence in Men Treated for Localized Prostate Cancer. *Prostate Cancer Prostatic Dis.* **2013**, *16*, 204–208.
- (62) Wulaningsih, W.; Holmberg, L.; Garmo, H.; Zethelius, B.; Wigertz, A.; Carroll, P.; Lambe, M.; Hammar, N.; Walldius, G.; Jungner, I.; Van Hemelrijck, M. Serum Glucose and Fructosamine in Relation to Risk of Cancer. *PLoS One* **2013**, *8*, e54944.
- (63) Liu, Y. Fatty Acid Oxidation Is a Dominant Bioenergetic Pathway in Prostate Cancer. *Prostate Cancer Prostatic Dis.* **2006**, *9*, 230–234.

(64) Liu, Y.; Zuckier, L. S.; Ghesani, N. V. Dominant Uptake of Fatty Acid over Glucose by Prostate Cells: A Potential New Diagnostic and Therapeutic Approach. *Anticancer Res.* **2010**, *30*, 369–374.

(65) Wu, X.; Daniels, G.; Lee, P.; Monaco, M. E. Lipid Metabolism in Prostate Cancer. *Am. J. Clin. Exp. Urol.* **2014**, *2*, 111–120.

(66) Richter, J. A.; Rodríguez, M.; Rioja, J.; Peñuelas, I.; Martí-Clement, J.; Garrastachu, P.; Quincoces, G.; Zudaire, J.; García-Velloso, M. J. Dual Tracer ¹¹C-Choline and FDG-PET in the Diagnosis of Biochemical Prostate Cancer Relapse after Radical Treatment. *Mol. Imaging Biol.* **2010**, *12*, 210–217.

(67) Jain, M.; Nilsson, R.; Sharma, S.; Madhusudhan, N.; Kitami, T.; Souza, A. L.; Kafri, R.; Kirschner, M. W.; Clish, C. B.; Mootha, V. K. Metabolite Profiling Identifies a Key Role for Glycine in Rapid Cancer Cell Proliferation. *Science* **2012**, *336*, 1040–1044.

(68) Rose, M. L.; Madren, J.; Bunzendahl, H.; Thurman, R. G. Dietary Glycine Inhibits the Growth of B16 Melanoma Tumors in Mice. *Carcinogenesis* **1999**, *20*, 793–798.

(69) Labuschagne, C. F.; van den Broek, N. J. F.; Mackay, G. M.; Vousden, K. H.; Maddocks, O. D. K. Serine, but Not Glycine, Supports One-Carbon Metabolism and Proliferation of Cancer Cells. *Cell Rep.* **2014**, *7*, 1248–1258.

(70) McDunn, J. E.; Li, Z.; Adam, K.-P.; Neri, B. P.; Wolfert, R. L.; Milburn, M. V.; Lotan, Y.; Wheeler, T. M. Metabolomic signatures of aggressive prostate cancer. *Prostate* **2013**, *73*, 1547–1560.

(71) Kumar, D.; Gupta, A.; Mandhani, A.; Sankhwar, S. N. NMR spectroscopy of filtered serum of prostate cancer: A new frontier in metabolomics. *Prostate* **2016**, *76*, 1106–1119.

(72) Xie, X.; Yu, H.; Wang, Y.; Zhou, Y.; Li, G.; Ruan, Z.; Li, F.; Wang, X.; Liu, H.; Zhang, J. Nicotinamide N-Methyltransferase Enhances the Capacity of Tumorigenesis Associated with the Promotion of Cell Cycle Progression in Human Colorectal Cancer Cells. *Arch. Biochem. Biophys.* **2014**, *564*, 52–66.

(73) Ramsden, D. B.; Waring, R. H.; Barlow, D. J.; Parsons, R. B. Nicotinamide N-Methyltransferase in Health and Cancer. *Int. J. Tryptophan Res.* **2017**, *10*, 117864691769173.

(74) Varisli, L. Identification of New Genes Downregulated in Prostate Cancer and Investigation of Their Effects on Prognosis. *Genet. Test. Mol. Biomarkers* **2013**, *17*, 562–566.

(75) Sirniö, P.; Väyrynen, J. P.; Klintrup, K.; Mäkelä, J.; Karhu, T.; Herzig, K.-H.; Minkkinen, I.; Mäkinen, M. J.; Karttunen, T. J.; Tuomisto, A. Alterations in Serum Amino-Acid Profile in the Progression of Colorectal Cancer: Associations with Systemic Inflammation, Tumour Stage and Patient Survival. *Br. J. Cancer* **2019**, *120*, 238–246.

(76) Neurauter, G.; Grahmann, A. V.; Klieber, M.; Zeimet, A.; Ledochowski, M.; Sperner-Unterweger, B.; Fuchs, D. Serum Phenylalanine Concentrations in Patients with Ovarian Carcinoma Correlate with Concentrations of Immune Activation Markers and of Isoprostane-8. *Cancer Lett.* **2008**, *272*, 141–147.

(77) Zhang, X.; Xu, L.; Shen, J.; Cao, B.; Cheng, T.; Zhao, T.; Liu, X.; Zhang, H. Metabolic Signatures of Esophageal Cancer: NMR-Based Metabolomics and UHPLC-Based Focused Metabolomics of Blood Serum. *Biochim. Biophys. Acta, Mol. Basis Dis.* **2013**, *1832*, 1207–1216.

Review

Metabolic Phenotyping in Prostate Cancer Using Multi-Omics Approaches

Nuria Gómez-Cebrián ¹, José Luis Poveda ², Antonio Pineda-Lucena ^{3,*} and Leonor Puchades-Carrasco ^{1,*}¹ Drug Discovery Unit, Instituto de Investigación Sanitaria La Fe, 46026 Valencia, Spain; nuria_gomez@iislafe.es² Pharmacy Department, Hospital Universitario y Politécnico La Fe, 46026 Valencia, Spain; poveda_josand@gva.es³ Molecular Therapeutics Program, Centro de Investigación Médica Aplicada, 31008 Navarra, Spain

* Correspondence: apinedal@unav.es (A.P.-L.); leonor_puchades@iislafe.es (L.P.-C.)

Simple Summary: Prostate cancer (PCa) is a hormone-dependent tumor characterized by a highly heterogeneous clinical outcome. This neoplastic process has become a leading cause of cancer worldwide, with over 1.4 million new cases and a total of 375,000 deaths in 2020. Despite the efforts to improve the diagnosis, risk stratification, and treatment of PCa patients, a number of challenges still need to be addressed. In this context, integration of different multi-omics datasets may represent a powerful approach for the development of novel metabolic signatures that could contribute to the clinical management of PCa patients. This review aims to provide the most relevant findings of recently published multi-omics studies with a particular focus on describing the metabolic alterations associated with PCa.

Abstract: Prostate cancer (PCa), one of the most frequently diagnosed cancers among men worldwide, is characterized by a diverse biological heterogeneity. It is well known that PCa cells rewire their cellular metabolism to meet the higher demands required for survival, proliferation, and invasion. In this context, a deeper understanding of metabolic reprogramming, an emerging hallmark of cancer, could provide novel opportunities for cancer diagnosis, prognosis, and treatment. In this setting, multi-omics data integration approaches, including genomics, epigenomics, transcriptomics, proteomics, lipidomics, and metabolomics, could offer unprecedented opportunities for uncovering the molecular changes underlying metabolic rewiring in complex diseases, such as PCa. Recent studies, focused on the integrated analysis of multi-omics data derived from PCa patients, have in fact revealed new insights into specific metabolic reprogramming events and vulnerabilities that have the potential to better guide therapy and improve outcomes for patients. This review aims to provide an up-to-date summary of multi-omics studies focused on the characterization of the metabolomic phenotype of PCa, as well as an in-depth analysis of the correlation between changes identified in the multi-omics studies and the metabolic profile of PCa tumors.

Keywords: prostate cancer; metabolism; multi-omics; metabolomics



Citation: Gómez-Cebrián, N.; Poveda, J.L.; Pineda-Lucena, A.; Puchades-Carrasco, L. Metabolic Phenotyping in Prostate Cancer Using Multi-Omics Approaches. *Cancers* **2022**, *14*, 596. <https://doi.org/10.3390/cancers14030596>

Academic Editor: Jerome Solassol

Received: 28 December 2021

Accepted: 20 January 2022

Published: 25 January 2022

Publisher's Note: MDPI stays neutral with regard to jurisdictional claims in published maps and institutional affiliations.



Copyright: © 2022 by the authors. Licensee MDPI, Basel, Switzerland. This article is an open access article distributed under the terms and conditions of the Creative Commons Attribution (CC BY) license (<https://creativecommons.org/licenses/by/4.0/>).

1. Introduction

Prostate cancer (PCa) is the second most frequent cancer and represents the fifth leading cause of cancer-related death in men worldwide [1]. According to the Global Cancer Incidence, Mortality, and Prevalence (GLOBOCAN) database, new PCa cases were estimated to account for almost 1.4 million, with a total of 375,000 cancer-related deaths in 2020 [1]. Clinically, PCa is characterized by a heterogeneous behavior, ranging from indolent phenotypes to a rapid progression into an aggressive metastatic disease [2]. Early PCa diagnosis mainly relies on prostate-specific antigen (PSA) tests, although this screening method exhibits several limitations as it is prostate-specific but not cancer-specific [3], leading to overdiagnosis and overtreatment [4–6]. Thus, histopathological evaluation

of biopsies, graded on the basis of the Gleason Score (GS) [7], is required to confirm the presence of PCa [8] and to determine the treatment strategy to follow [9]. However, prostate biopsy is an invasive procedure that might cause health complications (e.g., hematospermia, hematuria, fever, bleeding, urinary retention) [10,11]. In addition, although the grading system has been modified several times, there remains no classification scheme that allows accurately discriminating indolent from aggressive PCa stages [12]. Thus, there is a need for more precise and robust PCa biomarkers to improve diagnosis and risk stratification of patients.

In recent years, metabolic phenotyping has become a powerful approach for the identification of new molecular biomarkers and metabolic vulnerabilities that could represent novel therapeutic opportunities in oncological diseases [13–18]. Hence, several metabolomics analyses have been carried out on PCa samples (e.g., tissue, urine, serum, plasma, and seminal fluid) to characterize the specific metabolic profile associated with PCa progression and identify metabolic alterations that may potentially be used as clinical biomarkers (reviewed in [19–22]). Together, these studies have revealed a specific metabolic phenotype that could distinguish between healthy and PCa samples [23]. Healthy prostate cells accumulate high concentrations of zinc, which results in the inhibition of mitochondrial aconitase (ACO2) and consequently decreases citrate oxidation, thus disrupting the tricarboxylic acid (TCA) cycle metabolism [24]. In contrast, decreased zinc levels in PCa tumors enable the activation of ACO2 for citrate oxidation and subsequent re-establishment of the TCA cycle [23,25]. In line with this, metabolic studies have reported decreased citrate levels and increased concentrations of several TCA cycle intermediates (e.g., fumarate, malate, and succinate) in PCa tumor samples when compared with healthy prostate tissues, suggesting an increased TCA cycle metabolism [26–29]. In addition, other studies have reported lower levels of polyamines and sarcosine metabolism (e.g., spermine, spermidine, sarcosine) [29–33], as well as dysregulations of several amino acids (e.g., alanine, glutamate, arginine, tyrosine, phenylalanine) [26–28,34–39] and other metabolites involved in cellular membrane metabolism (e.g., choline, phospholipids) [26,27,40–44].

These metabolic alterations have been observed at different omics levels [45–47]. For instance, transcriptomics analyses facilitated the identification of three distinct metabolism-associated PCa clusters and the development of a six-gene metabolic signature associated with disease-free survival [47]. In addition, following a loss-of-function genetic screen, the glycolytic 6-phosphofructo-2-kinase/fructose-2,6-biphosphatase 4 (*PFKFB4*) enzyme was identified as an essential gene for PCa cell survival and evaluated as a potential therapeutic target for PCa treatment [48]. On the other hand, proteomics analyses carried out on PCa cell lines and tissue samples revealed that enzymes involved in the ketogenic metabolism pathway were overexpressed in high-grade PCa [49]. Furthermore, the characterization of the proteomics landscape of exosomes, isolated from primary prostate epithelial and PCa cell lines, identified four exosomal proteins (PDCD6IP, FASN, XPO1, and ENO1) as potential new candidate biomarkers for PCa [50]. Moreover, lipidomics, an emerging omics approach [51], has also demonstrated its potential as an alternative diagnostic tool in PCa, revealing specific associations between alterations in glycerophospholipid metabolism and fatty-acid synthesis and oxidation with PCa progression [52,53].

In summary, the information derived from different omics studies offers new avenues for better understanding the biological and molecular processes underlying metabolic changes occurring during cancer progression, as well as for developing novel molecular biomarkers to improve the clinical management of cancer patients. Moreover, a number of studies have demonstrated that the combination of multi-omics data can provide deeper insight into the metabolic changes associated with the progression of different oncological diseases than any of these omics on their own [54–57]. Thus, the integration of different omics platforms has emerged as a powerful and promising strategy for the elucidation of potential genetic and epigenetic alterations, changes in gene expression levels and signaling pathways, and other biological dysregulations that could be driving metabolic rewiring during cancer progression. Hence, this review aims to provide the most relevant

metabolic rewiring during cancer progression. Hence, this review aims to provide the most relevant findings reported in recently published multi-omics-based studies focused on the analysis of metabolic alterations associated with PCa initiation and progression (Figure 1). To that end, a literature search was conducted on PubMed, using different combinations of the following terms: “(omics OR multi-omics OR omics integration OR (metabolomics OR lipidomics) AND (metabolomics OR lipidomics OR transcriptomics OR genomics OR epigenomics OR proteomics) AND (metabol * OR metabolic profiling OR metabolic phenotype)) AND prostate cancer”. Then, titles and abstracts of the selected publications were examined to evaluate their eligibility according to their relevance on the issue of interest and to determine their inclusion in the review.

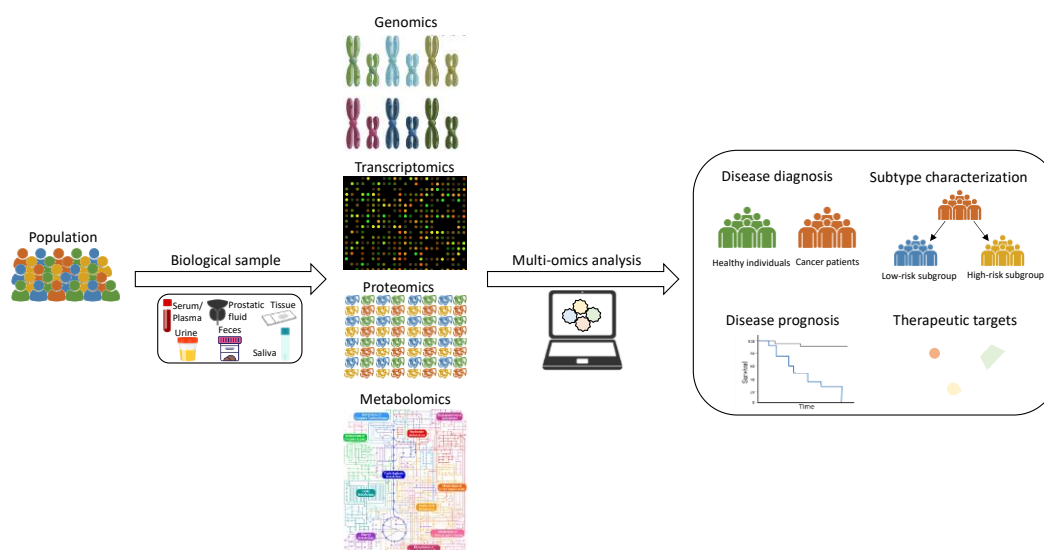


Figure 1. Graphical representation of different omics-based approaches and multi-omics analyses applied to the characterization of PCa-related metabolic alterations.

2. PCa Multi-Omics Studies

Between 2013 and 2021, 21 studies, focused on characterizing the specific metabolic profile associated with PCa, reported the integration of data from at least two different omics platforms. Tissue was by far the most frequently analyzed sample (15 studies), cell lines were harvested in four studies, biofluids (urine, serum) from Pca patients were collected in three of the studies, and only one of them relied on using murine models. Integration of transcriptomics and metabolomics was conducted in most of the studies, while transcriptomics, metabolomics, and lipidomics were only combined in two of them. Lastly, mass spectroscopy (MS) was preferentially chosen over nuclear magnetic resonance (NMR) as analytical platform for proteomics, metabolomics, or lipidomics analyses.

2.1. Benign Tissue vs. PCa Tumor

Nine of the studies discussed in this review relied on the analysis of benign prostate and PCa samples for identifying specific metabolic alterations associated with the metabolic phenotype of PCa patients (Table 1). Integration of transcriptomics and metabolomics data was the primary approach followed in these studies, and tissue samples were the biological specimens preferentially collected.

Table 1. Most relevant metabolic alterations reported in recent multi-omics studies focused on the characterization of the specific metabolic phenotype of PCa patients.

Study	Sample	Omics Data	Major Findings *
Meller et al. [58]	Tissue	M + T	↑ <i>ACC</i> , <i>ACLY</i> , <i>FASN</i> , <i>SCD</i> , 2-hydroxybehenic acid, cerebronic acid, glycerol phosphate, palmitic acid, GSH/GSSG, and spermidine ↓ putrescine and spermine
Li et al. [59]	Tissue	L + T	↑ <i>PLA2s</i> , free MUFA and PUFA, and <i>LPLATs</i> ↓ free SFA, PUFA-acyl, and ether-linked chains in PLs
Torrano et al. [60]	Cell lines	M + T	↓ <i>PGC1A</i> , FAO, and TCA cycle
Lima et al. [61]	Tissue	L + M	↑ amino-acid metabolism, nicotinate and nicotinamide metabolism, purine metabolism, and glycerophospholipid metabolism
Shao et al. [62]	Tissue	M + T	↑ fumarate, malate, succinate, 2-hydroxyglutaric acid, 2-ketoglutarate, glutamine, glutamate, PDH, GLS, <i>GLUD1</i> , <i>GLUD2</i> , and BCAA degradation enzymes
Tessem et al. [63]	Tissue	M + T	↑ <i>ACLY</i> , <i>ACACA</i> , <i>FASN</i> , <i>SAT1</i> , <i>SMOX</i> , <i>SRM</i> , and succinate, ↓ <i>ACO1</i> , <i>SDHD</i> , <i>SUCLA2</i> , putrescine, and citrate
Kaushik et al. [64]	Tissue	M + T	↑ HBP, <i>GNPNAT1</i> , <i>UAP1</i> , and UDP-GlcNAc
Ren et al. [65]	Tissue	M + T	↑ HBP, UDP-GlcNAc, and sphingosine
Lee et al. [66]	Urine	M + T	↑ <i>GOT1</i> and glutamate

ACACA: acetyl-CoA carboxylase alpha, *ACC*: acetyl-CoA carboxylase, *ACLY*: ATP citrate lyase, *ACO1*: aconitase, BCAA: branched-chain amino acids, FAO: fatty-acid oxidation, *FASN*: fatty-acid synthase, GLS: glutaminase, *GLUD1*: glutamate dehydrogenase 1, *GLUD2*: glutamate dehydrogenase 2, *GNPNAT1*: glucosamine-phosphate *N*-acetyltransferase 1, *GOT1*: glutamate oxaloacetate transaminase 1, GSH: reduced glutathione, GSSG: oxidized glutathione, HBP: hexosamine biosynthesis pathway, L: lipidomics, *LPLATs*: lysophospholipid acyltransferase, M: metabolomics, MUFA: mono-unsaturated fatty acids, PDH: pyruvate dehydrogenase, *PGC1A*: PPARγ coactivator 1 alpha, PLs: phospholipids, *PLA2s*: phospholipase A2, PUFA: polyunsaturated fatty acids, *SAT1*: spermidine/spermine *N1*-acetyltransferase 1, *SCD*: acyl-CoA desaturase, *SDHD*: succinate dehydrogenase complex subunit D, SFA: saturated fatty acids, *SMOX*: spermine oxidase, *SRM*: spermidine synthase, *SUCLA2*: succinate-CoA ligase ADP-forming beta subunit, T: transcriptomics, TCA: tricarboxylic acid, *UAP1*: UDP *N*-acetyl glucosamine pyrophosphate 1. * Direction of variation, considering the benign group as reference. Up and down arrows indicate direction of the variation observed in PCa samples.

Several of these studies reported alterations in enzymes and/or metabolites involved in fatty-acid metabolism. Among them, Meller et al. observed a highly deregulated metabolism of fatty acids, sphingolipids, and polyamines in malignant tissue [58]. Altered fatty-acid and sphingolipid metabolism was associated with increased expression of acetyl-CoA carboxylase (*ACC*), ATP citrate lyase (*ACLY*), fatty-acid synthase (*FASN*), and acyl-CoA desaturase (*SCD*) as well as with elevated concentrations of several fatty acids, such as 2-hydroxybehenic acid, cerebronic acid, glycerol phosphate, and palmitic acid. Furthermore, a higher ratio of reduced (GSH) to oxidized (GSSG) glutathione and alterations in the levels of several metabolites involved in polyamine metabolism, including putrescine, spermine, and spermidine, were detected in PCa tumors. These observations were based on the metabolomics, transcriptomics, and immunohistochemistry analysis of matched malignant and nonmalignant prostatectomy samples from 106 PCa patients. These results are in agreement with previous studies reporting *FASN* to be upregulated in PCa tumors [67–69], and *SCD* to promote PCa proliferation [70], as its inhibition resulted in a reduction in tumor growth [71]. Other studies reported higher glutathione reductase activity in PCa, leading to higher GSH levels, which could confer higher oxidative stress resistance to these tumors [72]. A recent study also showed that mTORC1 regulated polyamine synthesis as part of an essential oncogenic metabolic reprogramming in PCa [73].

Dysregulated lipid metabolism in PCa was also reported by Li et al., in a study focused on understanding the regulatory networks involved in adaptative transformation of lipid metabolism in PCa tissues [59]. Following a network-wide integrated mapping of lipid metabolism, including changes in the lipidome, transcript alterations, and post-transcriptional regulations, the authors observed a significant upregulation of de novo lipogenesis and a strengthened biosynthesis of phospholipids (PLs) via a de novo path-

way in PCa lipogenesis, together with a reprogrammed composition in membrane PLs. Overall, percentages of free mono- and polyunsaturated fatty acids (MUFAs and PUFAs, respectively) were elevated, while free saturated fatty acids (SFA) were reduced. Moreover, activated PL remodeling was characterized by enhanced activities of phospholipase A2 (*PLA2s*) and reduced lysophospholipid acyltransferase (*LPLATs*), which contributed to increased MUFA-acyl residues and reduced PUFA-acyl and ether-linked chains in PCa PLs. In fact, lipogenesis upregulation has been described as a hallmark of invasive cancers and termed the “lipogenic phenotype” [74]. Furthermore, several studies have associated changes in the PL content of the cellular membrane with PCa aggressiveness [27,75,76].

The characterization of relevant master regulators contributing to the metabolic switch in PCa was also evaluated in a multi-omics study conducted by Torrano et al. [60]. In this study, the analysis of the expression levels of several metabolic coregulators in five different PCa datasets revealed that only alterations in the transcriptional coactivator PPARC coactivator 1 alpha (*PPARGC1A* or *PGC1A*), PPARC coactivator 1 beta (*PPARGC1B* or *PGC1B*), and histone deacetylase 1 (*HDAC1*) expression were present in the majority or all datasets. Among them, *PGC1A* was the only coregulator negatively associated with GS. Additional integrative metabolomics analysis demonstrated that the tumor suppressive activity of *PGC1A* was associated with a global metabolic rewiring, leading to an enhanced fatty-acid β -oxidation and TCA cycle activity. TCA cycle downregulation has also been associated with PCa progression in other multi-omics studies [77], while upregulation of TCA cycle activity has been observed when comparing PCa tumor vs. adjacent prostate tissue [62]. Notably, the results from these studies are in agreement with a previously undescribed two-step metabolic shift in the TCA cycle during PCa development and progression, which was recently identified by Latonen et al. [77]. Further in vitro and in vivo analyses performed in this study demonstrated the role of *PGC1A* in tumor progression and metastatic dissemination, with these results also being in agreement with recent findings [78]. Moreover, a recent study showed that downregulation of *PGC1A* could promote PCa aggressiveness through activation of the polyamine pathway [79].

The comparison of benign and PCa tissue samples has also revealed additional changes in energy-related metabolic pathways. Thus, in a study conducted by Lima et al., an analysis of the metabolomics and lipidomics profiles of benign and PCa tissues by NMR and MS revealed metabolic dysregulations associated with PCa development [61]. The multivariate statistical analyses revealed that the levels of 26 metabolites, including different amino acids, organic acids, and nucleotide derivatives, and 21 phospholipid species were significantly altered between both groups. Furthermore, a metabolic pathway analysis revealed 11 dysregulated metabolic pathways associated with PCa development. Dysregulations in these pathways were confirmed by strong correlations among metabolites participating in the same pathway. The main metabolic pathways associated with PCa were amino-acid metabolism, nicotinate and nicotinamide metabolism, purine metabolism, and glycerophospholipid metabolism. Notably, metabolites involved in these pathways were upregulated in PCa tissues, being in accordance with other results published in previous studies [21–23]. Many of these pathways provide metabolic intermediates for the TCA cycle, nucleotide synthesis, and lipid synthesis, thus contributing to the production of high levels of cellular building blocks required for rapid proliferation of cancer cells [13,80].

Shao et al. also reported accumulation and upregulation of metabolites and genes related to the TCA cycle in another multi-omics-based study [62]. Metabolomics and transcriptomics analysis of PCa tumors and matched adjacent normal tissues revealed significant accumulations of key TCA metabolic intermediates (malate, fumarate, succinate, and 2-hydroxyglutaric acid) and enrichment in genes from different anaplerotic routes, including those involved in pyruvate, glutamine catabolism, and branched-chain amino-acid (BCAA) degradation. Associations between TCA cycle and the potential anaplerotic routes were supported by increased expression of pyruvate dehydrogenase (*PDH*) complex, higher expression levels of different BCAA degradation genes, glutaminase (*GLS*) and glutamate dehydrogenase (*GLUD1* and *GLUD2*), and higher α -ketoglutarate, glutamine, and gluta-

mate levels. Dysregulations in the TCA cycle were also identified in PCa tissues by Tessem et al. after accounting for the confounding effect of stroma [63]. In this study, integration of metabolomics and transcriptomics data revealed associations between increased succinate levels, also observed in other studies [29,81], and downregulation of succinate-CoA ligase ADP-forming subunit beta (*SUCLA2*) and succinate dehydrogenase complex subunit D (*SDHD*). Additional observations included lower citrate levels and decreased expression of *ACO1*, together with overexpression of fatty-acid synthesis genes *ACLY*, acetyl-CoA carboxylase alpha (*ACACA*), and *FASN*, suggesting an enhanced fatty-acid synthesis in these tissues. Reduced citrate concentrations and increased lipid synthesis are considered relevant metabolic features of PCa [23,82]. Furthermore, the authors observed relevant associations between reduced putrescine levels and upregulation of spermidine synthase (*SRM*), as well as lower spermine and increased spermidine/spermine *N*1-acetyltransferase 1 (*SAT1*) and spermine oxidase (*SMOX*) expression. In agreement with these results, other authors also reported a reduction in spermine and putrescine levels [34,58,74,75], as well as an overexpression of enzymes involved in the polyamine pathway [83–85].

In another study conducted by Kaushik et al., transcriptomics and metabolomics analyses were integrated, using a pathway-centric analytical framework that enabled the combination of the rankings of biochemical pathways enriched independently by gene expression and metabolic profiles in a single significance score [64]. Following this analysis, the hexosamine biosynthesis pathway (HBP) was found to be the most enriched pathway in treatment-naïve localized PCa, when compared to benign adjacent prostate tissues. Moreover, in silico analysis showed that the expression of glucosamine-phosphate *N*-acetyltransferase 1 (*GNPNAT1*) and UDP *N*-acetyl glucosamine pyrophosphate 1 (*UAP1*) were significantly elevated in PCa tumors. In contrast, HBP genes were significantly downregulated in castrate-resistant prostate cancer (CRPC) in comparison with localized PCa. The opposite effect of the HBP on the growth of androgen-dependent PCa and CRPC cells suggests the existence of metabolic rewiring during PCa progression. Moreover, on the basis of different in vitro and in vivo approaches, the authors concluded that downregulation of HBP in CRPC cells modulates progression via either PI3K/Akt or specific protein 1 (SP1)-regulated expression of carbohydrate response element-binding protein (ChREBP), depending on the androgen receptor variant. Previous studies have also reported several metabolic rewiring mechanisms associated with different androgen receptor variants [86]. Lastly, in this study, the authors evaluated the therapeutic efficacy of UDP-GlcNAc treatment, alone and in combination with anti-androgen therapy, for the treatment of CRPC-like tumors bearing different androgen receptor variants. Notably, in vivo UDP-GlcNAc treatment significantly reduced the proliferation in all assayed CRPC-like tumors. These findings are particularly relevant as CRPC cells containing the AR-V7 variant are essentially resistant to anti-androgen therapy. Interestingly, Ren et al. also reported increased activity of the HBP in PCa compared to adjacent prostate tissues [65]. In both studies, UDP-GlcNAc, the end product of the HBP and a key substrate for the *O*-linked *N*-acetyl-glucosamine transferase (OGT), which plays a vital role in *O*-GlcNAcylated modification of proteins, was found to be increased in PCa tissues [64,65]. Interestingly, posttranslational *O*-GlcNAcylation of chromatin is a significant feature of enhancers in the PCa genome [46,87]. In addition to the HBP, Ren et al. reported metabolic perturbations in other metabolic pathways, including the metabolism of cysteine and methionine and nucleotide sugars, glycerophospholipids, lysine, and sphingolipids. Moreover, nine metabolites showed potential utility as metabolic PCa biomarkers. Among them, sphingosine demonstrated high specificity and sensitivity for distinguishing PCa from benign prostatic hyperplasia (BPH), particularly in patients with low PSA levels. Other metabolomics studies have also reported alterations in the HBP and sphingolipid metabolism when analyzing the metabolic profile of PCa patients [27,28].

More recently, Lee et al. carried out a transcriptomics and metabolomics analysis of urine liquid biopsies from BPH, prostatitis, and PCa patients with a focus on the identification of PCa-specific biomarkers and the discovery of novel therapeutic targets for PCa treatment [66]. Significantly enriched pathways in PCa patients included the TCA

cycle and alanine, aspartate, and glutamate metabolism. Other metabolomics studies have also reported alterations in urine levels of metabolites involved in these pathways in PCa patients [36,88–90]. By examining the top 25 altered metabolites and corresponding genes, the authors identified a regulatory metabolic node that influenced both pathways and was mediated by changes in glutamate oxaloacetate transaminase 1 (GOT1)- and GOT2-related metabolism. Notably, *GOT1* expression was higher in PCa patients, and glutamate, the product of GOT1, also exhibited elevated levels in these patients. Moreover, knock-down of *GOT1* in LNCaP and PC3 cells resulted in a significant decrease in cell viability, consistent with previous studies where GOT1 repression suppressed tumor growth in different tumors [91,92]. Overall, these results suggest that the metabolic alterations observed in urine liquid biopsies obtained from PCa patients could reflect the specific changes already observed in PCa cells and tumors.

Altogether, in agreement with other studies where metabolomics was the only analytical platform used for analyzing the metabolic profile of PCa patients [39–41,93–97], the results from the multi-omics-based studies reviewed in this article suggest that the PCa-specific metabolic phenotype is characterized by alterations in the TCA cycle, polyamine synthesis, HBP, and nucleotide and lipid metabolism (Figure 2).

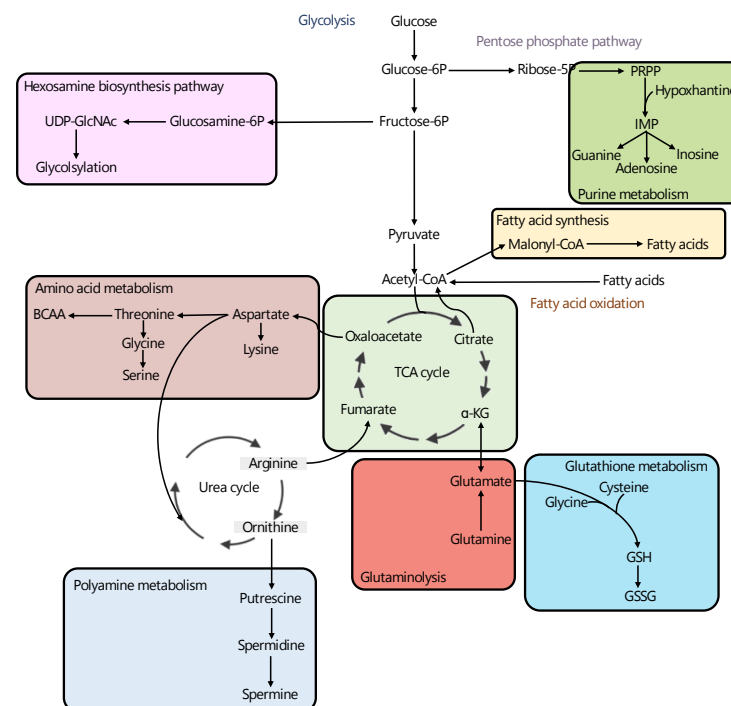


Figure 2. Overview of metabolic pathways most consistently reported to be altered in PCa in the multi-omics studies reviewed in this article, including: hexosamine biosynthesis pathway [64,65], purine metabolism [61], fatty acid synthesis [58,59,63], amino acid metabolism [61], TCA cycle [60,62], glutathione metabolism [58], glutaminolysis [62,66] and polyamine metabolism [58,63]. Thick lines highlight the metabolic pathways found to be upregulated in PCa tumors when compared with benign prostate tissue. References corresponding to the multi-omic studies describing alterations in each metabolic pathway are included. α -KG: alpha-ketoglutarate, Fructose-6P: fructose-6-phosphate, Glucosamine-6P: glucosamine-6-phosphate, Glucose-6P: glucose-6-phosphate, IMP: inosine monophosphate, PRPP: phosphoribosyl diphosphate, Ribose-5P: ribose-5-phosphate.

2.2. PCa Subtyping

Twelve of the multi-omics studies included in this review focused on the identification of metabolic alterations associated with specific subtypes of PCa (Table 2). Half of the studies combined transcriptomics and metabolomics analyses to characterize metabolic dysregulations in different subgroups of PCa patients, and the other half relied on the analysis of proteomics and lipidomics profiles. Tissue was the biological sample most often analyzed in these studies, whereas cell lines and biofluids were collected in only three and two studies, respectively. Different subgroups of PCa patients showed alterations in the TCA cycle and amino-acid, nucleotide, and lipid metabolism. Overall, these results correlate with metabolic changes, observed in previous studies, where metabolomics was the only analytical approach used to performed the analyses [26–28,75,98,99].

analysis of proteomics and lipidomics profiles. Tissue was the biological sample most often analyzed in these studies, whereas cell lines and biofluids were collected in only three and two studies, respectively. Different subgroups of PCa patients showed alterations in the TCA cycle and amino-acid, nucleotide, and lipid metabolism. Overall, these results correlate with metabolic changes, observed in previous studies, where metabolomics was the only analytical approach used to performed the analyses [26–28,75,98,99].

Table 2. Most relevant metabolic alterations reported in recent multi-omics studies focused on the characterization the metabolic phenotypes of different PCa subtypes.

Study	Sample	Omics Data	Group Comparison	Major Findings
Gómez-Cebrián et al. [100]	Urine, serum	M + T	Low- vs. high-grade PCa	High-grade: ↑ glucose, glycine, and 1-methylnicotinamide
Kiebish et al. [101]	Serum	L + M + P	non-BCR vs. BCR	BCR: ↑ TNC, APOA-IV, and 1-methyladenosine and ↓ phosphatidic acid
Liu et al. [102]	Tissue	G + M	PCa vs. metastatic	Metastatic Pca: ↑ <i>CYP1A1</i> , <i>PNP</i> , <i>SMS</i> , proline, cholesterol, sarcosine, spermidine, and spermine
Li et al. [103]	Tissue	M + T	PCa vs. metastatic	Metastatic PCa: ↓ histamine
Latonen et al. [77]	Tissue	E + G + P + T	PCa vs. CRPC	CRPC: ↓ <i>ACO2</i> , <i>OGDH</i> , <i>SUCLG1</i> , and <i>IDH3A</i> ; ↑ <i>MDH2</i>
Gao et al. [104]	Cell lines	L + M + T	LNCaP vs. SCNC	LNCaP: ↑ <i>PHGDH</i> , <i>PSAT1</i> , <i>PSPH</i> , <i>TDH</i> , <i>GCAT</i> , citrate, isocitrate, and succinate; ↓ fumarate, glutamate, glutamine, <i>IDH1</i> , <i>GLUD1</i> , <i>GLUD2</i> , carnitine, and short-chain acylcarnitines SCNC: ↑ lactate and <i>LDH</i> ; ↓ <i>G6P</i>
Joshi et al. [105]	Cell lines	M + T	<i>CPT1A</i> KD vs. <i>CPT1A</i> OE	<i>CPT1A</i> OE: ↑ <i>PHGDH</i> , <i>PSAT1</i> , <i>SHMT2</i> , <i>CTH</i> , <i>GSTO2</i> , dimethylglycine, cystathionine, cystathionine, and cysteine; ↓ glycolysis
Chen et al. [106]	Cell lines	M + T	ARCaP _E vs. ARCaP _M	ARCaP _M : ↑ malate, <i>ACO2</i> , <i>SDHA</i> , aspartate, <i>ASS1</i> , and <i>SRR</i> ; ↓ glycolysis, succinate, and citrate
Hansen et al. [107]	Tissue	L + M	<i>ERG</i> _{low} vs. <i>ERG</i> _{high}	<i>ERG</i> _{high} : ↑ ethanolamine, glycine, phosphocholine, phosphoethanolamine, <i>ACACA</i> , <i>FASN</i> , and <i>SAT1</i> ; ↓ <i>ACO2</i> , citrate, spermine, putrescine, and glucose
Yan et al. [108]	Tissue	L + M + T	<i>SPOP</i> <i>wt</i> vs. <i>SPOP</i> -mutant	<i>SPOP</i> -mutant: ↑ <i>ACADL</i> , <i>ELOVL2</i> , <i>FH</i> , fatty acids, fumarate, and malate
Andersen et al. [109]	Tissue	M + T	Low vs. high reactive stroma	High reactive stroma: ↑ taurine and leucine; ↓ citrate, spermine, and scyllo-inositol
Oberhuber et al. [110]	Tissue	M + P + T	<i>STAT3</i> _{low} vs. <i>STAT3</i> _{high}	<i>STAT3</i> _{low} : ↑ OXPHOS, TCA cycle, ribosomal activity, pyruvate, fumarate, and malate; ↓ <i>PDK4</i>

ACACA: acetyl-CoA carboxylase alpha, *ACADL*: acyl-CoA dehydrogenase, long chain, *ACO2*: aconitase, *APOA-IV*: apolipoprotein A1V, *ARCaP*: androgen-repressed prostate cancer cell, *ASS1*: arginosuccinate synthase 1, *BCR*: biochemical recurrence, *CPT1A*: carnitine palmitoyl transferase I, *CRPC*: castrate-resistant prostate cancer, *CTH*: cystathionine gamma-lyase, *CYP1A1*: cytochrome P450 family 1 subfamily A member 1, *E*: epigenomics, *ELOVL2*: ELOVL fatty acid elongase 2, *ERG*: ETS transcription factor *ERG*, *FASN*: fatty-acid synthase, *FH*: fumarate hydratase, *G*: genomics, *GSTO2*: glutathione S-transferase omega 2, *GCAT*: glycine C-acetyltransferase, *GLUD1*: glutamate dehydrogenase 1, *GLUD2*: glutamate dehydrogenase 2, *G6P*: glucose-6-phosphate, *IDH1*: isocitrate dehydrogenase (NADP(+)) 1, *IDH3A*: isocitrate dehydrogenase (NAD(+)) 3 catalytic subunit alpha, *KD*: knockdown, *L*: lipidomics, *LDH*: lactate dehydrogenase, *LNCaP*: lymph node carcinoma of the prostate, *M*: metabolomics, *OE*: overexpressed, *MDH2*: malate dehydrogenase 2, *OGDH*: oxoglutarate dehydrogenase, *OXPHOS*: oxidative phosphorylation, *P*: proteomics, *PCa*: prostate cancer, *PDK4*: pyruvate dehydrogenase kinase 4, *PHGDH*: D-3-phosphoglycerate dehydrogenase, *PNP*: purine nucleoside phosphorylase, *PSAT1*: phosphohydroxythreonine aminotransferase, *PSPH*: phosphoserine phosphatase, *SAT1*: spermidine N(1)-acetyltransferase, *SCNC*: small-cell neuroendocrine carcinoma, *SDHA*: succinate dehydrogenase complex flavoprotein subunit A, *SHMT2*: serine hydroxymethyltransferase, *SMS*: spermine synthase, *SPOP*: Speckle-type POZ protein, *SRR*: serine racemase, *STAT3*: signal transducer and activator of transcription 3, *SUCLG1*: succinate-CoA ligase alpha subunit, *T*: transcriptomics, *TCA*: tricarboxylic acid, *TDH*: threonine dehydrogenase, *TNC*: tenascin C.

Several studies have revealed specific metabolic alterations in PCa patients by comparing prostate tumors of different grade. Furthermore, different systemic and local metabolic alterations have consistently been associated with PCa risk and progression [111–116]. In line with this, in a recent study by Gómez-Cebrián et al., the specific metabolomics profile of high-grade PCa patients was characterized on the basis of the alterations in metabolite levels identified in the serum and urine of PCa patients with different tumor grades [100]. A gene set enrichment analysis (GSEA) of three publicly available Pca transcriptomics datasets facilitated a targeted analysis of the metabolomics profiles, with a focus on metabolites involved in potentially altered metabolic pathways in high-grade Pca patients. Statistically significant alterations in the levels of glucose, glycine, and 1-methylnicotinamide were found in high-grade PCa patients. Interestingly, dysregulations in the levels of these metabolites could be associated with different metabolic changes previously observed in PCa patients [35,99,117–119]. Particularly, in other multi-omics studies based on the analysis of tissue samples, glycine levels were found to be higher in PCa tumors enriched in the TMPRSS2–ERG gene fusion set [107], and nicotinamide metabolism was elevated in PCa tissues when compared with benign tissues [61]. In addition, Kiebish et al. recently investigated the metabolic profile of presurgical serum samples of PCa patients with a focus on selecting serum metabolic biomarkers that could be valuable for predicting biochemical recurrence (BCR) [101]. In this study, the integration of proteomics, metabolomics, and lipidomics data from PCa patients facilitated the identification of four analytes (tenascin C (TNC), apolipoprotein A-IV (APOA-IV), 1-methyladenosine, and phosphatidic acid 18:0–22:0) as potential biomarkers to discriminate BCR from non-BCR patients. Of note, TNC expression levels in PCa tumor tissues and stroma have previously been reported to predict poor prognosis in PCa patients [120–122], and different serum studies have described apolipoproteins as a potential biomarker for PCa [123,124]. The authors evaluated the association between the levels of each individual biomarker and survival, and they found that higher levels of serum TNC, APO-AIV and 1-methyladenosine and lower concentration of phosphatidic acid increased the probability of disease progression. The predictive potential of these markers was further validated in a testing cohort of patients. Overall, the combination of the four biomolecules resulted in a model with a predictive performance for differentiating PCa patients with and without BCR characterized by an AUC of 0.78, a value that increased to 0.89 after adding the pathological T stage and the GS to the model.

Furthermore, other multi-omics studies have focused on the analysis of local metabolic changes, as reflected in the metabolic profile of PCa tissues and cell lines. In a multi-omics study conducted by Liu et al., the authors developed an approach to improve the accuracy of PCa classification and risk evaluation [102]. According to the combined analysis of genomics and metabolomics data from benign prostate samples, as well as localized and metastatic PCa samples, the authors generated classifier models that proved to be informative for Pca prognosis in additional datasets. Following this approach, they found that arginine and proline metabolism, purine metabolism, and steroid hormone biosynthesis were relevant metabolic pathways for the discrimination between localized and metastatic PCa. Next, topologically important genes and metabolites involved in these pathways were selected as promising markers for PCa prognosis. Selected genes and metabolites included cytochrome P450 family 1 subfamily A member 1 (*CYP1A1*), purine nucleoside phosphorylase (*PNP*), spermine synthase (*SMS*), proline, cholesterol, sarcosine, spermidine, and spermine. Interestingly, elevated *PNP* expression has been observed in aggressive PCa cells [125], whereas alterations in the levels of some of the topologically relevant metabolites have been associated with PCa progression and aggressiveness, including sarcosine [126,127], proline [99], and spermine [41,128]. Moreover, the classification method achieved a more accurate overall performance compared to other existing classification methods across additional datasets.

Efforts to discover dysregulated metabolic pathways in metastatic stages were also made in another multi-omics study conducted by Li et al. In this study, the authors pro-

posed an analytical method, referred to as Subpathway-GM, aiming to identify biologically meaningful metabolic subpathways based on the combined analysis of metabolomics and transcriptomics data [103]. This method allowed the identification of disease-relevant subpathways that could go undetected on the basis of classical entire pathway identification methods. After applying this method to the analysis of a PCa dataset including data obtained from localized and metastatic tumors, 16 subpathways were identified as relevant in metastatic PCa. Among these metabolic routes, nine of them were involved in amino-acid metabolism, including glycine, serine, and threonine metabolism, tryptophan metabolism, cysteine, and methionine metabolism, and histidine metabolism. Interestingly, both tryptophan and histidine metabolism were not previously reported to be associated with metastatic PCa. Specifically, in the histidine metabolism pathway, the histamine region was accurately identified as a disease-relevant subpathway. On the basis of this information, the authors explored the effect of different histamine concentrations on PCa cell proliferation and migration. The results showed that high histamine concentrations inhibited cell migration in a dose-dependent manner, confirming that this metabolite could be associated with metastatic PCa. This finding is supplementary to other results included in previous studies where histamine altered the response to radiation in PCa tumors and significantly reduced proliferation of tumor cells compared with irradiation alone [129,130].

Other multi-omics studies have focused on the analysis of the metabolic profile associated with CRPC. Among them, the study by Latonen et al. was aimed at characterizing the distinct protein profiles of BPH, PCa, and CRPC patients [77]. To that end, the authors performed an integrated analysis of four different omics data. Following this experimental approach, it was found that gene copy number, DNA methylation, and RNA expression levels did not reliably predict proteomics changes in CRPC. These results suggested that proteomics data could be associated with alterations not detectable at the transcriptomic level. In fact, proteomics analyses revealed specific pathway alterations that were not previously reported in CRPC. Interestingly, no significant alterations were observed in the regulation of androgen receptor signaling at the mRNA or protein levels. The combined analysis by transcriptomics and proteomics identified alterations in different cell-cycle regulatory pathways, whereas changes in DNA repair pathways were only detected by proteomics. The combined analysis of the omics data also revealed a previously undescribed two-step modulation of the TCA cycle associated with metabolic changes occurring during PCa development and progression. This pathway exhibited two different metabolic shifts: a first one defined by the upregulation of most of TCA enzymes during initial PCa stages, and a second metabolic shift during PCa progression, involving the downregulation of *ACO2*, oxoglutarate dehydrogenase (*OGDH*), and succinate-CoA ligase alpha subunit (*SUCLG1*), together with elevated expression of malate dehydrogenase 2 (*MDH2*). Previous studies have already reported that PCa patients with *MDH2* overexpression have a significantly shorter period of relapse-free survival, and that stable knockdown of *MDH2* PCa cell lines decreased cell proliferation and increased docetaxel sensitivity, all suggesting that *MDH2* inhibition could be a viable strategy to target CRPC [131].

Additionally, other multi-omics studies have focused on characterizing metabolic dysregulations associated with specific PCa subtypes. In this context, Gao et al. integrated transcriptomics and metabolomics data to characterize the metabolic profile of two main types of PCa, adenocarcinoma (LNCaP), and small-cell neuroendocrine carcinoma (SCNC) [104]. By conducting an individual GSEA on SCNC and adenocarcinoma cell lines, a total of 62 and 112 genes, respectively, were found to be upregulated in each subgroup. Metabolomics and lipidomics analyses also revealed significant differences in 25 metabolite clusters. In particular, the LNCaP phenotype was characterized by an increased serine biosynthesis, a finding supported by elevated levels of serine, glycine, and threonine concentrations and higher expression of phosphoglycerate dehydrogenase (*PHGDH*), phosphoserine aminotransferase 1 (*PSAT1*), phosphoserine phosphatase (*PSPH*), threonine dehydrogenase (*TDH*), and glycine C-acetyltransferase (*GCAT*). This cell line also exhibited increased levels of citrate, isocitrate, and succinate, together with higher

expression of many enzymes involved in the TCA, as well as decreased levels of fumarate, glutamate, and glutamine and lower expression of isocitrate dehydrogenase (NADP(+)) 1 (*IDH1*), *GLUD1*, and *GLUD2*, an indication of a citrate accumulation phenotype. Furthermore, an enhanced alpha-linoleic acid, arachidonic acid, linoleic acid, fatty-acid, and sphingolipid metabolism was also observed in the LNCaP group, along with a reduced fatty-acid oxidation activity, suggested by the lower levels of carnitine and some short-chain acylcarnitines and the overexpression of genes involved in biosynthesis, as well as the use of acylcarnitines and members of the acyl-coenzyme A synthetase family. On the other hand, SCNC was characterized by an enhanced glycerolipid, glycerophospholipid, and ether lipid metabolism, as well as by an elevated pyruvate metabolism, which was supported by lower levels of glucose-6-phosphate and higher lactate concentrations together with increased expression of lactate dehydrogenase isoforms (*LDHA* and *LDHB*). Although a limited number of samples were included in this pilot study, the results highlight the potential of multi-omics approaches for the identification of novel therapeutic targets in specific subgroups of PCa. Furthermore, the integrated analysis of transcriptomics and metabolomics data carried out by Joshi et al. revealed an enhanced lipid catabolism in the carnitine palmitoyl transferase I (*CPT1A*) overexpressed (OE) phenotype, which was also associated with the elevated concentration of acyl-carnitine and higher lipase activity [105]. In this study, the analysis of molecular differences between *CPT1A* gain- and loss-of-function cellular models revealed genetic and metabolomics vulnerabilities associated with the progression to neuroendocrine differentiation in PCa. Cellular models overexpressing *CPT1A* were characterized by enhanced lipid metabolism, glycine and serine metabolism, and glutathione homeostasis. In addition, the OE phenotype exhibited lower glycolysis as glucose was preferentially shunted toward de novo serine biosynthesis. This finding was correlated with the increased expression of key serine/glycine pathway genes, including *PHGDH*, *PSAT1*, and serine hydroxymethyltransferase (*SHMT2*), together with elevated levels of some metabolites involved in the folate cycle (e.g., dimethylglycine and cystathionine). Furthermore, although cells overexpressing *CPT1A* showed increased levels of mitochondrial reactive oxygen species (ROS), elevated concentrations of metabolites involved in glutathione homeostasis, including overexpression of cystathionine gamma-lyase (*CTH*) and glutathione S-transferase omega 2 (*GSTO2*), were also found, indicating a key role of *CPT1A* in supporting adaptation to stress and antioxidant defense production. Lastly, the analysis of data derived from patients, available from public databases, provided evidence that lipid catabolism driven by *CPT1A* was associated with more aggressive disease, suggesting that *CPT1A* activity could rewire metabolism to promote growth and transformation in these patients.

Other multi-omics studies have focused on characterizing the metabolic features of PCa cells undergoing epithelial–mesenchymal transition (EMT). In the study carried out by Chen et al., two subclones derived from the androgen-repressed prostate cancer cell (ARCaP) line that exhibited epithelial and mesenchymal phenotypes, ARCaP_E and ARCaP_M, respectively, were used as EMT PCa models [106]. Integration of transcriptomics and metabolomics data revealed lower levels of glycolysis intermediates and decreased expression of several glucose metabolism-related genes in ARCaP_M, indicating a downregulation of glucose metabolism. In addition, this phenotype was characterized by exhibiting higher malate levels, as well as by overexpressing *ACO2* and succinate dehydrogenase complex flavoprotein subunit A (*SDHA*) enzymes. At the same time, authors found lower succinate and citrate levels, suggesting that TCA might be fueled by glutamine and aspartate in addition to glucose in these cells. Notably, upregulation of *ACO2* has been identified as an important event in prostate carcinogenesis [23], whereas lower citrate levels have been observed in PCa when compared to non-cancer epithelium [29,132]. Furthermore, malate has been associated with Gleason progression [99] and found to be altered between different PCa stages [133]. Additionally, increased aspartate and aspartate-derived metabolite levels and upregulation of important enzymes involved in aspartate metabolism, including

arginosuccinate synthase 1 (*ASS1*) and serine racemase (*SRR*), were observed in ARCaP_M cells, suggesting an enhanced aspartate metabolism.

A combination of metabolomics and transcriptomics data was also used by Hansen et al. to identify changes in PCa metabolism related to the Tmprss2-ERG gene fusion [107]. In this study, PCa patients were classified in two cohorts, ERG_{low} or ERG_{high}, as a function of specific enrichment of the ERG fusion gene set [134,135]. Multivariate analysis of metabolomic data revealed decreased concentrations of citrate, spermine, putrescine, and glucose, and higher levels of ethanolamine, glycine, phosphocholine, and phosphoethanolamine in ERG_{high} PCa patients included in two independent patient cohorts. Furthermore, a targeted analysis of genes involved in the metabolic pathways associated with these metabolic changes revealed an upregulation of genes involved in the polyamine pathway, together with a decrease in relevant genes in the TCA cycle and increased lipogenic phenotype. In particular, *N*(1)-acetyltransferase (*SAT1*), involved in spermine depletion, was highly expressed in ERG_{high} tumors. In addition, this group of patients also exhibited decreased expression of *ACO2* and elevated activity of the lipogenic enzymes *ACACA* and *FASN*, indicating that citrate might be preferentially derived from de novo lipid synthesis in these tumors. Several studies have also reported increased expression of *FASN* [67,68,136] and enhanced de novo fatty-acid synthesis in PCa [137] and PCa invasiveness [138]. Interestingly, in a different multi-omics study performed by Yan et al., the integration of data from three different omics platforms was used to analyze correlations between Speckle-type POZ protein (*SPOP*) mutations and changes in PCa metabolism [108]. *SPOP*, a cullin-based E3 ubiquitin ligase, has been identified as one of the most frequently mutated genes in PCa [139]. Several studies have shown that *SPOP* could directly bind to androgen receptor and contribute to its ubiquitination and degradation [140]. Interestingly, the authors found a strong upregulation of acyl-CoA dehydrogenase, long chain (*ACADL*), and ELOVL fatty-acid elongase 2 (*ELOVL2*) together with an increase in the levels of most fatty acids in *SPOP*-mutated patients. Relevant upregulations were also observed in the levels of two key intermediates of the TCA cycle (malate and fumarate) and fumarate hydratase (*FH*). Although *FH*, *ELOVL2*, and *ACADL* were identified as key genes in *SPOP*-mutated PCa patients in this study, their oncogenic role in PCa still needs to be proven.

Multi-omics studies have also focused on exploring specific metabolic alterations associated with PCa progression. Andersen et al. focused on identifying correlations between changes in genes and metabolites and high reactive stroma content in tumors [109], as it has been linked to worse clinical outcome and earlier BCR in Pca [141–145]. High reactive stroma samples were characterized by elevated levels of taurine and leucine, as well as by decreased levels of citrate, spermine, and scyllo-inositol. Interestingly, metastatic CRPC has previously been defined as leucine-dependent [146,147], and leucine deprivation has been shown to inhibit PCa growth [148]. The metabolic changes observed in high reactive stroma samples, together with the results from a gene enrichment analysis, indicated that immune processes and extracellular matrix remodeling were particularly important in these tumors. In a more recent study, Oberhuber et al. evaluated the correlation between the PCa transcriptomics and proteomics profiles with signal transducer and activator of transcription 3 (*STAT3*) expression looking for biomarkers associated with earlier BCR [110]. The integrative multi-omics analysis revealed enhanced oxidative phosphorylation (OXPHOS), TCA cycle, and ribosomal activity in the *STAT3*_{low} group of tumors. These findings were also observed in a PCa murine model, which showed enrichment of ribosomal gene sets and elevated TCA cycle and OXPHOS, as well as elevated pyruvate, fumarate, and malate levels in xenografts with loss of *STAT3*. The authors also observed that pyruvate dehydrogenase kinase 4 (*PDK4*) was significantly downregulated in *STAT3*_{low} samples. Expression of *PDK4* has already been reported to be significantly altered when comparing PCa patients with healthy individuals [149]. The analysis of the correlation between *PDK4* expression and BCR in primary and metastatic tumors demonstrated its ability to predict disease recurrence independently of diagnostic risk factors, such as grading, staging, and

PSA levels, thus suggesting its potential as a promising independent prognostic biomarker for distinguishing between a good and bad prognostic PCa.

3. Future Perspectives and Conclusions

Altered cell metabolism is a well-established hallmark of cancer [150]. Metabolism is dysregulated to support the metabolic requirements of uncontrolled proliferation in cancer cells [151,152]. This rewiring of cellular metabolism leads to characteristic metabolic phenotypes that can be used for the development of effective screening methods for early cancer detection, patient selection strategies, or evaluation of treatment responses [153,154]. Altered metabolism also results in unique metabolic vulnerabilities that can be exploited to develop novel therapeutic strategies in cancer, some of which are being evaluated in pre-clinical models or clinical trials [17,155–157]. Recently, the availability and advances in the development of different analytical platforms have prompted the application of new omics approaches for the characterization of specific cancer-associated metabolic phenotypes. Particularly, metabolomics approaches have greatly contributed to metabolically characterize the profile of PCa patients and to discover specific alterations associated with this disease [22,158,159]. However, compared with other omics (e.g., genomics, transcriptomics), the metabolome coverage is limited, thus adding difficulty to the final interpretation of the results [160]. In this context, the integration of different omics datasets could represent a powerful strategy to develop more robust and consistent metabolic signatures with a clinical impact on the management of cancer patients [161].

In this review, the most relevant findings reported in multi-omics studies focused on the characterization of the metabolic phenotype associated with PCa were summarized. Overall, the most frequently reported metabolic alterations associated with PCa onset and progression include differences in the TCA cycle, polyamine synthesis, HBP, and nucleotide and lipid metabolism, and the most widely applied multi-omics approach was the combination of transcriptomics and metabolomics data. In most of the reviewed studies, the different omics datasets were separately analyzed and only combined for the final interpretation of the metabolic changes. In this scenario, the development and implementation of novel computational tools, focused on the integrated analysis of different omics datasets that enable the assessment of the interplay between the different components of a biological system, would be greatly valuable [162,163]. Furthermore, although some studies included a vast number of samples [61,63,101,107,109], a major limitation in the majority of these studies was the lack of an external cohort of PCa patients/samples for confirming the reproducibility and robustness of the results. Thus, future studies including larger sample sizes and external datasets to increase the statistical power of the analyses and validate the findings of selected metabolites, together with confirmatory experiments to evaluate the clinical significance of these metabolic findings, are required. Lastly, access to publicly accessible databases integrating all metabolic alterations reported in the literature, associated with each tumor subtype, would greatly contribute to our understanding of the metabolic heterogeneity in PCa [164,165].

Author Contributions: Conceptualization, N.G.-C., L.P.-C. and A.P.-L.; writing—original draft preparation, N.G.-C. with input from L.P.-C.; writing—review and editing, J.L.P., L.P.-C. and A.P.-L. All authors have read and agreed to the published version of the manuscript.

Funding: N.G.-C. and L.P.-C. are supported by the European Regional Development Fund (FEDER) and Conselleria de Innovación, Universidades, Ciencia y Sociedad Digital (GV/2021/154). N.G.-C., L.P.-C., and A.P.-L. are supported by MCIN (PID2020-115875RB-I00/AEI/10.13039/501100011033).

Conflicts of Interest: The authors declare no conflict of interest.

References

1. Sung, H.; Ferlay, J.; Siegel, R.L.; Laversanne, M.; Soerjomataram, I.; Jemal, A.; Bray, F. Global Cancer Statistics 2020: GLOBOCAN Estimates of Incidence and Mortality Worldwide for 36 Cancers in 185 Countries. *CA Cancer J. Clin.* **2021**, *71*, 209–249. [[CrossRef](#)] [[PubMed](#)]
2. Sathianathen, N.J.; Konety, B.R.; Crook, J.; Saad, F.; Lawrentschuk, N. Landmarks in Prostate Cancer. *Nat. Rev. Urol.* **2018**, *15*, 627–642. [[CrossRef](#)] [[PubMed](#)]
3. Schalken, J.; Dijkstra, S.; Baskin-Bey, E.; van Oort, I. Potential Utility of Cancer-Specific Biomarkers for Assessing Response to Hormonal Treatments in Metastatic Prostate Cancer. *Ther. Adv. Urol.* **2014**, *6*, 245–252. [[CrossRef](#)] [[PubMed](#)]
4. Etzioni, R.; Penson, D.F.; Legler, J.M.; di Tommaso, D.; Boer, R.; Gann, P.H.; Feuer, E.J. Overdiagnosis Due to Prostate-Specific Antigen Screening: Lessons from U.S. Prostate Cancer Incidence Trends. *J. Natl. Cancer Inst.* **2002**, *94*, 981–990. [[CrossRef](#)]
5. Postma, R.; Schröder, F.H. Screening for Prostate Cancer. *Eur. J. Cancer* **2005**, *41*, 825–833. [[CrossRef](#)]
6. Ziglioli, F.; Granelli, G.; Cavalieri, D.; Bocchialini, T.; Maestroni, U. What Chance Do We Have to Decrease Prostate Cancer Overdiagnosis and Overtreatment? A Narrative Review. *Acta Biomed.* **2019**, *90*, 423–426. [[CrossRef](#)]
7. Gleason, D.F.; Mellinger, G.T. Prediction of Prognosis for Prostatic Adenocarcinoma by Combined Histological Grading and Clinical Staging. *J. Urol.* **1974**, *111*, 58–64. [[CrossRef](#)]
8. Hübner, N.; Shariat, S.; Remzi, M. Prostate Biopsy: Guidelines and Evidence. *Curr. Opin. Urol.* **2018**, *28*, 354–359. [[CrossRef](#)]
9. Mottet, N.; van den Bergh, R.C.N.; Briers, E.; Van den Broeck, T.; Cumberbatch, M.G.; De Santis, M.; Fanti, S.; Fossati, N.; Gandaglia, G.; Gillessen, S.; et al. EAU-EANM-ESTRO-ESUR-SIOG Guidelines on Prostate Cancer-2020 Update. Part 1: Screening, Diagnosis, and Local Treatment with Curative Intent. *Eur. Urol.* **2021**, *79*, 243–262. [[CrossRef](#)]
10. Kawachi, M.H.; Bahnson, R.R.; Barry, M.; Busby, J.E.; Carroll, P.R.; Carter, H.B.; Catalona, W.J.; Cookson, M.S.; Epstein, J.I.; Etzioni, R.B.; et al. NCCN Clinical Practice Guidelines in Oncology: Prostate Cancer Early Detection. *J. Natl. Compr. Cancer Netw.* **2010**, *8*, 240–262. [[CrossRef](#)]
11. Das, C.J.; Razik, A.; Sharma, S.; Verma, S. Prostate Biopsy: When and How to Perform. *Clin. Radiol.* **2019**, *74*, 853–864. [[CrossRef](#)] [[PubMed](#)]
12. Miles, B.; Ittmann, M.; Wheeler, T.; Sayeeduddin, M.; Cubilla, A.; Rowley, D.; Bu, P.; Ding, Y.; Gao, Y.; Lee, M.; et al. Moving Beyond Gleason Scoring. *Arch. Pathol. Lab. Med.* **2019**, *143*, 565–570. [[CrossRef](#)] [[PubMed](#)]
13. Zadra, G.; Loda, M. Metabolic Vulnerabilities of Prostate Cancer: Diagnostic and Therapeutic Opportunities. *Cold Spring Harb. Perspect. Med.* **2018**, *8*, a030569. [[CrossRef](#)] [[PubMed](#)]
14. Turanli, B.; Zhang, C.; Kim, W.; Benfeitas, R.; Uhlen, M.; Arga, K.Y.; Mardinoglu, A. Discovery of Therapeutic Agents for Prostate Cancer Using Genome-Scale Metabolic Modeling and Drug Repositioning. *EBioMedicine* **2019**, *42*, 386–396. [[CrossRef](#)] [[PubMed](#)]
15. Márquez, J.; Matés, J.M. Tumor Metabolome: Therapeutic Opportunities Targeting Cancer Metabolic Reprogramming. *Cancers* **2021**, *13*, 314. [[CrossRef](#)] [[PubMed](#)]
16. Pemovska, T.; Bigenzahn, J.W.; Srndic, I.; Lercher, A.; Bergthaler, A.; César-Razquin, A.; Kartnig, F.; Kornauth, C.; Valent, P.; Staber, P.B.; et al. Metabolic Drug Survey Highlights Cancer Cell Dependencies and Vulnerabilities. *Nat. Commun.* **2021**, *12*, 7190. [[CrossRef](#)]
17. Stine, Z.E.; Schug, Z.T.; Salvino, J.M.; Dang, C.V. Targeting Cancer Metabolism in the Era of Precision Oncology. *Nat. Rev. Drug Discov.* **2021**, *3*, 2–22. [[CrossRef](#)]
18. Martínez-Reyes, I.; Chandel, N.S. Cancer Metabolism: Looking Forward. *Nat. Rev. Cancer* **2021**, *21*, 669–680. [[CrossRef](#)]
19. Lima, A.R.; de Lourdes Bastos, M.; Carvalho, M.; de Pinho, P.G. Biomarker Discovery in Human Prostate Cancer: An Update in Metabolomics Studies. *Transl. Oncol.* **2016**, *9*, 357–370. [[CrossRef](#)]
20. Gómez-Cebrián, N.; Rojas-Benedicto, A.; Albors-Vaquer, A.; López-Guerrero, J.A.; Pineda-Lucena, A.; Puchades-Carrasco, L. Metabolomics Contributions to the Discovery of Prostate Cancer Biomarkers. *Metabolites* **2019**, *9*, 48. [[CrossRef](#)]
21. Kdadra, M.; Höckner, S.; Leung, H.; Kremer, W.; Schiffer, E. Metabolomics Biomarkers of Prostate Cancer: A Systematic Review. *Diagnostics* **2019**, *9*, 21. [[CrossRef](#)] [[PubMed](#)]
22. Lima, A.R.; Pinto, J.; Amaro, F.; Bastos, M.D.; Carvalho, M.; Guedes de Pinho, P. Advances and Perspectives in Prostate Cancer Biomarker Discovery in the Last 5 Years through Tissue and Urine Metabolomics. *Metabolites* **2021**, *11*, 181. [[CrossRef](#)] [[PubMed](#)]
23. Eidelman, E.; Twum-Ampofo, J.; Ansari, J.; Siddiqui, M.M. The Metabolic Phenotype of Prostate Cancer. *Front. Oncol.* **2017**, *7*, 131. [[CrossRef](#)] [[PubMed](#)]
24. Ahmad, F.; Cherukuri, M.K.; Choyke, P.L. Metabolic Reprogramming in Prostate Cancer. *Br. J. Cancer* **2021**, *125*, 1185–1196. [[CrossRef](#)] [[PubMed](#)]
25. Lima, A.R.; Araújo, A.M.; Pinto, J.; Jerónimo, C.; Henrique, R.; de Lourdes Bastos, M.; Carvalho, M.; de Pinho, P.G. Discrimination between the Human Prostate Normal and Cancer Cell Exometabolome by GC-MS. *Sci. Rep.* **2018**, *8*, 5539. [[CrossRef](#)] [[PubMed](#)]
26. Zheng, H.; Dong, B.; Ning, J.; Shao, X.; Zhao, L.; Jiang, Q.; Ji, H.; Cai, A.; Xue, W.; Gao, H. NMR-Based Metabolomics Analysis Identifies Discriminatory Metabolic Disturbances in Tissue and Biofluid Samples for Progressive Prostate Cancer. *Clin. Chim. Acta* **2020**, *501*, 241–251. [[CrossRef](#)] [[PubMed](#)]
27. Dudka, I.; Thysell, E.; Lundquist, K.; Antti, H.; Iglesias-Gato, D.; Flores-Morales, A.; Bergh, A.; Wikström, P.; Gröbner, G. Comprehensive Metabolomics Analysis of Prostate Cancer Tissue in Relation to Tumor Aggressiveness and TMPRSS2-ERG Fusion Status. *BMC Cancer* **2020**, *20*, 437. [[CrossRef](#)] [[PubMed](#)]

28. Franko, A.; Shao, Y.; Heni, M.; Hennenlotter, J.; Hoene, M.; Hu, C.; Liu, X.; Zhao, X.; Wang, Q.; Birkenfeld, A.L.; et al. Human Prostate Cancer Is Characterized by an Increase in Urea Cycle Metabolites. *Cancers* **2020**, *12*, 1814. [[CrossRef](#)]
29. Giskeødegård, G.F.; Bertilsson, H.; Selnæs, K.M.; Wright, A.J.; Bathen, T.F.; Viset, T.; Halgunset, J.; Angelsen, A.; Gribbestad, I.S.; Tessem, M.-B. Spermine and Citrate as Metabolic Biomarkers for Assessing Prostate Cancer Aggressiveness. *PLoS ONE* **2013**, *8*, e62375. [[CrossRef](#)]
30. Serkova, N.J.; Gamito, E.J.; Jones, R.H.; O'Donnell, C.; Brown, J.L.; Green, S.; Sullivan, H.; Hedlund, T.; Crawford, E.D. The Metabolites Citrate, Myo-Inositol, and Spermine Are Potential Age-Independent Markers of Prostate Cancer in Human Expressed Prostatic Secretions. *Prostate* **2008**, *68*, 620–628. [[CrossRef](#)] [[PubMed](#)]
31. Lynch, M.J.; Nicholson, J.K. Proton MRS of Human Prostatic Fluid: Correlations between Citrate, Spermine, and Myo-Inositol Levels and Changes with Disease. *Prostate* **1997**, *30*, 248–255. [[CrossRef](#)]
32. Cheng, L.L.; Wu, C.; Smith, M.R.; Gonzalez, R.G. Non-Destructive Quantitation of Spermine in Human Prostate Tissue Samples Using HRMAS 1H NMR Spectroscopy at 9.4 T. *FEBS Lett.* **2001**, *494*, 112–116. [[CrossRef](#)]
33. Tsoi, T.-H.; Chan, C.-F.; Chan, W.-L.; Chiu, K.-F.; Wong, W.-T.; Ng, C.-F.; Wong, K.-L. Urinary Polyamines: A Pilot Study on Their Roles as Prostate Cancer Detection Biomarkers. *PLoS ONE* **2016**, *11*, e0162217. [[CrossRef](#)] [[PubMed](#)]
34. Kumar, D.; Gupta, A.; Mandhani, A.; Sankhwar, S.N. Metabolomics-Derived Prostate Cancer Biomarkers: Fact or Fiction? *J. Proteome Res.* **2015**, *14*, 1455–1464. [[CrossRef](#)]
35. Kumar, D.; Gupta, A.; Mandhani, A.; Sankhwar, S.N. NMR Spectroscopy of Filtered Serum of Prostate Cancer: A New Frontier in Metabolomics. *Prostate* **2016**, *76*, 1106–1119. [[CrossRef](#)]
36. Pérez-Rambla, C.; Puchades-Carrasco, L.; García-Flores, M.; Rubio-Briones, J.; López-Guerrero, J.A.; Pineda-Lucena, A. Non-Invasive Urinary Metabolomic Profiling Discriminates Prostate Cancer from Benign Prostatic Hyperplasia. *Metabolomics* **2017**, *13*, 52. [[CrossRef](#)]
37. Giskeødegård, G.F.; Hansen, A.F.; Bertilsson, H.; Gonzalez, S.V.; Kristiansen, K.A.; Bruheim, P.; Mjøs, S.A.; Angelsen, A.; Bathen, T.F.; Tessem, M.-B. Metabolic Markers in Blood Can Separate Prostate Cancer from Benign Prostatic Hyperplasia. *Br. J. Cancer* **2015**, *113*, 1712–1719. [[CrossRef](#)]
38. Hahn, P.; Smith, I.C.; Leboldus, L.; Littman, C.; Somorjai, R.L.; Bezabeh, T. The Classification of Benign and Malignant Human Prostate Tissue by Multivariate Analysis of 1H Magnetic Resonance Spectra. *Cancer Res.* **1997**, *57*, 3398–3401.
39. Dereziński, P.; Klupczynska, A.; Sawicki, W.; Pałka, J.A.; Kokot, Z.J. Amino Acid Profiles of Serum and Urine in Search for Prostate Cancer Biomarkers: A Pilot Study. *Int. J. Med. Sci.* **2017**, *14*, 1–12. [[CrossRef](#)]
40. Madhu, B.; Shaw, G.L.; Warren, A.Y.; Neal, D.E.; Griffiths, J.R. Response of Degarelix Treatment in Human Prostate Cancer Monitored by HR-MAS 1H NMR Spectroscopy. *Metabolomics* **2016**, *12*, 120. [[CrossRef](#)]
41. Braadland, P.R.; Giskeødegård, G.; Sandsmark, E.; Bertilsson, H.; Euceda, L.R.; Hansen, A.F.; Guldvik, I.J.; Selnæs, K.M.; Grytli, H.H.; Katz, B.; et al. Ex Vivo Metabolic Fingerprinting Identifies Biomarkers Predictive of Prostate Cancer Recurrence Following Radical Prostatectomy. *Br. J. Cancer* **2017**, *117*, 1656–1664. [[CrossRef](#)] [[PubMed](#)]
42. Kühn, T.; Floegel, A.; Sookthai, D.; Johnson, T.; Rolle-Kampczyk, U.; Otto, W.; von Bergen, M.; Boeing, H.; Kaaks, R. Higher Plasma Levels of Lysophosphatidylcholine 18:0 Are Related to a Lower Risk of Common Cancers in a Prospective Metabolomics Study. *BMC Med.* **2016**, *14*, 13. [[CrossRef](#)] [[PubMed](#)]
43. Roberts, M.J.; Richards, R.S.; Chow, C.W.K.; Buck, M.; Yaxley, J.; Lavin, M.F.; Schirra, H.J.; Gardiner, R.A. Seminal Plasma Enables Selection and Monitoring of Active Surveillance Candidates Using Nuclear Magnetic Resonance-Based Metabolomics: A Preliminary Investigation. *Prostate Int.* **2017**, *5*, 149–157. [[CrossRef](#)] [[PubMed](#)]
44. Lin, H.-M.; Mahon, K.L.; Weir, J.M.; Mundra, P.A.; Spielman, C.; Briscoe, K.; Gurney, H.; Mallesara, G.; Marx, G.; Stockler, M.R.; et al. A Distinct Plasma Lipid Signature Associated with Poor Prognosis in Castration-Resistant Prostate Cancer. *Int. J. Cancer* **2017**, *141*, 2112–2120. [[CrossRef](#)]
45. Marzec, J.; Ross-Adams, H.; Pirrò, S.; Wang, J.; Zhu, Y.; Mao, X.; Gadaleta, E.; Ahmad, A.S.; North, B.V.; Kammerer-Jacquet, S.-F.; et al. The Transcriptomic Landscape of Prostate Cancer Development and Progression: An Integrative Analysis. *Cancers* **2021**, *13*, 345. [[CrossRef](#)]
46. Singh, R.; Mills, I.G. The Interplay Between Prostate Cancer Genomics, Metabolism, and the Epigenome: Perspectives and Future Prospects. *Front. Oncol.* **2021**, *11*, 704353. [[CrossRef](#)]
47. Zhang, Y.; Zhang, R.; Liang, F.; Zhang, L.; Liang, X. Identification of Metabolism-Associated Prostate Cancer Subtypes and Construction of a Prognostic Risk Model. *Front. Oncol.* **2020**, *10*, 598801. [[CrossRef](#)]
48. Ros, S.; Santos, C.R.; Moco, S.; Baenke, F.; Kelly, G.; Howell, M.; Zamboni, N.; Schulze, A. Functional Metabolic Screen Identifies 6-Phosphofructo-2-Kinase/Fructose-2,6-Biphosphatase 4 as an Important Regulator of Prostate Cancer Cell Survival. *Cancer Discov.* **2012**, *2*, 328–343. [[CrossRef](#)]
49. Saraon, P.; Cretu, D.; Musrap, N.; Karagiannis, G.S.; Batruch, I.; Drabovich, A.P.; van der Kwast, T.; Mizokami, A.; Morrissey, C.; Jarvi, K.; et al. Quantitative Proteomics Reveals That Enzymes of the Ketogenic Pathway Are Associated with Prostate Cancer Progression. *Mol. Cell. Proteom.* **2013**, *12*, 1589–1601. [[CrossRef](#)]
50. Duijvesz, D.; Burnum-Johnson, K.E.; Gritsenko, M.A.; Hoogland, A.M.; Vredenburg-van den Berg, M.S.; Willemsen, R.; Luijck, T.; Paša-Tolić, L.; Jenster, G. Proteomic Profiling of Exosomes Leads to the Identification of Novel Biomarkers for Prostate Cancer. *PLoS ONE* **2013**, *8*, e82589. [[CrossRef](#)]

51. Yang, K.; Han, X. Lipidomics: Techniques, Applications, and Outcomes Related to Biomedical Sciences. *Trends Biochem. Sci.* **2016**, *41*, 954–969. [[CrossRef](#)] [[PubMed](#)]
52. Chen, X.; Zhu, Y.; Jijiwa, M.; Nasu, M.; Ai, J.; Dai, S.; Jiang, B.; Zhang, J.; Huang, G.; Deng, Y. Identification of Plasma Lipid Species as Promising Diagnostic Markers for Prostate Cancer. *BMC Med. Inform. Decis. Mak.* **2020**, *20*, 223. [[CrossRef](#)] [[PubMed](#)]
53. Buszewska-Forajta, M.; Pomastowski, P.; Monedeiro, F.; Walczak-Skierska, J.; Markuszewski, M.; Matuszewski, M.; Markuszewski, M.J.; Buszewski, B. Lipidomics as a Diagnostic Tool for Prostate Cancer. *Cancers* **2021**, *13*, 2000. [[CrossRef](#)] [[PubMed](#)]
54. Hasin, Y.; Seldin, M.; Lusic, A. Multi-Omics Approaches to Disease. *Genome Biol.* **2017**, *18*, 83. [[CrossRef](#)]
55. Hakimi, A.A.; Reznik, E.; Lee, C.-H.; Creighton, C.J.; Brannon, A.R.; Luna, A.; Aksoy, B.A.; Liu, E.M.; Shen, R.; Lee, W.; et al. An Integrated Metabolic Atlas of Clear Cell Renal Cell Carcinoma. *Cancer Cell* **2016**, *29*, 104–116. [[CrossRef](#)]
56. Luo, X.; Yu, H.; Song, Y.; Sun, T. Integration of Metabolomic and Transcriptomic Data Reveals Metabolic Pathway Alteration in Breast Cancer and Impact of Related Signature on Survival. *J. Cell. Physiol.* **2019**, *234*, 13021–13031. [[CrossRef](#)]
57. Hoang, L.T.; Domingo-Sabugo, C.; Starren, E.S.; Willis-Owen, S.A.G.; Morris-Rosendahl, D.J.; Nicholson, A.G.; Cookson, W.O.C.M.; Moffatt, M.F. Metabolomic, Transcriptomic and Genetic Integrative Analysis Reveals Important Roles of Adenosine Diphosphate in Haemostasis and Platelet Activation in Non-Small-Cell Lung Cancer. *Mol. Oncol.* **2019**, *13*, 2406–2421. [[CrossRef](#)]
58. Meller, S.; Meyer, H.-A.; Bethan, B.; Dietrich, D.; Maldonado, S.G.; Lein, M.; Montani, M.; Reszka, R.; Schatz, P.; Peter, E.; et al. Integration of Tissue Metabolomics, Transcriptomics and Immunohistochemistry Reveals ERG- and Gleason Score-Specific Metabolomic Alterations in Prostate Cancer. *Oncotarget* **2016**, *7*, 1421–1438. [[CrossRef](#)]
59. Li, J.; Ren, S.; Piao, H.; Wang, F.; Yin, P.; Xu, C.; Lu, X.; Ye, G.; Shao, Y.; Yan, M.; et al. Integration of Lipidomics and Transcriptomics Unravels Aberrant Lipid Metabolism and Defines Cholesteryl Oleate as Potential Biomarker of Prostate Cancer. *Sci. Rep.* **2016**, *6*, 20984. [[CrossRef](#)]
60. Torrano, V.; Valcarcel-Jimenez, L.; Cortazar, A.R.; Liu, X.; Urosevic, J.; Castillo-Martin, M.; Fernández-Ruiz, S.; Morciano, G.; Caro-Maldonado, A.; Guiu, M.; et al. The Metabolic Co-Regulator PGC1 α Suppresses Prostate Cancer Metastasis. *Nat. Cell Biol.* **2016**, *18*, 645–656. [[CrossRef](#)]
61. Lima, A.R.; Carvalho, M.; Aveiro, S.S.; Melo, T.; Domingues, M.R.; Macedo-Silva, C.; Coimbra, N.; Jerónimo, C.; Henrique, R.; de Bastos, M.L.; et al. Comprehensive Metabolomics and Lipidomics Profiling of Prostate Cancer Tissue Reveals Metabolic Dysregulations Associated with Disease Development. *J. Proteome Res.* **2021**. [[CrossRef](#)]
62. Shao, Y.; Ye, G.; Ren, S.; Piao, H.-L.; Zhao, X.; Lu, X.; Wang, F.; Ma, W.; Li, J.; Yin, P.; et al. Metabolomics and Transcriptomics Profiles Reveal the Dysregulation of the Tricarboxylic Acid Cycle and Related Mechanisms in Prostate Cancer. *Int. J. Cancer* **2018**, *143*, 396–407. [[CrossRef](#)] [[PubMed](#)]
63. Tessem, M.-B.; Bertilsson, H.; Angelsen, A.; Bathen, T.F.; Drabløs, F.; Rye, M.B. A Balanced Tissue Composition Reveals New Metabolic and Gene Expression Markers in Prostate Cancer. *PLoS ONE* **2016**, *11*, e0153727. [[CrossRef](#)] [[PubMed](#)]
64. Kaushik, A.K.; Shojaie, A.; Panzitt, K.; Sonavane, R.; Venghatakrishnan, H.; Manikkam, M.; Zaslavsky, A.; Putluri, V.; Vasu, V.T.; Zhang, Y.; et al. Inhibition of the Hexosamine Biosynthetic Pathway Promotes Castration-Resistant Prostate Cancer. *Nat. Commun.* **2016**, *7*, 11612. [[CrossRef](#)] [[PubMed](#)]
65. Ren, S.; Shao, Y.; Zhao, X.; Hong, C.S.; Wang, F.; Lu, X.; Li, J.; Ye, G.; Yan, M.; Zhuang, Z.; et al. Integration of Metabolomics and Transcriptomics Reveals Major Metabolic Pathways and Potential Biomarker Involved in Prostate Cancer. *Mol. Cell. Proteom.* **2016**, *15*, 154–163. [[CrossRef](#)] [[PubMed](#)]
66. Lee, B.; Mahmud, I.; Marchica, J.; Dereziński, P.; Qi, F.; Wang, F.; Joshi, P.; Valerio, F.; Rivera, I.; Patel, V.; et al. Integrated RNA and Metabolite Profiling of Urine Liquid Biopsies for Prostate Cancer Biomarker Discovery. *Sci. Rep.* **2020**, *10*, 3716. [[CrossRef](#)]
67. Swinnen, J.V.; Roskams, T.; Joniau, S.; Van Poppel, H.; Oyen, R.; Baert, L.; Heyns, W.; Verhoeven, G. Overexpression of Fatty Acid Synthase Is an Early and Common Event in the Development of Prostate Cancer. *Int. J. Cancer* **2002**, *98*, 19–22. [[CrossRef](#)]
68. Van de Sande, T.; Roskams, T.; Lerut, E.; Joniau, S.; Van Poppel, H.; Verhoeven, G.; Swinnen, J.V. High-Level Expression of Fatty Acid Synthase in Human Prostate Cancer Tissues Is Linked to Activation and Nuclear Localization of Akt/PKB. *J. Pathol.* **2005**, *206*, 214–219. [[CrossRef](#)]
69. Myers, J.S.; von Lersner, A.K.; Sang, Q.-X.A. Proteomic Upregulation of Fatty Acid Synthase and Fatty Acid Binding Protein 5 and Identification of Cancer- and Race-Specific Pathway Associations in Human Prostate Cancer Tissues. *J. Cancer* **2016**, *7*, 1452–1464. [[CrossRef](#)]
70. Kim, S.-J.; Choi, H.; Park, S.-S.; Chang, C.; Kim, E. Stearoyl CoA Desaturase (SCD) Facilitates Proliferation of Prostate Cancer Cells through Enhancement of Androgen Receptor Transactivation. *Mol. Cells* **2011**, *31*, 371–377. [[CrossRef](#)]
71. Peck, B.; Schug, Z.T.; Zhang, Q.; Dankworth, B.; Jones, D.T.; Smethurst, E.; Patel, R.; Mason, S.; Jiang, M.; Saunders, R.; et al. Inhibition of Fatty Acid Desaturation Is Detrimental to Cancer Cell Survival in Metabolically Compromised Environments. *Cancer Metab.* **2016**, *4*, 6. [[CrossRef](#)] [[PubMed](#)]
72. Freitas, M.; Baldeiras, I.; Proença, T.; Alves, V.; Mota-Pinto, A.; Sarmiento-Ribeiro, A. Oxidative Stress Adaptation in Aggressive Prostate Cancer May Be Counteracted by the Reduction of Glutathione Reductase. *FEBS OpenBio* **2012**, *2*, 119–128. [[CrossRef](#)] [[PubMed](#)]
73. Zabala-Letona, A.; Arruabarrena-Aristorena, A.; Martín-Martín, N.; Fernandez-Ruiz, S.; Sutherland, J.D.; Clasquin, M.; Tomas-Cortazar, J.; Jimenez, J.; Torres, I.; Quang, P.; et al. MTORC1-Dependent AMD1 Regulation Sustains Polyamine Metabolism in Prostate Cancer. *Nature* **2017**, *547*, 109–113. [[CrossRef](#)] [[PubMed](#)]

74. Menendez, J.A.; Lupu, R. Fatty Acid Synthase (FASN) as a Therapeutic Target in Breast Cancer. *Expert Opin. Ther. Targets* **2017**, *21*, 1001–1016. [[CrossRef](#)] [[PubMed](#)]
75. Vandergrift, L.A.; Decelle, E.A.; Kurth, J.; Wu, S.; Fuss, T.L.; DeFeo, E.M.; Halpern, E.F.; Taupitz, M.; McDougal, W.S.; Olumi, A.F.; et al. Metabolomic Prediction of Human Prostate Cancer Aggressiveness: Magnetic Resonance Spectroscopy of Histologically Benign Tissue. *Sci. Rep.* **2018**, *8*, 4997. [[CrossRef](#)]
76. Zhou, X.; Mei, H.; Agee, J.; Brown, T.; Mao, J. Racial Differences in Distribution of Fatty Acids in Prostate Cancer and Benign Prostatic Tissues. *Lipids Health Dis.* **2019**, *18*, 189. [[CrossRef](#)]
77. Latonen, L.; Afyounian, E.; Jylhä, A.; Nättinen, J.; Aapola, U.; Annala, M.; Kivinummi, K.K.; Tammela, T.T.L.; Beuerman, R.W.; Uusitalo, H.; et al. Integrative Proteomics in Prostate Cancer Uncovers Robustness against Genomic and Transcriptomic Aberrations during Disease Progression. *Nat. Commun.* **2018**, *9*, 1176. [[CrossRef](#)]
78. Valcarcel-Jimenez, L.; Macchia, A.; Crosas-Molist, E.; Schaub-Clerigué, A.; Camacho, L.; Martín-Martín, N.; Cicogna, P.; Viera-Bardón, C.; Fernández-Ruiz, S.; Rodríguez-Hernandez, I.; et al. PGC1 α Suppresses Prostate Cancer Cell Invasion through ERR α Transcriptional Control. *Cancer Res.* **2019**, *79*, 6153–6165. [[CrossRef](#)]
79. Kaminski, L.; Torrino, S.; Dufies, M.; Djabari, Z.; Haider, R.; Roustan, F.-R.; Jaune, E.; Laurent, K.; Nottet, N.; Michiels, J.-F.; et al. PGC1 α Inhibits Polyamine Synthesis to Suppress Prostate Cancer Aggressiveness. *Cancer Res.* **2019**, *79*, 3268–3280. [[CrossRef](#)]
80. Yin, J.; Ren, W.; Huang, X.; Deng, J.; Li, T.; Yin, Y. Potential Mechanisms Connecting Purine Metabolism and Cancer Therapy. *Front. Immunol.* **2018**, *9*, 1697. [[CrossRef](#)]
81. Kami, K.; Fujimori, T.; Sato, H.; Sato, M.; Yamamoto, H.; Ohashi, Y.; Sugiyama, N.; Ishihama, Y.; Onozuka, H.; Ochiai, A.; et al. Metabolomic Profiling of Lung and Prostate Tumor Tissues by Capillary Electrophoresis Time-of-Flight Mass Spectrometry. *Metabolomics* **2013**, *9*, 444–453. [[CrossRef](#)] [[PubMed](#)]
82. Wu, X.; Daniels, G.; Lee, P.; Monaco, M.E. Lipid Metabolism in Prostate Cancer. *Am. J. Clin. Exp. Urol.* **2014**, *2*, 111–120. [[PubMed](#)]
83. Rhodes, D.R.; Barrette, T.R.; Rubin, M.A.; Ghosh, D.; Chinnaiyan, A.M. Meta-Analysis of Microarrays: Interstudy Validation of Gene Expression Profiles Reveals Pathway Dysregulation in Prostate Cancer. *Cancer Res.* **2002**, *62*, 4427–4433. [[PubMed](#)]
84. Goodwin, A.C.; Jadallah, S.; Toubaji, A.; Lecksell, K.; Hicks, J.L.; Kowalski, J.; Bova, G.S.; De Marzo, A.M.; Netto, G.J.; Casero, R.A. Increased Spermine Oxidase Expression in Human Prostate Cancer and Prostatic Intraepithelial Neoplasia Tissues. *Prostate* **2008**, *68*, 766–772. [[CrossRef](#)]
85. Peng, Q.; Wong, C.Y.-P.; Cheuk, I.W.-Y.; Teoh, J.Y.-C.; Chiu, P.K.-F.; Ng, C.-F. The Emerging Clinical Role of Spermine in Prostate Cancer. *Int. J. Mol. Sci.* **2021**, *22*, 4382. [[CrossRef](#)]
86. Shafi, A.A.; Putluri, V.; Arnold, J.M.; Tsouko, E.; Maity, S.; Roberts, J.M.; Coarfa, C.; Frigo, D.E.; Putluri, N.; Sreekumar, A.; et al. Differential Regulation of Metabolic Pathways by Androgen Receptor (AR) and Its Constitutively Active Splice Variant, AR-V7, in Prostate Cancer Cells. *Oncotarget* **2015**, *6*, 31997–32012. [[CrossRef](#)]
87. Kinnaird, A.; Zhao, S.; Wellen, K.E.; Michelakis, E.D. Metabolic Control of Epigenetics in Cancer. *Nat. Rev. Cancer* **2016**, *16*, 694–707. [[CrossRef](#)]
88. Clos-Garcia, M.; Loizaga-Iriarte, A.; Zuñiga-Garcia, P.; Sánchez-Mosquera, P.; Rosa Cortazar, A.; González, E.; Torrano, V.; Alonso, C.; Pérez-Cormenzana, M.; Ugalde-Olano, A.; et al. Metabolic Alterations in Urine Extracellular Vesicles Are Associated to Prostate Cancer Pathogenesis and Progression. *J. Extracell. Vesicles* **2018**, *7*, 1470442. [[CrossRef](#)]
89. Fernández-Peralbo, M.A.; Gómez-Gómez, E.; Calderón-Santiago, M.; Carrasco-Valiente, J.; Ruiz-García, J.; Requena-Tapia, M.J.; Luque de Castro, M.D.; Priego-Capote, F. Prostate Cancer Patients-Negative Biopsy Controls Discrimination by Untargeted Metabolomics Analysis of Urine by LC-QTOF: Upstream Information on Other Omics. *Sci. Rep.* **2016**, *6*, 38243. [[CrossRef](#)]
90. Yumba-Mpanga, A.; Struck-Lewicka, W.; Wawrzyniak, R.; Markuszewski, M.; Roslan, M.; Kaliszan, R.; Markuszewski, M.J. Metabolomic Heterogeneity of Urogenital Tract Cancers Analyzed by Complementary Chromatographic Techniques Coupled with Mass Spectrometry. *Curr. Med. Chem.* **2019**, *26*, 216–231. [[CrossRef](#)]
91. Kremer, D.M.; Nelson, B.S.; Lin, L.; Yarosz, E.L.; Halbrook, C.J.; Kerk, S.A.; Sajjakulnukit, P.; Myers, A.; Thurston, G.; Hou, S.W.; et al. GOT1 Inhibition Promotes Pancreatic Cancer Cell Death by Ferroptosis. *Nat. Commun.* **2021**, *12*, 4860. [[CrossRef](#)] [[PubMed](#)]
92. Son, J.; Lyssiotis, C.A.; Ying, H.; Wang, X.; Hua, S.; Ligorio, M.; Perera, R.M.; Ferrone, C.R.; Mullarky, E.; Shyh-Chang, N.; et al. Glutamine Supports Pancreatic Cancer Growth through a KRAS-Regulated Metabolic Pathway. *Nature* **2013**, *496*, 101–105. [[CrossRef](#)] [[PubMed](#)]
93. Goto, T.; Terada, N.; Inoue, T.; Kobayashi, T.; Nakayama, K.; Okada, Y.; Yoshikawa, T.; Miyazaki, Y.; Uegaki, M.; Utsunomiya, N.; et al. Decreased Expression of Lysophosphatidylcholine (16:0/OH) in High Resolution Imaging Mass Spectrometry Independently Predicts Biochemical Recurrence after Surgical Treatment for Prostate Cancer. *Prostate* **2015**, *75*, 1821–1830. [[CrossRef](#)] [[PubMed](#)]
94. Struck-Lewicka, W.; Kordalewska, M.; Bujak, R.; Yumba Mpanga, A.; Markuszewski, M.; Jacyna, J.; Matuszewski, M.; Kaliszan, R.; Markuszewski, M.J. Urine Metabolic Fingerprinting Using LC-MS and GC-MS Reveals Metabolite Changes in Prostate Cancer: A Pilot Study. *J. Pharm. Biomed. Anal.* **2015**, *111*, 351–361. [[CrossRef](#)]
95. Mondul, A.M.; Moore, S.C.; Weinstein, S.J.; Karoly, E.D.; Sampson, J.N.; Albanes, D. Metabolomic Analysis of Prostate Cancer Risk in a Prospective Cohort: The Alpha-Tocopherol, Beta-Carotene Cancer Prevention (ATBC) Study. *Int. J. Cancer* **2015**, *137*, 2124–2132. [[CrossRef](#)]
96. Huang, J.; Mondul, A.M.; Weinstein, S.J.; Karoly, E.D.; Sampson, J.N.; Albanes, D. Prospective Serum Metabolomic Profile of Prostate Cancer by Size and Extent of Primary Tumor. *Oncotarget* **2017**, *8*, 45190–45199. [[CrossRef](#)]

97. Lima, A.R.; Pinto, J.; Azevedo, A.I.; Barros-Silva, D.; Jerónimo, C.; Henrique, R.; de Lourdes Bastos, M.; Guedes de Pinho, P.; Carvalho, M. Identification of a Biomarker Panel for Improvement of Prostate Cancer Diagnosis by Volatile Metabolic Profiling of Urine. *Br. J. Cancer* **2019**, *121*, 857–868. [[CrossRef](#)]
98. Jung, K.; Reszka, R.; Kamlage, B.; Bethan, B.; Stephan, C.; Lein, M.; Kristiansen, G. Tissue Metabolite Profiling Identifies Differentiating and Prognostic Biomarkers for Prostate Carcinoma. *Int. J. Cancer* **2013**, *133*, 2914–2924. [[CrossRef](#)]
99. McDunn, J.E.; Li, Z.; Adam, K.-P.; Neri, B.P.; Wolfert, R.L.; Milburn, M.V.; Lotan, Y.; Wheeler, T.M. Metabolomic Signatures of Aggressive Prostate Cancer. *Prostate* **2013**, *73*, 1547–1560. [[CrossRef](#)]
100. Gómez-Cebrián, N.; García-Flores, M.; Rubio-Briones, J.; López-Guerrero, J.A.; Pineda-Lucena, A.; Puchades-Carrasco, L. Targeted Metabolomics Analyses Reveal Specific Metabolic Alterations in High-Grade Prostate Cancer Patients. *J. Proteome Res.* **2020**, *19*, 4082–4092. [[CrossRef](#)]
101. Kiebish, M.A.; Cullen, J.; Mishra, P.; Ali, A.; Milliman, E.; Rodrigues, L.O.; Chen, E.Y.; Tolstikov, V.; Zhang, L.; Panagopoulos, K.; et al. Multi-Omic Serum Biomarkers for Prognosis of Disease Progression in Prostate Cancer. *J. Transl. Med.* **2020**, *18*, 10. [[CrossRef](#)] [[PubMed](#)]
102. Liu, W.; Bai, X.; Liu, Y.; Wang, W.; Han, J.; Wang, Q.; Xu, Y.; Zhang, C.; Zhang, S.; Li, X.; et al. Topologically Inferring Pathway Activity toward Precise Cancer Classification via Integrating Genomic and Metabolomic Data: Prostate Cancer as a Case. *Sci. Rep.* **2015**, *5*, 13192. [[CrossRef](#)] [[PubMed](#)]
103. Li, C.; Han, J.; Yao, Q.; Zou, C.; Xu, Y.; Zhang, C.; Shang, D.; Zhou, L.; Zou, C.; Sun, Z.; et al. Subpathway-GM: Identification of Metabolic Subpathways via Joint Power of Interesting Genes and Metabolites and Their Topologies within Pathways. *Nucleic Acids Res.* **2013**, *41*, e101. [[CrossRef](#)]
104. Gao, B.; Lue, H.-W.; Podolak, J.; Fan, S.; Zhang, Y.; Serawat, A.; Alumkal, J.J.; Fiehn, O.; Thomas, G.V. Multi-Omics Analyses Detail Metabolic Reprogramming in Lipids, Carnitines, and Use of Glycolytic Intermediates between Prostate Small Cell Neuroendocrine Carcinoma and Prostate Adenocarcinoma. *Metabolites* **2019**, *9*, 82. [[CrossRef](#)] [[PubMed](#)]
105. Joshi, M.; Kim, J.; D'Alessandro, A.; Monk, E.; Bruce, K.; Elajaili, H.; Nozik-Grayck, E.; Goodspeed, A.; Costello, J.C.; Schlaepfer, I.R. CPT1A Over-Expression Increases Reactive Oxygen Species in the Mitochondria and Promotes Antioxidant Defenses in Prostate Cancer. *Cancers* **2020**, *12*, 3431. [[CrossRef](#)] [[PubMed](#)]
106. Chen, Y.; Wang, K.; Liu, T.; Chen, J.; Lv, W.; Yang, W.; Xu, S.; Wang, X.; Li, L. Decreased Glucose Bioavailability and Elevated Aspartate Metabolism in Prostate Cancer Cells Undergoing Epithelial-Mesenchymal Transition. *J. Cell. Physiol.* **2020**, *235*, 5602–5612. [[CrossRef](#)] [[PubMed](#)]
107. Hansen, A.F.; Sandsmark, E.; Rye, M.B.; Wright, A.J.; Bertilsson, H.; Richardsen, E.; Viset, T.; Bofin, A.M.; Angelsen, A.; Selnes, K.M.; et al. Presence of Tmprss2-ERG Is Associated with Alterations of the Metabolic Profile in Human Prostate Cancer. *Oncotarget* **2016**, *7*, 42071–42085. [[CrossRef](#)]
108. Yan, M.; Qi, H.; Li, J.; Ye, G.; Shao, Y.; Li, T.; Liu, J.; Piao, H.-L.; Xu, G. Identification of SPOP Related Metabolic Pathways in Prostate Cancer. *Oncotarget* **2017**, *8*, 103032–103046. [[CrossRef](#)]
109. Andersen, M.K.; Rise, K.; Giskeødegård, G.F.; Richardsen, E.; Bertilsson, H.; Størkersen, Ø.; Bathen, T.F.; Rye, M.; Tessem, M.-B. Integrative Metabolic and Transcriptomic Profiling of Prostate Cancer Tissue Containing Reactive Stroma. *Sci. Rep.* **2018**, *8*, 14269. [[CrossRef](#)]
110. Oberhuber, M.; Pecoraro, M.; Rusz, M.; Oberhuber, G.; Wieselberg, M.; Haslinger, P.; Gurnhofer, E.; Schleder, M.; Limberger, T.; Lager, S.; et al. STAT3-Dependent Analysis Reveals PDK4 as Independent Predictor of Recurrence in Prostate Cancer. *Mol. Syst. Biol.* **2020**, *16*, e9247. [[CrossRef](#)]
111. Cacciatore, S.; Wium, M.; Licari, C.; Ajayi-Smith, A.; Masieri, L.; Anderson, C.; Salukazana, A.S.; Kaestner, L.; Carini, M.; Carbone, G.M.; et al. Inflammatory Metabolic Profile of South African Patients with Prostate Cancer. *Cancer Metab.* **2021**, *9*, 29. [[CrossRef](#)] [[PubMed](#)]
112. Labbé, D.P.; Zadra, G.; Yang, M.; Reyes, J.M.; Lin, C.Y.; Cacciatore, S.; Ebot, E.M.; Creech, A.L.; Giunchi, F.; Fiorentino, M.; et al. High-Fat Diet Fuels Prostate Cancer Progression by Rewiring the Metabolome and Amplifying the MYC Program. *Nat. Commun.* **2019**, *10*, 4358. [[CrossRef](#)] [[PubMed](#)]
113. Röhnisch, H.E.; Kyrø, C.; Olsen, A.; Thysell, E.; Hallmans, G.; Moazzami, A.A. Identification of Metabolites Associated with Prostate Cancer Risk: A Nested Case-Control Study with Long Follow-up in the Northern Sweden Health and Disease Study. *BMC Med.* **2020**, *18*, 187. [[CrossRef](#)] [[PubMed](#)]
114. Schmidt, J.A.; Fensom, G.K.; Rinaldi, S.; Scalbert, A.; Appleby, P.N.; Achaintre, D.; Gicquiau, A.; Gunter, M.J.; Ferrari, P.; Kaaks, R.; et al. Pre-Diagnostic Metabolite Concentrations and Prostate Cancer Risk in 1077 Cases and 1077 Matched Controls in the European Prospective Investigation into Cancer and Nutrition. *BMC Med.* **2017**, *15*, 122. [[CrossRef](#)]
115. Xu, H.; Chen, Y.; Gu, M.; Liu, C.; Chen, Q.; Zhan, M.; Wang, Z. Fatty Acid Metabolism Reprogramming in Advanced Prostate Cancer. *Metabolites* **2021**, *11*, 765. [[CrossRef](#)]
116. Moazzami, A.A.; Zhang, J.-X.; Kamal-Eldin, A.; Aman, P.; Hallmans, G.; Johansson, J.-E.; Andersson, S.-O. Nuclear Magnetic Resonance-Based Metabolomics Enable Detection of the Effects of a Whole Grain Rye and Rye Bran Diet on the Metabolic Profile of Plasma in Prostate Cancer Patients. *J. Nutr.* **2011**, *141*, 2126–2132. [[CrossRef](#)]
117. Wright, J.L.; Plymate, S.R.; Porter, M.P.; Gore, J.L.; Lin, D.W.; Hu, E.; Zeliadt, S.B. Hyperglycemia and Prostate Cancer Recurrence in Men Treated for Localized Prostate Cancer. *Prostate Cancer Prostatic Dis.* **2013**, *16*, 204–208. [[CrossRef](#)]

118. Wulaningsih, W.; Holmberg, L.; Garmo, H.; Zethelius, B.; Wigertz, A.; Carroll, P.; Lambe, M.; Hammar, N.; Walldius, G.; Jungner, I.; et al. Serum Glucose and Fructosamine in Relation to Risk of Cancer. *PLoS ONE* **2013**, *8*, e54944. [[CrossRef](#)]
119. Varisli, L. Identification of New Genes Downregulated in Prostate Cancer and Investigation of Their Effects on Prognosis. *Genet. Test. Mol. Biomark.* **2013**, *17*, 562–566. [[CrossRef](#)]
120. Ni, W.-D.; Yang, Z.-T.; Cui, C.-A.; Cui, Y.; Fang, L.-Y.; Xuan, Y.-H. Tenascin-C Is a Potential Cancer-Associated Fibroblasts Marker and Predicts Poor Prognosis in Prostate Cancer. *Biochem. Biophys. Res. Commun.* **2017**, *486*, 607–612. [[CrossRef](#)]
121. San Martin, R.; Pathak, R.; Jain, A.; Jung, S.Y.; Hilsenbeck, S.G.; Piña-Barba, M.C.; Sikora, A.G.; Pienta, K.J.; Rowley, D.R. Tenascin-C and Integrin A9 Mediate Interactions of Prostate Cancer with the Bone Microenvironment. *Cancer Res.* **2017**, *77*, 5977–5988. [[CrossRef](#)] [[PubMed](#)]
122. Mishra, P.; Kiebish, M.A.; Cullen, J.; Srinivasan, A.; Patterson, A.; Sarangarajan, R.; Narain, N.R.; Dobi, A. Genomic Alterations of Tenascin C in Highly Aggressive Prostate Cancer: A Meta-Analysis. *Genes Cancer* **2019**, *10*, 150–159. [[CrossRef](#)] [[PubMed](#)]
123. Malik, G.; Ward, M.D.; Gupta, S.K.; Trosset, M.W.; Grizzle, W.E.; Adam, B.-L.; Diaz, J.I.; Semmes, O.J. Serum Levels of an Isoform of Apolipoprotein A-II as a Potential Marker for Prostate Cancer. *Clin. Cancer Res.* **2005**, *11*, 1073–1085. [[PubMed](#)]
124. Klee, E.W.; Bondar, O.P.; Goodmanson, M.K.; Dyer, R.B.; Erdogan, S.; Bergstralh, E.J.; Bergen, H.R.; Sebo, T.J.; Klee, G.G. Candidate Serum Biomarkers for Prostate Adenocarcinoma Identified by mRNA Differences in Prostate Tissue and Verified with Protein Measurements in Tissue and Blood. *Clin. Chem.* **2012**, *58*, 599–609. [[CrossRef](#)]
125. Kojima, S.; Chiyomaru, T.; Kawakami, K.; Yoshino, H.; Enokida, H.; Nohata, N.; Fuse, M.; Ichikawa, T.; Naya, Y.; Nakagawa, M.; et al. Tumour Suppressors MiR-1 and MiR-133a Target the Oncogenic Function of Purine Nucleoside Phosphorylase (PNP) in Prostate Cancer. *Br. J. Cancer* **2012**, *106*, 405–413. [[CrossRef](#)]
126. Sreekumar, A.; Poisson, L.M.; Rajendiran, T.M.; Khan, A.P.; Cao, Q.; Yu, J.; Laxman, B.; Mehra, R.; Lonigro, R.J.; Li, Y.; et al. Metabolomic Profiles Delineate Potential Role for Sarcosine in Prostate Cancer Progression. *Nature* **2009**, *457*, 910–914. [[CrossRef](#)]
127. Khan, A.P.; Rajendiran, T.M.; Ateeq, B.; Asangani, I.A.; Athanikar, J.N.; Yocum, A.K.; Mehra, R.; Siddiqui, J.; Palapattu, G.; Wei, J.T.; et al. The Role of Sarcosine Metabolism in Prostate Cancer Progression. *Neoplasia* **2013**, *15*, 491–501. [[CrossRef](#)] [[PubMed](#)]
128. Maxeiner, A.; Adkins, C.B.; Zhang, Y.; Taupitz, M.; Halpern, E.F.; McDougal, W.S.; Wu, C.-L.; Cheng, L.L. Retrospective Analysis of Prostate Cancer Recurrence Potential with Tissue Metabolomic Profiles. *Prostate* **2010**, *70*, 710–717. [[CrossRef](#)]
129. Johansson, S.; Landström, M.; Hellstrand, K.; Henriksson, R. The Response of Dunning R3327 Prostatic Adenocarcinoma to IL-2, Histamine and Radiation. *Br. J. Cancer* **1998**, *77*, 1213–1219. [[CrossRef](#)]
130. Johansson, S.; Landström, M.; Henriksson, R. Alterations of Tumour Cells, Stroma and Apoptosis in Rat Prostatic Adenocarcinoma Following Treatment with Histamine, Interleukin-2 and Irradiation. *Anticancer Res.* **1999**, *19*, 1961–1969.
131. Liu, Q.; Harvey, C.T.; Geng, H.; Xue, C.; Chen, V.; Beer, T.M.; Qian, D.Z. Malate Dehydrogenase 2 Confers Docetaxel Resistance via Regulations of JNK Signaling and Oxidative Metabolism. *Prostate* **2013**, *73*, 1028–1037. [[CrossRef](#)] [[PubMed](#)]
132. Andersen, M.K.; Giskeødegård, G.F.; Tessem, M.-B. Metabolic Alterations in Tissues and Biofluids of Patients with Prostate Cancer. *Curr. Opin. Endocr. Metab. Res.* **2020**, *10*, 23–28. [[CrossRef](#)]
133. Thysell, E.; Surowiec, I.; Hörnberg, E.; Crnalic, S.; Widmark, A.; Johansson, A.I.; Stattin, P.; Bergh, A.; Moritz, T.; Antti, H.; et al. Metabolomic Characterization of Human Prostate Cancer Bone Metastases Reveals Increased Levels of Cholesterol. *PLoS ONE* **2010**, *5*, e14175. [[CrossRef](#)] [[PubMed](#)]
134. Markert, E.K.; Mizuno, H.; Vazquez, A.; Levine, A.J. Molecular Classification of Prostate Cancer Using Curated Expression Signatures. *Proc. Natl. Acad. Sci. USA* **2011**, *108*, 21276–21281. [[CrossRef](#)] [[PubMed](#)]
135. Rye, M.B.; Bertilsson, H.; Drabløs, F.; Angelsen, A.; Bathen, T.F.; Tessem, M.-B. Gene Signatures ESC, MYC and ERG-Fusion Are Early Markers of a Potentially Dangerous Subtype of Prostate Cancer. *BMC Med. Genom.* **2014**, *7*, 50. [[CrossRef](#)] [[PubMed](#)]
136. Shah, U.S.; Dhir, R.; Gollin, S.M.; Chandran, U.R.; Lewis, D.; Acquafondata, M.; Pflug, B.R. Fatty Acid Synthase Gene Overexpression and Copy Number Gain in Prostate Adenocarcinoma. *Hum. Pathol.* **2006**, *37*, 401–409. [[CrossRef](#)]
137. Zadra, G.; Ribeiro, C.F.; Chetta, P.; Ho, Y.; Cacciatore, S.; Gao, X.; Syamala, S.; Bango, C.; Photopoulos, C.; Huang, Y.; et al. Inhibition of de Novo Lipogenesis Targets Androgen Receptor Signaling in Castration-Resistant Prostate Cancer. *Proc. Natl. Acad. Sci. USA* **2019**, *116*, 631–640. [[CrossRef](#)]
138. Bastos, D.C.; Ribeiro, C.F.; Ahearn, T.; Nascimento, J.; Pakula, H.; Clohessy, J.; Mucci, L.; Roberts, T.; Zanata, S.M.; Zadra, G.; et al. Genetic Ablation of FASN Attenuates the Invasive Potential of Prostate Cancer Driven by Pten Loss. *J. Pathol.* **2021**, *253*, 292–303. [[CrossRef](#)]
139. Barbieri, C.E.; Baca, S.C.; Lawrence, M.S.; Demichelis, F.; Blattner, M.; Theurillat, J.-P.; White, T.A.; Stojanov, P.; Van Allen, E.; Stransky, N.; et al. Exome Sequencing Identifies Recurrent SPOP, FOXA1 and MED12 Mutations in Prostate Cancer. *Nat. Genet.* **2012**, *44*, 685–689. [[CrossRef](#)]
140. An, J.; Wang, C.; Deng, Y.; Yu, L.; Huang, H. Destruction of Full-Length Androgen Receptor by Wild-Type SPOP, but Not Prostate-Cancer-Associated Mutants. *Cell Rep.* **2014**, *6*, 657–669. [[CrossRef](#)]
141. Ayala, G.; Tuxhorn, J.A.; Wheeler, T.M.; Frolov, A.; Scardino, P.T.; Otori, M.; Wheeler, M.; Spitler, J.; Rowley, D.R. Reactive Stroma as a Predictor of Biochemical-Free Recurrence in Prostate Cancer. *Clin. Cancer Res.* **2003**, *9*, 4792–4801. [[PubMed](#)]
142. Yanagisawa, N.; Li, R.; Rowley, D.; Liu, H.; Kadmon, D.; Miles, B.J.; Wheeler, T.M.; Ayala, G.E. Stromogenic Prostatic Carcinoma Pattern (Carcinomas with Reactive Stromal Grade 3) in Needle Biopsies Predicts Biochemical Recurrence-Free Survival in Patients after Radical Prostatectomy. *Hum. Pathol.* **2007**, *38*, 1611–1620. [[CrossRef](#)]

143. Tomas, D.; Spajić, B.; Milosević, M.; Demirović, A.; Marusić, Z.; Kruslin, B. Intensity of Stromal Changes Predicts Biochemical Recurrence-Free Survival in Prostatic Carcinoma. *Scand. J. Urol. Nephrol.* **2010**, *44*, 284–290. [[CrossRef](#)] [[PubMed](#)]
144. Billis, A.; Meirelles, L.; Freitas, L.L.L.; Polidoro, A.S.; Fernandes, H.A.; Padilha, M.M.; Magna, L.A.; Reis, L.O.; Ferreira, U. Adenocarcinoma on Needle Prostatic Biopsies: Does Reactive Stroma Predicts Biochemical Recurrence in Patients Following Radical Prostatectomy? *Int. Braz. J. Urol.* **2013**, *39*, 320–327. [[CrossRef](#)] [[PubMed](#)]
145. McKenney, J.K.; Wei, W.; Hawley, S.; Auman, H.; Newcomb, L.F.; Boyer, H.D.; Fazli, L.; Simko, J.; Hurtado-Coll, A.; Troyer, D.A.; et al. Histologic Grading of Prostatic Adenocarcinoma Can Be Further Optimized: Analysis of the Relative Prognostic Strength of Individual Architectural Patterns in 1275 Patients From the Canary Retrospective Cohort. *Am. J. Surg. Pathol.* **2016**, *40*, 1439–1456. [[CrossRef](#)] [[PubMed](#)]
146. Tee, A.R. Metastatic Castration-Resistant Prostate Cancer Hungers for Leucine. *J. Natl. Cancer Inst.* **2013**, *105*, 1427–1428. [[CrossRef](#)]
147. Wang, Q.; Tiffen, J.; Bailey, C.G.; Lehman, M.L.; Ritchie, W.; Fazli, L.; Metierre, C.; Feng, Y.J.; Li, E.; Gleave, M.; et al. Targeting Amino Acid Transport in Metastatic Castration-Resistant Prostate Cancer: Effects on Cell Cycle, Cell Growth, and Tumor Development. *J. Natl. Cancer Inst.* **2013**, *105*, 1463–1473. [[CrossRef](#)]
148. Otsuki, H.; Kimura, T.; Yamaga, T.; Kosaka, T.; Suehiro, J.-I.; Sakurai, H. Prostate Cancer Cells in Different Androgen Receptor Status Employ Different Leucine Transporters. *Prostate* **2017**, *77*, 222–233. [[CrossRef](#)]
149. Mengual, L.; Ars, E.; Lozano, J.J.; Bursset, M.; Izquierdo, L.; Ingelmo-Torres, M.; Gaya, J.M.; Algaba, F.; Villavicencio, H.; Ribal, M.J.; et al. Gene Expression Profiles in Prostate Cancer: Identification of Candidate Non-Invasive Diagnostic Markers. *Actas Urol. Esp.* **2014**, *38*, 143–149. [[CrossRef](#)]
150. Pavlova, N.N.; Thompson, C.B. The Emerging Hallmarks of Cancer Metabolism. *Cell Metab.* **2016**, *23*, 27–47. [[CrossRef](#)]
151. Hsu, P.P.; Sabatini, D.M. Cancer Cell Metabolism: Warburg and Beyond. *Cell* **2008**, *134*, 703–707. [[CrossRef](#)] [[PubMed](#)]
152. Vander Heiden, M.G.; Lunt, S.Y.; Dayton, T.L.; Fiske, B.P.; Israelsen, W.J.; Mattaini, K.R.; Vokes, N.I.; Stephanopoulos, G.; Cantley, L.C.; Metallo, C.M.; et al. Metabolic Pathway Alterations That Support Cell Proliferation. *Cold Spring Harb. Symp. Quant. Biol.* **2011**, *76*, 325–334. [[CrossRef](#)] [[PubMed](#)]
153. Cheung, P.K.; Ma, M.H.; Tse, H.F.; Yeung, K.F.; Tsang, H.F.; Chu, M.K.M.; Kan, C.M.; Cho, W.C.S.; Ng, L.B.W.; Chan, L.W.C.; et al. The Applications of Metabolomics in the Molecular Diagnostics of Cancer. *Expert Rev. Mol. Diagn.* **2019**, *19*, 785–793. [[CrossRef](#)] [[PubMed](#)]
154. Burton, C.; Ma, Y. Current Trends in Cancer Biomarker Discovery Using Urinary Metabolomics: Achievements and New Challenges. *Curr. Med. Chem.* **2019**, *26*, 5–28. [[CrossRef](#)] [[PubMed](#)]
155. Lyssiotis, C.A.; Nagrath, D. Metabolic Reprogramming and Vulnerabilities in Cancer. *Cancers* **2019**, *12*, 90. [[CrossRef](#)]
156. Harris, A.L. Development of Cancer Metabolism as a Therapeutic Target: New Pathways, Patient Studies, Stratification and Combination Therapy. *Br. J. Cancer* **2020**, *122*, 1–3. [[CrossRef](#)] [[PubMed](#)]
157. Luengo, A.; Gui, D.Y.; Vander Heiden, M.G. Targeting Metabolism for Cancer Therapy. *Cell Chem. Biol.* **2017**, *24*, 1161–1180. [[CrossRef](#)]
158. Gholizadeh, N.; Pundavela, J.; Nagarajan, R.; Dona, A.; Quadrelli, S.; Biswas, T.; Greer, P.B.; Ramadan, S. Nuclear Magnetic Resonance Spectroscopy of Human Body Fluids and in Vivo Magnetic Resonance Spectroscopy: Potential Role in the Diagnosis and Management of Prostate Cancer. *Urol. Oncol.* **2020**, *38*, 150–173. [[CrossRef](#)]
159. Manzi, M.; Riquelme, G.; Zabalegui, N.; Monge, M.E. Improving Diagnosis of Genitourinary Cancers: Biomarker Discovery Strategies through Mass Spectrometry-Based Metabolomics. *J. Pharm. Biomed. Anal.* **2020**, *178*, 112905. [[CrossRef](#)]
160. Pinu, F.R.; Beale, D.J.; Paten, A.M.; Kouremenos, K.; Swarup, S.; Schirra, H.J.; Wishart, D. Systems Biology and Multi-Omics Integration: Viewpoints from the Metabolomics Research Community. *Metabolites* **2019**, *9*, 76. [[CrossRef](#)]
161. Menyhárt, O.; Gyórfy, B. Multi-Omics Approaches in Cancer Research with Applications in Tumor Subtyping, Prognosis, and Diagnosis. *Comput. Struct. Biotechnol. J.* **2021**, *19*, 949–960. [[CrossRef](#)]
162. Lewis, J.E.; Kemp, M.L. Integration of Machine Learning and Genome-Scale Metabolic Modeling Identifies Multi-Omics Biomarkers for Radiation Resistance. *Nat. Commun.* **2021**, *12*, 2700. [[CrossRef](#)] [[PubMed](#)]
163. Eicher, T.; Kinnebrew, G.; Patt, A.; Spencer, K.; Ying, K.; Ma, Q.; Machiraju, R.; Mathé, A.E.A. Metabolomics and Multi-Omics Integration: A Survey of Computational Methods and Resources. *Metabolites* **2020**, *10*, 202. [[CrossRef](#)] [[PubMed](#)]
164. Das, T.; Andrieux, G.; Ahmed, M.; Chakraborty, S. Integration of Online Omics-Data Resources for Cancer Research. *Front. Genet.* **2020**, *11*, 578345. [[CrossRef](#)] [[PubMed](#)]
165. Chen, J.; Liu, X.; Shen, L.; Lin, Y.; Shen, B. CMBD: A Manually Curated Cancer Metabolic Biomarker Knowledge Database. *Database* **2021**, *2021*, baaa094. [[CrossRef](#)] [[PubMed](#)]